# Regularization-Scheme Dependence of QCD Amplitudes

---

**DISSERTATION**

zur

Erlangung der naturwissenschaftlichen Doktorwürde

(Dr. sc. nat.)

vorgelegt der

Mathematisch-naturwissenschaftlichen Fakultät

der

Universität Zürich

von

**ANDREA VISCONTI**

aus

Onsernone, TI

**Promotionskomitee**

Prof. Dr. Adrian Signer (Vorsitz)

Prof. Dr. Thomas Gehrmann

Prof. Dr. Michael Spira

Prof. Dr. Pierpaolo Mastrolia (Gutachter)

*Zürich, 2016*

*a mio padre*

## Abstract

To compute cross sections for processes at particle colliders such as the LHC, a perturbative expansion in the small coupling is needed. Moving beyond the leading order (LO) in this expansion, one can get a physical result by summing unphysical, divergent parts which have to be regularized to be mathematically consistent. These separate parts are scheme dependent, but they will give rise to a scheme independent quantity once they are summed together.

Nowadays most calculations are done using dimensional regularization, where the space-time dimension is shifted away from 4. However it is possible to define several variants of dimensional regularization (i.e. several variants of regularizations schemes). Certain powerful techniques to compute partial results can only be applied in specific schemes and are not defined in some others. Therefore it is essential to understand the relations between different variants of dimensional regularization and to know how to translate a partial result from one scheme to another.

At next-to-leading order (NLO) these relations are well understood. However, since nowadays many processes are computed in an expansion up to NNLO (and in some cases even beyond), it was imperative to complete the study of these schemes also beyond NLO. This has been done in the project presented in this thesis where a full description of the scheme dependence at NNLO is given. In particular, details on the use of schemes with four-dimensional external fields (such as the four-dimensional helicity scheme FDH) are outlined.

## Zusammenfassung

Um Wirkungsquerschnitte für Prozesse an Teilchenbeschleunigern wie dem *Large Hadron collider* (LHC) zu berechnen, sind Entwicklungen der Störungsreihe nach kleinen Kopplungen notwendig. Jenseits der führenden Ordnung in dieser Entwicklung kann man physikalische Ergebnisse erhalten, indem man unphysikalische, divergente Zwischenresultate summiert. Diese müssen regularisiert werden, um mathematisch konsistent zu sein und hängen vom Schema ab, welches für die Regularisierung der Divergenzen gewählt wurde. Die Summation liefert dann ein schemenunabhängiges Ergebnis.

Heutzutage werden die meisten Berechnungen mit Hilfe dimensionaler Regularisierung durchgeführt, bei der die Dimension der Raum-Zeit von 4 weg verschoben wird. Dabei ist es möglich, mehrere Varianten zu definieren. Einige leistungsfähige Hilfsmittel zur Berechnung von Teilergebnissen stehen nur für bestimmte Regularisierungen zur Verfügung und sind in anderen Schemen nicht definiert. Deshalb ist es zwingend notwendig, die Beziehungen zwischen den verschiedenen Varianten dimensionaler Regularisierung zu kennen und zu wissen, wie Teilergebnisse von einem Schema auf ein anderes übertragen werden können.

In nächst-führender Ordnung (*next-to-leading order*, NLO) sind diese Beziehungen gut verstanden. Da die meisten Prozesse heutzutage jedoch in der Entwicklung bis NNLO (*next-to-next-to leading order*) berechnet werden (und in manchen Fällen sogar darüber hinaus), ist eine Untersuchung der Regularisierungsschemen in höheren Ordnungen notwendig. Diese wird in der vorliegenden Arbeit in NNLO gegeben. Im Speziellen werden Einzelheiten über die Verwendung von Schemen mit vierdimensionalen externen Feldern wie FDH diskutiert.

## Contents

# 1 Introduction

The Standard Model (SM) of particle physics is arguably one of the most successful theories in the history of physics. It describes how the fundamental constituents of matter interact through the strong, weak, and electromagnetic force.

We can classify all the elementary particles in two families: the fermions, which constitute matter, and the vector bosons, which are the mediators of the fundamental interactions. The only exception in this picture is given by the only scalar field in the theory, the Higgs boson. The three fundamental forces described by the SM are a consequence of an underlying gauge symmetry: the electromagnetic, weak and strong forces are manifestations of $U(1)$, $SU(2)$, and $SU(3)$ gauge symmetry, respectively. The SM is a quantum field theory (QFT) based on these symmetries. Unfortunately there is no corresponding description of gravity so far, and its quantum nature remains unknown.

In the second half of the last century, it has been observed that the electromagnetic and the weak interactions are unified to form the so called electro-weak interaction. However the experimental evidence pertaining to the masses of the bosons responsible for the weak interaction suggested that the symmetry $SU(2) \times U(1)$ of the unified theory must be broken. This is achieved by breaking the gauge symmetry spontaneously through the Higgs mechanism. In this way the mediators of the electro-weak force (the $Z, W^+, W^-$ bosons) and fermions receive a mass term. On the other hand, the photon (the mediator of the electromagnetic interaction) remains massless. One consequence of the Higgs mechanism is the existence of a Higgs boson. Thus, the direct observation in 2012 of the Higgs boson at the Large Hadron Collider (LHC) was an extraordinary discovery which confirmed the validity of the Higgs mechanism in the theory. Finally the third interaction of the SM, the strong interaction, is described by Quantum Chromodynamics (QCD), an unbroken $SU(3)$ gauge symmetry mediated by the gluons, which remain massless.

Despite the extraordinary success of the SM, there are several pieces of evidence (dark matter, matter-antimatter asymmetry, hierarchy problem, ...) that there must be physics beyond it. Hence there is an extensive programme going on to search for new physics and scattering experiments at high-energy colliders play a decisive role in it. In order to fully exploit ever more precise experimental results, it is imperative to also increase the accuracy of theoretical predictions for cross sections. Such predictions usually rely on the application of perturbation theory and are obtained as an expansion in the couplings. To achieve the required precision, higher-order computations are required and there has been a huge effort in the community over the last few decades to push calculations up to (and in some cases even beyond) next-to-next-to leading order (NNLO). The current forefront of particle collider experiments is the LHC, where protons of several TeV in energy are collided. The dominating interaction in this case is QCD, the topic of interest in this dissertation.

There are several difficulties that occur in the perturbative computation of a cross section when hadrons are involved. In particular, we encounter the problem of confinement: at energies below $\sim 1$ GeV the strong coupling, $\alpha_s$, increases drastically. As a consequence, quarks and gluons combine to form hadrons, like protons, neutrons, and pions. At this energy scale QCD is not in a perturbative regime, nor are gluons and quarks the appropriate degrees of freedom. On the other hand, at high energies (above several GeV), the strong coupling is small enough and QCD can be approximated perturbatively by interactions between (asymptotically free) gluons and quarks. Hence, a full description of a scattering process requires a careful separation of the various scales involved.

Schematically high-energy scattering of hadrons can be split into several parts. Constituents (quarks or gluons) of the hadrons might produce a high-energy collision. While the probability of finding a particular constituent within a hadron, described by the so called Parton Distribution Functions (PDF) is a non-perturbative quantity, the large energy transfer in the scattering of the quarks and gluons ensures that this process can be described perturbatively. After the hard interaction, gluons and quarks are emitted from the partons that have been produced in the scattering. This sequence of emissions, called parton shower, is predominantly soft and/or collinear to the initial high-energy partons. However, it can still be described using perturbation theory. During this process the initial hard partons evolve into jet-like structures. Finally, once the energy of the partons is small enough, due to confinement they transform into the hadrons observed in the detector. This last part, called hadronization, is obviously non-perturbative. In order to minimize the impact of hadronization usually observables are chosen such that they depend mainly on energy flow. This leads to jet cross sections or similar quantities. The crucial feature of such quantities is that they have to be infrared safe, i.e. they must not depend on whether or not a final-state parton splits into two collinears or emit an additional soft one.

The research presented in this thesis focuses on technical aspects regarding the computation of the perturbative partonic cross section and particularly on the analysis of the regularization-scheme dependences of QCD amplitudes. Turning now to the region of our interest we give more details on the technical aspects that one encounters in the computation of the hard scattering cross section $d\hat{\sigma}$. Practically, we can write a generic fixed-order differential cross section (excluding parton shower and hadronization) in a hadronic collision through the factorization theorem [1] via

$$d\sigma^{H_1,H_2}(k_1,k_2) = \sum_{ab} \int dx_1 dx_2 f_a^{H_1}(x_1) f_b^{H_2}(x_2) d\hat{\sigma}_{ab}(x_1 k_1, x_2 k_2)\,, \tag{1.1}$$

where $H_1$ and $H_2$ are the interacting hadrons in the initial state carrying momentum $k_1$ and $k_2$. The functions $f^{H_i}(x)$ are the PDF and $x$ denotes the momentum fraction of the parton. In the subtracted partonic cross section $d\hat{\sigma}$, initial collinear

singularities have been cancelled by some counterterms (we will discuss the nature of such singularities in Section 2). The sum in the equation runs over all the flavours contributing to the process.

Computing the perturbative partonic cross section beyond tree level, several complications arise. In particular one encounters the problem of ultraviolet (UV) and infrared (IR) singularities in partial results. These singularities need to be regularized in order to obtain mathematically well-defined expressions. Of course, a final physical result has to be free of singularities. While UV poles are absorbed via renormalization, the IR divergences cancel out when we sum over degenerate states that contribute to the same physical jet cross section. Beyond tree level, the partonic cross section consist of several components: at NLO there is a virtual (one-loop diagrams) and a real component (tree-level diagrams with an additional parton in the final state); at NNLO, there is a double virtual (two-loop diagrams), a double real (tree-level diagrams with two additional partons in the final state) and a real-virtual (one-loop diagrams with an additional parton in the final state) contribution.

At NLO the cancellation of IR singularities works as follows: virtual amplitudes generate IR singularities due to the integration of the loop momentum, while real emission diagrams are finite, but nevertheless they become divergent once we perform the phase-space integration over regions where the emitted partons become soft or collinear. The final physical cross section is then a sum of these two quantities. If we regularize such singularities in dimensional regularization (where one uses $D = 4-2\epsilon$ for the dimension of the space-time) one schematically finds for the cancellation of IR singularities

$$\underbrace{\frac{1}{\epsilon}}_{\text{virtual}} + \underbrace{(Q^2)^\epsilon \int_0^{m_{jet}^2} \frac{dk^2}{(k^2)^{1+\epsilon}}}_{\text{real}} \quad \Rightarrow \ln(m_{jet}^2/Q^2). \tag{1.2}$$

Here $Q^2$ is the energy scale of the hard scattering and $m_{jet}^2$ is the limit in the integration of the phase-space for the radiated gluon, which depends on the physical observable considered (e.g. the jet mass). We immediately see that the residual logarithm surviving the cancellation can become very large when $m_{jet}^2 \ll Q^2$. If $\alpha_s \ln(m_{jet}^2/Q^2) \lesssim 1$, the fixed order expansion in the coupling is then spoiled by such logarithms (called Sudakov logarithms) as they occur at all orders in perturbation theory. A resummation of the terms $[\alpha_s \ln(m_{jet}^2/Q^2)]^n$ is often required for a reliable prediction of a cross section.

Apart from standard perturbation theory in QCD, one can also make use of effective theories (EFTs) for calculating physical quantities. They are well adapted to dealing with problems containing two (or more) widely separate scales, as e.g. $m_{jet}^2 \ll Q^2$ above. Basically this technique allows for a decomposition of a problem into contributions due to the different energy scales, which can be evaluated

individually. This usually simplifies the problem and is often a powerful method to compute physical observables. More precisely, the effective theory we use is called Soft-Collinear-Effective-Theory (SCET) [2–10]. It is a formalism that allows us to derive a factorization theorem using an effective Lagrangian. This then allows the resummation of the Sudakov logarithms using renormalization group evolution (RGE) techniques. As can be seen from Eq. (1.2) these logarithms are intimately linked to the $1/\epsilon$ singularities which in turn are linked to the regularization-scheme dependence we want to study in this thesis. Hence, this method has been our main approach in the study of regularization-scheme dependences.

An important issue is the one-to-one correspondence of SCET diagrams with the suitably expanded QCD one: separating QCD diagrams into contributions from different energy regions is a way to build an effective Lagrangian that reproduces the expansion of such diagrams. In our context, the even more important aspect is that the effective theory (in this case SCET) reproduces the long distance behaviour of the full theory and so has the same IR behaviour as QCD. Furthermore, in SCET on-shell integrals are scaleless and, therefore, vanish[1]. Hence, IR singularities in SCET (and QCD) can be determined by UV singularities of SCET. This allows us to fully reproduce the IR singularities of QCD and their scheme dependence by analysing the UV structure of SCET. The advantage of this approach is that we can use RGE techniques that are well established.

This thesis is organized as follows: we start by giving an overview of the different schemes in 1.1. We then describe some basics of QCD and SCET in Section 2 and Section 3. In Section 4 we give a precise definition of conventional dimensional regularization (CDR), the 't Hooft-Veltman scheme (HV), the four-dimensional helicity scheme (FDH), and dimensional reduction (DRED). Section 5 and Section 6 contain a discussion of how the various regularization schemes affect the UV and IR structure of scattering amplitudes. It turns out that the IR structure is governed by anomalous dimensions that contain the scheme dependence. Section 7 is devoted to the computation of the anomalous dimensions that are required for the IR structure in massless QCD. These computations are done in SCET. In Section 8 we use these results to obtain explicit transition rules for two-loop amplitudes between HV and FDH, as well as between FDH and DRED. The transition rules are then checked with explicit examples. To extend the result to the massive case, the "massive" form factors, soft functions and their corresponding anomalous dimensions are computed in Section 9. Our conclusions, including a discussion of the scheme independence of cross sections at NNLO, are presented in Section 10. Finally, we give some explicit results in Appendix A and list the required anomalous dimensions and $\beta$ functions in all schemes in Appendix B.

The results presented in this thesis are based on [11, 12].

[1] We will show some specific examples in Section 3.1.

### 1.1 Introduction to regularization schemes

Higher-order calculations in QCD result in loop integrals that are UV and/or IR divergent. The standard method to deal with these singularities is dimensional regularization, where space-time is shifted from 4 to $D \equiv 4 - 2\epsilon$ dimensions. The UV and IR singularities then manifest themselves as poles of the form $1/\epsilon^k$.

There are several variants of dimensional regularization. The most common scheme is conventional dimensional regularization (CDR), where all vector bosons are treated as $D$-dimensional. From a conceptual point of view this is the simplest possibility and guarantees a consistent treatment. However, CDR has some disadvantages. Apart from breaking supersymmetry, it is also not directly compatible with the helicity method and other computational techniques that rely on 4 dimensions and, hence, leads to more tedious expressions in intermediate steps of a calculation. Therefore, it is often advantageous to use other schemes, such as the 't Hooft-Veltman scheme (HV) [13], dimensional reduction (DRED) [14] or the four-dimensional helicity scheme (FDH) [15].

The result for a physical quantity such as a cross section is of course finite and must not depend on the regularization scheme that has been used. However, in practise such a result is obtained as a sum of several contributions, which are usually individually divergent. Therefore, these partial results can depend on the regularization scheme. It is often advantageous to use regularization schemes that are adapted to the technique used for the computation of a particular contribution. In order to be able to consistently combine the various partial results it is then imperative to have full control over the scheme dependence.

The key observation is that the scheme dependence is actually intimately linked to the structure of UV and IR singularities. The singularity structure in FDH and DRED is best understood if the (quasi) 4-dimensional gluons[2] $g$ are split into $D$-dimensional gluons $\hat{g}$ and $N_\epsilon = 2\epsilon$ scalars $\tilde{g}$. From a conceptual point of view these so-called $\epsilon$-scalars $\tilde{g}$ can be treated as independent fields with an initially arbitrary multiplicity $N_\epsilon$. The identification $N_\epsilon = 2\epsilon$ is to be made only at the end of a calculation. The decomposition of $g$ into $\hat{g}$ and $\tilde{g}$ has to be made in DRED as well as in FDH. This seems to be a disadvantage of these schemes. However, it is useful to gain insight and to derive the scheme dependence, and for practical purposes, such an explicit separation is often not required.

The contributions of the $\epsilon$-scalars are UV and IR divergent, resulting in terms of the form $(N_\epsilon)^i/\epsilon^k$. It is precisely these terms that – after setting $N_\epsilon = 2\epsilon$ – induce the scheme dependence in partial results. For a physical cross section the poles in $\epsilon$ have to cancel, including poles of the form $N_\epsilon/\epsilon$. This entails that the scheme dependence for a (finite) physical result can be at most $\mathcal{O}(N_\epsilon\,\epsilon^0)$ and, hence, will

[2]The distinction between quasi 4-dimensional space and strictly 4-dimensional space will be discussed in details in Section 4.

vanish in the limit $\epsilon \to 0$. At next-to-leading order (NLO) this has been explicitly demonstrated [16]. However, virtual corrections are generally UV and IR divergent and, therefore, scheme dependent. To find this scheme dependence the structure of UV and IR singularities has to be understood for a gauge theory with gluons and $\epsilon$-scalars.

Regarding the UV singularities, the main point is that treating the $\epsilon$-scalars as independent fields induces additional couplings. The independence of these couplings and their UV renormalization was already required in the equivalence proof of DRED and CDR [17–19] and in explicit multi-loop calculations in DRED [20–22]. It has to be stressed that also in FDH the couplings have to be treated as independent [16, 23].

The development regarding the scheme dependence related to the IR divergent part beyond NLO is more recent. The structure of the IR singularities for massless gauge amplitudes has a remarkably simple form [24–27]. It can be expressed in terms of the cusp anomalous dimension $\gamma_{\text{cusp}}$ and the anomalous dimensions of the quark and gluon, $\gamma_q$ and $\gamma_g$, respectively. These anomalous dimensions have been extracted from explicit results of form factors computed in CDR and are consistent with other processes.

It seems natural to assume that this structure can be extended to other schemes by applying the split of $g$ into $\hat{g}$ and $\tilde{g}$. This results in modified (i.e. scheme dependent) anomalous dimensions. At NLO, this leads to results that are consistent with the well-known scheme dependence of NLO amplitudes [28]. Based on this assumption, $\gamma_{\text{cusp}}$, $\gamma_q$ and $\gamma_g$ have been extracted in the FDH scheme at NNLO [29, 30], by comparing the generalized IR structure to explicit results of two-loop amplitudes for the $\gamma^* \to q\bar{q}$ and $H \to gg$ form factors and the process $q\bar{q} \to g\gamma$. Considering all these processes together yields an over-constrained system for the extraction of $\gamma_{\text{cusp}}$, $\gamma_q$ and $\gamma_g$ in the FDH scheme. The fact that there is a solution to this system suggests that FDH is a well defined scheme beyond NLO.

The main results presented in this thesis are the following: first, we will provide further evidence that with a proper definition the four-dimensional helicity scheme (FDH) can be used for loop calculations beyond NLO. To this end we show that the anomalous dimensions $\gamma_{\text{cusp}}$, $\gamma_q$ and $\gamma_g$ can be computed directly in SCET by relating them to the jet- and soft functions. We repeat the original calculation of the quark-jet function [31] and gluon-jet function [32] in the FDH scheme and also determine the soft function in FDH. This gives us an independent determination of $\gamma_{\text{cusp}}$, $\gamma_q$ and $\gamma_g$ in the FDH scheme and the results we find are in agreement with previous findings. Note that the FDH as we use it [16, 29] is slightly different from previous implementations [33].

Second, we extend the scheme dependence study to dimensional reduction (DRED). While the anomalous dimensions in DRED are the same as in FDH we also need to consider amplitudes with external $\epsilon$-scalars. Determination of the IR structure of these amplitudes requires the knowledge of $\gamma_\epsilon$, the anomalous dimen-

sion of the $\epsilon$-scalar $\tilde{g}$. We compute $\gamma_\epsilon$ in SCET via the calculation of the $\tilde{g}$-jet and soft functions and give the generalization of the IR structure to amplitudes with external $\tilde{g}$. Furthermore, we verify that this result for $\gamma_\epsilon$ is in agreement with the result extracted from an explicit computation of $H \to \tilde{g}\tilde{g}$ at NNLO [34]. To complete our study, we then generalize the results to the massive case by computing the corresponding anomalous dimensions ($\gamma_Q$ and $\gamma_{\text{cusp}}(\beta)$) from the massive form factor and the heavy to light decay and by checking them through an independent SCET approach by computing the relevant soft functions. We thus obtain a complete understanding of the relations between NNLO amplitudes in QCD in CDR, HV, FDH, and DRED.

Finally, we gain insights into how the regularization-scheme dependence cancels for fully differential cross sections at NNLO. While a complete study of this issue is beyond the scope of this work, our calculations in SCET show that the jet- and soft functions are separately scheme independent. The same is true for the hard function. Hence, if the cross section is written as a convolution of hard-, soft-, and jet functions it is manifestly regularization-scheme independent. Recently, there has been a lot of activity in performing fully differential NNLO calculations using the SCET framework. This development started with the computation of top-quark decay [35] and has subsequently been extended to more generic cases [36–45]. The results of our work show how to apply a particular regularization scheme for the calculation of either the hard-, soft- or jet function. For each of these building blocks separately, the most convenient regularization scheme can be used. This opens up possibilities for further technical advances.

# 2 Dimensional regularization, UV and IR divergences in QCD

## 2.1 Origin of the UV divergences

In order to discuss the UV origin in loop integrals, let us consider a simple example:

$$\text{Int} = \int \frac{d^4k}{(2\pi)^4} \frac{1}{k^2 - m^2 + i\delta}. \tag{2.1}$$

To evaluate this integral we can consider it as a contour integral and make use of the Wick rotation. The integral then becomes

$$\text{Int} = \int_{-\infty}^{+\infty} \frac{d^3\vec{k}}{(2\pi)^4} \int_{-i\infty}^{+i\infty} dk_0 \frac{1}{k_0^2 - \vec{k}^2 - m^2 + i\delta} \tag{2.2}$$

$$= \frac{-i}{(2\pi)^4} \int d\Omega_4 \int_0^{+\infty} dk_E \frac{k_E^3}{k_E^2 + m^2 - i\delta}\,, \tag{2.3}$$

where in the last step we made the substitution $k_0 = ik_0'$ and calculated the integral in four-dimensional spherical coordinates in the euclidean space. The UV divergence then shows up explicitly in the limit $k_E \to \infty$, which makes the integral divergent. There are several methods to regularize such infinities, but one of the most elegant one is dimensional regularization, where space-time is shifted from 4 to $D = 4 - 2\epsilon$ dimensions. We can then recompute the above integral in $D$ dimensions and get the following result:

$$\text{Int} = \int \frac{d^Dk}{(2\pi)^D} \frac{1}{k^2 - m^2 + i\delta} = -i \int \frac{d\Omega_D}{(2\pi)^D} \int_0^{+\infty} dk_E \frac{k_E^{D-1}}{k_E^2 + m^2 - i\delta}. \tag{2.4}$$

The first term is the area of a unit sphere in $D$ dimensions and is given by

$$\int d\Omega_D = \frac{2\pi^{D/2}}{\Gamma(D/2)}. \tag{2.5}$$

The second term is

$$\int_0^{\infty} dk_E \frac{k_E^{D-1}}{k_E^2 + m^2} = \frac{1}{2} \int_0^{\infty} d(l^2) \frac{(l^2)^{\frac{D}{2}-1}}{l^2 + m^2}$$

$$= \frac{1}{2} \Big(\frac{1}{m^2}\Big)^{1-\frac{D}{2}} \int_0^1 dx\, x^{-\frac{D}{2}} (1-x)^{\frac{D}{2}-1}, \tag{2.6}$$

where we set $x = m^2/(l^2 + m^2)$. At this stage we can use the relation

$$\int_0^1 dx\, x^{\alpha-1}(1-x)^{\beta-1} = \frac{\Gamma(\alpha)\Gamma(\beta)}{\Gamma(\alpha+\beta)} \tag{2.7}$$

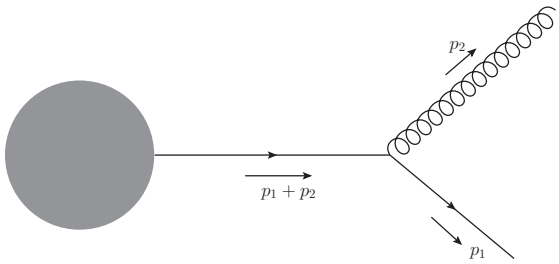


**Figure 1**. Origin of the IR singularities.

and finally get the result

$$\text{Int} = \frac{-i}{(4\pi)^{D/2}} \frac{\Gamma(1-\frac{D}{2})}{\Gamma(1)} \big(\frac{1}{m^2}\big)^{1-\frac{D}{2}}. \tag{2.8}$$

By setting $D = 4-2\epsilon$ and series expanding the gamma function, we then obtain the UV divergence as a pole in $\epsilon$

$$\Gamma(1-D/2) = \Gamma(-1+\epsilon) = -\frac{1}{\epsilon} - 1 + \gamma_E + \mathcal{O}(\epsilon)\,, \tag{2.9}$$

where $\gamma_E \approx 0.5772$ is the Euler-Mascheroni constant. In a renormalizable theory like QCD, we can subtract the UV divergences through the renormalization, i.e. by expressing the bare parameters of the Lagrangian in terms of renormalized quantities.

### 2.2 Origin of the IR divergences

In addition to the UV divergences there are another type of singularities, which have a different origin and are called IR divergences. To better understand how they are generated, let us consider the general diagram of Figure 1, where an on-shell gluon is emitted from a final state on-shell massless quark.

The singularities originate then from the intermediate propagator

$$\frac{1}{(p_1+p_2)^2} = \frac{1}{2p_1p_2} = \frac{1}{2E_1E_2(1-\cos\theta)} \simeq \frac{1}{E_1E_2\theta^2}\,. \tag{2.10}$$

We see immediately that the amplitude diverges if the emitted gluon becomes soft ($E_2 \to 0$) and/or collinear to the final quark ($\theta \to 0$). Such singularities arise in real diagrams when one performs the phase space integration and in virtual diagrams due to the loop integrals. We can regularize such infinities in exactly the same way as for the UV singularities, by applying dimensional regularization. For example we get for the following integral

$$i\pi^{-D/2}\mu^{4-D} \int d^Dk \frac{1}{[k^2+i0]\big[(k+p_1)^2+i0\big]\big[(k+p_1+p_2)^2+i0\big]} =$$

$$-\frac{\Gamma^2(1-\epsilon)\Gamma(1+\epsilon)}{\Gamma(1-2\epsilon)}\frac{1}{s}\Big[\frac{1}{\epsilon^2}-\frac{1}{\epsilon}\ln\Big(\frac{-s+i0}{\mu^2}\Big)+\frac{1}{2}\ln^2\Big(\frac{-s+i0}{\mu^2}\Big)\Big]+\mathcal{O}(\varepsilon)\,, \tag{2.11}$$

where $s=(p_1+p_2)^2$ and the double pole originates from the momentum of integration becoming both, soft and collinear at the same time. The structure of such singularities has been studied in CDR up to two-loop in [25, 27, 46, 47] and up to three-loop in [48]. Contrary to the UV divergences, the IR singularities are not subtracted through renormalization. However, a physical quantity can not be divergent and such infinities have to cancel in some way. This is indeed the case and once we add real and virtual contributions in the final state, the IR divergences cancel out. For the initial state things are a bit more complicated since there is not a full cancellation of IR singularities between virtual and real contributions and one needs to add the counterterm from the PDF in order to cancel out remaining initial state collinear singularities. IR cancellations occur at any order in the perturbation series and any infrared safe QCD observable is guaranteed to be finite.

# 3 Soft-collinear effective theory

In this section we closely follow what is given in [9] and we refer to it for more details.

The advantage of using an effective theory is that in many cases it simplifies the calculation of a given process. It can be applied whenever one encounters two widely different energy scales. The simplest possibility is to deal with exactly two different scales, but the method also applies if there are more. The general idea of an effective theory is to integrate out the large energy mode of the full theory from the Lagrangian and build effective fields that can only reproduce the low-energy behaviour. The large energy mode (also called hard contribution) is in that way embedded in the so called Wilson coefficients, which are the effective couplings of the new Lagrangian. These coefficients are determined by matching the effective theory with the full one at a given energy scale. By construction, the effective theory can only reproduce the low-energy behaviour of the full theory.

EFTs have been constructed for many different kinematic situations. For our case, to approximate QCD amplitudes needed at high-energy colliders, the appropriate EFT is SCET. It has also the peculiarity to deal with more energy scales (namely hard, soft and collinear). In that way SCET diagrams are intrinsically linked to the QCD ones, expanded around the high-energy limit. To expand the QCD loop diagrams one can use the so called *strategy of regions* technique, which also allows one to perform the matching and determine the Wilson coefficient. We turn now to this technique and discuss it in more detail.

## 3.1 The strategy of regions

The strategy of regions is an efficient method to compute loop-integrals approximately in particular kinematic regions. Basically one has to separate the original integral into different regions (e.g. hard, soft and collinear) and then expand the integrand in each sector to get an approximate result. In SCET we instead split the fields of the full Lagrangian into effective fields, which describe the behaviour of any single region. At the end the expanded integrals from the technique of the strategy of regions will correspond to the diagrams computed in SCET through effective fields. As an example let us consider the following off-shell integral with massless momenta:

$$I = i\pi^{-D/2}\mu^{4-D}\int d^D k \frac{1}{[k^2+i0]\,[(k+l)^2+i0]\,[(k+p)^2+i0]}\,, \tag{3.1}$$

where $D = 4-2\epsilon$. We also define

$$L^2 \equiv -l^2 - i0\,, \qquad P^2 \equiv -p^2 - i0\,, \qquad Q^2 \equiv -(l-p)^2 - i0\,. \tag{3.2}$$

The final goal is then to calculate the integral in Eq. (3.1) for $L^2 \sim P^2 \ll Q^2$.

At this point we also need to introduce some notation used in SCET. We define two light-like reference vectors, one along the direction of the momentum $p$ and the

other in the direction of $l$ according to the reference frame in which $\vec{Q} = 0$,

$$n_\mu = (1, 0, 0, 1) \quad \text{and} \quad \bar{n}_\mu = (1, 0, 0, -1) \tag{3.3}$$

with the properties

$$n^2 = \bar{n}^2 = 0\,, \quad \text{and} \quad n \cdot \bar{n} = 2\,. \tag{3.4}$$

Thanks to these reference vectors we can then decompose any momentum in three components; one proportional to $n$, a second proportional to $\bar{n}$, and the last perpendicular to both

$$p^\mu = (n \cdot p)\frac{\bar{n}^\mu}{2} + (\bar{n} \cdot p)\frac{n^\mu}{2} + p_\perp^\mu \equiv p_+^\mu + p_-^\mu + p_\perp^\mu\,. \tag{3.5}$$

For the square and scalar product we get

$$p^2 = (n \cdot p)(\bar{n} \cdot p) + p_\perp^2\,, \tag{3.6}$$

$$p \cdot q = p_+ \cdot q_- + p_- \cdot q_+ + p_\perp \cdot q_\perp\,. \tag{3.7}$$

In the following we give the momenta in terms of their components and use the notation

$$p^\mu = (\underbrace{n \cdot p}_{\text{“+ comp.”}}, \underbrace{\bar{n} \cdot p}_{\text{“− comp.”}}, p_\perp^\mu)\,. \tag{3.8}$$

In order to define all the different regions in which we want to split our integral, we need to introduce an expansion parameter $\lambda$

$$\lambda^2 \sim \frac{P^2}{Q^2} \sim \frac{L^2}{Q^2}\,, \qquad \text{and} \qquad p^2 \sim l^2 \sim \lambda^2 Q^2\,. \tag{3.9}$$

The reference vectors are then chosen such that $p^\mu \approx Qn^\mu/2$ and $l^\mu \approx Q\bar{n}^\mu/2$. We get the following scaling for the components of $p$ and $l$:

$$p^\mu \sim \left(\lambda^2, 1, \lambda\right) Q\,, \qquad \text{and} \qquad l^\mu \sim \left(1, \lambda^2, \lambda\right) Q\,, \tag{3.10}$$

At this point we are finally able to define all the regions of interest in which we will split our integral, namely:

- **hard region** where the integration momentum scales as $k^\mu \sim (1, 1, 1)\, Q$,
- **region collinear to** $p$ where $k$ scales as $k^\mu \sim (\lambda^2, 1, \lambda)\, Q$,
- **region collinear to** $l$ where $k$ scales as $k^\mu \sim (1, \lambda^2, \lambda)\, Q$,
- **soft region** where $k$ scales as $k^\mu \sim (\lambda^2, \lambda^2, \lambda^2)\, Q$.

Once again we stress that any region we have just described above is represented in SCET by a different effective field. The contribution of the hard region is given by taking the leading contribution $\mathcal{O}(1)$ of the propagators appearing in our integrals,

$$(k+l)^2 = \overbrace{k^2}^{\mathcal{O}(1)} + 2(\overbrace{k_+\cdot l_-}^{\mathcal{O}(\lambda^2)} + \overbrace{k_-\cdot l_+}^{\mathcal{O}(1)} + \overbrace{k_\perp\cdot l_\perp}^{\mathcal{O}(\lambda)}) + \overbrace{l^2}^{\mathcal{O}(\lambda^2)} = k^2 + 2k_-\cdot l_+ + \mathcal{O}(\lambda)\,, \quad (3.11)$$

and, similarly

$$(k+p)^2 = k^2 + 2k_+\cdot p_- + \mathcal{O}(\lambda)\,. \quad (3.12)$$

The hard region contributes to the integral $I$ as follows

$$I_h = i\pi^{-D/2}\mu^{4-D}\int d^Dk \frac{1}{[k^2+i0]\,[k^2+2k_-\cdot l_+ + i0]\,[k^2+2k_+\cdot p_- + i0]}\,; \quad (3.13)$$

it is identical to the one of an on-shell form factor integral (i.e. with $p^2 = l^2 = 0$). The result of the integral is given by

$$\begin{aligned} I_h &= \frac{\Gamma(1+\epsilon)}{2l_+\cdot p_-}\frac{\Gamma^2(-\epsilon)}{\Gamma(1-2\epsilon)}\left(\frac{\mu^2}{2l_+\cdot p_-}\right)^\epsilon \\ &= \frac{\Gamma(1+\epsilon)}{Q^2}\left(\frac{1}{\epsilon^2}+\frac{1}{\epsilon}\ln\frac{\mu^2}{Q^2}+\frac{1}{2}\ln^2\frac{\mu^2}{Q^2}-\frac{\pi^2}{6}\right)+\mathcal{O}(\epsilon)\,, \end{aligned} \quad (3.14)$$

where all divergences are infrared.

We now investigate the region collinear to $p$ where the momentum scales as $k^\mu \sim (\lambda^2, 1, \lambda)Q$. In this region $k^2 \sim \lambda^2 Q^2$, while

$$(k+l)^2 = 2k_-\cdot l_+ + \mathcal{O}(\lambda^2)\,, \qquad (k+p)^2 = \mathcal{O}(\lambda^2)\,. \quad (3.15)$$

By considering only the leading term one obtains

$$\begin{aligned} I_c &= i\pi^{-D/2}\mu^{4-D}\int d^Dk \frac{1}{[k^2+i0]\,[2k_-\cdot l_+ + i0]\,[(k+p)^2+i0]} \\ &= -\frac{\Gamma(1+\epsilon)}{2l_+\cdot p_-}\frac{\Gamma^2(-\epsilon)}{\Gamma(1-2\epsilon)}\left(\frac{\mu^2}{P^2}\right)^\epsilon \\ &= \frac{\Gamma(1+\epsilon)}{Q^2}\left(-\frac{1}{\epsilon^2}-\frac{1}{\epsilon}\ln\frac{\mu^2}{P^2}-\frac{1}{2}\ln^2\frac{\mu^2}{P^2}+\frac{\pi^2}{6}\right)+\mathcal{O}(\epsilon)\,. \end{aligned} \quad (3.16)$$

The integral in the collinear region scales as $P^{-2\epsilon}$ and the poles are of UV origin. Note that this integral is scaleless for $p^2 = 0$ and so it vanishes if it is computed on-shell. This is a general property of loop integrals in SCET. The region collinear to $l$ corresponds to the one collinear to $p$ by replacing $P^2$ with $L^2$ in the final result.

The last region to consider is the soft one, where all the components are proportional to $\lambda^2$. We get

$$k^2 = \mathcal{O}(\lambda^4)\,, \quad (k+l)^2 = 2k_-\cdot l_+ + l^2 + \mathcal{O}(\lambda^3)\,, \text{ and } \quad (k+p)^2 = 2k_+\cdot p_- + p^2 + \mathcal{O}(\lambda^3)\,. \quad (3.17)$$

The integral is then given by

$$
\begin{aligned}
I_s &= i\pi^{-D/2}\mu^{4-D}\int d^Dk \frac{1}{[k^2+i0]\,[2k_-\cdot l_+ + l^2 + i0]\,[2k_+\cdot p_- + p^2 + i0]} \\
&= -\frac{\Gamma\,(1+\epsilon)}{2l_+\cdot p_-}\Gamma(\epsilon)\Gamma\,(-\epsilon)\left(\frac{2l_+\cdot p_-\mu^2}{L^2P^2}\right)^{\epsilon} \\
&= \frac{\Gamma(1+\epsilon)}{Q^2}\left(\frac{1}{\epsilon^2}+\frac{1}{\epsilon}\ln\frac{\mu^2Q^2}{L^2P^2}+\frac{1}{2}\ln^2\frac{\mu^2Q^2}{L^2P^2}+\frac{\pi^2}{6}\right)+\mathcal{O}\,(\epsilon)\;,
\end{aligned}
\tag{3.18}
$$

where all divergences are UV.

At this stage we can sum all the contributions of any single region and get the integral in Eq. (3.1) in the limit in which $L^2 \sim P^2 \ll Q^2$.

$$
\begin{aligned}
I_h &= \frac{\Gamma\,(1+\epsilon)}{Q^2}\left(\frac{1}{\epsilon^2}+\frac{1}{\epsilon}\ln\frac{\mu^2}{Q^2}+\frac{1}{2}\ln^2\frac{\mu^2}{Q^2}-\frac{\pi^2}{6}+\mathcal{O}(\lambda)\right) \\
I_c &= \frac{\Gamma\,(1+\epsilon)}{Q^2}\left(-\frac{1}{\epsilon^2}-\frac{1}{\epsilon}\ln\frac{\mu^2}{P^2}-\frac{1}{2}\ln^2\frac{\mu^2}{P^2}+\frac{\pi^2}{6}+\mathcal{O}(\lambda)\right) \\
I_{\bar{c}} &= \frac{\Gamma\,(1+\epsilon)}{Q^2}\left(-\frac{1}{\epsilon^2}-\frac{1}{\epsilon}\ln\frac{\mu^2}{L^2}-\frac{1}{2}\ln^2\frac{\mu^2}{L^2}+\frac{\pi^2}{6}+\mathcal{O}(\lambda)\right) \\
I_s &= \frac{\Gamma\,(1+\epsilon)}{Q^2}\left(\frac{1}{\epsilon^2}+\frac{1}{\epsilon}\ln\frac{\mu^2Q^2}{L^2P^2}+\frac{1}{2}\ln^2\frac{\mu^2Q^2}{L^2P^2}+\frac{\pi^2}{6}+\mathcal{O}(\lambda)\right) \\
\hline
I \equiv I_h+I_c+I_{\bar{c}}+I_s &= \frac{1}{Q^2}\left(\ln\frac{Q^2}{L^2}\ln\frac{Q^2}{P^2}+\frac{\pi^2}{3}+\mathcal{O}(\lambda)\right)\;.
\end{aligned}
\tag{3.19}
$$

We immediately see that the final result does not depend on $\epsilon$. We also want to stress that the IR poles from the hard region cancel out against the UV divergences from the soft and collinear contributions. This fact suggests important constraints on the IR pole structure of a general amplitude. In other words, knowing the UV behaviour of SCET allows one to reproduce the structure of the IR divergences of the hard part. This property is of fundamental importance in our study and we will return to it later.

### 3.2 Scalar SCET

As already mentioned before, we can build an effective theory that directly reproduces the hard, collinear and soft region of the integral studied in the previous paragraph. In the following we only consider the case of scalar $\phi^3$ theory, since the procedure is similar to the case of QCD, but considerably simpler. We refer once again to [9] for the generalization to QCD.

Consider now the scalar Lagrangian

$$
\mathcal{L}\,(\phi) = \frac{1}{2}\partial_\mu\phi(x)\partial^\mu\phi(x) - \frac{g}{3!}\phi^3(x)\,,
\tag{3.20}
$$

where $g$ is the coupling constant and $\phi$ is the scalar field. The goal is to directly reproduce the integral we computed above using effective fields. We then split the scalar field into a collinear field to the momentum $p$, to the momentum $l$ and into a soft component, according to the regions defined before

$$\phi(x) \to \phi_c(x) + \phi_{\bar{c}}(x) + \phi_s(x)\,. \tag{3.21}$$

We note that there is no hard component of the field. This is not needed, since the hard contributions are absorbed into the so called Wilson coefficients, which are prefactors of the operators constructed from soft and collinear fields. In others words, the Wilson coefficients are the coupling constants of the effective theory and they can be adjusted in such a way that one reproduces the full theory. By replacing the split of Eq. (3.21) into the Lagrangian (3.20) we get

$$\mathcal{L}(\phi) = \underbrace{\mathcal{L}\left(\phi_c\right)}_{\equiv\mathcal{L}_c} + \underbrace{\mathcal{L}\left(\phi_{\bar{c}}\right)}_{\equiv\mathcal{L}_{\bar{c}}} + \underbrace{\mathcal{L}\left(\phi_s\right)}_{\equiv\mathcal{L}_s} + \mathcal{L}_{c+s}\left(\phi_c, \phi_{\bar{c}}, \phi_s\right)\,, \tag{3.22}$$

where the first three contributions are identical to the original Lagrangian in which we replace the full scalar field by one collinear to $p$, one collinear to $l$ and one soft. The last term describes the interaction between collinear and soft fields and is given by

$$\mathcal{L}_{c+s}\left(\phi_c, \phi_{\bar{c}}, \phi_s\right) = -\frac{g}{2}\phi_c^2\phi_s - \frac{g}{2}\phi_{\bar{c}}^2\phi_s\,. \tag{3.23}$$

At this point we still need to make a derivative (also called multipole) expansion, which means expanding each term in the small momentum components. At the end one obtains for the leading power scalar SCET Lagrangian

$$\begin{aligned}\mathcal{L}_{\text{eff}} = {} & \frac{1}{2}\partial_\mu\phi_c(x)\partial^\mu\phi_c(x) - \frac{g}{3!}\phi_c^3(x) + \frac{1}{2}\partial_\mu\phi_{\bar{c}}(x)\partial^\mu\phi_{\bar{c}}(x) - \frac{g}{3!}\phi_{\bar{c}}^3(x) \\ & + \frac{1}{2}\partial_\mu\phi_s(x)\partial^\mu\phi_s(x) - \frac{g}{3!}\phi_s^3(x) - \frac{g}{2}\phi_c^2(x)\phi_s(x_-) - \frac{g}{2}\phi_{\bar{c}}^2(x)\phi_s(x_+)\,.\end{aligned} \tag{3.24}$$

### 3.3 Factorization and RGE

We now consider the case of the Sudakov form factor, in which it is possible to factorize the soft and collinear interactions through so called jet ($\mathcal{J}$) and soft ($\mathcal{S}$) functions [9]. The hard contribution is instead integrated out into the Wilson coefficient $\tilde{C}_V\left(Q^2, \mu^2\right)$. The factorization is schematically shown in Figure 2. Mathematically we get

$$F\left(Q^2, L^2, P^2\right) = \tilde{C}_V\left(Q^2, \mu^2\right)\mathcal{J}\left(L^2, \mu^2\right)\mathcal{J}\left(P^2, \mu^2\right)\mathcal{S}\left(\Lambda_s^2, \mu^2\right)\,, \tag{3.25}$$

where $\Lambda_s^2 = L^2P^2/Q^2$. Any separate term on the r.h.s. of Eq. (3.25) fulfils a similar renormalization group equation (RGE)

$$\frac{d}{d\ln\mu}\tilde{C}_V(Q^2, \mu^2) = \left[C_F\gamma_{\text{cusp}}(\alpha_s)\ln\frac{Q^2}{\mu^2} + \gamma_V(\alpha_s)\right]\tilde{C}_V(Q^2, \mu^2)\,,$$

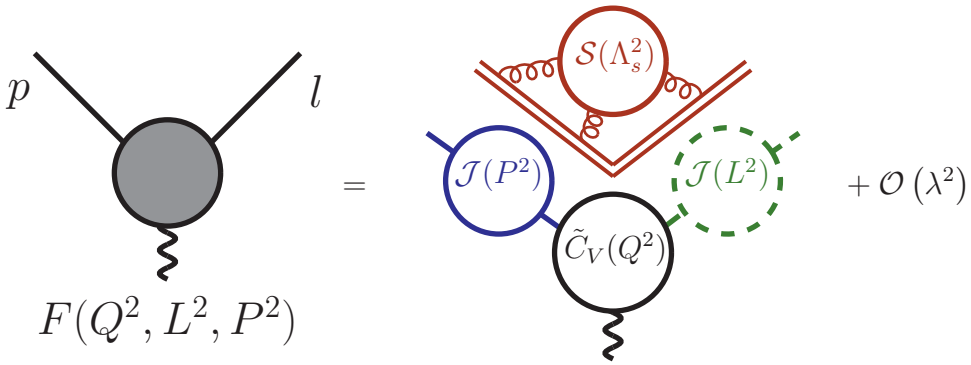


**Figure 2**. Factorization of the Sudakov form factor into hard, soft and jet functions. Figure taken from [9].

$$\begin{aligned}\frac{d}{d\ln\mu}\mathcal{J}\left(L^2,\mu^2\right) &= -\left[C_F\gamma_{\text{cusp}}\left(\alpha_s\right)\ln\frac{L^2}{\mu^2}+\gamma_J\left(\alpha_s\right)\right]\mathcal{J}\left(L^2,\mu^2\right)\,,\\ \frac{d}{d\ln\mu}\mathcal{S}\left(\Lambda_s^2,\mu^2\right) &= \left[C_F\gamma_{\text{cusp}}\left(\alpha_s\right)\ln\frac{\Lambda_s^2}{\mu^2}+\gamma_S\left(\alpha_s\right)\right]\mathcal{S}\left(\Lambda_s^2,\mu^2\right)\,.\end{aligned} \tag{3.26}$$

However, the full expression has also to be independent of the scale $\mu$

$$\frac{d}{d\ln\mu}\left[\tilde{C}_V\left(Q^2,\mu^2\right)\mathcal{J}\left(L^2,\mu^2\right)\mathcal{J}\left(P^2,\mu^2\right)\mathcal{S}\left(\Lambda_s^2,\mu^2\right)\right]=0\,. \tag{3.27}$$

By plugging the expressions in (3.26) into Eq. (3.27) we finally obtain

$$C_F\gamma_{\text{cusp}}\ln\frac{Q^2}{\mu^2}+\gamma_V-C_F\gamma_{\text{cusp}}\left(\ln\frac{L^2}{\mu^2}+\ln\frac{P^2}{\mu^2}\right)-2\gamma_J-C_F\gamma_{\text{cusp}}\ln\frac{\mu^2}{\Lambda_s^2}+\gamma_S=0\,. \tag{3.28}$$

In order to get a full cancellation of the $\mu$-dependence it is mandatory that the coefficient $\gamma_{\text{cusp}}$ in front of the logarithms is identical in all RGE. The last equation is crucial for our study of the scheme dependences and we will come back to it later when we discuss the IR structure in the various regularization schemes.

### 3.4 IR structure of QCD amplitudes

In this section we show that the IR divergences of QCD amplitudes are related to the UV divergences of SCET. The crucial point is that on-shell amplitudes in QCD match up with the Wilson coefficients. Basically we need to compute the same quantity in the full and the effective theory and then perform the matching to determine the Wilson coefficients. One possibility is the calculation of $n$-jet on-shell amplitudes. We denote an $n$-particle amplitude by

$$|\mathcal{M}_n(\epsilon,\{\underline{p}\})\rangle.$$

We compute the amplitude on-shell and as a consequence we find that all loop corrections in SCET vanish, since all the soft and collinear integrals are scaleless for

$p_i^2 = 0$. The matching between the full and the effective theory then directly relate the Fourier-transformed bare Wilson coefficients $\tilde{\mathcal{C}}_n\left(\epsilon, \{\underline{p}\}\right)$ with the on-shell amplitude:

$$|\mathcal{M}_n(\epsilon, \{\underline{p}\})\rangle = |\tilde{\mathcal{C}}_n(\epsilon, \{\underline{p}\})\rangle \times (\text{“spinors and polarization vectors”})\,. \tag{3.29}$$

At this stage we are able to relate the IR structure of QCD with the UV of SCET: the left-hand side of Eq. (3.29) contains only IR poles, which then have to be identical to the UV poles of the Wilson coefficient on the r.h.s. of the equation. This is a consequence of the fact that the on-shell loop integrals in SCET have both UV and IR singularities which cancelled each other out

$$\underbrace{\frac{1}{\epsilon_{\text{IR}}}}_{\text{on-shell amplitude}} = \underbrace{\frac{1}{\epsilon_{\text{UV}}}}_{\text{Wilson coeff.}} + \underbrace{\left(\frac{1}{\epsilon_{\text{IR}}} - \frac{1}{\epsilon_{\text{UV}}}\right)}_{\text{soft and coll. loop integrals}}\,. \tag{3.30}$$

Eq. (3.30) seems to be in contradiction to Eq. (3.14) where the singularities of the hard part have an IR origins. However, according to the SCET framework, the Wilson coefficient is the coupling of the effective Lagrangian and so it can only contain UV singularities. Furthermore, SCET does not reproduce the full QCD, but only its low-energy behaviour. This means that the high energy modes of SCET, which are described by the Wilson coefficient, have to match up with the low energy modes of the QCD hard part: this is the “border” of validity of SCET. In other words, the IR singularities of the hard part in QCD are the “upper limit” (i.e. UV limit) of the range accessible by SCET. In that sense the IR singularities of the hard region in QCD can only be interpreted as UV in the framework of SCET and no contradiction occurs.

We can subtract the UV divergences of the Wilson coefficient via a multiplicative matrix $\mathbf{Z}$ in colour space [26, 27]:

$$|\tilde{\mathcal{C}}_n(\{\underline{p}\}, \mu)\rangle = \lim_{\epsilon \to 0} \mathbf{Z}^{-1}(\epsilon, \{\underline{p}\}, \mu)|\tilde{\mathcal{C}}_n(\epsilon, \{\underline{p}\})\rangle\,. \tag{3.31}$$

As a consequence the IR singularities in the amplitude can be subtracted by the same factor $\mathbf{Z}$ and its structure is related to the renormalization group equation. Starting from the RGE of the Wilson coefficient we have

$$\frac{d}{d\ln\mu}|\tilde{\mathcal{C}}_n(\{\underline{p}\}, \mu)\rangle = \mathbf{\Gamma}(\{\underline{p}\}, \mu)|\tilde{\mathcal{C}}_n(\{\underline{p}\}, \mu)\rangle\,, \tag{3.32}$$

where the anomalous dimension $\mathbf{\Gamma}$ is also a matrix in color space. In that way we can relate the anomalous dimension to the renormalization factor and obtain

$$\mathbf{\Gamma}(\{\underline{p}\}, \mu) = -\mathbf{Z}^{-1}(\epsilon, \{\underline{p}\}, \mu)\frac{d}{d\ln\mu}\mathbf{Z}(\epsilon, \{\underline{p}\}, \mu)\,, \tag{3.33}$$

or equivalently

$$\mathbf{Z}(\epsilon, \{\underline{p}\}, \mu) = \mathbf{P} \exp \int_{\mu}^{\infty} \frac{d\mu'}{\mu'} \mathbf{\Gamma}(\{\underline{p}\}, \mu') \,. \tag{3.34}$$

From Eq. (3.30) we see that the UV singularities of the Wilson coefficient are also related to the UV singularities of the loops integrals. This means that we are able to extract the anomalous dimension $\mathbf{\Gamma}$ by computing off-shell jets and soft functions, so that we screen the IR singularities and can read off the UV poles.

### 3.5 A conjecture for $\mathbf{\Gamma}$

In [24–27] the following conjecture for the structure of $\mathbf{\Gamma}$ is given

$$\mathbf{\Gamma}(\{\underline{p}\}, \mu) = \sum_{(i,j)} \frac{\mathbf{T}_i \cdot \mathbf{T}_j}{2} \gamma_{\text{cusp}}(\alpha_s) \ln \frac{\mu^2}{-s_{ij}} + \sum_{i=1}^{n} \gamma_i(\alpha_s) \,, \tag{3.35}$$

where the first sum in means that we have to consider all unordered pairs $(i, j)$, $(i, j \in \{1, 2, \cdots, n\}$ with $n$ the number of external legs) but without the case $i = j$. This conjecture has been proven to be correct up to two-loop. It is of particular relevance that it only involves two-parton correlations and no other complicated structures appear. The exact definition of the colour matrix $\mathbf{T}$ and others details regarding Eq. (3.35) will be given later. What is conceptually relevant from Eq. (3.35) is that it gives the full description of the IR structure of any QCD amplitude with massless partons and it only requires the knowledge of the universal cusp anomalous dimension $\gamma_{\text{cusp}}(\alpha_s)$ and of the external partons $\gamma_i(\alpha_s)$, which can be either a quark or a gluon. As we will see later, these anomalous dimensions will be the key point of our study concerning regularization schemes.

### 3.6 Generalization to the massive case

If we assume there are only massive external legs in a given amplitude, we are then allowed to factorize a cross section in the soft region in terms of an hard function and a soft function. The structure of the IR divergences has been generalized in [47] to the case in which both, massless and massive external partons are present. To this end, a combination of SCET and Heavy Quark Effective Theory (HQET) has been used. As a result the soft function describing such an amplitude depends on both, massless and massive Wilson lines. If we assume that the amplitude contains massive partons, then the anomalous dimension has fewer constraints than the massless case and other more complicated color structures will show up at a given order. To be more precise, we can decompose the anomalous dimension of an amplitude containing both massive and massless external legs in a part which contains only one- and two-

parton correlations given by

$$\begin{aligned}\mathbf{\Gamma}\left(\{\underline{p}\},\{\underline{m}\},\mu\right)\big|_{\text{2-parton}} = &\sum_{(i,j)}\frac{\mathbf{T}_i\cdot\mathbf{T}_j}{2}\gamma_{\text{cusp}}(\alpha_s)\ln\frac{\mu^2}{-s_{ij}}+\sum_i\gamma_i(\alpha_s)\\ &-\sum_{(IJ)}\frac{\mathbf{T}_I\cdot\mathbf{T}_J}{2}\gamma_{\text{cusp}}(\beta_{IJ},\alpha_s)+\sum_I\gamma_I(\alpha_s)\\ &+\sum_{(Ij)}\frac{\mathbf{T}_I\cdot\mathbf{T}_j}{2}\gamma_{\text{cusp}}(\alpha_s)\ln\frac{m_I\mu}{-s_{Ij}}\,,\end{aligned}\tag{3.36}$$

where the capital indices $I, J$ refer to the massive partons and the angle $\beta_{IJ}$ is defined as

$$\beta_{IJ}=\text{arcosh}(\frac{-s_{IJ}}{2m_Im_J}),\tag{3.37}$$

with $s_{ij}=2\sigma_{ij}p_ip_j+i0$, $p_i^2=m_i^2$ and the sign factor $\sigma_{ij}=+1$ if $p_i$ and $p_j$ are both incoming or outgoing, and $\sigma_{ij}=-1$ otherwise. The remaining contribution to the anomalous dimension is a three-parton correlation function and is given by

$$\begin{aligned}\mathbf{\Gamma}\left(\{\underline{p}\},\{\underline{m}\},\mu\right)|_{\text{3-partons}} = &\,if^{abc}\sum_{(I,J,K)}\mathbf{T}_I^a\mathbf{T}_J^b\mathbf{T}_K^cF_1\left(\beta_{IJ},\beta_{JK},\beta_{KI}\right)\\ &+if^{abc}\sum_{(I,J)}\sum_k\mathbf{T}_I^a\mathbf{T}_J^b\mathbf{T}_k^cf_2\left(\beta_{IJ},\ln\left(\frac{-\sigma_{Ik}v_I\cdot p_k}{-\sigma_{Jk}v_J\cdot p_k}\right)\right).\end{aligned}\tag{3.38}$$

The functions $F_1$ and $f_2$ are defined as

$$F_1\left(\beta_{12},\beta_{23},\beta_{31}\right)=\left(\frac{\alpha_s}{4\pi}\right)^2\frac{4}{3}\sum_{(I,J,K)}\epsilon_{IJK}\,g\left(\beta_{IJ}\right)\beta_{KI}\coth\beta_{KI}\,,\tag{3.39}$$

where

$$g\left(\beta\right)=\coth\beta\left[\beta^2+2\beta\ln(1-e^{-2\beta})-\text{Li}_2(e^{-2\beta})+\frac{\pi^2}{6}\right]-\beta^2-\frac{\pi^2}{6}\tag{3.40}$$

and

$$f_2\left(\beta_{12},\ln\left(\frac{-\sigma_{23}v_2\cdot p_3}{-\sigma_{13}v_1\cdot p_3}\right)\right)=-\left(\frac{\alpha_s}{4\pi}\right)^2 4g\left(\beta_{12}\right)\ln\left(\frac{-\sigma_{23}v_2\cdot p_3}{-\sigma_{13}v_1\cdot p_3}\right).\tag{3.41}$$

In the equations above we have used the four-velocities for a massive particle, defined as

$$v_I^\mu\equiv\frac{p_I^\mu}{m_I}\,,\quad v_I^2=1\,.\tag{3.42}$$

As in the massless case, we can then subtract the IR divergences of loop amplitudes in QCD by means of a **Z**-factor. However in the effective theory the virtual corrections

from the heavy quarks are integrated out and the coupling constant entering in $\mathbf{Z}$ is only defined for a massless theory, while in the massive case we also need to take into account contributions from heavy-quark loops. In other words the $\mathbf{Z}$-factor we get from the effective low-energy theory reproduces the IR behaviour of massive QCD amplitudes after we perform a matching of the coupling constant into the massless effective theory,

$$\lim_{\epsilon\to 0}\ \mathbf{Z}^{-1}(\alpha_s)\left[\left|\mathcal{M}_n(\alpha_s^f)\right\rangle\right]_{\alpha_s^f\to\zeta_{\alpha_s}\alpha_s} \;=\; \text{finite}\ . \tag{3.43}$$

Here, $\alpha_s$ is a coupling in the effective theory, meaning that the heavy quark flavours have been integrated out. It is related to the corresponding coupling of the full theory via the decoupling relation $\alpha_s^f = \zeta_{\alpha_s}\alpha_s$. The matching factor has been calculated in [49] for $N_H$ heavy-quark flavours and it is given by

$$\zeta_{\alpha_s} = 1 + \left(\frac{\alpha_s}{4\pi}\right) N_H\, \frac{2}{3}\ln(\frac{\mu^2}{m^2}) + \mathcal{O}(\alpha^2)\,. \tag{3.44}$$

We will come back to this point later and give more details on the computation of such decoupling transformations in any regularization scheme.

# 4 Regularization schemes

In dimensional regularization the most common scheme is CDR where all vector bosons are treated as $D$-dimensional. However it is often advantageous from a computational point of view to use schemes which rely on 4 dimensions as much as possible. Since loop momenta are always $D$-dimensional objects, it follows that if a 4-dimensional treatment of the vector bosons is applied (i.e. $\gamma$-matrices and gauge fields remain 4-dimensional), two types of metric tensors can then appear in the calculations of Feynman diagrams. For instance one can get the 4-dimensional metric $g^{\mu\nu}$ from gluon propagators and the $D$-dimensional metric $\hat{g}^{\mu\nu}$ from a $D$-dimensional integral such as $\int d^D k[k^\mu k^\nu f(k^2)]$. If we decompose the 4-dimensional metric tensor $g^{\mu\nu}$ into a $D$-dimensional subspace component $\hat{g}^{\mu\nu}$ and an orthogonal $(4-D)$-dimensional subspace with metric tensor $\tilde{g}^{\mu\nu}$, we get the following relations:

$$g^{\mu\nu} = \hat{g}^{\mu\nu} + \tilde{g}^{\mu\nu} \qquad g^{\mu\nu}g_{\mu\nu} = 4 \qquad \hat{g}^{\mu\nu}\hat{g}_{\mu\nu} = D \qquad \tilde{g}^{\mu\nu}\tilde{g}_{\mu\nu} = 4 - D \tag{4.1a}$$

$$g^{\mu\nu}\hat{g}_\nu{}^\rho = \hat{g}^{\mu\rho} \qquad g^{\mu\nu}\tilde{g}_\nu{}^\rho = \tilde{g}^{\mu\rho} \qquad \hat{g}^{\mu\nu}\tilde{g}_\nu{}^\rho = 0 \tag{4.1b}$$

## 4.1 Consistent regularization

By applying a naive use of the above relations we can get into mathematical inconsistencies [50]. These can only be avoided by a proper and consistent use of the regularization [51]. To illustrate such an inconsistency [50] we note that we can project any 4-dimensional object $a^\mu$ into a $D$-dimensional component $\hat{a}^\mu = \hat{g}^{\mu\nu}a_\nu$ and the orthogonal one $\tilde{a}^\mu = \tilde{g}^{\mu\nu}a_\nu$. If this is done for the $\epsilon$-tensor we can write down the expression

$$\hat{\epsilon}^{\mu\nu\rho\sigma}\,\tilde{\epsilon}_{\alpha\beta\gamma\delta}\,\hat{\epsilon}_{\mu\nu\rho\sigma}\,\tilde{\epsilon}^{\alpha\beta\gamma\delta} \tag{4.2}$$

and evaluate it in two ways by using the 4-dimensional relation

$$\epsilon^{\mu_1\mu_2\mu_3\mu_4}\,\epsilon^{\nu_1\nu_2\nu_3\nu_4} \propto \det(g^{\mu_i\nu_j})\,. \tag{4.3}$$

First if we contract the first and second factor in (4.2) we obtain zero. However the contraction of the first and third factor yields $D(D-1)(D-2)(D-3)$ while the contraction of the second and fourth factor results in $(D-1)(D-2)(D-3)(D-4)$. As a consequence we conclude that the expression in (4.2) is not well defined for general $D$ since it entails

$$0 = D(D-1)^2(D-2)^2(D-3)^2(D-4)\,, \tag{4.4}$$

which is not satisfied for $D = 4-2\epsilon$. The inconsistency is solved by realizing that the objects $g^{\mu\nu}$, $\hat{g}^{\mu\nu}$ and $\tilde{g}^{\mu\nu}$ do not belong to a proper 4-dimensional space and therefore do not respect (4.3). This can be understood by requiring that the relation

$$\not{p}\not{p} = \frac{1}{2}p_\mu p_\nu\{\gamma^\mu,\gamma^\nu\} = p_\mu p_\nu g^{\mu\nu} = p^2 \tag{4.5}$$

| | CDR | HV | FDH | DRED |
|---|---|---|---|---|
| internal gluon | $\hat{g}^{\mu\nu}$ | $\hat{g}^{\mu\nu}$ | $g^{\mu\nu}$ | $g^{\mu\nu}$ |
| external gluon | $\hat{g}^{\mu\nu}$ | $\bar{g}^{\mu\nu}$ | $\bar{g}^{\mu\nu}$ | $g^{\mu\nu}$ |

**Table 1**. Different use of the metric tensor in the four schemes. Figure taken from [16].

holds for $D$-dim. momenta to ensure that e.g. a Dirac propagator $(\not{p}+m)/(p^2-m^2)$ can indeed be expressed as the inverse of $(\not{p}-m)$. As a consequence we get

$$g^{\mu\nu}\hat{g}^{\rho}_{\nu} = \hat{g}^{\mu\rho}\,, \tag{4.6}$$

meaning that the $D$-dimensional space has to be a subspace of the 4-dimensional one. However it is known that the $D$-dim. space can be realized only formally and it is an infinite dimensional vector space [52, 53]. To avoid any inconsistency we are then forced to realize the metric $g^{\mu\nu}$ to belong to a "quasi-4-dimensional" space $(Q4S)$ which in fact is also infinite-dimensional.

It follows that in order to define new schemes one needs to distinguish three spaces:

- the original 4-dimensional space $(4S)$ with metric tensor $\overline{g}^{\mu\nu}$ (a proper 4-dimensional vector space)
- the "quasi-$D$-dimensional space" $(QDS)$ with metric tensor $\hat{g}^{\mu\nu}$ (in fact an infinite-dimensional vector space)
- the "quasi-4-dimensional space" $(Q4S)$ with metric tensor $g^{\mu\nu}$ (in fact an infinite-dimensional vector space)

which are characterized by the following relations:

$$\begin{aligned}(4S)&: \ \overline{g}^{\mu\nu}\overline{g}_{\mu\nu} = 4\\ (QDS)&: \ \hat{g}^{\mu\nu}\hat{g}_{\mu\nu} = D = 4-2\epsilon\\ (Q4S)&: \ g^{\mu\nu}g_{\mu\nu} = D_s = 4\end{aligned} \tag{4.7}$$

and

$$g^{\mu\nu}\hat{g}^{\rho}_{\nu} = \hat{g}^{\mu\rho}, \quad g^{\mu\nu}\overline{g}^{\rho}_{\nu} = \overline{g}^{\mu\rho}, \quad \hat{g}^{\mu\nu}\overline{g}^{\rho}_{\nu} = \overline{g}^{\mu\rho}\,, \tag{4.8}$$

which entails $Q4S \supset QDS \supset 4S$.

### 4.2 Variants of dimensional regularization and dimensional reduction

Having defined the different spaces, we are allowed to introduce other schemes than CDR that differ among themselves by the regularization of the gluons[3]. It is not needed to regularize all the gluons, but only the ones that are either virtual and part of a one-particle irreducible loop diagram or, collinear or soft gluons in real correction diagrams. We follow the notation given in [16] and refer to these gluons as "internal gluons", all other gluons are then defined as "external gluons". Since only the internal vector bosons need to be regularized, we are allowed to distinguish two variants of dimensional regularization:

- CDR ("conventional dimensional regularization"): internal and external gluons are all treated as $D$-dimensional.
- HV ("'t Hooft Veltman scheme"): internal gluons are treated as $D$-dimensional but external ones are treated as strictly 4-dimensional.

and two variants of dimensional reduction:

- DRED ("original/old dimensional reduction"): internal and external gluons are all treated as quasi-4-dimensional.
- FDH ("four-dimensional helicity scheme"): internal gluons are treated as quasi-4-dimensional but external ones are treated as strictly 4-dimensional.

The different treatment of the metric tensor in the four schemes is illustrated in Table 1.

Note that in order to obtain a mathematically consistent scheme, the metric tensor for internal gluons either belongs to $Q4S$ or to $QDS$, but never to the $4S$, as discussed in the previous section. On the other hand, any of the three metrics is allowed for external ones. As an example, Figure 3 shows the same diagram computed in the different four schemes, where the two final gluons are collinear and so internal according to our definition.

Any scheme has some advantages and disadvantages. As already mentioned in the introduction, the simplest scheme from the conceptual point of view is CDR, since there is no need to distinguish between internal and external gluons and it makes use of the "standard" $QDS$ metric tensor. On the other hand, schemes such as HV and FDH are conceptually more complicated but they have the advantage of being compatible with the helicity method. DRED has been introduced to preserve supersymmetry (contrary to CDR) and it does not make any distinction between internal or external gluons (contrary to FDH and HV). However, as we will see

[3]Since we are assuming to work in QCD, the only vector bosons are gluons and we will often refer to them as a general statement valid for any other vector bosons in different theories.

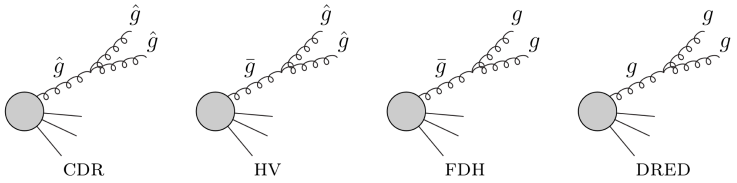


**Figure 3**. Two collinear gluons in the final state described in the four schemes. Note that the gluons in the final state are defined as internal and the gluon propagator as external, according to our definition. Figure taken from [16].

later, the use of the $Q4S$ metric tensor $g^{\mu\nu}$ introduces some complications in the UV renormalization (the same obviously occurs for FDH) and once again DRED is not compatible with the use of the helicity method. FDH has been introduced with the aim of combining the use of helicity method with the preservation of supersymmetry. At the end the choice of the scheme relies on the simplifications you can get by using one scheme instead of another in the various parts of a calculation. In that sense, knowing how to translate results from one scheme to another will allow one to get the benefit and the flexibility to use different schemes in the computation of a physical quantity (e.g. computing the virtual corrections in FDH and add the real contribution calculated in CDR).

### 4.3 Decomposition of the gluon field in FDH and DRED

With the metric tensors defined before, we can decompose a quasi-4-dimensional gluon field $A^\mu$ as

$$A^\mu = \hat{g}^{\mu\nu} A_\nu + \tilde{g}^{\mu\nu} A_\nu = \hat{A}^\mu + \tilde{A}^\mu \tag{4.9}$$

into a $D$-dimensional gauge field $\hat{A}^\mu$ and an associated $\epsilon$-scalar field $\tilde{A}^\mu$ with multiplicity $N_\epsilon = \tilde{g}^{\mu\nu}\tilde{g}_{\mu\nu} = 2\epsilon$.[4] Correspondingly, there are two types of particles in the regularized theory: $D$-dimensional gluons $\hat{g}$ and $\epsilon$-scalars $\tilde{g}$. The unregularized external gluons $\bar{g}$ of FDH are a part of $\hat{g}$.

The regularized Lagrangian of massless QCD then reads

$$\mathcal{L}_{QCD,\,\text{regularized}} = -\frac{1}{4}\hat{F}_a^{\mu\nu}\hat{F}_{\mu\nu,a} - \frac{1}{2\xi}(\partial^\mu \hat{A}_{\mu,a})^2 + i\,\overline{\psi}\hat{\not{D}}\psi + \partial^\mu \overline{c}_a \hat{D}_\mu c_a + \mathcal{L}_\epsilon, \tag{4.10a}$$

$$\mathcal{L}_\epsilon = -\frac{1}{2}(\hat{D}^\mu \tilde{A}^\nu)_a(\hat{D}_\mu \tilde{A}_\nu)_a - g_e\,\overline{\psi}\tilde{\not{A}}\psi - \frac{1}{4!}\left(g_{4\epsilon}^2\right)^{\alpha\beta\gamma\delta}_{abcd}\,\tilde{A}_{\alpha,a}\tilde{A}_{\beta,b}\tilde{A}_{\gamma,c}\tilde{A}_{\delta,d}. \tag{4.10b}$$

[4] In many applications of FDH the dimensionality of $Q4S$ is left as a variable $D_s$, which is eventually set to $D_s = 4$. The multiplicity of $\epsilon$-scalars is then $N_\epsilon = D_s - D$ [33].

Here, $\hat{F}^{\mu\nu}$ and $\hat{D}^{\mu} = \partial^{\mu} + ig_s\hat{A}^{\mu}$ denote the non-abelian field strength tensor and the covariant derivative in $D$ dimensions; $\psi$ and $c$ are the quark and ghost fields, respectively. In Eq. (4.10b) the coupling of $\epsilon$-scalars to (anti-)quarks is given by the evanescent Yukawa-like coupling $g_e$. This could in principle be set equal to the strong coupling $g_s$. But, since both couplings renormalize differently, this would only hold at tree-level and for one particular renormalization scale [19]; the same results for the quartic $\epsilon$-scalar coupling $g_{4\epsilon}$[5]. Ignoring this distinction one may obtain a non-cancellation of the divergences, wrong results and violation of unitarity [23]. The decomposition of these external gluons into $\hat{g}$ and $\tilde{g}$ also allows to avoid all problems related to factorization theorems [54] in DRED regularized QCD. In Eq. (4.10b) we introduce an abbreviation that includes the appearing Lorentz and colour structure: $(g_{4\epsilon}^2)_{abcd}^{\alpha\beta\gamma\delta} := g_{4\epsilon}^2(f_{abe}f_{cde}\tilde{g}^{\alpha\gamma}\tilde{g}^{\beta\delta} + \text{perm.})$, where "perm." denotes the 5 permutations arising from symmetrization in the multi-indices $(a,\alpha)\dots(c,\gamma)$. In the following we use all couplings in the form $\alpha_i = \frac{g_i^2}{4\pi}$ with $i = s, e, 4\epsilon$.

### 4.4 Feynman rules and Dirac algebra in FDH and DRED

From the Lagrangian given in Eq. (4.10b) we can derive the following Feynman rules (in addition to the usual ones already needed in CDR):

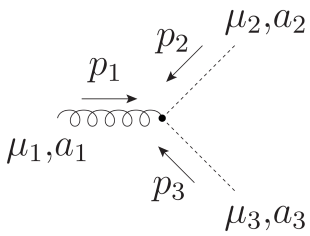


$$= g_s f^{a_1a_2a_3}\tilde{g}^{\mu_2\mu_3}(p_2 - p_3)^{\mu}$$

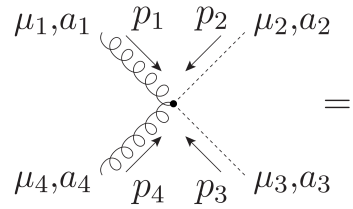


$$= -ig_s^2\Big[f^{a_1a_2e}f^{a_4a_3e}\Big(\hat{g}^{\mu_1\mu_4}\tilde{g}^{\mu_2\mu_3}\Big) + f^{a_1a_3e}f^{a_4a_2e}\Big(\hat{g}^{\mu_1\mu_4}\tilde{g}^{\mu_2\mu_3}\Big)\Big]$$

[5] Formally there are three different couplings (i.e. one per color structure) for the 4-$\epsilon$-scalar vertex. However for the study presented in this thesis no distinction is needed and the three couplings can be set equal.

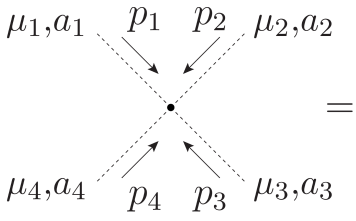


$$= -ig_{4\epsilon}^2 \Big[ f^{a_1 a_2 e} f^{a_4 a_3 e} \Big( \tilde{g}^{\mu_1\mu_4} \tilde{g}^{\mu_2\mu_3} - \tilde{g}^{\mu_1\mu_3} \tilde{g}^{\mu_2\mu_4} \Big) + f^{a_1 a_4 e} f^{a_2 a_3 e} \Big( \tilde{g}^{\mu_1\mu_2} \tilde{g}^{\mu_4\mu_3} - \tilde{g}^{\mu_1\mu_3} \tilde{g}^{\mu_2\mu_4} \Big) + f^{a_1 a_3 e} f^{a_2 a_4 e} \Big( \tilde{g}^{\mu_1\mu_2} \tilde{g}^{\mu_4\mu_3} - \tilde{g}^{\mu_1\mu_4} \tilde{g}^{\mu_2\mu_3} \Big) \Big]$$

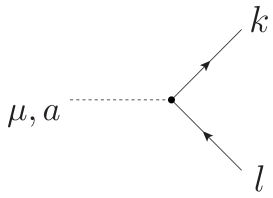


$$= ig_e \tilde{\gamma}^\mu t^a_{kl}$$

where the dash lines represent the $\epsilon$-scalar.

In addition to the Feynman rules related to the $\epsilon$-scalar, we get the following properties in the Dirac algebra:

$$\not{p} = \hat{p}_\mu \gamma^\mu = \hat{p}_\mu (\hat{\gamma}^\mu + \tilde{\gamma}^\mu) = \hat{p}_\mu \hat{\gamma}^\mu + \underbrace{\hat{g}_{\nu\mu} \tilde{g}^{\mu\rho}}_{=0} \hat{p}^\nu \tilde{\gamma}_\rho = \hat{p}_\mu \hat{\gamma}^\mu \,, \tag{4.11}$$

$$\hat{\gamma^\mu} \tilde{\gamma^\nu} = \hat{g}^{\sigma\mu} \tilde{g}^{\rho\nu} \gamma_\sigma \gamma_\rho = \hat{g}^{\sigma\mu} \tilde{g}^{\rho\nu} (2 g_{\sigma\rho} - \gamma_\rho \gamma_\sigma) = 2 \underbrace{\hat{g}^\mu_\rho \tilde{g}^{\rho\nu}}_{=0} - \tilde{\gamma}^\nu \hat{\gamma}^\mu = -\tilde{\gamma}^\nu \hat{\gamma}^\mu \,, \tag{4.12}$$

$$\tilde{\gamma}^\mu \tilde{\gamma}_\mu = \frac{1}{2} \tilde{g}_{\mu\nu} \{\tilde{\gamma}^\mu, \tilde{\gamma}^\nu\} = \tilde{g}_{\mu\nu} \tilde{g}^{\mu\nu} = N_\epsilon \,, \tag{4.13}$$

$$\hat{\gamma}^\mu \tilde{\gamma}_\mu = \underbrace{\tilde{g}_{\nu\mu} \hat{g}^{\mu\sigma}}_{=0} \gamma_\sigma \gamma^\nu = 0. \tag{4.14}$$

## 5 UV renormalization in FDH and DRED

Scheme differences have their origin in UV and IR divergent contributions due to the $\epsilon$-scalars. These contributions are of the form $(N_\epsilon)^i/\epsilon^k$ and after setting $N_\epsilon \to 2\epsilon$ result in the scheme differences. This connection to UV and IR singular terms allows for a completely systematic treatment of the regularization-scheme (RS) dependence[6].

Regarding UV renormalization, FDH and DRED behave in the same way. The possible split of internal gluons into gauge fields and $\epsilon$-scalars implies that in principle five different couplings need to be distinguished (see in particular [19, 20, 23]): the gauge coupling $\alpha_s$, the $\tilde{g}q\bar{q}$ coupling $\alpha_e$, and three different independent quartic $\tilde{g}$-couplings $\alpha_{4\epsilon,i}$ with $i = 1, 2, 3$. In general, we write the perturbative expansion of an RS-dependent quantity $X^{\rm RS}(\{\alpha\})$ as

$$X^{\rm RS}(\{\alpha\}) = \sum_{m,n,k,l,j}^{\infty} \left(\frac{\alpha_s}{4\pi}\right)^m \left(\frac{\alpha_e}{4\pi}\right)^n \left(\frac{\alpha_{4\epsilon,1}}{4\pi}\right)^k \left(\frac{\alpha_{4\epsilon,2}}{4\pi}\right)^l \left(\frac{\alpha_{4\epsilon,3}}{4\pi}\right)^j X^{\rm RS}_{mnklj}\,. \tag{5.1}$$

Accordingly, the $\beta$ functions for $\alpha_s$ and $\alpha_e$ in full generality are written as

$$\mu^2\frac{d}{d\mu^2}\frac{\alpha_s}{4\pi} = -\epsilon\frac{\alpha_s}{4\pi} - \sum_{\Sigma\geq 2} \left(\frac{\alpha_s}{4\pi}\right)^m \left(\frac{\alpha_e}{4\pi}\right)^n \left(\frac{\alpha_{4\epsilon,1}}{4\pi}\right)^k \left(\frac{\alpha_{4\epsilon,2}}{4\pi}\right)^l \left(\frac{\alpha_{4\epsilon,3}}{4\pi}\right)^j \beta^{s\,\rm RS}_{mnklj}, \tag{5.2a}$$

$$\mu^2\frac{d}{d\mu^2}\frac{\alpha_e}{4\pi} = -\epsilon\frac{\alpha_e}{4\pi} - \sum_{\Sigma\geq 2} \left(\frac{\alpha_s}{4\pi}\right)^m \left(\frac{\alpha_e}{4\pi}\right)^n \left(\frac{\alpha_{4\epsilon,1}}{4\pi}\right)^k \left(\frac{\alpha_{4\epsilon,2}}{4\pi}\right)^l \left(\frac{\alpha_{4\epsilon,3}}{4\pi}\right)^j \beta^{e\,\rm RS}_{mnklj} \tag{5.2b}$$

with analogous expansions for the $\beta$ functions for $\alpha_{4\epsilon,i}$. In the sums, $\Sigma \geq 2$ is an abbreviation for $m + n + k + l + j \geq 2$. The later results will show that the $\beta$ functions of the $\alpha_{4\epsilon,i}$ are not needed for our study and that we do not need to distinguish between them; hence we will often denote them generically by $\alpha_{4\epsilon}$.[7] Note that in Eq. (5.2) all quantities are finite and the scheme dependence is $\mathcal{O}(N_\epsilon)$. Thus, after setting $N_\epsilon \to 2\epsilon$ and then $\epsilon \to 0$, the scheme dependence disappears and we refrain from using an RS label on the l.h.s. of Eq. (5.2). In particular we write $\alpha_s$ and $\alpha_e$ without an RS label.

[6] From now on we will refer to any regularisation schemes by the abbreviation RS and to only CDR, HV and FDH by RS*.

[7] We remark that in practice the couplings can often be identified; only the bare couplings and the associated renormalization constants and $\beta$ functions must be kept different. Section 8 will provide further discussion and examples.

### 5.1 $\beta$ functions and coupling renormalization

The renormalization of the couplings $\alpha_s, \alpha_e$, and $\alpha_{4\epsilon}$ is done by replacing the bare couplings with the renormalized ones. For renormalization purposes we choose a modified version of the $\overline{\text{MS}}$ scheme: as in Ref. [30] we treat the multiplicity $N_\epsilon$ of the $\epsilon$-scalars as an initially arbitrary quantity and subtract divergences of the form $\left(\frac{N_\epsilon}{\epsilon}\right)^n$. As a consequence, the corresponding $\beta$ functions depend on $N_\epsilon$: $\overline{\beta}^i \equiv \mu^2 \frac{\mathrm{d}}{\mathrm{d}\mu^2}\left(\frac{\alpha_i}{4\pi}\right) = \overline{\beta}^i(\alpha_s, \alpha_e, \alpha_{4\epsilon}, N_\epsilon)$, with $i = s, e, 4\epsilon$. They are given in Refs. [29, 30] and read (for $\bar{\beta}^s$ and $\bar{\beta}^e$)

$$\begin{aligned}\overline{\beta}^s =& -\left(\frac{\alpha_s}{4\pi}\right)^2\left[C_A\left(\frac{11}{3}-\frac{N_\epsilon}{6}\right)-\frac{2}{3}N_F\right]\\ &-\left(\frac{\alpha_s}{4\pi}\right)^3\left[C_A^2\left(\frac{34}{3}-\frac{7}{3}N_\epsilon\right)-\frac{10}{3}C_A N_F-2C_F N_F\right]\\ &-\left(\frac{\alpha_s}{4\pi}\right)^2\left(\frac{\alpha_e}{4\pi}\right)\left[C_F N_F N_\epsilon\right]+\mathcal{O}(\alpha^4),\end{aligned} \tag{5.3a}$$

$$\overline{\beta}^e = -\left(\frac{\alpha_s}{4\pi}\right)\left(\frac{\alpha_e}{4\pi}\right)6\,C_F-\left(\frac{\alpha_e}{4\pi}\right)^2\left[C_A(2-N_\epsilon)+C_F(-4+N_\epsilon)-N_F\right]+\mathcal{O}(\alpha^3). \tag{5.3b}$$

In addition we also provide a list of renormalization factors:

$$\text{wave fct } q: \quad Z_{qq} = 1+\left(\frac{1}{4\pi}\right)\frac{1}{\epsilon}C_F\left[-\alpha_s-\alpha_e\frac{N_\epsilon}{2}\right], \tag{5.4}$$

$$\text{wave fct } g: \quad Z_{gg} = 1+\left(\frac{\alpha_s}{4\pi}\right)\frac{1}{\epsilon}\left[C_A\left(\frac{5}{3}-\frac{N_\epsilon}{6}\right)-\frac{4N_F T_R}{3}\right], \tag{5.5}$$

$$\text{wave fct } \tilde{g}: \quad Z_{\tilde{g}\tilde{g}} = 1+\left(\frac{1}{4\pi}\right)\frac{1}{\epsilon}\left[\alpha_s\,(2C_A)-\alpha_e\,(2N_F T_R)\right], \tag{5.6}$$

$$\text{vertex } q\bar{q}g: \quad Z_{qqg} = 1+\left(\frac{1}{4\pi}\right)\frac{1}{\epsilon}\left[-\alpha_s\left(C_A+C_F\right)-\alpha_e C_F\frac{N_\epsilon}{2}\right], \tag{5.7}$$

$$\text{vertex } q\bar{q}\tilde{g}: \quad Z_{qq\tilde{g}} = 1+\left(\frac{1}{4\pi}\right)\frac{1}{\epsilon}\left[\alpha_s\left(C_A-4C_F\right)+\frac{\alpha_e}{2}\left(C_A-2C_F\right)\left(-2+N_\epsilon\right)\right]. \tag{5.8}$$

As an example Figure 4 shows the explicit diagrams contributing to the vertex $q\bar{q}g$ in FDH and DRED.

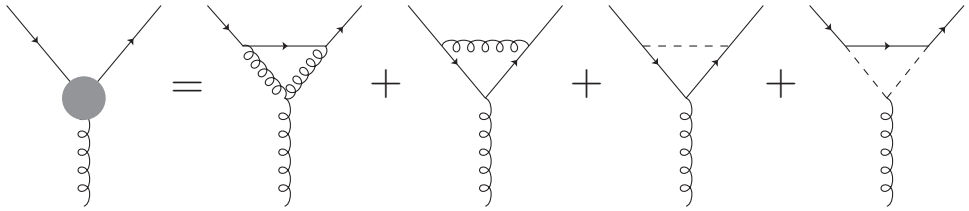

**Figure 4**. *Vertex $q\bar{q}g$ in* FDH *and* DRED.

Thanks to these expressions we can then obtain the coupling constants renormalization and so the above $\beta$ functions by computing the following expressions

$$\text{coupling } gq\bar{q}: \quad Z_{g_s} = Z_{qqg} Z_{gg}^{-1/2} Z_{qq}^{-1}, \tag{5.9}$$

$$\text{coupling } \tilde{g}q\bar{q}: \quad Z_{g_e} = Z_{qq\tilde{g}} Z_{\tilde{g}\tilde{g}}^{-1/2} Z_{qq}^{-1}. \tag{5.10}$$

# 6 IR structure in various regularization schemes

## 6.1 IR structure in CDR, HV and FDH

After UV renormalization, on-shell scattering amplitudes in massless QCD still contain IR poles $1/\epsilon^k$. In the framework of CDR it has been shown that these singularities can be subtracted in the $\overline{\text{MS}}$ scheme, using the procedure described in [24–27, 55–57], via a multiplicative renormalization factor $\mathbf{Z}$ which is a matrix in colour space (as also discussed previously in Sections 3.4 and 3.5) . This can be generalized not only to the HV but also to the FDH and DRED schemes [29, 30].

For the following discussion we find more convenient to work with amplitudes squared. More precisely, we consider

$$\mathcal{M}^{\text{RS}*}(\epsilon, N_\epsilon, \{p\}) \equiv 2\,\text{Re}\,\langle \mathcal{A}_0^{\text{RS}*}(\epsilon, N_\epsilon, \{p\})|\mathcal{A}^{\text{RS}*}(\epsilon, N_\epsilon, \{p\})\rangle\,, \tag{6.1}$$

where $|\mathcal{A}^{\text{RS}*}(\epsilon, N_\epsilon, \{p\})\rangle$ is a UV renormalized, on-shell $n$-parton scattering amplitude containing IR poles and $\langle \mathcal{A}_0^{\text{RS}*}(\epsilon, N_\epsilon, \{p\})|$ is the corresponding tree-level amplitude[8]. Both the $\epsilon$- and the $N_\epsilon$-dependence differ in the four regularization schemes. For the moment we restrict ourselves to CDR, HV, FDH, as indicated by the label RS*. Then the regularized external gluons behave completely as gauge fields and do not have to be split into gauge fields and $\epsilon$-scalars. The set $\{p\}$ denotes the set of partons of the process under consideration and contains only quarks or gluons.

The regularization-scheme dependence of $\mathcal{M}^{\text{RS}*}$ is related to the IR poles and can be absorbed by a scheme-dependent factor $(\mathbf{Z}^{\text{RS}*})^{-1}$. We can define IR subtracted finite squared amplitudes as

$$\mathcal{M}_{\text{sub}}^{\text{RS}*}(\epsilon, N_\epsilon, \{p\}, \mu) = 2\,\text{Re}\langle \mathcal{A}_0^{\text{RS}*}(\epsilon, N_\epsilon, \{p\})|\big(\mathbf{Z}^{\text{RS}*}(\epsilon, N_\epsilon, \{p\}, \mu)\big)^{-1}|\mathcal{A}^{\text{RS}*}(\epsilon, N_\epsilon, \{p\})\rangle\,, \tag{6.2}$$

where $\mu$ represents the factorization scale. The expression on the l.h.s. of Eq. (6.2), $\mathcal{M}_{\text{sub}}^{\text{RS}*}$, denotes the finite remainder of the amplitude where the poles have been subtracted in a minimal way. $\mathcal{M}_{\text{sub}}^{\text{RS}*}$ still depends on $\epsilon$ (and $N_\epsilon$) but does not contain poles $1/\epsilon^k$ any longer. Hence, the limit $\epsilon \to 0$ can be taken and then we obtain a scheme independent finite matrix element squared

$$\mathcal{M}_{\text{fin}}(\{p\}, \mu) = \lim_{(N)_\epsilon \to 0} \mathcal{M}_{\text{sub}}^{\text{RS}*}(\epsilon, N_\epsilon, \{p\}, \mu)\,. \tag{6.3}$$

The limit $(N)_\epsilon \to 0$ indicates that first we set $N_\epsilon \to 2\epsilon$ and then $\epsilon \to 0$. To put it differently, after setting $N_\epsilon \to 2\epsilon$, the scheme dependence of $\mathcal{M}_{\text{sub}}^{\text{RS}*}$ is only in the terms $\mathcal{O}(\epsilon)$.

[8] Strictly speaking, the tree-level amplitudes in the RS*-schemes do not depend on $N_\epsilon$. Nevertheless, we keep the dependence on $N_\epsilon$ in the notation to simplify the generalization to DRED in Section 6.2.

The starting point for a typical NNLO calculation is the computation of the two-loop virtual corrections in a particular regularization scheme. This corresponds to $\mathcal{M}^{\text{RS}*}$ as defined in Eq. (6.1). To understand the IR divergence structure and obtain transition rules between schemes we want to exploit the relation of the scheme-dependent $\mathcal{M}^{\text{RS}*}$ to the scheme-independent $\mathcal{M}_{\text{fin}}$. The key quantity for this is the scheme dependent factor $\mathbf{Z}^{\text{RS}*}$ to which we turn now.

The all-order amplitude $|\mathcal{A}^{\text{RS}*}(\epsilon, N_\epsilon, \{p\})\rangle$ in Eq. (6.2) is independent of the factorization scale $\mu$. It follows that the IR subtracted amplitude squared satisfies a renormalization group equation (RGE)

$$\frac{d}{d\ln\mu}\mathcal{M}^{\text{RS}*}_{\text{sub}}(\epsilon, N_\epsilon, \{p\}, \mu) = \mathbf{\Gamma}^{\text{RS}*}(N_\epsilon, \{p\}, \mu)\,\mathcal{M}^{\text{RS}*}_{\text{sub}}(\epsilon, N_\epsilon, \{p\}, \mu)\,, \tag{6.4}$$

where the anomalous dimension $\mathbf{\Gamma}^{\text{RS}*}(N_\epsilon, \{p\}, \mu)$ is related to the $\mathbf{Z}^{\text{RS}*}$ factor through

$$\mathbf{\Gamma}^{\text{RS}*}(N_\epsilon, \{p\}, \mu) = -\big(\mathbf{Z}^{\text{RS}*}(\epsilon, N_\epsilon, \{p\}, \mu)\big)^{-1}\frac{d}{d\ln\mu}\mathbf{Z}^{\text{RS}*}(\epsilon, N_\epsilon, \{p\}, \mu)\,, \tag{6.5}$$

as already shown in Eq. (3.33) for CDR. This equation can be formally solved to obtain a path-ordered exponential with respect to colour matrices

$$\mathbf{Z}^{\text{RS}*}(\epsilon, N_\epsilon, \{p\}, \mu) = \mathcal{P}\exp\int_\mu^\infty \frac{d\mu'}{\mu'}\mathbf{\Gamma}^{\text{RS}*}(N_\epsilon, \{p\}, \mu')\,. \tag{6.6}$$

In [24–27] it has been shown that in CDR the general structure of the anomalous dimension operator $\mathbf{\Gamma}$, which controls the IR divergences of QCD scattering amplitudes, is exactly known up to two-loop level and only involves colour dipoles (see Eq. (3.35)). Generalizing this from CDR to other schemes and suppressing the dependence on $N_\epsilon$, we write according to Refs. [29, 30]

$$\mathbf{\Gamma}^{\text{RS}*}(\{p\}, \mu) = \sum_{(i,j)}\frac{\mathbf{T}_i\cdot\mathbf{T}_j}{2}\,\gamma^{\text{RS}*}_{\text{cusp}}\,\ln\frac{\mu^2}{-s_{ij}} + \sum_{i=1}^{n}\gamma_i^{\text{RS}*}\,, \tag{6.7}$$

where $s_{ij} = \pm 2p_i\cdot p_j + i0$, the sign "+" is chosen when both momenta $p_i$ and $p_j$ are incoming or outgoing and the sign "−" when one momentum is incoming and the other one outgoing. The first sum in Eq. (6.7) runs over all pairs $i \neq j$ of distinct parton indices $i, j \in \{1, 2, \ldots, n\}$, where $n$ is the number of external partons. The universal quantity $\gamma^{\text{RS}*}_{\text{cusp}}$ that appears as coefficient of the two-particle correlation term, $\mathbf{T}_i\cdot\mathbf{T}_j \equiv \mathbf{T}_i^c\mathbf{T}_j^c$, is called "cusp" anomalous dimension. The quantity $\gamma_i^{\text{RS}*}$ is a single-particle term which depends on the type of the external particle, $\gamma_q^{\text{RS}*} \equiv \gamma_{\bar{q}}^{\text{RS}*}$ in the case of a (anti)quark and $\gamma_g^{\text{RS}*}$ in the case of a gluon. The explicit form of the colour generator associated to the $i$-th parton, $\mathbf{T}_i^a$, is as follows: for final-state quarks or initial-state antiquarks, the colour matrices $\mathbf{T}$ are defined by $(\mathbf{T}^c)_{ba} = t^c_{ba}$, where $t^c$ is a SU($N$) generator. For final-state antiquarks or initial state quarks one has instead $(\mathbf{T}^c)_{ba} = -t^c_{ab}$, while for gluons $(\mathbf{T}^c)_{ba} = if^{abc}$.

As a consequence the IR structure can be described by a set of three constants, which depend on the scheme

$$\text{RS}* \in \{\text{CDR}, \text{HV}, \text{FDH}\}: \quad \gamma_{\text{cusp}}^{\text{RS}*}, \gamma_q^{\text{RS}*}, \gamma_g^{\text{RS}*}. \tag{6.8}$$

Thanks to the simple structure of the anomalous dimension matrix $\mathbf{\Gamma}$, one can find an explicit solution for the perturbative expansion of $\mathbf{Z}$. It is also possible to drop the path-ordering symbol in Eq. (6.6) since the colour structure of $\mathbf{\Gamma}$ is independent of $\mu$. The following notation is often introduced

$$\Gamma'^{\text{RS}*}(\{p\}) \equiv \frac{\partial}{\partial \ln \mu} \mathbf{\Gamma}^{\text{RS}*}(\{p\}, \mu) = -\gamma_{\text{cusp}}^{\text{RS}*} \sum_i C_i \,, \tag{6.9}$$

where the last equality follows from colour conservation, $C_i = C_{\bar{q}} = C_q = C_F$ for (anti)quarks and $C_i = C_g = C_A$ for gluons.

All scheme-dependent quantities introduced so far potentially depend on all couplings $\{\alpha(\mu)\} \equiv \{\alpha_s(\mu), \alpha_e(\mu), \alpha_{4\epsilon,i}(\mu)\}$. Thus, in general the perturbative expansion is of the form of Eq. (5.1).

Solving the differential equation Eq. (6.5) one obtains a perturbative expression for $\ln \mathbf{Z}^{\text{RS}*}$ which also depends on the $\beta$ functions. Suppressing the arguments, in particular the dependence on the process $\{p\}$, it can be written up to NNLO as

$$\begin{aligned}
\ln \mathbf{Z}^{\text{RS}*} = {} & \left(\frac{\vec{\alpha}}{4\pi}\right) \cdot \left(\frac{\vec{\Gamma}_1'^{\,\text{RS}*}}{4\epsilon^2} + \frac{\vec{\mathbf{\Gamma}}_1^{\text{RS}*}}{2\epsilon}\right) \\
& + \sum_{\Sigma=2} \left(\frac{\alpha_s}{4\pi}\right)^m \left(\frac{\alpha_e}{4\pi}\right)^n \left(\frac{\alpha_{4\epsilon,1}}{4\pi}\right)^k \left(\frac{\alpha_{4\epsilon,2}}{4\pi}\right)^l \left(\frac{\alpha_{4\epsilon,3}}{4\pi}\right)^j \\
& \left( - \frac{3\vec{\beta}_{mnklj}^{\text{RS}*} \cdot \vec{\Gamma}_1'^{\,\text{RS}*}}{16\epsilon^3} - \frac{\vec{\beta}_{mnklj}^{\text{RS}*} \cdot \vec{\mathbf{\Gamma}}_1^{\text{RS}*}}{4\epsilon^2} + \frac{\Gamma'^{\text{RS}*}_{mnklj}}{16\epsilon^2} + \frac{\mathbf{\Gamma}^{\text{RS}*}_{mnklj}}{4\epsilon} \right) + \mathcal{O}(\alpha^3) \,.
\end{aligned} \tag{6.10}$$

Here the sum $\Sigma = 2$ denotes a sum over all terms satisfying $m + n + k + l + j = 2$, and the following vector notation for terms involving pure one-loop quantities has been used:

$$\vec{\alpha} \cdot \vec{\mathbf{\Gamma}}_1^{\text{RS}*} \equiv \alpha_s \, \mathbf{\Gamma}^{\text{RS}*}_{10000} + \alpha_e \, \mathbf{\Gamma}^{\text{RS}*}_{01000} + \alpha_{4\epsilon,1} \, \mathbf{\Gamma}^{\text{RS}*}_{00100} + \alpha_{4\epsilon,2} \, \mathbf{\Gamma}^{\text{RS}*}_{00010} + \alpha_{4\epsilon,3} \, \mathbf{\Gamma}^{\text{RS}*}_{00001} \,, \tag{6.11a}$$

$$\begin{aligned}
\vec{\beta}_{mnklj}^{\text{RS}*} \cdot \vec{\mathbf{\Gamma}}_1^{\text{RS}*} \equiv {} & \beta^{s\,\text{RS}*}_{mnklj} \, \mathbf{\Gamma}^{\text{RS}*}_{10000} + \beta^{e\,\text{RS}*}_{mnklj} \, \mathbf{\Gamma}^{\text{RS}*}_{01000} \\
& + \beta^{4\epsilon,1\,\text{RS}*}_{mnklj} \, \mathbf{\Gamma}^{\text{RS}*}_{00100} + \beta^{4\epsilon,2\,\text{RS}*}_{mnklj} \, \mathbf{\Gamma}^{\text{RS}*}_{00010} + \beta^{4\epsilon,3\,\text{RS}*}_{mnklj} \, \mathbf{\Gamma}^{\text{RS}*}_{00001} \,,
\end{aligned} \tag{6.11b}$$

and analogously for the combinations involving $\vec{\Gamma}_1'$. The dependence of $\mathbf{\Gamma}$ on the individual couplings and the appearance of the different $\beta$ functions constitutes an important difference to the CDR case, where only the $\alpha_s$ and $\beta^s$ terms appear. It can be obtained by setting $\alpha_e, \alpha_{4\epsilon,i} \to 0$ in Eq. (6.10) and identifying $\mathbf{\Gamma}_{m0000} = \mathbf{\Gamma}_m$ etc.

Eq. (6.10) shows that the one-loop IR divergences are described by the one-loop coefficients of $\Gamma'$, which depend on the process-independent quantity $\gamma_{\text{cusp}}^{\text{RS}*}$, and of $\mathbf{\Gamma}$. Both anomalous dimensions depend on the partons involved in the process. At the two-loop level, the full $1/\epsilon^3$ and parts of the $1/\epsilon^2$ divergences are predicted by one-loop $\beta$ and $\Gamma$ coefficients. The remaining $1/\epsilon^2$ and the $1/\epsilon$ poles are described by genuine two-loop anomalous dimensions.

Eq. (6.2) together with Eq. (6.10) allows to describe the RS dependence of the squared amplitude $\mathcal{M}^{\text{RS}*}$:

- CDR-HV: since internal gluons are treated in the same way in CDR and HV we have $\mathbf{Z}^{\text{CDR}} = \mathbf{Z}^{\text{HV}}$ and all the anomalous dimensions are the same in these two schemes. The difference in the squared matrix element comes entirely from using different metric tensors for the polarization sum due to external gluons. In CDR, where external gluons are $D$-dimensional, this polarization sum involves $\hat{g}^{\mu\nu}$, whereas in HV $\bar{g}^{\mu\nu}$ is to be used.

- HV-FDH: since internal gluons are treated differently in HV and FDH we have $\mathbf{Z}^{\text{HV}} \neq \mathbf{Z}^{\text{FDH}}$ and the anomalous dimensions are not the same in these two schemes. This results in further scheme differences of the squared matrix element. However, external gluons are treated in the same way in HV and FDH and the metric tensors in polarization sums are the same in the two schemes.

### 6.2 IR structure in DRED

Understanding the IR structure of DRED processes with external gluons is more complicated. Each external quasi-4-dimensional gluon can be split into a $\hat{g}$ and a $\tilde{g}$, and the squared matrix element for a process with $\#g$ external gluons can be decomposed into $2^{\#g}$ terms. Following Ref. [16], we can write for the amplitude squared for such a process

$$\mathcal{M}^{\text{DRED}}(\dots g_1 \dots g_{\#g} \dots) = \sum_{\breve{g}_1 \in \{\hat{g},\tilde{g}\}} \dots \sum_{\breve{g}_{\#g} \in \{\hat{g},\tilde{g}\}} \mathcal{M}^{\text{DRED}}(\dots \breve{g}_1 \dots \breve{g}_{\#g} \dots)\,. \tag{6.12}$$

Reinstating all variables explicitly, we write the same relation in a more compact way as

$$\mathcal{M}^{\text{DRED}}(\epsilon, N_\epsilon, \{p\}, \mu) = \sum_{\{\breve{p}\}} \mathcal{M}^{\text{DRED}}(\epsilon, N_\epsilon, \{\breve{p}\}, \mu)\,. \tag{6.13}$$

Hence, the partons appearing in the list $\{\breve{p}\}$ on the r.h.s. can be either quarks or $\hat{g}$, $\tilde{g}$, but not full quasi-4-dimensional gluons. We stress that practical calculations are not as complicated as implied by Eqs. (6.12) and (6.13). The l.h.s. will typically be computed directly as a whole with quasi-4-dimensional gluons, i.e. 4-dimensional numerator algebra. Even the renormalized couplings $\alpha_s$, $\alpha_e$, $\alpha_{4\epsilon}$ can be identified, see

section 8 for further discussion. However, from a conceptual point of view each term in the sum on the r.h.s. of Eqs. (6.12) and (6.13) can be considered as an independent process and the couplings as independent. Then, each of these processes behaves as the processes in CDR, HV, FDH discussed in the previous subsection, and it becomes possible to understand the IR structure and construct IR subtraction terms and transition rules to other schemes.

For each process on the r.h.s. of Eqs. (6.12) and (6.13) a corresponding factor $\mathbf{Z}(\epsilon, N_\epsilon, \{\breve{p}\}, \mu)$ and a subtracted squared amplitude $\mathcal{M}^{\text{DRED}}_{\text{sub}}(\epsilon, N_\epsilon, \{\breve{p}\}, \mu)$ can be constructed, like for $\mathcal{M}^{\text{RS*}}$ in Eq. (6.1) and Eq. (6.2). Overall, one can then define the full subtracted squared amplitude in DRED as

$$\mathcal{M}^{\text{DRED}}_{\text{sub}}(\epsilon, N_\epsilon, \{p\}, \mu) = \sum_{\{\breve{p}\}} \mathcal{M}^{\text{DRED}}_{\text{sub}}(\epsilon, N_\epsilon, \{\breve{p}\}, \mu)\,. \tag{6.14}$$

It satisfies an equation analogous to Eq. (6.4),

$$\frac{d}{d\ln\mu}\mathcal{M}^{\text{DRED}}_{\text{sub}}(\epsilon, N_\epsilon, \{p\}, \mu) = \sum_{\{\breve{p}\}} \mathbf{\Gamma}^{\text{DRED}}(\{\breve{p}\}, \mu)\mathcal{M}^{\text{DRED}}_{\text{sub}}(\epsilon, N_\epsilon, \{\breve{p}\}, \mu)\,. \tag{6.15}$$

The $\mathbf{\Gamma}^{\text{DRED}}$'s for the individual parton sets $\{\breve{p}\}$ satisfy relations analogous to Eqs. (6.5), (6.6) and (6.7). Likewise, the subtraction factors $\mathbf{Z}$ can be written as

$$\begin{aligned}\ln \mathbf{Z}^{\text{DRED}} = &\left(\frac{\vec{\alpha}}{4\pi}\right)\cdot\left(\frac{\vec{\Gamma}'^{\,\text{DRED}}_1}{4\epsilon^2} + \frac{\vec{\mathbf{\Gamma}}^{\text{DRED}}_1}{2\epsilon}\right)\\ &+\sum_{\Sigma=2}\left(\frac{\alpha_s}{4\pi}\right)^m\left(\frac{\alpha_e}{4\pi}\right)^n\left(\frac{\alpha_{4\epsilon,1}}{4\pi}\right)^k\left(\frac{\alpha_{4\epsilon,2}}{4\pi}\right)^l\left(\frac{\alpha_{4\epsilon,3}}{4\pi}\right)^j\\ &\left(-\frac{3\vec{\beta}^{\text{DRED}}_{mnklj}\cdot\vec{\Gamma}'^{\,\text{DRED}}_1}{16\epsilon^3} - \frac{\vec{\beta}^{\text{DRED}}_{mnklj}\cdot\vec{\mathbf{\Gamma}}^{\text{DRED}}_1}{4\epsilon^2} + \frac{\Gamma'^{\,\text{DRED}}_{mnklj}}{16\epsilon^2} + \frac{\mathbf{\Gamma}^{\text{DRED}}_{mnklj}}{4\epsilon}\right) + \mathcal{O}(\alpha^3)\,.\end{aligned} \tag{6.16}$$

Like in the corresponding Eq. (6.10) the arguments are suppressed. An important difference to the RS* schemes is that in DRED the individual split processes $\{\breve{p}\}$ have to be used. This implies that the set of $\gamma$'s needed to describe the IR structure is different in DRED compared to the other schemes,

$$\text{DRED}: \quad \gamma^{\text{DRED}}_{\text{cusp}}, \gamma^{\text{DRED}}_q, \gamma^{\text{DRED}}_{\hat{g}}, \gamma^{\text{DRED}}_{\tilde{g}}\,. \tag{6.17}$$

This should be compared with Eq. (6.8). There are however several obvious relations, since internal gluons are treated equally in FDH and DRED:

$$\bar{\gamma}_{\text{cusp}} \equiv \gamma^{\text{FDH}}_{\text{cusp}} = \gamma^{\text{DRED}}_{\text{cusp}}, \tag{6.18a}$$
$$\bar{\gamma}_q \equiv \gamma^{\text{FDH}}_q = \gamma^{\text{DRED}}_q, \tag{6.18b}$$
$$\bar{\gamma}_g \equiv \gamma^{\text{FDH}}_g = \gamma^{\text{DRED}}_{\hat{g}}\,. \tag{6.18c}$$

Thus, the $\epsilon$-scalar anomalous dimension $\gamma_{\tilde{g}}^{\text{DRED}}$ is the only additional ingredient in DRED. To highlight this, we introduce the notation $\bar{\gamma}_\epsilon$ for this quantity,

$$\bar{\gamma}_\epsilon \equiv \gamma_{\tilde{g}}^{\text{DRED}} \,. \tag{6.19}$$

It is instructive to compare the individual processes with external $\hat{g}$ or $\tilde{g}$ in DRED to a process in FDH. The squared amplitude for a process with at least one external $\tilde{g}$ has an overall factor $N_\epsilon$ from the $\epsilon$-scalar polarization sum. As long as we consider the UV renormalized, but not yet IR subtracted matrix element, we cannot set $(N)_\epsilon \to 0$ since there are still IR poles present. However, once these have been subtracted, the squared matrix element is free of poles in $\epsilon$ and still contains a factor $N_\epsilon$. Hence,

$$\mathcal{M}_{\text{fin}}^{\text{DRED}}(\ldots\tilde{g}\ldots) = \lim_{(N)_\epsilon\to 0} \mathcal{M}_{\text{sub}}^{\text{DRED}}(\ldots\tilde{g}\ldots) = 0 \tag{6.20}$$

and

$$\lim_{(N)_\epsilon\to 0} \mathcal{M}_{\text{sub}}^{\text{DRED}}(\ldots g_1\ldots g_{\#g}\ldots) = \lim_{(N)_\epsilon\to 0} \mathcal{M}_{\text{sub}}^{\text{DRED}}(\ldots \hat{g}_1\ldots \hat{g}_{\#g}\ldots) = \mathcal{M}_{\text{fin}}(\ldots g\ldots)\,, \tag{6.21}$$

i.e. once the amplitudes are properly subtracted and the limit $(N)_\epsilon \to 0$ is taken, processes with external $\tilde{g}$ do not contribute any longer and the finite squared amplitude is equal in all four regularization schemes.

# 7 SCET approach to scheme dependence

In Section 4 it has been shown that the regularization-scheme dependence of any massless QCD amplitude can be absorbed into a re-definition of the factor **Z**. Hence, it is important to study the scheme dependence of the anomalous dimension **Γ** governing the RG equation for the **Z**-factor. We work at NNLO, and at this order the anomalous dimension has a sum-over-dipoles structure. Thus, we need to compute the three relevant anomalous dimensions in Eq. (6.7), $\gamma_{\rm cusp}$, $\gamma_q$ and $\gamma_g$ in the several schemes considered in this work, particularly in FDH (in DRED, also $\gamma_\epsilon$ is needed). In principle $\gamma_q$ and $\gamma_g$ can be directly extracted from the IR divergences of the on-shell quark and gluon form factors computed in the three schemes. This approach [29, 30], which at first glance seems to be totally straightforward, turned out to hide highly non-trivial technical complications related to the UV renormalization procedure in schemes like FDH and DRED.

Here we show that the same $\gamma$'s can be also extracted by combining the anomalous dimensions of the quark and gluon jet functions together with the anomalous dimensions of the corresponding soft functions (for Drell-Yan or Higgs production) defined through SCET operators. The soft and the jet functions can be computed with a standard diagrammatic procedure, and they are free of the renormalization difficulties that appear in the form factor calculations. This is an easier and more direct way to perform such a calculation. We have carried out this calculation at NNLO. In addition, the computation has also been checked with the results obtained in [34] by using the more traditional method. This gives an independent check of the results presented in this work and shows that the scheme dependence of these anomalous dimensions is universal and does not depend on the particular process analyzed.

## 7.1 Outline of the method

In the following we present the procedure for the direct calculation of the relevant anomalous dimensions in the four schemes via a SCET approach, in a similar way as already shown in Section 3.3. The anomalous dimensions are obtained not from QCD scattering amplitudes but from soft and jet functions defined in SCET. Schematically, we get

$$\text{soft function} \quad \Rightarrow \quad \gamma^{\rm RS}_{\rm cusp}, \gamma^{\rm RS}_{W_{\{\rm DY,\,H\}}}\,, \tag{7.1a}$$

$$\text{jet function} \quad \Rightarrow \quad \gamma^{\rm RS}_{\rm cusp}, \gamma^{\rm RS}_{J_{\{q,g\}}}\,, \tag{7.1b}$$

where $\gamma^{\rm RS}_{W_{\{\rm DY,\,H\}}}$ governs the single-logarithmic evolution of the soft function for the case with an initial quark and an anti-quark (Drell-Yan) or two initial gluons (Higgs production), respectively. $\gamma^{\rm RS}_{J_{\{q,g\}}}$ is defined similarly via the jet function. In DRED, one has to distinguish the jet functions for $D$-dimensional gluons $\hat{g}$ and $\epsilon$-scalars $\tilde{g}$

and the corresponding $\gamma^{\text{DRED}}_{J_{\hat{g}}}$ and $\gamma^{\text{DRED}}_{J_\epsilon}$. The present discussion applies to these two cases in an analogous way.

Thus, the cusp anomalous dimension $\gamma^{\text{RS}}_{\text{cusp}}$ and its scheme dependence can be easily extracted independently either from the soft or the jet functions. The situation is slightly more involved for the quark and the gluon anomalous dimensions where we need to exploit some known relations between anomalous dimensions to determine $\gamma^{\text{RS}}_q$ and $\gamma^{\text{RS}}_g$. In the case of Drell-Yan and Higgs production, these relations hold as a consequence of the factorization of the cross section in the threshold region [58]. In particular one finds

$$\gamma^{\text{RS}}_{W_{\{\text{DY, H}\}}} = 2\gamma^{\text{RS}}_{\phi_{\{q,g\}}} + 2\gamma^{\text{RS}}_{\{q,g\}}\,, \tag{7.2}$$

where $\gamma^{\text{RS}}_{\phi_{\{q,g\}}}$ is one half the coefficient of the $\delta(1-x)$ term in the Altarelli-Parisi splitting functions and controls the PDFs evolution. A similar relation involving the jet anomalous dimension instead of the soft anomalous dimension is found for DIS [59]

$$\gamma^{\text{RS}}_{\phi_{\{q,g\}}} = \gamma^{\text{RS}}_{J_{\{q,g\}}} - 2\gamma^{\text{RS}}_{\{q,g\}}\,. \tag{7.3}$$

By combining Eq. (7.2) with Eq. (7.3) to eliminate the universal PDF anomalous dimension one obtains [58]

$$\gamma^{\text{RS}}_{\{q,g\}} = \gamma^{\text{RS}}_{J_{\{q,g\}}} - \frac{\gamma^{\text{RS}}_{W_{\{\text{DY, H}\}}}}{2}\,. \tag{7.4}$$

The validity of Eq. (7.3) is a consequence of the factorization theorem for deep-inelastic scattering in the threshold region. The factorization proof is explicitly derived in [59] only for the quark current. Nevertheless by replacing the photon with a Higgs boson and after integrating out the heavy top loop, the factorization theorem for a gluon current follows in total analogy to the quark case. Indeed it can be explicitly checked that this relation holds both for the quark and gluon cases up to two-loop order by directly substituting the known expressions for the anomalous dimensions in CDR.

Before we turn to the evaluation of the various anomalous dimensions we introduce some notations. As explained in Section 6.2 the anomalous dimensions in FDH and DRED are equal, except for the appearance of the additional $\bar{\gamma}_\epsilon \equiv \gamma^{\text{DRED}}_{\tilde{g}}$, see Eqs. (6.18) and (6.19). Likewise, the anomalous dimensions in CDR and HV are equal. Thus, we will drop the label RS whenever possible and denote FDH/DRED quantities with a bar, schematically

$$\gamma \equiv \gamma^{\text{CDR}} = \gamma^{\text{HV}}, \qquad\qquad \bar{\gamma} \equiv \gamma^{\text{FDH}} = \gamma^{\text{DRED}}. \tag{7.5}$$

In principle all perturbative expansions are carried out in terms of the five couplings $\{\alpha\}$, as indicated in Eq. (5.1). However, for the results presented in this thesis it is not

necessary to distinguish the various $\alpha_{4\epsilon,i}$. Therefore, a coefficient in the perturbative expansion of the quantity $X$ will have at most three labels, $X_{mnk}$, indicating the power of $\alpha_s$, $\alpha_e$ and $\alpha_{4\epsilon}$, respectively. Very often, the quantities do not depend on $\alpha_{4\epsilon}$, i.e. the last of the three indices is zero. In this case we often drop this label altogether and write the perturbative expansion with two labels only by setting $X_{mn} = X_{mn0}$.[9]

We mention two special cases. First, the $\beta$ functions are defined with a negative sign,

$$\beta^{s\,\mathrm{RS}} = -\sum_{mn} \left(\frac{\alpha_s}{4\pi}\right)^m \left(\frac{\alpha_e}{4\pi}\right)^n \beta^{s\,\mathrm{RS}}_{mn}\,, \tag{7.6}$$

so the one-loop renormalization factors of $\alpha_s$ and $\alpha_e$ in the various schemes are given by

$$Z^{\mathrm{RS}}_{\alpha_s} = 1 - \beta^{s\,\mathrm{RS}}_{20}\frac{\alpha_s}{4\pi\epsilon} + \mathcal{O}(\alpha^2) \tag{7.7a}$$

$$Z^{\mathrm{RS}}_{\alpha_e} = 1 - \beta^{e\,\mathrm{RS}}_{11}\frac{\alpha_s}{4\pi\epsilon} - \beta^{e\,\mathrm{RS}}_{02}\frac{\alpha_e}{4\pi\epsilon} + \mathcal{O}(\alpha^2) \tag{7.7b}$$

where the explicit form of the coefficients of the $\beta$ functions are listed in Appendix B. Second, we also introduce an abbreviation for the cusp anomalous dimension multiplied with a colour factor,

$$\Gamma^{\mathrm{RS}}_{\mathrm{cusp}} \equiv C_R\,\gamma^{\mathrm{RS}}_{\mathrm{cusp}} = \sum_{mn} \left(\frac{\alpha_s}{4\pi}\right)^m \left(\frac{\alpha_e}{4\pi}\right)^n \Gamma^{\mathrm{RS}}_{mn}\,, \tag{7.8}$$

where the colour factor $C_R$ is either $C_F$ or $C_A$, depending on the quantity under consideration. For brevity we omit the superscript cusp in the expansion coefficients $\Gamma^{\mathrm{RS}}_{mn}$ of $\Gamma^{\mathrm{RS}}_{\mathrm{cusp}}$.

### 7.2 Computation and scheme dependence of the soft functions and $\gamma_W$

In this subsection we describe the calculation of the two-loop soft functions for Drell-Yan and Higgs production in momentum space and the extraction of the soft anomalous dimensions $\gamma_{W_{\mathrm{DY}}}$ and $\gamma_{W_{\mathrm{H}}}$ in the different regularization schemes considered in this work. In the partonic threshold region, where the emitted gluons in the final state are soft, the Drell-Yan and Higgs production hard-scattering kernels factorize into the product of soft functions and hard functions. The factorization proof can be found in [9, 58]. The soft functions describe the real emission of soft gluons and contain singular distributions of the gluon energy while the hard functions depend on the virtual corrections and are regular functions of their variables. The soft matrix elements $\hat{W}_{\{\mathrm{DY,H}\}}(x)$ arise in the cross section after the decoupling transformation which separates the soft and collinear sectors in the leading power SCET Lagrangian.

[9] In the CDR and HV schemes, all quantities of course only depend on $\alpha_s$. However, our notation will be adapted for the cases of FDH and DRED, unless noted otherwise.

The building blocks for the soft functions are the soft Wilson lines

$$\mathbf{S}_i(x) = \mathcal{P}\exp\left(ig_s\int_{-\infty}^{0} ds\, n_i\cdot A_s^a(x+sn_i)\mathbf{T}_i^a\right), \tag{7.9}$$

where $A_s^a(x)$ is a soft gluon field in SCET and $n_i = \{n, \bar{n}\}$ ($n_\mu = (1,0,0,1)$, $\bar{n}_\mu = (1,0,0,-1)$ are light-like reference vectors in the direction of the two incoming partons). The path-ordering acts on the colour generators $\mathbf{T}_i^a$ in the representation appropriate for the $i$th field. For the conjugate quark fields one finds $\mathbf{T}_i^a = -(t^a)^T$ which turns into anti-path-ordering. The soft matrix elements $\hat{W}_{\{\text{DY,H}\}}(x)$ are defined in terms of a soft operator

$$\mathbf{O}_s(x) = \left[\mathbf{S}_{\bar{n}}\mathbf{S}_n\right](x), \tag{7.10}$$

as an expectation value of products of soft Wilson lines forming a closed Wilson loop

$$\hat{W}_{\{\text{DY,H}\}}(x) = \frac{1}{d_R}\text{tr}\langle 0|\bar{T}\big(\mathbf{O}_s^\dagger(x)\big)T\big(\mathbf{O}_s(0)\big)|0\rangle, \tag{7.11}$$

where $d_R = N_c$ for Drell-Yan and $d_R = N_c^2 - 1$ for Higgs production, $T$ and $\bar{T}$ are the time-ordering and anti-time-ordering operators, respectively.

Since the collinear and soft sectors no longer interact, it is worth noting that $\hat{W}_{\{\text{DY,H}\}}(x)$ in Eq. (7.11) still contains the information about the colour and the direction of the initial quarks/gluons, but it is insensitive to the spin of the external particles due to the eikonal approximation. The soft function is defined as the Fourier transform of the soft matrix element $\hat{W}_{\{\text{DY,H}\}}(x)$ in Eq. (7.11):

$$S_{\{\text{DY,H}\}}(\omega) = \int\frac{dx^0}{4\pi}\, e^{ix^0\omega/2}\,\hat{W}_{\{\text{DY,H}\}}(x^0, \vec{x}=0). \tag{7.12}$$

The Drell-Yan and Higgs production soft functions are closely related to each other; up to NNNLO they differ by Casimir scaling replacements [60]. At NNLO the situation is even simpler and the following replacement holds [61]:

$$S_{\text{H}}(\omega) = S_{\text{DY}}(\omega)\big|_{C_F\to C_A} + \mathcal{O}(\alpha_s^3). \tag{7.13}$$

Thus, we directly compute the soft function for Drell-Yan and obtain the Higgs soft function by using Eq. (7.13). In the DRED scheme the soft function for external $\epsilon$-scalars is also needed. Since soft gluon interactions are insensitive to the spinorial structure of the external particles, it turns out that the soft function for external $\epsilon$-scalars is the same as the one for external gluons. Therefore we will not discuss it further.

In momentum space it is more convenient to rewrite the soft function in Eq. (7.12) as a squared amplitude by inserting a complete set of states

$$S(\omega) = \frac{1}{d_R}\sum_{X_s}\text{tr}\langle 0|\bar{T}\big(\mathbf{O}_s^\dagger(0)\big)|X_s\rangle\langle X_s|T\big(\mathbf{O}_s(0)\big)|0\rangle\delta(\omega - 2E_{X_s}), \tag{7.14}$$

where $X_s$ refers to a final state made of unobserved soft gluons carrying energy $E_{X_s}$. For simplicity in Eq. (7.14) we drop the subscripts $\{\mathrm{DY}, \mathrm{H}\}$. To perform this calculation, we need not only the usual QCD Feynman rules but also the momentum-space Feynman rules for gluons emitted from Wilson lines up to $\mathcal{O}(\alpha_s^2)$. In order to derive such Feynman rules, we can expand the soft Wilson line. If we consider for instance an incoming quark (or an outgoing anti-quark), one has to expand

$$S_n(x) = \mathbf{P} \exp\left[ i g_s \int_{-\infty}^{0} ds\, n \cdot A_s^a(x + sn)\, t^a \right] \tag{7.15}$$

in the coupling constant. It turns out that at order $g_s$, there is only one gluon emission from the collinear direction $n$, and by performing the Fourier representation of the gluon field one get the eikonal vertex approximation

$$\begin{aligned} S_n(x) &= 1 + i g_s \int_{-\infty}^{0} ds\, n \cdot A_s^a(x + sn) t^a \, + \mathcal{O}(g_s^2) \\ &= 1 + i g_s \int_{-\infty}^{0} ds \int \frac{d^4k}{(2\pi)^4}\, e^{-ik\cdot(x+sn)} n \cdot \mathcal{A}_s^a(k)\, t^a \, + \mathcal{O}(g_s^2) \\ &= 1 + \int \frac{d^4k}{(2\pi)^4}\, e^{-ik\cdot x} \underbrace{\left( -g_s \frac{n^\mu}{n\cdot k}\, t^a \right)}_{\text{Eikonal Feynman rule}} \mathcal{A}_{s\,\mu}^a(k) \, + \mathcal{O}(g_s^2)\,, \end{aligned} \tag{7.16}$$

which is shown in the first line of Fig. 5. By moving at order $g_s^2$ (needed for the two-loop computation) in the expansion of the Wilson line one instead finds

$$\begin{aligned} &- \frac{g_s^2}{2} \left[ \int_{-\infty}^{0} dt \int_{t}^{0} ds\, n \cdot A(x + sn)\, n \cdot A(x + tn) \, + \, \big( s \leftrightarrow t \big) \right] \\ &= - \frac{g_s^2}{2} \left[ \int_{-\infty}^{0} dt \int_{t}^{0} ds \int_{k_1} \int_{k_2} e^{-ik_1\cdot(x+sn)} e^{-ik_2\cdot(x+tn)} n \cdot \mathcal{A}(k_1)\, n \cdot \mathcal{A}(k_2) \, + \begin{pmatrix} s \leftrightarrow t \\ k_1 \leftrightarrow k_2 \end{pmatrix} \right] \\ &= \frac{g_s^2}{2} \left[ \int_{k_1} \int_{k_2} e^{-i(k_1+k_2)\cdot x} \left( \frac{n^{\mu_1} n^{\mu_2}}{n\cdot k_2\, n\cdot(k_1+k_2)} \right) \mathcal{A}^{\mu_1}(k_1)\, \mathcal{A}^{\mu_2}(k_2) \, + \begin{pmatrix} k_1 \leftrightarrow k_2 \\ \mu_1 \leftrightarrow \mu_2 \end{pmatrix} \right], \end{aligned} \tag{7.17}$$

where $A \equiv A^a\, t^a$ and we used the notation

$$\int_k \equiv \int \frac{d^4k}{(2\pi)^4}\,. \tag{7.18}$$

The Feynman rules can finally be extracted from Eq. (7.17) by summing over the two possible permutations of the gluon momenta and indices. If we then replace the $t$ matrices by the colour space generators $\mathbf{T}$, one obtains the Feynman rule given in the second line of Fig. 5. In a similar way we can also obtain the Feynman rules for collinear Wilson lines needed for the jet function.

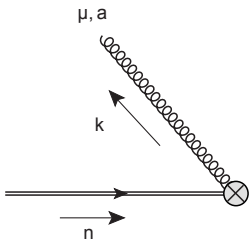


$$\rightarrow \quad g_s \frac{n^\mu}{n\cdot k}\,\mathbf{T}^a$$

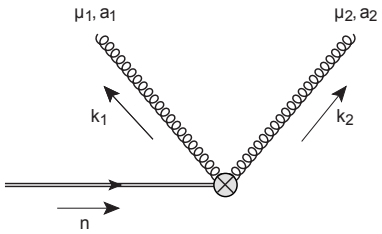


$$\rightarrow \quad g_s^2\, n^{\mu_1} n^{\mu_2} \left[ \frac{\mathbf{T}^{a_1}\mathbf{T}^{a_2}}{n\cdot k_2\, n\cdot(k_1+k_2)} + \frac{\mathbf{T}^{a_2}\mathbf{T}^{a_1}}{n\cdot k_1\, n\cdot(k_1+k_2)} \right]$$

**Figure 5**. Feynman rules for the emission of one and two gluons from a Wilson line. Figure taken from [9].

The $\mathcal{O}(\alpha_s^2)$ [62] Drell-Yan soft functions in the CDR scheme have been originally calculated in position space directly from the definition in Eq. (7.11). An exclusive soft function for Drell-Yan at $\mathcal{O}(\alpha_s^2)$ has been computed in [63]. The state of the art $\mathcal{O}(\alpha_s^3)$ soft functions for Higgs and Drell-Yan production have been computed very recently in a series of papers [60, 64, 65]. We also mention that related soft functions for thrust distribution and N-jettiness have been computed at $\mathcal{O}(\alpha_s^2)$ in [66, 67] and [68] respectively.

In order to study the higher-order corrections of the soft functions in the regularization schemes different from CDR, we define expansion coefficients of the perturbative series as

$$S^{\rm RS}_{\rm bare}(\omega) = \delta(\omega) + a_s(\omega)\, S^{\rm RS}_{10}(\omega) + a_s^2(\omega)\, S^{\rm RS}_{20}(\omega) + \dots\,, \tag{7.19}$$

where we have introduced the superscript RS to indicate the scheme dependence. In the above equation we have introduced

$$a_s(\omega) \equiv e^{-\epsilon\gamma_E}(4\pi)^\epsilon \left(\frac{1}{\omega^2}\right)^\epsilon \frac{\alpha_s^{\rm bare}}{4\pi} = \left(\frac{\mu^2}{\omega^2}\right)^\epsilon \frac{Z^{\rm RS}_{\alpha_s}\alpha_s}{(4\pi)} \tag{7.20}$$

and expressed the bare coupling $\alpha_s^{\rm bare}$ in terms of the renormalized coupling $\alpha_s \equiv \alpha_s(\mu)$ in the $\overline{\rm MS}$ scheme. Note that $a_s(\omega)$ and $\alpha_s^{\rm bare}$ are actually scheme independent,

but if expressed in terms of the $\overline{\text{MS}}$ coupling $\alpha_s(\mu)$ depend on the scheme-dependent renormalization factor $Z_{\alpha_s}^{\text{RS}}$. The all-order bare soft function in Eq. (7.19) is independent of the renormalization scale $\mu$. Up to NNLO the soft function depends only on $\alpha_s$ and not on $\alpha_e$ or $\alpha_{4\epsilon}$.

At NLO only two diagrams contribute to the soft functions; they describe the real emission of one soft gluon from the Wilson lines. At NLO the bare soft function turns out to be scheme independent,

$$\bar{S}_{10}(\omega) = \frac{8}{\omega} C_R \frac{e^{\epsilon\gamma_E}\Gamma(-\epsilon)}{\Gamma(1-2\epsilon)} \,. \tag{7.21}$$

As a result, the soft anomalous dimensions must be scheme independent, too. This reproduces the well-known fact that $\gamma_{\text{cusp}}$ is scheme independent at NLO, and it implies $\gamma_{10}^{W\,\text{RS}} = 0$ in all RS. The reason is that for the FDH and DRED schemes there are no additional diagrams involving $\epsilon$-scalars compared to CDR and HV. This is a consequence of the fact that dot products of a $\epsilon$-scalar field $\tilde{A}$ with the vectors $n$, $\bar{n}$ are vanishing, i.e. $n \cdot \tilde{A} = \bar{n} \cdot \tilde{A} = 0$. It follows that soft $\epsilon$-scalars cannot be emitted from the Wilson lines. This explains in a direct way the result [16] that the scheme dependence of general NLO amplitudes is contained in the parton anomalous dimensions.

At NNLO the situation is more involved; diagrams with two real soft emissions and virtual diagrams with one real soft emission are present. The soft functions and soft anomalous dimensions at NNLO have a scheme dependence, which originates from the $\epsilon$-scalar cut bubble contributing to the second diagram in Figure 6. The grey blob represents the quark, gluon, ghosts and $\epsilon$-scalar contributions. The latter is present only in FDH and DRED. After calculating the non-vanishing integrals using the techniques described in [69, 70] and summing all the contributions we obtain the NNLO coefficient in Eq. (7.19) in FDH/DRED,

$$\bar{S}_{20}(\omega) = \frac{1}{\omega} C_R \left[ C_A \, \bar{S}_A + N_F T_R \, \bar{S}_f + C_R \, \bar{S}_R \right] \,, \tag{7.22}$$

with

$$\begin{aligned}
\bar{S}_A = {} & \frac{1}{\epsilon^2}\left(-\frac{44}{3} + \frac{2N_\epsilon}{3}\right) + \frac{1}{\epsilon}\left(\frac{16N_\epsilon}{9} + \frac{4\pi^2}{3} - \frac{268}{9}\right) - \frac{7\pi^2 N_\epsilon}{9} + \frac{104 N_\epsilon}{27} \\
& + 56\zeta_3 + \frac{154\pi^2}{9} - \frac{1616}{27} + \left( - \frac{124 N_\epsilon \zeta_3}{9} - \frac{56\pi^2 N_\epsilon}{27} \right. \\
& \left. + \frac{640 N_\epsilon}{81} + \frac{2728\zeta_3}{9} - \frac{4\pi^4}{9} + \frac{938\pi^2}{27} - \frac{9712}{81} \right)\epsilon + \mathcal{O}(\epsilon^2) \,,
\end{aligned} \tag{7.23a}$$

$$\bar{S}_f = \frac{16}{3\epsilon^2} + \frac{80}{9\epsilon} - \frac{56\pi^2}{9} + \frac{448}{27} + \left( -\frac{992\zeta_3}{9} + \frac{2624}{81} - \frac{280\pi^2}{27} \right)\epsilon + \mathcal{O}(\epsilon^2) \,, \tag{7.23b}$$

$$\bar{S}_R = -\frac{32}{\epsilon^3} + \frac{112\pi^2}{3\epsilon} + \frac{1984\zeta_3}{3} + \frac{4\pi^4\epsilon}{5} + \mathcal{O}(\epsilon^2) \,, \tag{7.23c}$$

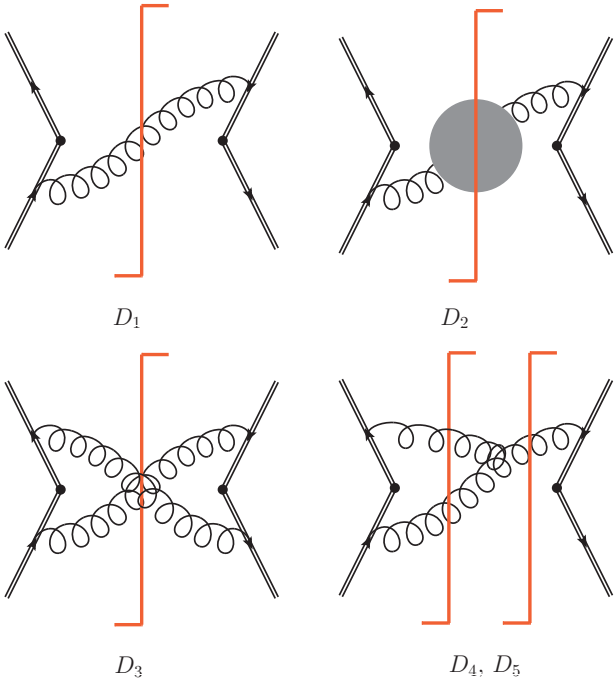


**Figure 6**. Selected non-zero Feynman diagrams contributing to the one-loop and two-loop soft functions. A complete list of diagrams can be found in [62]. Double lines indicate the direction of Wilson lines while the red vertical cut indicates on-shell partons. The scheme dependence originates from the diagram $D_2$. Diagrams $D_2$, $D_3$ and $D_4$ represent double real soft emissions while diagram $D_5$ represents a single virtual-real emission.

where $C_R = C_F$ for Drell-Yan and $C_R = C_A$ for Higgs production.

We now turn to the determination of the soft and cusp anomalous dimension from the soft function. In order to do this we need to discuss the singularities of the soft function that remain after coupling renormalization. From the point of view of ordinary QCD computations, these remaining singularities are closely related to IR singularities. However, from the SCET point of view they simply correspond to UV singularities and are to be removed by renormalization within the effective theory. For convenience this is done in Laplace space by introducing the Laplace transformed soft function as

$$s^{\rm RS}(\kappa) = \int_0^\infty d\omega \exp\left(-\frac{\omega}{\kappa\, e^{\gamma_E}}\right) S^{\rm RS}(\omega)\,, \tag{7.24}$$

where the integral transform can be easily carried out by using the relation

$$\int_0^\infty d\omega \exp\left(-b\omega\right) \omega^{-1-n\epsilon} = \Gamma(-n\epsilon) b^{n\epsilon}\,. \tag{7.25}$$

The remaining UV divergences of the soft function can be subtracted multiplicatively,

$$s^{\rm RS}_{\rm sub}(\kappa,\mu) = Z^{\rm RS}_s(\kappa,\mu)\, s^{\rm RS}_{\rm bare}(\kappa)\,. \tag{7.26}$$

Like in the case of general amplitudes in Eq. (6.4) and Eq. (6.5), the RGE

$$\frac{d}{d\ln\mu}\, s_{\rm sub}^{\rm RS}(\kappa,\mu) = \frac{d\, Z_s^{\rm RS}(\kappa,\mu)}{d\ln\mu}\big(Z_s^{\rm RS}(\kappa,\mu)\big)^{-1}\, s_{\rm sub}^{\rm RS}(\kappa,\mu) \tag{7.27}$$

holds, and the corresponding anomalous dimension has a structure similar to Eq. (6.7),

$$\frac{d}{d\ln\mu} s_{\rm sub}^{\rm RS}(\kappa,\mu) = \left[-4\,\Gamma_{\rm cusp}^{\rm RS}\, L_\kappa - 2\gamma_W^{\rm RS}\right] s_{\rm sub}^{\rm RS}(\kappa,\mu)\,, \tag{7.28}$$

which is derived from the RG invariance of the cross sections in the threshold region in analogy to the CDR case in Ref. [58]. In Eq. (7.28) we have defined $L_\kappa \equiv \ln(\kappa/\mu)$ and $C_R = C_F$ for Drell-Yan and $C_R = C_A$ for Higgs production. Comparison of the previous two equations yields an expression for the FDH renormalization factor $\bar{Z}_s(\kappa,\mu) \equiv Z_s^{\rm FDH}(\kappa,\mu)$ in terms of the soft and cusp anomalous dimensions. This expression has the same structure as Eq. (6.10), but can be written in a simpler form because up to NNLO the soft function does not depend on $\alpha_e$ and $\alpha_{4\epsilon}$:

$$\begin{aligned}\ln \bar{Z}_s = {}& \left(\frac{\alpha_s}{4\pi}\right)\left[-\frac{\bar{\Gamma}_{10}}{\epsilon^2} + \frac{1}{\epsilon}\left(2\bar{\Gamma}_{10}L_\kappa + \bar{\gamma}_{10}^W\right)\right] \\ & + \left(\frac{\alpha_s}{4\pi}\right)^2\left[\frac{3\bar{\beta}_{20}^s\bar{\Gamma}_{10}}{4\epsilon^3} - \frac{\bar{\beta}_{20}^s}{2\epsilon^2}\left(2\bar{\Gamma}_{10}L_\kappa + \bar{\gamma}_{10}^W\right) - \frac{\bar{\Gamma}_{20}}{4\epsilon^2} + \frac{1}{2\epsilon}\left(2\,\bar{\Gamma}_{20}L_\kappa + \bar{\gamma}_{20}^W\right)\right] \\ & + \mathcal{O}(\alpha_s^3)\,.\end{aligned} \tag{7.29}$$

By requiring that the renormalization factor $\bar{Z}_s$ in Eq. (7.29) minimally subtracts all of the divergences of the bare soft function (in FDH, treating $N_\epsilon$ as an independent multiplicity), we extract the expressions for the anomalous dimensions in the FDH scheme

$$\begin{aligned}\bar{\Gamma}_{\rm cusp} = {}& \left(\frac{\alpha_s}{4\pi}\right) C_R\,(4) \\ & + \left(\frac{\alpha_s}{4\pi}\right)^2 C_R\left[C_A\left(\frac{268}{9} - \frac{4}{3}\pi^2\right) - \frac{80}{9}T_R N_F - N_\epsilon\frac{16}{9}C_A\right] + \mathcal{O}(\alpha^3)\,, \qquad (7.30a) \\ \bar{\gamma}_W = {}& \left(\frac{\alpha_s}{4\pi}\right)^2 C_R\left[C_A\left(-\frac{808}{27} + \frac{11}{9}\pi^2 + 28\zeta_3 + N_\epsilon\frac{52}{27} - N_\epsilon\frac{\pi^2}{18}\right) + T_R N_F\left(\frac{224}{27} - \frac{4}{9}\pi^2\right)\right] \\ & + \mathcal{O}(\alpha^3)\,. \qquad (7.30b)\end{aligned}$$

The fact that $\bar{\Gamma}_{\rm cusp} = C_R\bar{\gamma}_{\rm cusp}$, with the known expression of the cusp anomalous dimension in the FDH scheme, $\bar{\gamma}_{\rm cusp}$, is a consistency check of the method. $\bar{\gamma}_W$ is a new result. The corresponding expressions in CDR/HV can be obtained by simply using the appropriate $\beta$ functions and anomalous dimensions in Eq. (7.29) and by setting $N_\epsilon = 0$ in Eq. (7.30). They are consistent with the literature [58].

Finally we remark that in analogy to Eq. (6.3) we can obtain a finite and scheme independent soft function $s_{\rm fin}$ through

$$s_{\rm fin}(\kappa,\mu) = \lim_{(N)_\epsilon\to 0} s_{\rm sub}^{\rm RS}(\kappa,\mu)\,. \tag{7.31}$$

The explicit expression for $s_{\rm fin}$ is given in Eq. (A.2) of Appendix A.

### 7.3 Computation and scheme dependence of the quark jet function and $\gamma_{Jq}$

The quark jet function has been calculated at NNLO in CDR [31]. Referring to [31] for more details, we describe here the corresponding calculation in FDH (which is identical to the one in DRED, but for simplicity we will only refer to FDH in the present subsection). The jet function is given in terms of the hard-collinear quark propagator

$$\begin{aligned}\frac{\bar{n}\!\!\!/}{2}\,\bar{n}\cdot p\,\mathcal{J}_q^{\rm RS}(p^2) &= \int d^4x\, e^{ipx}\langle 0|T\{\chi_{hc}(x)\bar{\chi}_{hc}(0)\}|0\rangle \\ &= \int d^4x\, e^{ipx}\langle 0|T\{\frac{\bar{n}\!\!\!/\,n\!\!\!/}{4}W^\dagger(x)\psi(x)\bar{\psi}(0)W(0)\frac{n\!\!\!/\,\bar{n}\!\!\!/}{4}\}|0\rangle\,, \end{aligned} \tag{7.32}$$

with Wilson lines

$$W(x) = \mathcal{P}\,\exp\left(ig_s\int_{-\infty}^{0} ds\,\bar{n}\,\cdot\,A(x+s\bar{n})\right), \tag{7.33}$$

where $A^\mu = A_a^\mu\, t^a$. The field $\chi_{hc}(x)$ is the gauge-invariant (under both soft and hard-collinear gauge transformations) effective-theory field for a massless quark after a decoupling transformation has been applied, which removes the interactions of soft gluons with hard-collinear fields in the leading-power SCET Lagrangian. As shown in Eq. (7.32), we can rewrite the propagator in terms of standard QCD fields.

The hard-collinear quark propagator $\mathcal{J}_q^{\rm RS}$ as defined in Eq. (7.32) is scheme dependent. The fields $\chi_{hc}$ and $\psi$ on the r.h.s. of Eq. (7.32) are Heisenberg fields, so applying the usual perturbative expansion results in loop diagrams contributing to the propagator. The scheme dependence is related to UV singularities of such diagrams. Examples of two-loop diagrams are shown in Figure 7. In FDH the computation is similar to the CDR scheme. However there are additional diagrams, which include the $\epsilon$-scalars and also depend on the coupling $\alpha_e$. An example of a two-loop diagram needed for the jet function in FDH (and not present in the CDR scheme) is shown in Figure 7 $(b)$. Since $\bar{n}$ is a $D$-dimensional vector, there are no $\epsilon$-scalars originating from the Wilson lines. Indeed, the scalar product in Eq. (7.33) will vanish in the case of the $\epsilon$-scalar.

The jet function $J_q^{\rm RS}(p^2)$ is the discontinuity of the propagator, i.e.

$$J_q^{\rm RS}(p^2) = \frac{1}{\pi}{\rm Im}\Big[i\,\mathcal{J}_q^{\rm RS}(p^2)\Big]\,, \tag{7.34}$$

which is directly given by using

$$\frac{1}{\pi}{\rm Im}\Big[(-p^2-i0)^a\Big] = -\theta(p^2)\frac{\sin(\pi a)}{\pi}(p^2)^a. \tag{7.35}$$

To highlight the similarities with the discussion in Section 6 and the soft function it is convenient to work in Laplace space, so we define $j_q^{\rm RS}(Q^2)$, the Laplace transform

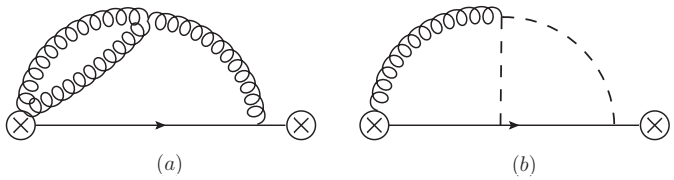


**Figure 7**. Examples of two-loop diagrams contributing to the quark jet function. Gluons emitted from the crossed circles originate from the Wilson lines. Diagram (a) contributes in CDR and FDH, whereas diagram (b) with two $\epsilon$-scalars contributes only in FDH.

of the jet function as

$$j_q^{\rm RS}(Q^2) \equiv \int_0^\infty dp^2 \, \exp\left(-\frac{p^2}{Q^2 e^{\gamma_E}}\right) J_q^{\rm RS}(p^2)\,. \tag{7.36}$$

The analogous equation in the case of the soft function is Eq. (7.24).

To compute the propagator in the FDH scheme, $\bar{\mathcal{J}}_q(p^2)$, the diagrams have been generated with QGRAF [71] and the colour algebra has been done with Color-Math [72]. For the reduction of the integrals, Reduze 2 [73] has been used. The master integrals needed for the FDH jet function are the same as for the CDR scheme. After taking the imaginary part and performing the Laplace transform, the bare quark jet function at NNLO in FDH is obtained as

$$\begin{aligned}
\bar{j}_{q\,\rm bare}(Q^2) = 1 &+ a_s(Q^2)\, C_F \left(\frac{4}{\epsilon^2} + \frac{3}{\epsilon} + 7 - \frac{2\,\pi^2}{3} + \epsilon\Big(14 - \frac{\pi^2}{2} - 8\zeta_3\Big)\right) \\
&+ a_e(Q^2)\, C_F\, N_\epsilon \left(-\frac{1}{2\,\epsilon} - 1 + \epsilon\Big(-2 + \frac{\pi^2}{12}\Big)\right) \\
&+ a_s^2(Q^2) \left(C_F^2\, \bar{j}_{20}^{q;F} + C_F C_A\, \bar{j}_{20}^{q;A} + C_F T_R N_F\, \bar{j}_{20}^{q;f}\right) \\
&+ a_e^2(Q^2) \left(C_F^2\, \bar{j}_{02}^{q;F} + C_F C_A\, \bar{j}_{02}^{q;A} + C_F T_R N_F\, \bar{j}_{02}^{q;f}\right) \\
&+ a_s(Q^2) a_e(Q^2) \left(C_F^2\, \bar{j}_{11}^{q;F} + C_F C_A\, \bar{j}_{11}^{q;A}\right) + \mathcal{O}(a^3)\,.
\end{aligned} \tag{7.37}$$

In analogy to Eq. (7.20) we have defined

$$a_s(Q^2) \equiv e^{-\epsilon\gamma_E}(4\pi)^\epsilon \left(\frac{1}{Q^2}\right)^\epsilon \frac{\alpha_s^{\rm bare}}{4\pi} = \left(\frac{\mu^2}{Q^2}\right)^\epsilon \frac{\bar{Z}_{\alpha_s}\alpha_s}{(4\pi)}\,, \tag{7.38}$$

with an analogous equation for $a_e$. The explicit expressions for the two-loop coefficients are given in Appendix A. Note that $\bar{j}_{q\,\rm bare}(Q^2)$ is independent of $\mu$.

The renormalization procedure in any regularization scheme can easily be generalized from the corresponding procedure in CDR [31]. A renormalization factor $Z_{J_q}^{\rm RS}(Q^2,\mu)$ absorbing the UV divergences of the bare jet function is introduced such that

$$j_{q\,\rm sub}^{\rm RS}(Q^2,\mu) = Z_{J_q}^{\rm RS}(Q^2,\mu)\, j_{q\,\rm bare}^{\rm RS}(Q^2) \tag{7.39}$$

is finite. This equation is analogous to Eqs. (6.2) and (7.26). Requiring minimal subtraction with $N_\epsilon$ as an independent multiplicity determines the explicit form of $Z_{J_q}^{\rm RS}(Q^2,\mu)$ uniquely in terms of the bare quark jet function $\bar{\jmath}_{q\,\rm bare}(Q^2)$. In principle, $Z_{J_q}^{\rm RS}$ depends on all couplings $\{\alpha\}$. However, in FDH, up to NNLO there is no dependence on $\alpha_{4\epsilon}$.

To relate $Z_{J_q}^{\rm RS}(Q^2,\mu)$ to the cusp anomalous dimension $\gamma_{\rm cusp}^{\rm RS}$ and the quark jet anomalous dimension $\gamma_{J_q}^{\rm RS}$, we follow the same procedure as for the soft anomalous dimension. We compare the RGE of the quark jet function in the form

$$\frac{d}{d\ln\mu}\,\jmath_{q\,\rm sub}^{\rm RS}(Q^2,\mu) = \frac{d\,Z_{J_q}^{\rm RS}(Q^2,\mu)}{d\ln\mu}\,\Big(Z_{J_q}^{\rm RS}(Q^2,\mu)\Big)^{-1}\,\jmath_{q\,\rm sub}^{\rm RS}(Q^2,\mu) \tag{7.40}$$

to the RGE written in terms of $\Gamma_{\rm cusp}^{\rm RS}$ and $\gamma_{J_q}^{\rm RS}$,

$$\frac{d}{d\ln\mu}\jmath_{q\,\rm sub}^{\rm RS}(Q^2,\mu) = \Big[-2\Gamma_{\rm cusp}^{\rm RS}\,L_Q - 2\gamma_{J_q}^{\rm RS}\Big]\,\jmath_{q\,\rm sub}^{\rm RS}(Q^2,\mu)\,. \tag{7.41}$$

This relation is analogous to Eqs. (6.4) and (7.28); we have used $L_Q \equiv \ln(Q^2/\mu^2)$ and $\Gamma_{\rm cusp}^{\rm RS} = C_F\gamma_{\rm cusp}^{\rm RS}$. With the help of Eqs. (7.40) and (7.41) we can express $\bar{Z}_{J_q}$ in terms of the FDH anomalous dimensions. Up to NNLO, the expression for $\ln\bar{Z}_{J_q}$ has the same structure as Eqs. (6.10) and (7.29). We write it explicitly, using that up to NNLO only the two couplings $\alpha_s$ and $\alpha_e$ appear:

$$\begin{aligned}
\ln\bar{Z}_{J_q} = {}& \frac{\alpha_s}{4\pi}\Big[-\frac{\bar\Gamma_{10}}{\epsilon^2}+\frac{1}{\epsilon}\Big(\bar\Gamma_{10}\,L_Q+\bar\gamma_{10}^{J_q}\Big)\Big]+\frac{\alpha_e}{4\pi}\Big[-\frac{\bar\Gamma_{01}}{\epsilon^2}+\frac{1}{\epsilon}\Big(\bar\Gamma_{01}\,L_Q+\bar\gamma_{01}^{J_q}\Big)\Big]\\
&+\Big(\frac{\alpha_s}{4\pi}\Big)^2\Big[\frac{3\,\big(\bar\beta_{20}^s\bar\Gamma_{10}+\bar\beta_{20}^e\bar\Gamma_{01}\big)}{4\epsilon^3}-\frac{\bar\beta_{20}^s}{2\,\epsilon^2}\Big(\bar\Gamma_{10}\,L_Q+\bar\gamma_{10}^{J_q}\Big)-\frac{\bar\beta_{20}^e}{2\,\epsilon^2}\Big(\bar\Gamma_{01}\,L_Q+\bar\gamma_{01}^{J_q}\Big)\\
&\qquad-\frac{\bar\Gamma_{20}}{4\,\epsilon^2}+\frac{1}{2\,\epsilon}\Big(\bar\Gamma_{20}\,L_Q+\bar\gamma_{20}^{J_q}\Big)\Big]\\
&+\Big(\frac{\alpha_e}{4\pi}\Big)^2\Big[\frac{3\,\big(\bar\beta_{02}^s\bar\Gamma_{10}+\bar\beta_{02}^e\bar\Gamma_{01}\big)}{4\epsilon^3}-\frac{\bar\beta_{02}^s}{2\,\epsilon^2}\Big(\bar\Gamma_{10}\,L_Q+\bar\gamma_{10}^{J_q}\Big)-\frac{\bar\beta_{02}^e}{2\,\epsilon^2}\Big(\bar\Gamma_{01}\,L_Q+\bar\gamma_{01}^{J_q}\Big)\\
&\qquad-\frac{\bar\Gamma_{02}}{4\,\epsilon^2}+\frac{1}{2\,\epsilon}\Big(\bar\Gamma_{02}\,L_Q+\bar\gamma_{02}^{J_q}\Big)\Big]\\
&+\Big(\frac{\alpha_s}{4\pi}\Big)\Big(\frac{\alpha_e}{4\pi}\Big)\Big[\frac{3\,\big(\bar\beta_{11}^s\bar\Gamma_{10}+\bar\beta_{11}^e\bar\Gamma_{01}\big)}{4\epsilon^3}-\frac{\bar\beta_{11}^s}{2\,\epsilon^2}\Big(\bar\Gamma_{10}\,L_Q+\bar\gamma_{10}^{J_q}\Big)-\frac{\bar\beta_{11}^e}{2\,\epsilon^2}\Big(\bar\Gamma_{01}\,L_Q+\gamma_{01}^{J_q}\Big)\\
&\qquad-\frac{\bar\Gamma_{11}}{4\,\epsilon^2}+\frac{1}{2\,\epsilon}\Big(\bar\Gamma_{11}\,L_Q+\bar\gamma_{11}^{J_q}\Big)\Big]+\mathcal{O}(\alpha^3)\,.
\end{aligned} \tag{7.42}$$

On the one hand this formula gives strong consistency checks. It allows for an independent extraction of the cusp anomalous dimension and the coefficients of the $\beta$ functions of $\alpha_s$ and $\alpha_e$ in the FDH scheme. These coefficients agree with the well-known results in the literature [29, 30].

On the other hand, comparing Eq. (7.42), in particular the $1/\epsilon$ pole, to the explicit result for the bare quark jet function allows to read off the anomalous dimension

$\bar{\gamma}_{J_q}$. We obtain the following explicit expression in the FDH scheme:

$$\begin{aligned}\bar{\gamma}_{J_q} &= \left(\frac{\alpha_s}{4\pi}\right)(-3\,C_F) + \left(\frac{\alpha_e}{4\pi}\right)\frac{N_\epsilon}{2}\,C_F \\ &+ \left(\frac{\alpha_s}{4\pi}\right)^2\Big[C_F^2\Big(-\frac{3}{2}+2\pi^2-24\zeta_3\Big) + C_F C_A\Big(-\frac{1769}{54}-\frac{11\pi^2}{9}+40\zeta_3\Big) \\ &\qquad + C_F T_R N_F\Big(\frac{242}{27}+\frac{4\pi^2}{9}\Big) + \frac{N_\epsilon}{2}\Big(\frac{271}{54}+\frac{\pi^2}{9}\Big)C_F C_A\Big] \\ &+ \left(\frac{\alpha_s}{4\pi}\right)\left(\frac{\alpha_e}{4\pi}\right)\Big[\frac{N_\epsilon}{2}\Big(11 C_F C_A - 4C_F^2 - \frac{2}{3}C_F^2\pi^2\Big)\Big] \\ &+ \left(\frac{\alpha_e}{4\pi}\right)^2\Big[-\frac{N_\epsilon^2}{8}C_F^2 - \frac{3\,N_\epsilon}{2}\,C_F T_R N_F\Big] + \mathcal{O}(\alpha^3)\,. \end{aligned} \tag{7.43}$$

Using this expression together with Eqs. (7.4) and (7.30b) the quark anomalous dimension in the FDH scheme, $\bar{\gamma}_q$ can be found. Thus the computation of the soft and quark jet functions provides an alternative determination of $\bar{\gamma}_q$. The result agrees with previous determinations [29, 30] and is listed in Appendix B for completeness. Of course, setting $N_\epsilon = 0$ only the pure $\alpha_s$ terms survive and the well known results in the CDR/HV scheme are recovered.

This is also true for the quark jet function as a whole. In analogy to Eq. (7.31) we can define

$$\jmath_{q\,\mathrm{fin}}(Q^2,\mu) = \lim_{(N)_\epsilon\to 0}\jmath^{\mathrm{RS}}_{q\,\mathrm{sub}}(Q^2,\mu)\,, \tag{7.44}$$

so the finite quark jet function is scheme independent and can be obtained using any of the regularization schemes. The explicit result is given in Appendix A.

### 7.4 Computation and scheme dependence of the gluon jet function and $\gamma_{Jg}$

The discussion of the previous subsection can be readily adapted to the gluon case. We closely follow Ref. [32], where the gluon jet function $J_g(p^2)$ has been calculated at NNLO in CDR. The starting point is the gauge-invariant field $\mathcal{A}^\mu$, related to the collinear gluon field $A_c^\mu(x)$ through

$$\mathcal{A}^\mu(x) = \mathcal{A}^{a\mu}(x)t_a = W^\dagger(x)[iD_c^\mu W(x)]\,. \tag{7.45}$$

The treatment of this vector field depends on the regularization scheme; we will give the details below. In all schemes the field $\mathcal{A}^\mu$ satisfies $\bar{n}\cdot\mathcal{A} = 0$; hence it can be decomposed as $\mathcal{A}^\mu = \mathcal{A}_\perp^\mu + (n\cdot\mathcal{A})\bar{n}^\mu/2$ and the leading term is $\mathcal{A}_\perp^\mu$. The gluon jet propagator $\mathcal{J}_g(p^2)$ is then defined as

$$\delta^{ab}g_s^2\,(-g_\perp^{\mu\nu})\,\mathcal{J}_g^{\mathrm{RS}}(p^2) = \int d^4x\,e^{ipx}\langle 0|T\{\mathcal{A}_\perp^{a\mu}(x)\mathcal{A}_\perp^{b\nu}(0)\}|0\rangle\,. \tag{7.46}$$

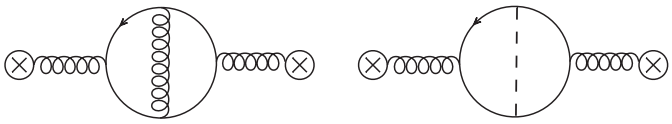


**Figure 8**. Sample two-loop diagrams contributing to the gluon jet function. Diagram (a) is present both in CDR and FDH, diagram (b) including an $\epsilon$-scalar contributes only in FDH.

For the calculation of $\mathcal{J}_g^{\text{RS}}(p^2)$ it is actually more convenient to use an equivalent definition in terms of the time-ordered product of the full fields $\mathcal{A}^\mu$,

$$\delta^{ab} g_s^2 \Big[ \Big( -g_{\mu\nu} + \frac{\bar{n}_\mu p_\nu + p_\mu \bar{n}_\nu}{\bar{n}\cdot p} \Big) \mathcal{J}_g^{\text{RS}}(p^2) + \frac{\bar{n}_\mu \bar{n}_\nu}{(\bar{n}\cdot p)^2} \mathcal{K}_g^{\text{RS}}(p^2) \Big] \tag{7.47}$$
$$= \int d^4x e^{ipx} \langle 0 | T\{ \mathcal{A}_\mu^a(x) \mathcal{A}_\nu^b(0) \} | 0 \rangle$$

and then extract $\mathcal{J}_g^{\text{RS}}(p^2)$ using a projection. The gluon jet function $J_g^{\text{RS}}(p^2)$ is the discontinuity of the leading part of the propagator, more precisely $J_g^{\text{RS}}(p^2) = \text{Im}[i\,\mathcal{J}_g^{\text{RS}}(p^2)]/\pi$. The function $K_g^{\text{RS}}$ is related to power-suppressed terms and will not be considered any further in this thesis.

As in the case of the quark jet function, after decoupling of the soft fields, the collinear Lagrangian is equivalent to the QCD Lagrangian. Exploiting the gauge invariance of $\mathcal{J}_g^{\text{RS}}$ we work in the light-cone gauge $\bar{n}\cdot A = 0$. This is particularly convenient as in this gauge $W(x) = 1$ and, therefore, no diagrams with additional emission of gluons from the Wilson lines have to be considered. Therefore, for the calculation of $\mathcal{J}_g^{\text{RS}}$ only standard QCD Feynman rules are required. Of course, ghost loops are also absent in this gauge.

Now we give details on the regularization scheme dependence. Typical examples of two-loop diagrams contributing to $\mathcal{J}_g^{\text{RS}}$ are shown in Figure 8. In CDR all gluons are $D$-dimensional gluons $\hat{g}$ and no $\epsilon$-scalar diagrams are present. Correspondingly, the metric tensor in Eq. (7.47) is $\hat{g}^{\mu\nu}$ in CDR. In HV and FDH the external gluons are understood to be strictly 4-dimensional. Thus, the gluons attached to the Wilson lines in Figure 8 are to be interpreted as $\bar{g}$, and the metric tensor in Eq. (7.47) is $\bar{g}^{\mu\nu}$ in these schemes. Furthermore, in FDH internal gluons are treated as $g$ and hence are decomposed into $\hat{g}$ and $\tilde{g}$, as indicated in the left and right panel of Figure 8. In DRED the definitions of the present subsection apply to external $D$-dimensional gluons $\hat{g}$. For these, the calculation and the result are the same as the corresponding FDH calculation, see Eq. (6.18). Hence for simplicity we will only refer to FDH in the remainder of the subsection.

After an explicit calculation of the diagrams in FDH, taking the imaginary part and performing the Laplace transform, we obtain for the bare gluon jet function in

FDH

$$\bar{\jmath}_{g\,\mathrm{bare}}(Q^2) = 1 + a_s\Big(C_A\Big[\frac{4}{\epsilon^2} + \frac{11}{3\epsilon} + \frac{67}{9} - \frac{2\pi^2}{3} + \epsilon\,\big(\frac{404}{27} - \frac{11\pi^2}{18} - 8\zeta_3\big)\Big] + N_F T_R\Big[-\frac{4}{3\epsilon} - \frac{20}{9} + \epsilon\,\big(\frac{2\pi^2}{9} - \frac{112}{27}\big)\Big] + \frac{N_\epsilon}{2}\,C_A\Big[-\frac{1}{3\epsilon} - \frac{8}{9} + \epsilon\big(\frac{\pi^2}{18} - \frac{52}{27}\big)\Big]\Big) + a_s^2\left(C_A^2\,\bar{\jmath}_{20}^{g;\,AA} + C_A N_F T_R\,\bar{\jmath}_{20}^{g;\,Af} + C_F N_F T_R\,\bar{\jmath}_{20}^{g;\,Ff} + N_F^2 T_R^2\,\bar{\jmath}_{20}^{g;\,ff}\right) + a_s a_e\left(C_A N_F T_R\,\bar{\jmath}_{11}^{g;\,Af} + C_F N_F T_R\,\bar{\jmath}_{11}^{g;\,Ff}\right) + \mathcal{O}(\alpha^3)\,. \tag{7.48}$$

The explicit results of the two-loop coefficients are given in Appendix A. In the limit $N_\epsilon \to 0$ all terms proportional to $\alpha_e$ vanish and we obtain the results in CDR, in agreement with Ref. [32].

The renormalization procedure is the same as for the quark jet function. In Laplace space, the renormalized gluon jet function in the FDH scheme is obtained by multiplying Eq. (7.48) by a factor $\bar{Z}_{J_g}$. This factor is the same as in Eq. (7.42) apart from the replacement $\bar{\gamma}_{ij}^{J_q} \to \bar{\gamma}_{ij}^{J_g}$ and $\Gamma_{\mathrm{cusp}}^{\mathrm{RS}} = C_A \gamma_{\mathrm{cusp}}^{\mathrm{RS}}$. After renormalization of the coupling, all divergences of the bare gluon jet function have to be absorbed by $\bar{Z}_{J_g}(Q^2,\mu)$. This allows to determine the anomalous dimension of the gluon jet in the FDH scheme as

$$\bar{\gamma}_{J_g} = \Big(\frac{\alpha_s}{4\pi}\Big)\left(-\frac{11}{3}C_A + \frac{4}{3}N_F T_R + \frac{N_\epsilon}{6}C_A\right) + \Big(\frac{\alpha_s}{4\pi}\Big)^2\Big[C_A^2\Big(-\frac{1096}{27} + \frac{11\pi^2}{9} + 16\zeta_3\Big) + C_A N_F T_R\Big(\frac{368}{27} - \frac{4\pi^2}{9}\Big) + 4C_F T_R N_F + \frac{N_\epsilon}{2}\Big(\frac{248}{27} - \frac{\pi^2}{9}\Big)C_A^2\Big] + \Big(\frac{\alpha_s}{4\pi}\Big)\Big(\frac{\alpha_e}{4\pi}\Big)\Big[-N_\epsilon\,(2\,C_F N_F T_R)\Big] + \mathcal{O}(\alpha^3)\,. \tag{7.49}$$

Of course, it is again also possible to extract the cusp anomalous dimension as well as the $\beta$ functions of $\alpha_s$ and $\alpha_e$ from $\bar{Z}_{J_g}(Q^2,\mu)$. The fact that we obtain again the same results for these quantities is a strong consistency check on the procedure.

From $\bar{\gamma}_{J_g}$ we can determine $\bar{\gamma}_g$ with the help of Eq. (7.4). The result is in agreement with previous determinations [29, 30] and is listed in Appendix B for completeness, but the present procedure provides a more direct alternative determination of $\bar{\gamma}_g$.

Finally, as for the soft and quark jet function, we can obtain a finite and scheme independent gluon jet function as

$$\jmath_{g\,\mathrm{fin}}(Q^2,\mu) = \lim_{(N)_\epsilon \to 0} \jmath_{g\,\mathrm{sub}}^{\mathrm{RS}}(Q^2,\mu)\,. \tag{7.50}$$

For completeness the explicit result is listed in Appendix A.

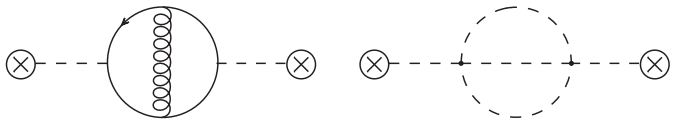


**Figure 9**. Sample two-loop diagrams contributing to the $\epsilon$-scalar jet function both. Diagram (a) is proportional to $\alpha_s\alpha_e$ whereas diagram (b) is $\sim \alpha_{4\epsilon}^2$

### 7.5 Computation of the $\epsilon$-scalar jet function, $\gamma_{J\epsilon}$ and result for $\bar{\gamma}_\epsilon$ in DRED

In DRED processes with external $\epsilon$-scalars need to be considered. The discussion of Section 7.1 applies analogously, and we can determine the anomalous dimension of $\epsilon$-scalars from an equation like Eq. (7.4),

$$\gamma_{\tilde{g}}^{\text{DRED}} \equiv \bar{\gamma}_\epsilon = \bar{\gamma}_{J_\epsilon} - \frac{\gamma_{W_\epsilon}^{\text{DRED}}}{2}\,. \tag{7.51}$$

As mentioned in Section 7.2 the soft function is the same as for external gluons, hence $\gamma_{W_\epsilon}^{\text{DRED}} = \bar{\gamma}_W$, from Eq. (7.30b). For $\bar{\gamma}_{J_\epsilon}$ an $\epsilon$-scalar jet function is needed. Such an object can be defined and computed in close analogy to the calculation of the gluon jet function, with the difference that now the time-ordered product of two fields $\tilde{\mathcal{A}}_\mu = \tilde{g}_{\mu\nu}\mathcal{A}^\nu$ has to be considered. In light-cone gauge these fields reduce to the $\epsilon$-scalar field $\tilde{A}_\mu$. Starting from the propagator $\bar{\mathcal{J}}_\epsilon(p^2) \equiv \mathcal{J}_\epsilon^{\text{DRED}}(p^2)$ given by

$$\delta^{ab} g_s^2\,(-\tilde{g}_{\mu\nu})\,\bar{\mathcal{J}}_\epsilon(p^2) = \int d^4x e^{ipx}\langle 0|T\{\tilde{\mathcal{A}}_\mu^a(x)\tilde{\mathcal{A}}_\nu^b(0)\}|0\rangle \tag{7.52}$$

the $\epsilon$-scalar jet function is obtained as $\bar{J}_\epsilon(p^2) = \text{Im}[i\,\bar{\mathcal{J}}_\epsilon(p^2)]/\pi$.

Two examples of diagrams contributing (in light-cone gauge) at two-loop order are shown in Figure 9. A new feature is the appearance of the quartic coupling $\alpha_{4\epsilon}$. We do not need to distinguish the three different $\alpha_{4\epsilon}$ since the quartic coupling only appears at the two-loop level and hence the associated renormalization constants and $\beta$ functions do not appear. The only non-vanishing diagram $\sim \alpha_{4\epsilon}^2$ is depicted in Figure 9 b.

Performing a computation analogous to previous cases, the bare two-loop $\epsilon$-scalar jet function in Laplace space is found to be

$$\begin{aligned}\bar{J}_{\epsilon\,\text{bare}}(Q^2) = 1 &+ a_s\,C_A\Big(\frac{4}{\epsilon^2} + \frac{4}{\epsilon} + 8 - \frac{2\pi^2}{3} + \epsilon\big(16 - \frac{2\pi^2}{3} - 8\zeta_3\big)\Big)\\ &+ a_e\,N_F T_R\Big(-\frac{2}{\epsilon} - 4 + \epsilon\big(-8 + \frac{\pi^2}{3}\big)\Big)\\ &+ a_s^2\left(C_A^2\,\bar{j}_{200}^{\epsilon;\,AA} + C_A N_F T_R\,\bar{j}_{200}^{\epsilon;\,Af}\right)\end{aligned}$$

$$
\begin{aligned}
&+ a_e^2\, N_F T_R \left( C_A\, \bar{j}_{020}^{\epsilon;\,Af} + C_F\, \bar{j}_{020}^{\epsilon;\,Ff} + N_F T_R\, \bar{j}_{020}^{\epsilon;\,ff} \right) \\
&+ a_{4\epsilon}^2\, C_A^2\, \bar{j}_{002}^{\epsilon;\,AA} \\
&+ a_s a_e\, N_F T_R \left( C_A\, \bar{j}_{110}^{\epsilon;\,Af} + C_F\, \bar{j}_{110}^{\epsilon;\,Ff} \right) + \mathcal{O}(a^3)\,. \qquad (7.53)
\end{aligned}
$$

Due to the presence of $\alpha_{4\epsilon}$, the various coefficients have now three labels, with the last one indicating the power of $\alpha_{4\epsilon}$. The explicit NNLO expressions are given in Appendix A.

Once more, the UV divergences of the bare jet function are absorbed by a renormalization factor $Z_\epsilon^{\text{DRED}}(Q^2,\mu)$, which has a structure similar to Eq. (6.10) or Eqs. (7.29) and (7.42). In fact, it can be written as Eq. (6.16),

$$
\begin{aligned}
\ln Z_\epsilon^{\text{DRED}} &= \left(\frac{\vec{\alpha}}{4\pi}\right) \cdot \left( \frac{\vec{\Gamma}_1'^{\,\text{DRED}}}{4\epsilon^2} + \frac{\vec{\mathbf{\Gamma}}_1^{\text{DRED}}}{2\epsilon} \right) \qquad (7.54) \\
&\quad + \sum_{\Sigma=2} \left(\frac{\alpha_s}{4\pi}\right)^m \left(\frac{\alpha_e}{4\pi}\right)^n \left(\frac{\alpha_{4\epsilon}}{4\pi}\right)^k \\
&\quad \left( - \frac{3\vec{\beta}_{mnk}^{\,\text{DRED}} \cdot \vec{\Gamma}_1'^{\,\text{DRED}}}{16\epsilon^3} - \frac{\vec{\beta}_{mnk}^{\,\text{DRED}} \cdot \vec{\mathbf{\Gamma}}_1^{\text{DRED}}}{4\epsilon^2} + \frac{\Gamma'^{\,\text{DRED}}_{mnk}}{16\epsilon^2} + \frac{\mathbf{\Gamma}^{\text{DRED}}_{mnk}}{4\epsilon} \right) + \mathcal{O}(\alpha^3)
\end{aligned}
$$

with the identification

$$
\Gamma'^{\,\text{DRED}} = -4\, C_A\, \bar{\gamma}_{\text{cusp}}, \qquad \mathbf{\Gamma}^{\text{DRED}} = 2\, C_A\, \bar{\gamma}_{\text{cusp}}\, L_Q + 2\, \bar{\gamma}_{J_\epsilon}\,. \qquad (7.55)
$$

We refrain from using the explicit form of Eq. (7.42) since the dependence on $\alpha_{4\epsilon}$ leads to a proliferation of similar terms. The only simplification used is the identification of the couplings $\alpha_{4\epsilon,i}$, which is possible since the explicit results show that these couplings appear not at one-loop but only in the genuine two-loop coefficients.

By comparing with the explicit result for the $\epsilon$-scalar jet function we determine the renormalization factor using minimal subtraction and extract from this the anomalous dimension of the $\epsilon$-scalar jet as

$$
\begin{aligned}
\bar{\gamma}_{J_\epsilon} &= \left(\frac{\alpha_s}{4\pi}\right) (-4\, C_A) + \left(\frac{\alpha_e}{4\pi}\right) (2 N_F T_R) \\
&\quad + \left(\frac{\alpha_s}{4\pi}\right)^2 \left[ C_A^2 \Big( -\frac{4603}{108} + \frac{13\pi^2}{9} + 16\zeta_3 + N_\epsilon \frac{337}{108} + N_\epsilon \frac{\pi^2}{18} \Big) + C_A N_F T_R \Big( \frac{338}{27} + \frac{4\pi^2}{9} \Big) \right] \\
&\quad + \left(\frac{\alpha_s}{4\pi}\right) \left(\frac{\alpha_e}{4\pi}\right) \left[ 10\, C_F N_F T_R - \frac{4\pi^2}{3} C_A N_F T_R \right] \\
&\quad + \left(\frac{\alpha_e}{4\pi}\right)^2 \left[ N_F T_R \big( 2\, C_A - 4\, C_F - N_\epsilon (C_A + C_F) \big) \right] \\
&\quad + \left(\frac{\alpha_{4\epsilon}}{4\pi}\right)^2 \left[ C_A^2 \frac{3}{4} (-1 + N_\epsilon) \right] + \mathcal{O}(\alpha^3)\,. \qquad (7.56)
\end{aligned}
$$

Combining this result as prescribed by Eq. (7.51) with the soft anomalous dimension, which has only $\alpha_s^2$ contributions, we find the $\epsilon$-scalar anomalous dimension

$$
\bar{\gamma}_\epsilon = \left(\frac{\alpha_s}{4\pi}\right) (-4\, C_A) + \left(\frac{\alpha_e}{4\pi}\right) (2 N_F T_R)
$$

$$
\begin{aligned}
&+\left(\frac{\alpha_s}{4\pi}\right)^2\left[C_A^2\Big(-\frac{2987}{108}+\frac{5\pi^2}{6}+2\zeta_3+N_\epsilon\frac{233}{108}+N_\epsilon\frac{\pi^2}{12}\Big)+C_AN_FT_R\Big(\frac{226}{27}+\frac{2\pi^2}{3}\Big)\right]\\
&+\left(\frac{\alpha_s}{4\pi}\right)\left(\frac{\alpha_e}{4\pi}\right)\left[10\,C_FN_FT_R-\frac{4\pi^2}{3}C_AN_FT_R\right]\\
&+\left(\frac{\alpha_e}{4\pi}\right)^2\left[N_FT_R\big(2\,C_A-4\,C_F-N_\epsilon(C_A+C_F)\big)\right]\\
&+\left(\frac{\alpha_{4\epsilon}}{4\pi}\right)^2\left[C_A^2\frac{3}{4}(-1+N_\epsilon)\right]+\mathcal{O}(\alpha^3)\,.
\end{aligned}
\tag{7.57}
$$

As discussed in Section 6.2, $\bar{\gamma}_\epsilon$ is needed to relate two-loop matrix elements computed in DRED to those computed in other schemes such as FDH. With this new result all anomalous dimensions needed for the massless case are known at the two-loop level in all four schemes.

# 8 Cross check with explicit processes

The results of the previous sections allow us to predict the differences between UV renormalized virtual two-loop amplitudes squared, as defined in Eq. (6.1), computed in different regularization schemes. In this section we will make these transition rules more explicit and will check them with explicit examples.

The following discussions will also shed more light on the role of the various couplings $\alpha_s$, $\alpha_e$ and $\alpha_{4\epsilon,i}$. In the practical computation of the genuine two-loop diagrams it is no problem to set these couplings equal from the beginning. In the process of UV renormalization, i.e. in lower-order diagrams with counterterm insertions, the bare couplings and the associated renormalization constants appear. It is unavoidable to keep these distinct, regardless whether FDH or DRED is used. Once renormalization has been performed, it is possible to set the renormalized couplings equal and to identify $N_\epsilon$ and $2\epsilon$. Likewise, the derivation of the IR subtraction formulas and the transition rules requires the couplings to be treated independently, but in the end the transition rules can be easily written down for the special case of equal couplings.

We will consider the transition rules FDH $\leftrightarrow$ HV, as well as FDH $\leftrightarrow$ DRED. To make connection to the scheme that is most often used, CDR, we remind the reader of the discussion in Section 6.1. The only difference in the squared matrix element between HV and CDR is due to the use of different metric tensors for the polarization sum of external gluons. All anomalous dimensions are the same in the two schemes.

## 8.1 Transition between FDH and HV

Since external gluons are treated in the same way in FDH and HV, we can actually relate directly virtual amplitudes and do not need to work with squared amplitudes. The finite remainders of the scattering amplitudes are scheme independent. More precisely

$$\begin{aligned} |\mathcal{A}_{\text{fin}}(\{p\},\mu)\rangle &= \lim_{\epsilon\to 0} \mathbf{Z}^{-1}(\epsilon,\{p\},\mu)|\mathcal{A}(\epsilon,\{p\})\rangle \\ &= \lim_{(N)_\epsilon\to 0} \bar{\mathbf{Z}}^{-1}(\epsilon,N_\epsilon,\{p\},\mu)|\bar{\mathcal{A}}(\epsilon,N_\epsilon,\{p\})\rangle\,, \end{aligned} \tag{8.1}$$

where $|\mathcal{A}\rangle = |\mathcal{A}^{\text{HV}}\rangle$ and $\mathbf{Z} = \mathbf{Z}^{\text{HV}}$ denote quantities in the HV scheme and $|\bar{\mathcal{A}}\rangle = |\mathcal{A}^{\text{FDH}}\rangle$ and $\bar{\mathbf{Z}} = \mathbf{Z}^{\text{FDH}}$ are the corresponding quantities in the FDH scheme. Suppressing the arguments of the amplitudes, setting $N_\epsilon = 2\epsilon$ and writing $\mathbf{Z}^{-1} = 1 + \delta\mathbf{Z}$ in both schemes, we can rewrite this equation as

$$|\mathcal{A}\rangle + \delta\mathbf{Z}|\mathcal{A}\rangle = |\bar{\mathcal{A}}\rangle + \delta\bar{\mathbf{Z}}|\bar{\mathcal{A}}\rangle + \mathcal{O}(\epsilon)\,. \tag{8.2}$$

If the expansion coefficients $\delta\mathbf{Z}$ are known to $\mathcal{O}(\alpha^n)$ and the amplitudes $|\mathcal{A}\rangle$ are known to $\mathcal{O}(\alpha^{n-1})$, this equation allows to obtain a relation between the $\mathcal{O}(\alpha^n)$

amplitudes computed in HV and FDH, up to $\mathcal{O}(\epsilon)$ terms. We now give the explicit results up to the two-loop level.

The tree-level amplitudes in the two schemes are the same $|\bar{\mathcal{A}}_0\rangle = |\mathcal{A}_0\rangle$. At one-loop we can relate the $\mathcal{O}(\alpha_s)$ and $\mathcal{O}(\alpha_e)$ corrections in the FDH scheme, denoted by $|\bar{\mathcal{A}}_{10}\rangle$ and $|\bar{\mathcal{A}}_{01}\rangle$ respectively, to $|\mathcal{A}_1\rangle$, the $\mathcal{O}(\alpha_s)$ corrections in the HV scheme

$$|\bar{\mathcal{A}}_{01}\rangle = -\delta\bar{\mathbf{Z}}_{01}|\mathcal{A}_0\rangle + \mathcal{O}(\epsilon)\,, \tag{8.3a}$$

$$|\bar{\mathcal{A}}_{10}\rangle - |\mathcal{A}_1\rangle = (\delta\mathbf{Z}_1 - \delta\bar{\mathbf{Z}}_{10})|\mathcal{A}_0\rangle + \mathcal{O}(\epsilon)\,. \tag{8.3b}$$

In the above equation we have also introduced the expansion coefficients $\delta\mathbf{Z}_m$ and $\delta\bar{\mathbf{Z}}_{mn}$ of $\mathbf{Z}^{-1} = 1+\delta\mathbf{Z}$ in the HV and FDH scheme, respectively. Substituting in the last equations the explicit expressions of these expansion coefficients, the explicit form of the differences for a process with $\#q$ external massless quarks and $\#g$ external gluons read

$$|\bar{\mathcal{A}}_{01}\rangle = \frac{\#q\,\bar{\gamma}^q_{01}}{2\epsilon}|\mathcal{A}_0\rangle + \mathcal{O}(\epsilon) = \#q\frac{C_F}{2}|\mathcal{A}_0\rangle + \mathcal{O}(\epsilon)\,, \tag{8.4a}$$

$$|\bar{\mathcal{A}}_{10}\rangle - |\mathcal{A}_1\rangle = \frac{\#g\,(\bar{\gamma}^g_{10} - \gamma^g_{10})}{2\epsilon}|\mathcal{A}_0\rangle + \mathcal{O}(\epsilon) = \#g\frac{C_A}{6}|\mathcal{A}_0\rangle + \mathcal{O}(\epsilon)\,, \tag{8.4b}$$

which agrees with the results in [16, 28]. In Eq. (8.4) and what follows we use the notation $\gamma_{m0} \equiv \gamma_m^{\rm HV}$ (see footnote in Section 7.1) for the anomalous dimensions (and the $\beta$-functions) in the HV scheme. Since in the HV scheme the anomalous dimensions depend only on $\alpha_s$ but not on $\alpha_e$ the second label is always zero. Of course, this is not the case in the corresponding quantities in the FDH scheme, $\bar{\gamma}_{mn}$. To obtain Eq. (8.4) we have used $\gamma^q_{10} = \bar{\gamma}^q_{10}$ and $\gamma^{\rm cusp}_{10} = \bar{\gamma}^{\rm cusp}_{10}$.

Moving to the two-loop level, the corresponding equations are

$$|\bar{\mathcal{A}}_{02}\rangle = -\delta\bar{\mathbf{Z}}_{01}|\bar{\mathcal{A}}_{01}\rangle - \delta\bar{\mathbf{Z}}_{02}|\mathcal{A}_0\rangle + \mathcal{O}(\epsilon)\,, \tag{8.5a}$$

$$|\bar{\mathcal{A}}_{20}\rangle - |\mathcal{A}_2\rangle = \delta\mathbf{Z}_1|\mathcal{A}_1\rangle - \delta\bar{\mathbf{Z}}_{10}|\bar{\mathcal{A}}_{10}\rangle + (\delta\mathbf{Z}_2 - \delta\bar{\mathbf{Z}}_{20})|\mathcal{A}_0\rangle + \mathcal{O}(\epsilon)\,, \tag{8.5b}$$

$$|\bar{\mathcal{A}}_{11}\rangle = -\delta\bar{\mathbf{Z}}_{01}|\bar{\mathcal{A}}_{10}\rangle - \delta\bar{\mathbf{Z}}_{10}|\bar{\mathcal{A}}_{01}\rangle - \delta\bar{\mathbf{Z}}_{11}|\mathcal{A}_0\rangle + \mathcal{O}(\epsilon)\,. \tag{8.5c}$$

The expressions given in (8.5a), (8.5b) and (8.5c) allow one to move from FDH to HV (and vice versa) for any process with $\#g$ external gluons and $\#q$ external massless quarks in QCD up to two-loop order. Exploiting $\gamma^q_{10} = \bar{\gamma}^q_{10}$ and $\gamma^{\rm cusp}_{10} = \bar{\gamma}^{\rm cusp}_{10}$ we obtain

$$\begin{aligned}|\bar{\mathcal{A}}_{02}\rangle = &\left[\frac{-1}{8\epsilon^2}\#q\bar{\gamma}^q_{01}(2\bar{\beta}^e_{02} + \#q\bar{\gamma}^q_{01}) + \frac{1}{4\epsilon}\#q\bar{\gamma}^q_{02}\right]|\mathcal{A}_0\rangle \\ &+ \left[\frac{1}{2\epsilon}\#q\bar{\gamma}^q_{01}\right]|\bar{\mathcal{A}}_{01}\rangle + \mathcal{O}(\epsilon)\,,\end{aligned} \tag{8.6a}$$

$$
\begin{aligned}
|\bar{\mathcal{A}}_{20}\rangle - |\mathcal{A}_2\rangle = &\left[\frac{-3}{16\epsilon^3}\Big[(C_A\#g + C_F\#q)(\beta_{20}^s - \bar{\beta}_{20}^s)\gamma_{10}^{\text{cusp}}\Big]\right. \\
&+ \frac{1}{16\epsilon^2}\Big[(C_A\#g + C_F\#q)(\gamma_{20}^{\text{cusp}} - \bar{\gamma}_{20}^{\text{cusp}}) - 2\#g(-2\beta_{20}^s\gamma_{10}^g + \#g(\gamma_{10}^g - \bar{\gamma}_{10}^g)^2 \\
&+ 2\bar{\beta}_{20}^s\bar{\gamma}_{10}^g) + (\beta_{20}^s - \bar{\beta}_{20}^s)\Big(4\#q\gamma_{10}^q + 2\gamma_{10}^{\text{cusp}}\sum_{(i,j)}\mathbf{T}_i\cdot\mathbf{T}_j\ln(\frac{\mu^2}{-s_{ij}})\Big)\Big] \\
&+ \frac{1}{8\epsilon}\Big[2\#g(\bar{\gamma}_{20}^g - \gamma_{20}^g) + 2\#q(\bar{\gamma}_{20}^q - \gamma_{20}^q) \\
&\quad + (\bar{\gamma}_{20}^{\text{cusp}} - \gamma_{20}^{\text{cusp}})\sum_{(i,j)}\mathbf{T}_i\cdot\mathbf{T}_j\ln(\frac{\mu^2}{-s_{ij}})\Big]\Big]|\mathcal{A}_0\rangle \\
&+ \left[\frac{-1}{4\epsilon^2}(C_A\#g + C_F\#q)\gamma_{10}^{\text{cusp}}\right. \\
&+ \frac{1}{4\epsilon}\Big(2\#g\bar{\gamma}_{10}^g + 2\#q\gamma_{10}^q + \gamma_{10}^{\text{cusp}}\sum_{(i,j)}\mathbf{T}_i\cdot\mathbf{T}_j\ln(\frac{\mu^2}{-s_{ij}})\Big)\Big]|\mathcal{A}_{10}^{\text{diff}}\rangle \\
&+ \left[\frac{1}{2\epsilon}\#g(\bar{\gamma}_{10}^g - \gamma_{10}^g)\right]|\mathcal{A}_1^{\text{fin}}\rangle + \mathcal{O}(\epsilon)\,, \qquad (8.6b)\\
|\bar{\mathcal{A}}_{11}\rangle = &\left[\frac{-1}{4\epsilon^2}\#q\Big(\bar{\beta}_{11}^e + \#g(\bar{\gamma}_{10}^g - \gamma_{10}^g)\Big)\bar{\gamma}_{01}^q + \frac{1}{4\epsilon}(\#g\bar{\gamma}_{11}^g + \#q\bar{\gamma}_{11}^q)\right]|\mathcal{A}_0\rangle \\
&+ \left[-\frac{1}{4\epsilon^2}(C_A\#g + C_F\#q)\gamma_{10}^{\text{cusp}}\right. \\
&+ \frac{1}{4\epsilon}\Big(2\#g\bar{\gamma}_{10}^g + 2\#q\gamma_{10}^q + \gamma_{10}^{\text{cusp}}\sum_{(i,j)}\mathbf{T}_i\cdot\mathbf{T}_j\ln(\frac{\mu^2}{-s_{ij}})\Big)\Big]|\bar{\mathcal{A}}_{01}\rangle \\
&+ \left[\frac{1}{2\epsilon}\#q\bar{\gamma}_{01}^q\right]|\mathcal{A}_{10}^{\text{diff}}\rangle + \left[\frac{1}{2\epsilon}\#q\bar{\gamma}_{01}^q\right]|\mathcal{A}_1^{\text{fin}}\rangle + \mathcal{O}(\epsilon)\,, \qquad (8.6c)
\end{aligned}
$$

where we have defined

$$
|\mathcal{A}_{10}^{\text{diff}}\rangle = |\bar{\mathcal{A}}_{10}\rangle - |\mathcal{A}_1\rangle\,, \qquad (8.7a)
$$

$$
|\mathcal{A}_1^{\text{fin}}\rangle = \lim_{\epsilon\to 0}\Big[\delta\mathbf{Z}_1|\mathcal{A}_0\rangle + |\mathcal{A}_1\rangle\Big] = \lim_{\epsilon\to 0}\Big[\delta\bar{\mathbf{Z}}_{10}|\mathcal{A}_0\rangle + |\bar{\mathcal{A}}_{10}\rangle\Big]\,. \qquad (8.7b)
$$

$|\mathcal{A}_1^{\text{fin}}\rangle$ is the NLO approximation to $|\mathcal{A}_{\text{fin}}\rangle$ and, thus, a finite and scheme independent quantity. The one-loop quantities $|\mathcal{A}_{10}^{\text{diff}}\rangle$ and $|\bar{\mathcal{A}}_{01}\rangle$ have to be known up to $\mathcal{O}(\epsilon^2)$ terms.

We remark that Eq. (8.5a) allows to obtain the $\mathcal{O}(\alpha_e^2)$ contribution of a two-loop amplitude in FDH up to $\mathcal{O}(\epsilon)$ terms directly from the tree-level amplitude. This is due to the fact that $\bar{\gamma}_{01}^q \sim N_\epsilon \sim \epsilon$ and hence the coefficient multiplying $|\bar{\mathcal{A}}_{01}\rangle$ in Eq. (8.6a) is finite. Therefore, we can use Eq. (8.3a) and with the explicit expressions

of the anomalous dimensions we get

$$|\bar{\mathcal{A}}_{02}\rangle = C_F\,\#q\left[\frac{2\,C_F - C_A + N_F T_R}{2\,\epsilon} + \frac{1}{8}\big(4\,C_A + C_F\,(\#q-4) - 6\,N_F T_R\big)\right]|\mathcal{A}_0\rangle + \mathcal{O}(\epsilon)\,. \tag{8.8}$$

For a process with no external quarks, $\#q = 0$ there are no $\mathcal{O}(\alpha_e^2)$ terms at NNLO, as can easily be confirmed on a diagrammatic level.

As mentioned several times, once the UV renormalization has been carried out, there is no need any longer to distinguish between the different couplings. After setting $\alpha_e = \alpha_s$ the full difference is given by

$$\begin{aligned}
|\bar{\mathcal{A}}_2\rangle - |\mathcal{A}_2\rangle = \Bigg[ & -\frac{1}{4\epsilon^2} C_A(\#g\,C_A + \#q\,C_F) \\
& + \frac{1}{36\epsilon}\Big[ -14\,C_A^2\#g - 18\,C_F\#q(C_F - N_F T_R) + C_A(-19\,C_F\#q + 8\,N_F\#g T_R) \\
& + 6\,C_A \sum_{(i,j)} \mathbf{T}_i\cdot\mathbf{T}_j \ln(\frac{\mu^2}{-s_{ij}})\Big] \\
& + \frac{1}{216}\Big[C_A^2\#g(398 - 3\#g - 3\pi^2) + C_A C_F\#q(869 - 18\#g + 9\pi^2) \\
& - 9\,C_F\Big(C_F\#q\big(3\#q + 4(9+\pi^2)\big) + 6\,N_F(4\#g + 3\#q)T_R\Big) \\
& - 96\,C_A \sum_{(i,j)} \mathbf{T}_i\cdot\mathbf{T}_j \ln(\frac{\mu^2}{-s_{ij}})\Big]\Bigg]|\mathcal{A}_0\rangle \\
& + \Bigg[ -\frac{1}{\epsilon^2}(\#g C_A + \#q C_F) \\
& + \frac{1}{6\epsilon}\Big[ -11\,C_A\#g - 9\,C_F\#q + 4\,N_F\#g T_R + 6\sum_{(i,j)} \mathbf{T}_i\cdot\mathbf{T}_j \ln(\frac{\mu^2}{-s_{ij}})\Big] \\
& + \frac{1}{6}(\#g C_A + 3\#q C_F)\Bigg]|\mathcal{A}_1^{\text{diff}}\rangle \\
& + \left[\frac{1}{6}(\#g C_A + 3\#q C_F)\right]|\mathcal{A}_1^{\text{fin}}\rangle\,,
\end{aligned} \tag{8.9}$$

where we have introduced the notation

$$|\bar{\mathcal{A}}_2\rangle = |\bar{\mathcal{A}}_{20}\rangle + |\bar{\mathcal{A}}_{02}\rangle + |\bar{\mathcal{A}}_{11}\rangle\,, \tag{8.10a}$$

$$|\mathcal{A}_1^{\text{diff}}\rangle = |\bar{\mathcal{A}}_{10}\rangle + |\bar{\mathcal{A}}_{01}\rangle - |\mathcal{A}_1\rangle\,. \tag{8.10b}$$

### 8.2 NNLO $2 \to 2$ amplitudes in HV and FDH in massless QCD

As an example for the transition rules derived in the previous subsection, we consider the two-loop amplitudes $gg \to gg$ and $q\bar{q} \to gg$ for massless quarks. Initially

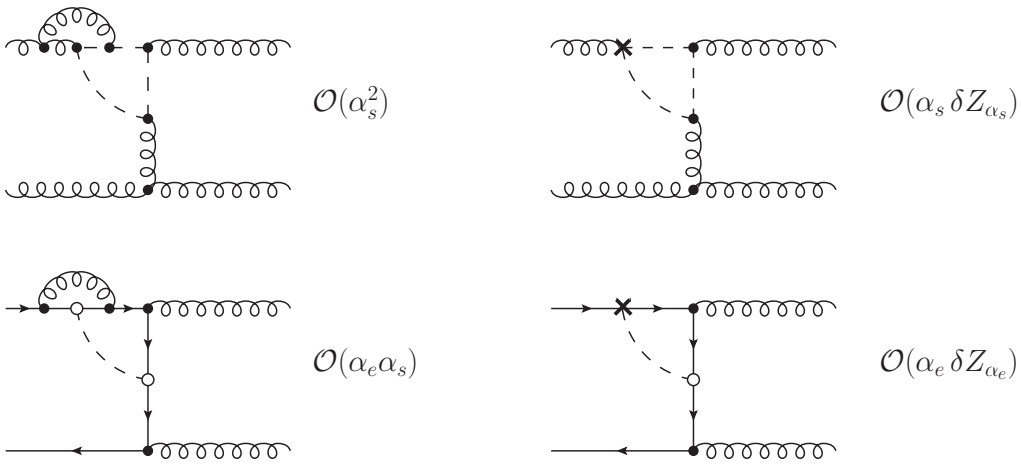


**Figure 10**. Examples of two-loop (left panel) and one-loop counterterm (right panel) diagrams for $gg \to gg$ (top panel) and $q\bar{q} \to gg$ (bottom panel). Black vertices denote couplings $g_s$ whereas white vertices denote couplings $g_e$, and crosses denote counterterm insertions. For $gg \to gg$ at one-loop, there are no contributions with couplings $g_e$. The order is given relative to the Born term $|\mathcal{A}_0\rangle \sim \mathcal{O}(\alpha_s)$.

the interference of these two-loop amplitudes with the tree-level amplitudes was calculated in CDR [74, 75]. Later the helicity amplitudes were computed and explicit results in the HV and FDH scheme were given [76, 77]. However, for the computation and the UV renormalization procedure in the FDH scheme, no distinction between $\alpha_s$ and $\alpha_e$ (and $\alpha_{4\epsilon,i}$) was made. For the process $gg \to gg$ this is of no consequence, but for $q\bar{q} \to gg$ this will lead to an incorrect UV renormalization. As shown in Refs. [18, 19, 29] this leads to incorrect finite terms which violate unitarity. For our purposes it also matters because an incorrectly renormalized amplitude cannot be consistent with the IR structure and transition rules discussed above.

Hence, in order to check the validity of the transition rules, we first need to correct the renormalization of the $q\bar{q} \to gg$ result of Ref. [77]. Figure 10 shows diagrams which illustrate the problem. The left panels show genuine two-loop diagrams to $gg \to gg$ and $q\bar{q} \to gg$. One of them depends on $\alpha_e$, but setting $\alpha_e = \alpha_s$ in these two-loop diagrams causes no problem. However, the diagrams have subdivergences, which should be cancelled by suitable counterterm diagrams, such as the ones in the right panels. The first of these counterterm diagrams depends on the one-loop renormalization constant $\delta Z_{\alpha_s}$, but the second one depends on $\delta Z_{\alpha_e}$, which differs by a divergent amount. If, as in Ref. [77], this renormalization constant is effectively replaced by $\delta Z_{\alpha_s}$, the subdivergence is not properly subtracted, and the final result will not be correct.

The correct renormalization procedure requires to compute the lower-order am-

plitudes for individual couplings. At tree-level, the amplitudes $|\bar{\mathcal{A}}_0\rangle$ for both processes are proportional to $\alpha_s$ and hence are correctly renormalized by multiplying with $Z_{\alpha_s}$. At the one-loop level, the amplitudes receive contributions of $\mathcal{O}(\alpha_s)$ or $\mathcal{O}(\alpha_e)$ relative to tree-level. The latter contribution $|\bar{\mathcal{A}}_{01}\rangle$ must be renormalized by multiplication with $Z_{\alpha_s} Z_{\alpha_e}$.

The difference between the two processes $gg \to gg$ and $q\bar{q} \to gg$ is that for the former process, $|\bar{\mathcal{A}}_{01}\rangle$ happens to vanish. This is the reason why for this process the identification $\alpha_s = \alpha_e$ causes no problem. In order to restore the correct renormalization for the latter process, we have computed the $\mathcal{O}(\alpha_s\,\alpha_e)$ contribution to the one-loop amplitudes. We have then renormalized this contribution using $Z_{\alpha_s} Z_{\alpha_e}$ and add the resulting NNLO term to the explicit results of Ref. [77]. We also subtracted the corresponding terms obtained with the renormalization factor $Z_{\alpha_s}^2$ that had been applied in Ref. [77].

We have compared the difference between the FDH and HV amplitudes for both processes with the prediction given by Eq. (8.9) and have found full agreement. This is a further non-trivial confirmation that our treatment of the scheme dependence is process independent and applicable at least to NNLO. It is also an independent verification of the correctness of the anomalous dimensions in FDH.

### 8.3 Transition between FDH and DRED

The transition rules between DRED and FDH can be derived similarly but are more involved. To illustrate their structure let us first consider a process with a single external gluon. The explicit calculation of the UV renormalized matrix element in DRED yields $\mathcal{M}^{\text{DRED}}(g)$ that can be written as

$$\mathcal{M}^{\text{DRED}}(g) = \mathcal{M}^{\text{DRED}}(\hat{g}) + \mathcal{M}^{\text{DRED}}(\tilde{g}) = 2\,\text{Re}\,\langle \mathcal{A}_0^{\hat{g}} | \mathcal{A}^{\hat{g}} \rangle + 2\,\text{Re}\,\langle \mathcal{A}_0^{\epsilon} | \mathcal{A}^{\epsilon} \rangle\,, \tag{8.11}$$

where we have introduced the shorthand notation $\mathcal{A}^{\hat{g}} \equiv \mathcal{A}^{\text{DRED}}(\hat{g})$ and $\mathcal{A}^{\epsilon} \equiv \mathcal{A}^{\text{DRED}}(\tilde{g})$ etc, and suppressed other arguments compared to Section 6.2. We would like to find a relation between $\mathcal{M}^{\text{DRED}}(g)$ and the corresponding result in FDH,

$$\mathcal{M}^{\text{FDH}}(g) = 2\,\text{Re}\,\langle \bar{\mathcal{A}}_0^{g} | \bar{\mathcal{A}}^{g} \rangle \equiv 2\,\text{Re}\,\langle \mathcal{A}_0^{\text{FDH}}(g) | \mathcal{A}^{\text{FDH}}(g) \rangle\,. \tag{8.12}$$

To do so, we start from the equality of the IR subtracted amplitudes computed in DRED and FDH, written with a similar shorthand notation for the $\mathbf{Z}$-factors as

$$\langle \mathcal{A}_0^{\hat{g}} | \big(\mathbf{Z}^{\hat{g}}\big)^{-1} | \mathcal{A}^{\hat{g}} \rangle + \langle \mathcal{A}_0^{\epsilon} | \big(\mathbf{Z}^{\epsilon}\big)^{-1} | \mathcal{A}^{\epsilon} \rangle = \langle \bar{\mathcal{A}}_0^{g} | \big(\bar{\mathbf{Z}}^{g}\big)^{-1} | \bar{\mathcal{A}}^{g} \rangle + \mathcal{O}(\epsilon)\,, \tag{8.13}$$

where we have set $N_\epsilon = 2\epsilon$. Writing $\mathbf{Z}^{-1} = 1 + \delta\mathbf{Z}$, where $\delta\mathbf{Z}$ denote the perturbatively expanded higher-order terms, we obtain an equation analogous to (8.2),

$$\begin{aligned} &\mathcal{M}^{\text{DRED}}(g) + 2\,\text{Re}\,\langle \mathcal{A}_0^{\hat{g}} | \delta\mathbf{Z}^{\hat{g}} | \mathcal{A}^{\hat{g}} \rangle + 2\,\text{Re}\,\langle \mathcal{A}_0^{\epsilon} | \delta\mathbf{Z}^{\epsilon} | \mathcal{A}^{\epsilon} \rangle \\ &= \mathcal{M}^{\text{FDH}}(g) + 2\,\text{Re}\,\langle \bar{\mathcal{A}}_0^{g} | \delta\bar{\mathbf{Z}}^{g} | \bar{\mathcal{A}}^{g} \rangle + \mathcal{O}(\epsilon)\,. \end{aligned} \tag{8.14}$$

If the expansion coefficients $\delta\mathbf{Z}$ are known to $\mathcal{O}(\alpha^n)$ and the amplitudes $|\mathcal{A}\rangle$ are known to $\mathcal{O}(\alpha^{n-1})$, Eq. (8.14) allows to obtain a relation between the $\mathcal{O}(\alpha^n)$ squared matrix element computed in DRED and FDH, up to $\mathcal{O}(\epsilon)$ terms. For this relation, the knowledge of $\mathbf{Z}^\epsilon \equiv \mathbf{Z}^{\text{DRED}}(\tilde{g})$ is required, even though Eq. (8.13) is still correct if the second term on the l.h.s. containing $\mathbf{Z}^\epsilon$ is dropped.

As a concrete example we consider the process $H \to g\,g$ in FDH and DRED and work out the transition rules between the two schemes for the UV renormalized two-loop squared amplitudes. For simplicity we also set $\alpha_e = \alpha_{4\epsilon} = \alpha_s$.

As we have $\#g = 2$ external gluons, in DRED the squared matrix element is to be written as a sum over $2^{\#g} = 4$ terms. However, in this particular case two of these terms vanish to all orders, resulting in

$$\mathcal{M}^{\text{DRED}}(g,g) = \mathcal{M}(\hat{g},\hat{g}) + \mathcal{M}(\tilde{g},\tilde{g})\,. \tag{8.15}$$

Writing explicitly the equality of the subtracted matrix elements in FDH and DRED we get

$$\begin{aligned}
&\langle\bar{\mathcal{A}}_0|\left(1+\delta\bar{\mathbf{Z}}_1\left(\frac{\alpha_s}{4\pi}\right)+\delta\bar{\mathbf{Z}}_2\left(\frac{\alpha_s}{4\pi}\right)^2\right)\left(|\bar{\mathcal{A}}_0\rangle+|\bar{\mathcal{A}}_1\rangle\left(\frac{\alpha_s}{4\pi}\right)+|\bar{\mathcal{A}}_2\rangle\left(\frac{\alpha_s}{4\pi}\right)^2\right)\\
&=\langle\mathcal{A}_0^{\hat{g}\hat{g}}|\left(1+\delta\mathbf{Z}_1^{\hat{g}\hat{g}}\left(\frac{\alpha_s}{4\pi}\right)+\delta\mathbf{Z}_2^{\hat{g}\hat{g}}\left(\frac{\alpha_s}{4\pi}\right)^2\right)\left(|\mathcal{A}_0^{\hat{g}\hat{g}}\rangle+|\mathcal{A}_1^{\hat{g}\hat{g}}\rangle\left(\frac{\alpha_s}{4\pi}\right)+|\mathcal{A}_2^{\hat{g}\hat{g}}\rangle\left(\frac{\alpha_s}{4\pi}\right)^2\right)\\
&+\langle\mathcal{A}_0^{\epsilon\epsilon}|\left(1+\delta\mathbf{Z}_1^{\epsilon\epsilon}\left(\frac{\alpha_s}{4\pi}\right)+\delta\mathbf{Z}_2^{\epsilon\epsilon}\left(\frac{\alpha_s}{4\pi}\right)^2\right)\left(|\mathcal{A}_0^{\epsilon\epsilon}\rangle+|\mathcal{A}_1^{\epsilon\epsilon}\rangle\left(\frac{\alpha_s}{4\pi}\right)+|\mathcal{A}_2^{\epsilon\epsilon}\rangle\left(\frac{\alpha_s}{4\pi}\right)^2\right)\\
&+\mathcal{O}(\epsilon)+\mathcal{O}(\alpha^3)\,.
\end{aligned} \tag{8.16}$$

In Eq. (8.16) we have introduced a compact notation for the perturbative coefficients of the amplitudes and $\mathbf{Z}^{-1}$ in DRED: $|\mathcal{A}_2^{\epsilon\epsilon}\rangle \equiv |\mathcal{A}_2(\tilde{g},\tilde{g})\rangle$ and

$$\mathbf{Z}^{-1}(\hat{g},\hat{g}) = 1+\delta\mathbf{Z}_1^{\hat{g}\hat{g}}\left(\frac{\alpha_s}{4\pi}\right)+\delta\mathbf{Z}_2^{\hat{g}\hat{g}}\left(\frac{\alpha_s}{4\pi}\right)^2+\mathcal{O}(\alpha^3)\,, \tag{8.17}$$

with analogous expressions for other partonic processes. Comparing the order $\alpha_s$ terms yields

$$\begin{aligned}
\mathcal{M}_1^{\text{DRED}}(g,g)-\mathcal{M}_1^{\text{FDH}}(g,g) &= \mathcal{M}_0^{\text{DRED}}(\tilde{g},\tilde{g})\frac{(\bar{\gamma}^\epsilon_{010}+\bar{\gamma}^\epsilon_{100}-\bar{\gamma}^g_{100})}{\epsilon}\\
&= \mathcal{M}_0^{\text{DRED}}(\tilde{g},\tilde{g})\frac{(2\,N_F T_R - C_A)}{3\epsilon}+\mathcal{O}(\epsilon)\,.
\end{aligned} \tag{8.18}$$

This one-loop transition rule is in agreement[10] with Ref. [16]. To make this agreement more explicit we write the transition in a more general way as

$$\mathcal{M}_1^{\text{DRED}}(g,g)-\mathcal{M}_1^{\text{FDH}}(g,g) = \left(\mathcal{M}_0^{\text{DRED}}(g,\tilde{g})+\mathcal{M}_0^{\text{DRED}}(\tilde{g},g)\right)\frac{(2\,N_F T_R - C_A)}{6\epsilon}+\mathcal{O}(\epsilon)\,. \tag{8.19}$$

[10]Note that in Ref. [16] a different convention for the $\gamma$'s has been used.

Note that the difference is finite, since the tree-level matrix element squared on the r.h.s. of Eq. (8.18) or Eq. (8.19) are of $\mathcal{O}(\epsilon)$.

In order to write the scheme difference at NNLO we introduce a similar shorthand notation for the squared matrix elements as for the amplitudes, denoting the full tree-level and one-loop contribution for the $H \to \tilde{g}\tilde{g}$ process by $\mathcal{M}_0^{\epsilon\epsilon} \equiv \mathcal{M}_0(\tilde{g},\tilde{g})$ and $\mathcal{M}_1^{\epsilon\epsilon} \equiv \mathcal{M}_1(\tilde{g},\tilde{g})$, respectively. The difference can then be written as

$$\begin{aligned}
&\mathcal{M}_2^{\text{DRED}}(g,g) - \mathcal{M}_2^{\text{FDH}}(g,g) = \frac{1}{2\epsilon^3}\, C_A\, \mathcal{M}_0^{\epsilon\epsilon} \bar{\gamma}_{100}^{\text{cusp}} \big(\bar{\gamma}_{010}^{\epsilon} + \bar{\gamma}_{100}^{\epsilon} - \bar{\gamma}_{100}^{g}\big) \\
&- \frac{1}{2\epsilon^2}\Big[\mathcal{M}_0^{\epsilon\epsilon}\big(\bar{\beta}_{020}^{e}\bar{\gamma}_{010}^{\epsilon} + \bar{\beta}_{110}^{e}\bar{\gamma}_{010}^{\epsilon} + \bar{\beta}_{200}(\bar{\gamma}_{100}^{\epsilon} - \bar{\gamma}_{100}^{g}) + (\bar{\gamma}_{010}^{\epsilon} + \bar{\gamma}_{100}^{\epsilon})^2 - (\bar{\gamma}_{100}^{g})^2\big) \\
&\quad + C_A \mathcal{M}_1^{\text{diff}} \bar{\gamma}_{100}^{\text{cusp}} - C_A \mathcal{M}_0^{\epsilon\epsilon} \bar{\gamma}_{100}^{\text{cusp}} \bar{\gamma}_{010}^{\epsilon} \ln(-\frac{\mu^2}{s})\Big] \\
&+ \frac{1}{2\epsilon}\Big[2\,\mathcal{M}_1^{\epsilon\epsilon}(\bar{\gamma}_{010}^{\epsilon} + \bar{\gamma}_{100}^{\epsilon} - \bar{\gamma}_{100}^{g}) + \mathcal{M}_0^{\epsilon\epsilon}(\bar{\gamma}_{002}^{\epsilon} + \bar{\gamma}_{020}^{\epsilon} + \bar{\gamma}_{110}^{\epsilon} + \bar{\gamma}_{200}^{\epsilon} - \bar{\gamma}_{110}^{g} - \bar{\gamma}_{200}^{g}) \\
&\quad + 2\,\mathcal{M}_1^{\text{diff}} \bar{\gamma}_{100}^{g} - C_A \mathcal{M}_1^{\text{diff}} \bar{\gamma}_{100}^{\text{cusp}} \ln(-\frac{\mu^2}{s})\Big] + \mathcal{O}(\epsilon)\,,
\end{aligned} \tag{8.20}$$

where we have introduced the one-loop difference

$$\mathcal{M}_1^{\text{diff}} \equiv \mathcal{M}_1^{\text{DRED}}(g,g) - \mathcal{M}_1^{\text{FDH}}(g,g)\,. \tag{8.21}$$

Note that the squared matrix elements $\mathcal{M}_0^{\epsilon\epsilon}$ and $\mathcal{M}_1^{\epsilon\epsilon}$ are of $\mathcal{O}(\epsilon)$ and $\mathcal{M}_1^{\text{diff}}$ needs to be known up to $\mathcal{O}(\epsilon^2)$. Using the explicit results for the anomalous dimensions Eq. (8.20) translates into

$$\begin{aligned}
\mathcal{M}_2^{\text{DRED}} - \mathcal{M}_2^{\text{FDH}} = &-\frac{2}{3\epsilon^3} C_A \mathcal{M}_0^{\epsilon\epsilon}\,(C_A - 2\,N_F T_R) + \frac{1}{\epsilon^2}\Big[-\frac{2}{3}(3\,C_A\,\mathcal{M}_1^{\text{diff}} + 2\,C_A^2 \mathcal{M}_0^{\epsilon\epsilon} \\
&- 5\,C_A\,N_F T_R \mathcal{M}_0^{\epsilon\epsilon} + 3\,C_F\,N_F T_R \mathcal{M}_0^{\epsilon\epsilon}) + 4\,C_A\,N_F T_R \ln(-\frac{\mu^2}{s})\mathcal{M}_0^{\epsilon\epsilon}\Big] \\
&+ \frac{1}{18\epsilon}\Big[C_A(-66\,\mathcal{M}_1^{\text{diff}} - 6\,\mathcal{M}_1^{\epsilon\epsilon} + C_A \mathcal{M}_0^{\epsilon\epsilon}(-37 + 2\pi^2)) \\
&+ 2\,N_F\,T_R(12\,\mathcal{M}_1^{\text{diff}} - 9\,C_F \mathcal{M}_0^{\epsilon\epsilon} + 6\,\mathcal{M}_1^{\epsilon\epsilon} - 2\,C_A \mathcal{M}_0^{\epsilon\epsilon}(-11 + \pi^2)) \\
&- 36\,C_A \mathcal{M}_1^{\text{diff}} \ln(-\frac{\mu^2}{s})\Big] + \frac{1}{3} C_A(\mathcal{M}_1^{\text{diff}} - \mathcal{M}_1^{\epsilon\epsilon}) + \mathcal{O}(\epsilon)\,.
\end{aligned} \tag{8.22}$$

We have checked our prediction Eq. (8.22) with the explicit calculation of the gluon form factor in DRED and FDH [34] and we have obtained full agreement. This was of course to be expected, as we have verified that the extraction of $\bar{\gamma}^{\epsilon}$ from the form factor for $H \to \tilde{g}\tilde{g}$ is in agreement with its determination in SCET.

## 9 Scheme dependence for massive external legs

Exactly as in the massless case, the key point of the scheme dependences relies on the anomalous dimensions. In the massive case this implies that we have to compute $\gamma_Q$ and $\gamma_{\text{cusp}}(\beta_{IJ})$ in the various schemes. According to the discussion related to the massless case, the expression in (3.36) has to be extended for the FDH case[11], by expanding the coefficients in all possible couplings $\{\alpha\}$. Since in FDH the functions in (3.38) do not receive evaneschent contributions form the $\epsilon$-scalar, at NNLO Eq. (3.38) is a scheme-independent quantity. Its value in FDH is therefore the same as in CDR.

We can then extract $\gamma_Q$ and $\gamma_{\text{cusp}}(\beta_{IJ})$ by computing the heavy quark form factor in FDH at NNLO. However this process alone does not allow us to disentangle the two anomalous dimensions and obtain them separately. For that reason we also compute the heavy to light form factor. We finally get a full knowledge of Eq. (3.36) in the various schemes.

We turn now to the computation of the two form factors and discuss in detail the technology needed at NNLO.

### 9.1 Heavy quark form factor

In order to study the scheme dependence in the case of massive QCD, we have to compute the anomalous dimensions given in (3.36). One way to get them is via the computation of the heavy form factor in the different schemes. The CDR result of the form factor has been computed up to NNLO in [78]. Referring to [78], we describe here the corresponding calculation in FDH (which is identical to the one in DRED). We express the QCD vertex of a virtual photon decaying into two massive quarks as

$$\bar{V}^{\mu}_{c_1c_2}(p_1,p_2) = \bar{u}_{c_1}(p_1)\,\bar{\Gamma}^{\mu}_{c_1c_2}(p_1,p_2)\,v_{c_2}(p_2)\,, \tag{9.1a}$$

with

$$\bar{\Gamma}^{\mu}_{c_1c_2}(p_1,p_2) = -i\,v_Q\,\delta_{c_1c_2}\left[\bar{F}_1(s)\,\hat{\gamma}^{\mu} + \frac{1}{2m}\bar{F}_2(s)\,i\,\hat{\sigma}^{\mu\nu}q_{\nu}\right], \tag{9.1b}$$

where $p_1$, $p_2$ are the momenta of the two on-shell massive external quarks with colours $c_1$ and $c_2$ and mass $p_1^2 = p_2^2 = m^2$. $\bar{u}_{c_1}(p_1), v_{c_2}(p_2)$ denote the spinors, $\sigma^{\mu\nu} = \frac{i}{2}[\gamma^{\mu},\gamma^{\nu}]$ and $\bar{F}_i(s)$ are dimensionless scalar form factors depending on the dimensionless variable

$$s = \frac{(p_1+p_2)^2}{m^2}\,. \tag{9.2}$$

The charge of the heavy quark $Q_Q$ is given in terms of the positron charge $e$ by

$$v_Q = e\,Q_Q\,. \tag{9.3}$$

[11]The anomalous dimension related to massive partons are identically in FDH and DRED and we will then refer only to FDH in the following, but the same statements will be also valid in DRED.

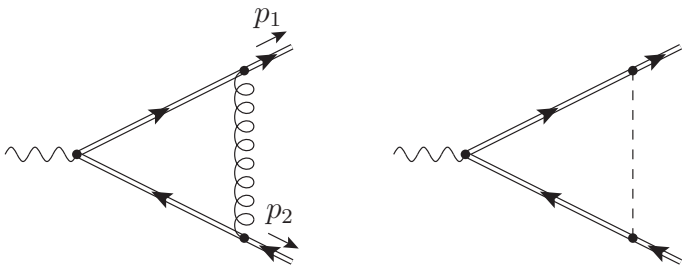


**Figure 11**. One-loop diagrams contributing to the heavy quark form factor in FDH.

The gamma matrices appearing in (9.1b) are scheme dependent. However, since we are only interested in the structure of $F_1(s)$ in the various schemes, we can treat them always as $D-$dimensional quantities in any scheme (although this is not formally correct) and use an unique projector operator $P_\mu^{(i)}$ to extract $F_1(s)$. With

$$P_\mu^{(i)}(m,p_1,p_2) = \frac{\not{p}_2 - m}{m}\left[i\, g_1^{(i)}\gamma_\mu + \frac{i}{2m} g_2^{(i)} t_\mu\right]\frac{\not{p}_1 + m}{m}, \tag{9.4}$$

we get

$$\mathrm{Tr}\left(P_\mu^{(i)}(m,p_1,p_2)\Gamma^\mu(p_1,p_2)\right) = F_i(s), \tag{9.5}$$

where $t^\mu = p_2^\mu - p_1^\mu$ and the constants are

$$g_1^{(1)} = -\frac{1}{v_Q N_c}\frac{1}{4(1-\epsilon)}\frac{1}{(s-4)}\,, \tag{9.6}$$

$$g_2^{(1)} = \frac{1}{v_Q N_c}\frac{(3-2\epsilon)}{(1-\epsilon)}\frac{1}{(s-4)^2}\,, \tag{9.7}$$

$$g_1^{(2)} = \frac{1}{v_Q N_c}\frac{1}{(1-\epsilon)}\frac{1}{s(s-4)}\,, \tag{9.8}$$

$$g_2^{(2)} = -\frac{1}{v_Q N_c}\frac{1}{(1-\epsilon)}\frac{1}{(s-4)^2}\left[\frac{4}{s} + 2 - 2\epsilon\right]\,. \tag{9.9}$$

We performed the integral reduction using Reduze 2 and we expressed the final result in terms of 1-dimensional harmonic polylogarithms (HPLs) [79, 80] of the variable

$$x = \frac{\sqrt{-s+4} - \sqrt{-s}}{\sqrt{-s+4} + \sqrt{-s}}, \qquad (0 \le x \le 1)\,. \tag{9.10}$$

The master integrals [81, 82] are identical to those needed in CDR.

We express the result as a series expansion in $a_s$ and $a_e$:

$$\begin{aligned}\bar{F}_1(x) = 1 &+ a_s(m^2)\,\bar{\mathcal{F}}_{10}(x) + a_e(m^2)\,\bar{\mathcal{F}}_{01}(x) + a_s^2(m^2)\,\bar{\mathcal{F}}_{20}(x)\\ &+ a_e^2(m^2)\,\bar{\mathcal{F}}_{02}(x) + a_s(m^2)a_e(m^2)\,\bar{\mathcal{F}}_{11}(x) \;+\mathcal{O}(a^3)\,,\end{aligned} \tag{9.11}$$

where the coupling constant $a_s$ (and similar for $a_e$) is defined as

$$a_s(m^2) \equiv e^{-\epsilon\gamma_E}(4\pi)^\epsilon\left(\frac{1}{m^2}\right)^\epsilon\frac{\alpha_s^{\mathrm{bare}}}{4\pi} = \left(\frac{\mu^2}{m^2}\right)^\epsilon\frac{Z_{\alpha_s}^{\mathrm{RS}}\alpha_s}{4\pi}. \tag{9.12}$$

At one-loop there are only two diagrams contributing and they are shown in Figure 11. We then get for the expression of the bare one-loop result

$$\begin{aligned}
\bar{\mathcal{F}}_{10}(x) = \frac{2}{\epsilon}\Bigg\{ & C_F\left[\frac{1}{2}+\left(1-\frac{1}{1+x}-\frac{1}{1-x}\right)H(0;x)\right]\Bigg\} \\
& + 2C_F\Bigg[\frac{1}{2}\left(1-\frac{2}{1-x}\right)H(0;x) - \left(1-\frac{1}{1+x}-\frac{1}{1-x}\right)\big(\zeta(2) \\
& - H(0;x) - H(0,0;x) + 2H(-1,0;x)\big)\Bigg] \\
& - 2\epsilon\Bigg\{ C_F\Bigg[\frac{1}{2}\left(1-\frac{2}{1-x}\right)\big(\zeta(2) - H(0,0;x) + 2H(-1,0;x)\big) \\
& + \left(1-\frac{1}{1+x}-\frac{1}{1-x}\right)\big(\zeta(2)+2\zeta(3) \\
& - (4-\zeta(2))H(0;x) - 2\zeta(2)H(-1;x) - H(0,0;x) \\
& + 2H(-1,0;x) - H(0,0,0;x) + 2H(-1,0,0;x) \\
& + 2H(0,-1,0;x) - 4H(-1,-1,0;x)\big) \\
& - \frac{\pi^2}{12}\left(\frac{1}{2}+\left(1-\frac{1}{1+x}-\frac{1}{1-x}\right)H(0;x)\right)\Bigg]\Bigg\} + \mathcal{O}\left(\epsilon^2\right), \qquad (9.13)
\end{aligned}$$

$$\begin{aligned}
\bar{\mathcal{F}}_{01}(x) = & \; 2C_F N_\epsilon\Bigg\{\frac{1}{4\epsilon} + \frac{1+x+(1-x)H(0;x)}{4(1+x)} \\
& + \epsilon\Big(\frac{6-\pi^2+6x+\pi^2 x - 6(-1+x)(H(0;x)-2H(-1,0;x)+H(0,0;x))}{24(1+x)} + \frac{\pi^2}{48}\Big)\Bigg\} \\
& + \mathcal{O}\left(\epsilon^2\right). \qquad (9.14)
\end{aligned}$$

The CDR result can be obtained directly by taking the limit $N_\epsilon \to 0$ and it agrees with [78].

At two-loop the computation is more involved and several more diagrams need to be computed. Some examples of two-loop diagrams contributing to the form factor in FDH are given in Figure 12.

Although the computation of the bare result in FDH is almost equivalent to the one in CDR from the technical point of view, the renormalization is unfortunately a bit more involved. One reason for that is due to the absence of any symmetry protecting the $\epsilon$-scalar from acquiring an effective mass due to higher-order quantum effects. This is not happening in the massless case where no additional complications occur. It is exactly the contribution of diagram $(c)$ in Figure 12 that makes the $\epsilon$-scalar massive and we are obliged to restore the condition of zero mass in the renormalization procedure by introducing a $\epsilon$-mass counterterm.

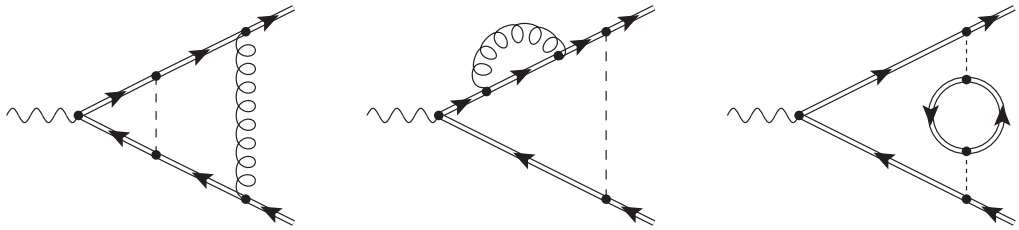

**Figure 12**. Sample two-loop diagrams contributing to the heavy quark form factor in FDH.

We will turn now to that problem and discuss the renormalization in FDH in detail.

### 9.1.1 Epsilon mass renormalization

Let us first consider for simplicity the QED case and study the photon two-point function. The well known sum of the 1-particle-irreducible ($1PI$) insertion into the photon propagator is given by $i\Pi^{\mu\nu}(q)$ and is graphically shown in Figure 13.

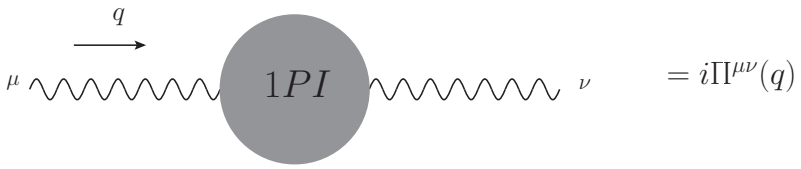


**Figure 13**. 1-particle-irreducible diagrams insert into the photon propagator.

The Ward identity guarantees that the tensor structure cannot contain a mass term and we get the following expression

$$\Pi^{\mu\nu}(q) = \Big(q^\mu q^\nu - q^2 g^{\mu\nu}\Big)\Pi(q^2). \tag{9.15}$$

If we now sum over all the $1PI$ contributions and we use again the Ward identity by taking into account that at least one end of this two-point function will connect to a fermion line in any $S$-matrix calculation, one finds that the exact two-point function of the photon reads as

$$\frac{-ig_{\mu\nu}}{q^2\Big(1+\Pi(q^2)\Big)}. \tag{9.16}$$

Since $\Pi(q^2)$ is regular at $q^2 = 0$, the propagator has a pole at $q^2 = 0$, which means that the photon remains massless at any order in perturbation theory. This is not the case for the $\epsilon$-scalar, where there is no Ward identity protecting the structure of $i\Pi^{\mu\nu}(q)$. As we will see the vacuum polarization of the $\epsilon$-scalar contains a term $\propto m^2 g^{\mu\nu}$ (where $m$ is the mass of the fermion). As a consequence, the $\epsilon$-scalar's

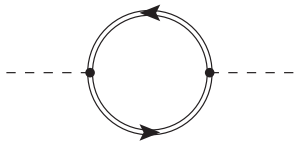

**Figure 14**. Diagram generating the mass shift of the $\epsilon$-scalar. The fermion loop is massive and we denote the fermion-multiplicity by $N_H$.

mass is effectively shifted away from zero, even if the $\epsilon$-scalar is massless at tree-level. Therefore we have to introduce a mass counterterm in the Lagrangian to restore the initial on-shell condition of a vanishing $\epsilon$-scalar mass [83].

If we now turn back to QCD, there is only one diagram at one-loop that effectively generates a mass term in the two-point $\epsilon$-scalar propagator, see Figure 14.

To compute the $\epsilon$-scalar mass counterterm (which we define as $\delta m_\epsilon^2$), we need to compute the full two-point function for the $\epsilon$-scalar as we have done before for the photon propagator. In this case the tensor structure is simply given by

$$-i\tilde{\Pi}^{\mu\nu}(q^2, m^2) = -i\Big(q^2\tilde{g}^{\mu\nu}\Big)\tilde{\Pi}(q^2, m^2)\,, \tag{9.17}$$

where

$$\tilde{\Pi}(q^2, m^2) = A + \frac{m^2}{q^2}B \tag{9.18}$$

and $A$ and $B$ are dimensionless quantities. We can then get the expression for $\delta m_\epsilon^2$ by noticing that, summing over all the $1PI$ diagrams results in

$$\frac{-i\tilde{g}_{\mu\nu}}{q^2\Big(1+\tilde{\Pi}(q^2, m^2)\Big) + \delta m_\epsilon^2} = \frac{-i\tilde{g}_{\mu\nu}}{q^2(1+A) + m^2 B + \delta m_\epsilon^2}\,. \tag{9.19}$$

In the expansion above we have explicitly inserted the $\delta m_\epsilon^2$ counterterm in the sum of the $1PI$ diagrams. Finally, in order to keep the $\epsilon$-scalar massless, we require for $\delta m_\epsilon^2$

$$\delta m_\epsilon^2 = -m^2 B = -a_e m^2 N_H \left(\frac{2}{\epsilon} + 2 + \epsilon\frac{12+\pi^2}{6} + \mathcal{O}\left(\epsilon^2\right)\right), \tag{9.20}$$

where $N_H$ denotes the number of heavy quark flavours. As a consequence, any time we encounter a massive loop diagram insertion as in Figure 14, we have to add the mass counterterm (9.20) in order to impose the on-shell condition of a massless $\epsilon$-scalar.

### 9.1.2 On shell $Z_{2,h}$, $Z_m$ and $\delta m$ in FDH

Let us start by first considering the calculation in CDR. We can compute $Z_{2,h}$ and $Z_m$ in the on-shell scheme from the perturbative expansion of the bare self energy

$\Sigma(p)$ as a function of the bare coupling $g_0$ and the bare mass $m_0$. $Z_{2,h}$ is then given by calculating the bare Feynman propagator

$$S_F(p) \equiv \frac{1}{\not{p} - m_0 - \Sigma(p)} = \frac{Z_{2,h}}{\not{p} - m} + (\text{terms regular at } p^2 = m^2)\,, \tag{9.21}$$

where $m$ is the renormalized mass. The bare self energy has the following structure,

$$\Sigma(p) = \sum_{n=1}^{\infty} \left[\frac{g_0^2}{(4\pi)^{D/2} p^{2\epsilon}}\right]^n \left(m_0 A_n(m_0^2/p^2) + (\not{p} - m_0) B_n(m_0^2/p^2)\right), \tag{9.22}$$

where the coefficients $A_n$ and $B_n$ are dimensionless functions. The expression of $Z_m$ and $Z_{2,h}$ can be written as a series expansion

$$\begin{aligned} \frac{m_0}{m} \equiv Z_m &= 1 + \sum_{n=1}^{\infty} \left[\frac{g_0^2}{(4\pi)^{D/2} m^{2\epsilon}}\right]^n M_n \\ (\not{p} - m) S_F(p) \mid_{\not{p}=m} \equiv Z_{2,h} &= 1 + \sum_{n=1}^{\infty} \left[\frac{g_0^2}{(4\pi)^{D/2} m^{2\epsilon}}\right]^n F_n. \end{aligned} \tag{9.23}$$

At this point we can substitute Eq. (9.22) into (9.21) and use the expressions in (9.23) to get the following relations for the coefficients:

$$\begin{aligned} M_1 &= -A_1 \\ M_2 &= -A_2 + A_1(A_1 + 2A_1' - B_1) \\ F_1 &= B_1 - 2\epsilon A_1 - 2A_1' \\ F_2 &= B_2 - 4\epsilon A_2 - 2A_2' + (2A_1' - B_1)^2 + 4A_1(A_1'' - B_1) \\ &\quad + 2(1+2\epsilon)A_1(\epsilon A_1 + 3A_1') - 6\epsilon A_1 B_1\,, \end{aligned} \tag{9.24}$$

where all the terms $A$ and $B$ are evaluated at $m_0^2/p^2 = 1$. In order to compute the derivatives we can differentiate directly the diagrams with respect to the bare mass and then compute the integrals on-shell. For example in the case of $A_1$ we can compute the derivative as follows

$$\frac{\partial A_1(x)}{\partial x} = \frac{\partial A_1(p^2/m_0^2)}{\partial m_0^2} \frac{\partial m_0^2}{\partial x} = -\frac{m_0^4}{p^2} \frac{\partial A_1}{\partial m_0^2}\,, \tag{9.25}$$

where we have defined $x = p^2/m_0^2$. In practice we differentiate the diagrams before applying the tensor reduction and then we impose the on-shell condition $p^2 = m_0^2$ to compute the integrals. This allows one to simplify the calculation and no off-shell integrals need to be calculated.

When we move to FDH there are basically two complications that we have to take into account. The first one is the usual inconvenience that the $\epsilon$-scalar introduces the new coupling $g_e$, which means that the previous expansions have to be computed

**Figure 15**. Sample two-loop contributions to the field renormalization of the heavy quark. The diagram on the r.h.s. shows the insertion of the mass counterterm $\delta m_\epsilon^2$.

in both $\alpha_s$ and $\alpha_e$. Secondly one has to introduce the $\epsilon$-scalar's mass counterterm, as described in the previous section. Concretely this means that one has to add the counterterm diagram in Figure 15, when we compute the bare self energy $\Sigma(p)$ in FDH.

The expression for $\bar{Z}_{2,h}$ in the on-shell scheme (OS-scheme) in FDH in terms of the bare couplings finally reads

$$\begin{aligned}
\bar{Z}_{2,h} = 1 &+ a_s(m^2)\, C_F \left[ -\frac{3}{\epsilon} - 4 - \epsilon\Big(8 + \frac{\pi^2}{4}\Big)\right] + a_e(m^2)\, C_F\, N_\epsilon \left[ -\frac{1}{2\epsilon} - \frac{1}{2} - \epsilon\Big(\frac{1}{2} + \frac{\pi^2}{24}\Big)\right] \\
&+ a_s^2(m^2) \left\{ C_F^2 \left[ \frac{9}{2\epsilon^2} + \frac{51}{4\epsilon} + \frac{433}{8} - \frac{49}{4}\pi^2 + 16\pi^2 \ln(2) - 24\zeta(3)\right] \right. \\
&\qquad + C_A C_F \left[ -\frac{11}{2\epsilon^2} - \frac{101}{4\epsilon} - \frac{803}{8} + \frac{49}{12}\pi^2 - 8\pi^2\ln(2) + 12\zeta(3) \right. \\
&\qquad\qquad \left. + N_\epsilon \Big(\frac{1}{4\epsilon^2} + \frac{11}{8\epsilon} + \frac{5}{24}\pi^2 + \frac{81}{16}\Big)\right] \\
&\qquad + C_F N_F \left[ \frac{1}{\epsilon^2} + \frac{9}{2\epsilon} + \frac{59}{4} + \frac{5}{6}\pi^2 \right] + C_F N_H \left[ \frac{2}{\epsilon^2} + \frac{19}{6\epsilon} + \frac{1139}{36} - \frac{7}{3}\pi^2 \right] \Big\} \\
&+ a_e^2(m^2)\, N_\epsilon \left\{ C_F^2 \left[ \frac{1}{\epsilon^2} + \frac{2}{\epsilon} + \frac{\pi^2}{2} - 3 + N_\epsilon\Big( -\frac{1}{8\epsilon^2} - \frac{3}{16\epsilon} - \frac{13}{48}\pi^2 + \frac{91}{32}\Big)\right] \right. \\
&\qquad + C_A C_F \left[ \Big( -\frac{1}{2\epsilon^2} - \frac{1}{\epsilon} - \frac{\pi^2}{4} + \frac{3}{2}\Big)\Big(1 - \frac{N_\epsilon}{2}\Big)\right] \\
&\qquad + C_F N_F \left[ \frac{1}{4\epsilon^2} + \frac{7}{8\epsilon} + \frac{21}{16} + \frac{5}{24}\pi^2 \right] + C_F N_H \left[ \frac{1}{4\epsilon^2} + \frac{7}{8\epsilon} - \frac{3}{16} + \frac{\pi^2}{24} \right] \Big\} \\
&+ a_s(m^2)\, a_e(m^2)\, N_\epsilon \left\{ C_F^2 \left[ \frac{3}{2\epsilon} + \frac{47}{4} - \pi^2 \right] + C_A C_F \left[ -\frac{9}{4\epsilon} - \frac{77}{8} + \frac{\pi^2}{6} \right] \right\} + \mathcal{O}(a^3)\,.
\end{aligned} \tag{9.26}$$

In order to renormalise the form factor we also need the expression for $\delta m$, which is easily obtained from $\bar{Z}_m$ by $\delta m = m - m_0 = m(1 - \bar{Z}_m)$ (where we denote $m$ to be

the renormalized mass) and it reads

$$\begin{aligned}
\frac{\delta m}{m} &= a_s(m^2)\,C_F\left[\frac{3}{\epsilon}+4+\epsilon\Big(8+\frac{\pi^2}{4}\Big)\right]+a_e(m^2)\,C_F\,N_\epsilon\left[\frac{1}{2\epsilon}+\frac{1}{2}+\epsilon\Big(\frac{1}{2}+\frac{\pi^2}{24}\Big)\right]\\
&\quad+a_s^2(m^2)\left\{C_F^2\left[-\frac{9}{2\epsilon^2}-\frac{45}{4\epsilon}-\frac{199}{8}+\frac{17}{4}\pi^2-8\pi^2\ln(2)+12\zeta(3)\right]\right.\\
&\qquad+C_AC_F\left[\frac{11}{2\epsilon^2}+\frac{91}{4\epsilon}+\frac{605}{8}-\frac{5}{12}\pi^2+4\pi^2\ln(2)-6\zeta(3)\right.\\
&\qquad\qquad\left.+N_\epsilon\Big(-\frac{1}{4\epsilon^2}-\frac{9}{8\epsilon}-\frac{5}{24}\pi^2-\frac{63}{16}\Big)\right]\\
&\qquad+C_FN_F\left[-\frac{1}{\epsilon^2}-\frac{7}{2\epsilon}-\frac{45}{4}-\frac{5}{6}\pi^2\right]\\
&\qquad\left.+C_FN_H\left[-\frac{1}{\epsilon^2}-\frac{7}{2\epsilon}-\frac{69}{4}+\frac{7}{6}\pi^2\right]\right\}\\
&\quad+a_e^2(m^2)\,N_\epsilon\left\{C_F^2\left[-\frac{1}{\epsilon^2}-\frac{3}{\epsilon}+\frac{\pi^2}{6}-6+N_\epsilon\Big(\frac{1}{8\epsilon^2}+\frac{13}{16\epsilon}-\frac{11}{48}\pi^2+\frac{75}{32}\Big)\right]\right.\\
&\qquad+C_AC_F\left[\Big(\frac{1}{2\epsilon^2}+\frac{3}{2\epsilon}-\frac{\pi^2}{12}+3\Big)\Big(1-\frac{N_\epsilon}{2}\Big)\right]\\
&\qquad+C_FN_F\left[-\frac{1}{4\epsilon^2}-\frac{5}{8\epsilon}-\frac{11}{16}-\frac{5}{24}\pi^2\right]\\
&\qquad\left.+C_FN_H\left[-\frac{1}{4\epsilon^2}-\frac{5}{8\epsilon}-\frac{3}{16}-\frac{\pi^2}{24}\right]\right\}\\
&\quad+a_s(m^2)\,a_e(m^2)\,N_\epsilon\left\{C_F^2\left[\frac{3}{2\epsilon}+\frac{23}{4}-\pi^2\right]+C_AC_F\left[\frac{3}{4\epsilon}+\frac{11}{8}+\frac{\pi^2}{2}\right]\right\}+\mathcal{O}(a^3)
\end{aligned}\tag{9.27}$$

up to the two-loop level.

### 9.1.3 UV renormalization of the form factor

Having calculated $\bar{Z}_{2,h}$, $\delta m$ and $\delta m_\epsilon^2$ we have now all the ingredients needed for the renormalization of the form factor. We also need the coupling renormalization, which is however identical to the one of the massless case (up to the introduction of the heavy quark flavour multiplicity), since the mass term does not introduce any UV singularity. The expressions for $Z_\alpha$ are then given by the simple replacement $N_F \to N_F + N_H$ in the expression used in the massless case.

We perform the UV renormalization as follows:

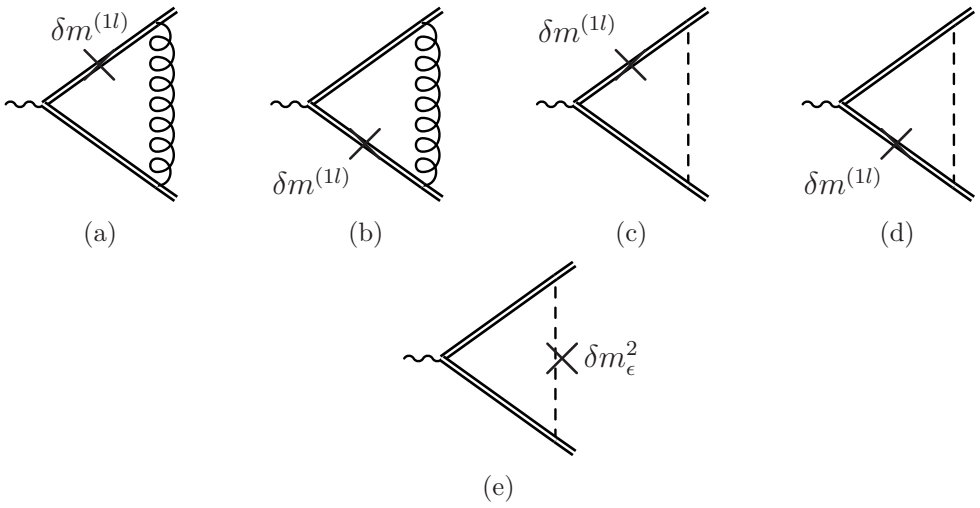


**Figure 16**. Counterterm diagrams originated from the mass renormalization (diagrams (a)–(d)) and from the $\epsilon$-scalar mass counterterm (diagram (e)).

- Add the wave function renormalization counterterm to the bare result.
- Then add the mass counterterm.
- Then add the $\epsilon$-scalar mass counterterm.
- Renormalise the coupling constants.

The wave-function renormalization counterterm is simply given by multiplying the bare result with $\bar{Z}_{2,h}$ given in (9.26). The mass counterterm is obtained by rewriting the bare mass as $m_0 = m - \delta m$ in the bare one-loop expression (before doing the tensor reduction) and then expanding in $\alpha_s$, $\alpha_e$. A similar procedure occurs for the $\epsilon$-scalar mass counterterm.

Schematically, the diagrams needed for the mass and $\epsilon$-scalar mass renormalization are listed in Figure 16.

For instance the diagram (a) in Figure 16 is given by

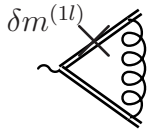


$$\stackrel{def}{=} -\frac{1}{m}\,\delta m^{(1l)}\left(\epsilon, m, \frac{\mu^2}{m^2}\right) \times \left( m \right), \tag{9.28}$$

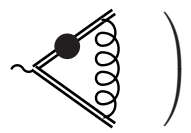

where the diagram on the r.h.s of Eq. (9.28) is defined as

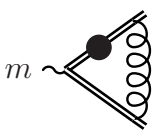


$$= m\, C_F\, a_s(m^2)$$

$$\times \int \mathfrak{D}^D k \, \frac{\mathcal{U}^\mu}{\left[(p_1+k)^2-m^2\right]^2\left[(p_2-k)^2-m^2\right]k^2}, \tag{9.29}$$

with $\mathfrak{D}^D k$ defined as

$$\int \mathfrak{D}^D k = \frac{1}{e^{-\epsilon\gamma_E}(4\pi)^\epsilon}\left(\frac{m^2}{\mu^2}\right)^\epsilon \int \frac{d^D k}{(2\pi)^{2(1-\epsilon)}}\,, \tag{9.30}$$

and the numerator given by

$$\mathcal{U}^\mu = v_Q\,\hat{\gamma}_\sigma[\not{p}_1+\not{k}+m][\not{p}_1+\not{k}+m]\hat{\gamma}^\mu[\not{k}-\not{p}_2+m]\hat{\gamma}_\sigma\,. \tag{9.31}$$

The diagram (e) in Figure 16 is instead given by

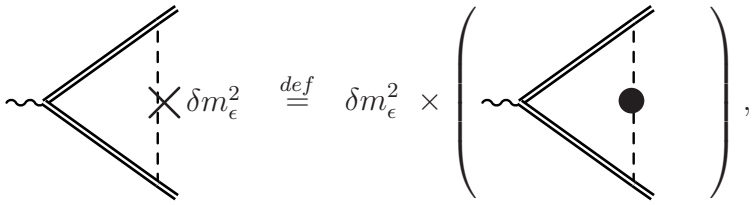


, (9.32)

where the diagram on the r.h.s. of Eq. (9.32) is defined as

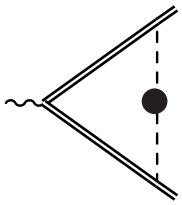

$= C_F\, a_e(m^2)$

$$\times \int \mathfrak{D}^D k \, \frac{\mathcal{U}^\mu}{\left[(p_1+k)^2-m^2\right]\left[(p_2-k)^2-m^2\right]k^4}, \tag{9.33}$$

and the numerator given by

$$\mathcal{U}^\mu = v_Q\,\tilde{\gamma}_\sigma[\not{p}_1+\not{k}+m]\hat{\gamma}^\mu[\not{k}-\not{p}_2+m]\tilde{\gamma}_\sigma\,. \tag{9.34}$$

With these expressions we can finally get the renormalized heavy quark form factor. The difference between the renormalized FDH result and the CDR up to two-loops is given by

$$\begin{aligned}\bar{F}_1(x) - F_1(x) = \left(\frac{\alpha_s}{4\pi}\right)^2 \Bigg\{ & C_A C_F \left[\frac{1}{3\epsilon}-\frac{8}{9}\right]\left(-1+\frac{x^2+1}{x^2-1}H(0;x)\right) \\ & + C_F^2\left[\frac{2\,(x^2-1)\,H(0;x) - 4\,(x^2+1)\,H(0,0;x)}{(x+1)^2}\right] + \mathcal{O}(\epsilon^1)\Bigg\} \\ & + \mathcal{O}(\alpha_s^3)\,,\end{aligned} \tag{9.35}$$

where we have set $\alpha_e = \alpha_s$ and $N_\epsilon = 2\epsilon$. This difference has to match with the difference given by the condition

$$\lim_{(N)_\epsilon \to 0} \bar{\mathbf{Z}}^{-1}(\{\alpha\}) \left[\left|\mathcal{M}_n(\{\alpha\}^f)\right\rangle\right]_{\alpha_i^f \to \zeta_{\alpha_i}\alpha_i} =$$

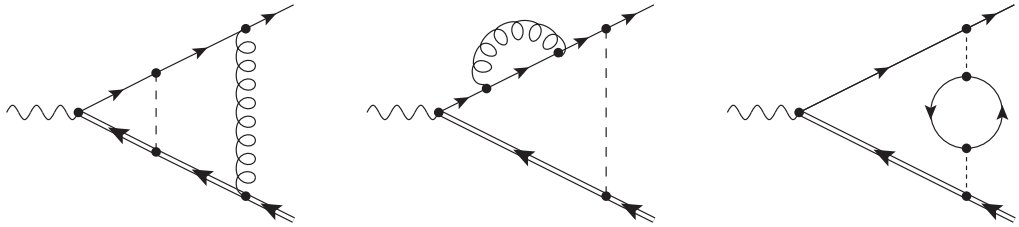

**Figure 17**. Sample two-loop diagrams contributing to the heavy-to-light form factor in FDH.

$$= \lim_{\epsilon\to 0}\ \mathbf{Z}^{-1}(\alpha_s)\left[\,|\mathcal{M}_n(\alpha_s^f)\rangle\right]_{\alpha_s^f\to\zeta_{\alpha_s}\alpha_s}\,, \tag{9.36}$$

which, after some algebra, is then given by

$$\begin{aligned}\bar{F}_1(x) - F_1(x) = \left(\frac{\alpha_s}{4\pi}\right)^2\Bigg\{ &-\frac{1}{\epsilon^2}\,C_F\left(\bar{\beta}^s_{20}-\beta^s_{20}\right)\left(-1+\frac{x^2+1}{x^2-1}H(0;x)\right)\\ &+\frac{1}{4\epsilon}\Bigg[C_F\left(\bar{\gamma}^{\rm cusp}_{20}(\beta)-\gamma^{\rm cusp}_{20}(\beta)-8\,\mathcal{F}_1^{\rm diff}\right)+2\left(\bar{\gamma}^{Q}_{20}-\gamma^{Q}_{20}\right)\\ &+8\,C_F\,\mathcal{F}_1^{\rm diff}\,\frac{x^2+1}{x^2-1}\,H(0;x)\Bigg]+\mathcal{O}(\epsilon^1)\Bigg\}+\mathcal{O}(\alpha_s^3)\,.\end{aligned} \tag{9.37}$$

Here $\mathcal{F}_1^{\rm diff} = \bar{\mathcal{F}}_{10}^{\rm ren} + \bar{\mathcal{F}}_{01}^{\rm ren} - \mathcal{F}_1^{\rm ren}$ is the difference of the UV renormalized one-loop coefficients. By comparing Eq. (9.35) with Eq. (9.37) it is already possible to read off the anomalous dimensions[12].

The FDH two-loop result in terms of $\alpha_s, \alpha_e$ and $N_\epsilon$ is given in Appendix A.

### 9.2 Heavy-to-light quark decay

The decay process $b \to uW^* \to ul\bar{\nu}_l$ has been computed in CDR at NNLO in [84–87]. Following the procedure applied in [84], we extend here the calculation to FDH. Examples of Feynman diagrams contributing to the NNLO corrections in FDH are shown in Figure 17.

The tensor structure of the vertex is the following:

$$\begin{aligned}\bar{\Gamma}^\mu(p_1,p_2) = {}& \bar{F}_1(q^2)\,\hat{\gamma}^\mu + \frac{1}{2m}\bar{F}_2(q^2)\,\hat{\sigma}^{\mu\nu}\,q_\nu + \frac{i}{2m}\bar{F}_3(q^2)\,q^\mu + \bar{G}_1(q^2)\,\hat{\gamma}^\mu\,\gamma_5\\ &+\frac{i}{2m}\bar{G}_2(q^2)\,\gamma_5\,q^\mu + \frac{i}{2m}\bar{G}_3(q^2)\,\gamma_5\,(p_1^\mu - p_2^\mu)\,.\end{aligned} \tag{9.38}$$

We are only interested in the form factor $\bar{F}_1$ and we can get it through a projector operator, similar to before. We compute the bare diagrams and perform the UV

[12]The explicit results for the anomalous dimensions, as well as the computation of the decoupling transformation, will be given in Section 9.3.

**Figure 18**. Non-vanishing diagrams contributing to the wave function renormalization of the light quark.

renormalization exactly as in the case of the heavy quark form factor (taking into account that here only one leg is massive). Again we will have to add a counterterm to subtract the $\epsilon$-scalar mass shift. The only missing term that was not present in the heavy form factor is the two-loop wave function renormalization $\bar{Z}_{2,l}$ of the light quark. The non-vanishing diagrams contributing to $\bar{Z}_{2,l}$ are shown in Figure 18. There is no one-loop contribution, since there is no scale entering in the corresponding diagrams. For the same reason, there is no contribution from the $\epsilon$-scalar mass counterterm at the two-loop level.

The expression for $\bar{Z}_{2,l}$ is given by

$$\bar{Z}_{2,l} = 1+C_F N_H \left[ a_s^2(m^2)\left(\frac{1}{2\epsilon}-\frac{5}{12}\right)+a_e^2(m^2)\, N_\epsilon \left(-\frac{1}{4\epsilon^2}+\frac{3}{8\epsilon}-\frac{13}{16}-\frac{\pi^2}{24}\right)+\mathcal{O}(\epsilon)\right]+\mathcal{O}(a^3)\,. \tag{9.39}$$

Following the notation of Eq. (9.11) we get for the bare one-loop result expressed in terms of the variable $y = q^2/m^2$

$$\begin{aligned}\bar{\mathcal{F}}_{10}(y) = -\,C_F \Bigg[ & \frac{1}{\epsilon^2} + \frac{1+2\,H(1;y)}{\epsilon} + 4 + \frac{\pi^2}{12} + 3\,H(1;y) + 2\,H(0,1;y) + 4\,H(1,1;y) \\ & + \epsilon \Bigg( 8 + \frac{\pi^2}{12} - \frac{\zeta(3)}{3} + \left(8+\frac{\pi^2}{6}\right) H(1;y) + 3\,H(0,1;y) + 6\,H(1,1;y) \\ & \quad + 8\,H(1,1,1;y) + 4\,H(-1,0,-1;-y) + 4\,H(0,-1,-1;-y) \\ & \quad + 2\,H(0,0,1;y)\Bigg)\Bigg] + \mathcal{O}\left(\epsilon^2\right)\,, \end{aligned} \tag{9.40a}$$

$$\bar{\mathcal{F}}_{01}(y) = C_F \left[1+\epsilon\Big(1+H(1;y)\Big)\right] + \mathcal{O}\left(\epsilon^2\right)\,. \tag{9.40b}$$

The renormalized difference between the FDH and the CDR result up to two-loop is given by

$$\bar{F}_1(y) - F_1(y) = \left(\frac{\alpha_s}{4\pi}\right)\frac{C_F}{2}$$

$$
\begin{aligned}
&+\left(\frac{\alpha_s}{4\pi}\right)^2\Bigg\{C_A C_F\left[-\frac{1}{4\epsilon^2}+\frac{-\frac{25}{36}-\frac{1}{3}H(1;y)-\frac{L}{6}}{\epsilon}+\frac{965}{216}+\frac{\pi^2}{24}+\frac{8}{9}H(1;y)+\frac{4}{9}L\right]\\
&\qquad-C_F^2\left[-\frac{1}{2\epsilon^2}+\frac{\frac{9}{4}+2H(1;y)+L}{\epsilon}+\frac{49}{8}+\frac{\pi^2}{4}+\big(6+4L\big)H(1;y)\right.\\
&\qquad\qquad\left.+8H(1,1;y)+2H(0,1;y)+\frac{7}{2}L+L^2\right]\\
&\qquad+C_F N_F\left[\frac{1}{4\epsilon}-\frac{3}{8}\right]-C_F N_H\,\frac{L}{2}+\mathcal{O}(\alpha_s^3)\,,
\end{aligned}
\tag{9.41}
$$

where $L=\ln\left(\frac{\mu^2}{m^2}\right)$ and we have set $\alpha_e=\alpha_s$ and $N_\epsilon=2\epsilon$. As for the massive form factor we can express the difference in terms of the anomalous dimensions

$$
\begin{aligned}
\bar{F}_1(y)-F_1(y)&=\left(\frac{\alpha_s}{4\pi}\right)\frac{\bar{\gamma}^q_{01}}{2\epsilon}\\
&+\left(\frac{\alpha_s}{4\pi}\right)^2\Bigg\{\frac{3}{16\epsilon^3}\,C_F\gamma_{10}^{\rm cusp}\Big(\bar{\beta}^s_{20}-\beta^s_{20}\Big)\\
&\qquad+\frac{1}{16\epsilon^2}\Bigg[\Big(\bar{\beta}^s_{20}-\beta^s_{20}\Big)\Big(8\,C_F-4\left(\gamma^Q_{10}+\gamma^q_{10}\right)+2\,C_F\gamma_{10}^{\rm cusp}\big(2\,H(1;y)+L\big)\Big)\\
&\qquad\quad-\bar{\gamma}^q_{01}\Big(4(\bar{\beta}^e_{11}+\bar{\beta}^e_{02})+2\bar{\gamma}^q_{01}\Big)-C_F\Big(\bar{\gamma}_{20}^{\rm cusp}-\gamma_{20}^{\rm cusp}-8\bar{\gamma}^q_{01}\Big)-4\,C_F\gamma_{10}^{\rm cusp}\mathcal{F}_1^{\rm diff}\Bigg]\\
&\qquad+\frac{1}{4\epsilon}\Bigg[-\frac{1}{2}C_F\big(2\,H(1;y)+L\big)\Big(\bar{\gamma}_{20}^{\rm cusp}-\gamma_{20}^{\rm cusp}+2\,\gamma_{10}^{\rm cusp}\,\mathcal{F}_1^{\rm diff}\Big)\\
&\qquad\quad+(\bar{\gamma}^Q_{20}-\gamma^Q_{20})+(\bar{\gamma}^q_{20}-\gamma^q_{20})+\bar{\gamma}^q_{11}+\bar{\gamma}^q_{02}-2\,N_H\,\bar{\gamma}^q_{01}\,L\\
&\qquad\quad+2\,\mathcal{F}_1^{\rm diff}\left(\gamma^Q_{10}+\gamma^q_{10}+\bar{\gamma}^q_{01}\right)+2\,\bar{\gamma}^q_{01}\,\mathcal{F}_1^{\rm fin}\Bigg]\Bigg\}\,,
\end{aligned}
\tag{9.42}
$$

with

$$
\mathcal{F}_1^{\rm diff}=\bar{\mathcal{F}}_{10}^{\rm ren}+\bar{\mathcal{F}}_{01}^{\rm ren}-\mathcal{F}_{10}^{\rm ren}\,,
\tag{9.43a}
$$

$$
\mathcal{F}_1^{\rm fin}=\lim_{\epsilon\to0}\left[\bar{\mathcal{F}}_{10}^{\rm ren}+\delta\bar{\mathbf{Z}}_{10}\right]=\lim_{\epsilon\to0}\left[\mathcal{F}_{10}^{\rm ren}+\delta\mathbf{Z}_1\right].
\tag{9.43b}
$$

The two-loop renormalized expression in terms of $\alpha_s,\alpha_e$ and $N_\epsilon$ is given in Appendix A.

### 9.3 Anomalous dimensions and decoupling transformation

Having calculated the heavy quark and the heavy-to-light form factors in FDH, we are finally able to extract the anomalous dimensions through Eq. (3.36) (expressed

in terms of $\alpha_s$ and $\alpha_e$ as in the massless case) by imposing the condition

$$\lim_{(N)_\epsilon \to 0} \bar{\mathbf{Z}}^{-1}(\{\alpha\}) \left[ |\mathcal{M}_n(\{\alpha\}^f)\rangle \right]_{\alpha_i^f \to \zeta_{\alpha_i} \alpha_i} = \text{finite} \tag{9.44}$$

as in Eq. (3.43) for CDR. For this we need the decoupling coefficients. $\zeta_{\alpha_s}$ has already been calculated in [49], while the coefficient $\zeta_{\alpha_e}$ will be calculated below. Using the results in Eq. (9.52) we finally get for $\gamma_{\text{cusp}}(\beta_{IJ})$ and $\gamma_Q$ in FDH

$$\begin{aligned}
\bar{\gamma}_{\text{cusp}}(\beta, \alpha_s) = \bar{\gamma}_{\text{cusp}}(\alpha_s)\, \beta \coth \beta + 8\, C_A \left(\frac{\alpha_s}{4\pi}\right)^2 \Bigg\{ & \beta^2 + \frac{\pi^2}{6} + \zeta_3 \\
& + \coth \beta \left[ \text{Li}_2(e^{-2\beta}) - 2\beta \ln(1 - e^{-2\beta}) - \frac{\pi^2}{6}(1+\beta) - \beta^2 - \frac{\beta^3}{3} \right] \\
& + \coth^2 \beta \left[ \text{Li}_3(e^{-2\beta}) + \beta\, \text{Li}_2(e^{-2\beta}) - \zeta_3 + \frac{\pi^2}{6}\beta + \frac{\beta^3}{3} \right] \Bigg\} + \mathcal{O}(\alpha^3)\,,
\end{aligned}$$

$$\begin{aligned}
\bar{\gamma}_Q = & \left(\frac{\alpha_s}{4\pi}\right)(-2C_F) \\
& + \left(\frac{\alpha_s}{4\pi}\right)^2 \left\{ C_A C_F \left[ -\frac{98}{9} + \frac{2}{3}\pi^2 - 4\zeta(3) + \frac{8}{9} N_\epsilon \right] + C_F N_F \frac{20}{9} \right\} + \mathcal{O}(\alpha^3).
\end{aligned} \tag{9.45}$$

The scheme dependence of $\bar{\gamma}_{\text{cusp}}(\beta, \alpha_s)$ is fully described by the already known $\bar{\gamma}_{\text{cusp}}(\alpha_s)$ from the massless case and no other scheme dependence enters in the expression. We also notice that there is no $\alpha_e$ term in both anomalous dimensions. Eq. (9.45) also shows that there is no scheme dependence at the one-loop level, as already discussed in [88]. With these results we have now the full understanding of the scheme dependence for any QCD process up to two-loops.

In the last part of this chapter we now focus on the calculation of the decoupling transformation.

In order to compute the decoupling transformations needed in Eq. (9.44) we apply the procedure described in Ref. [89] and build an effective Lagrangian in which the heavy quark flavors have been integrated out. As a consequence, the parameters and fields of the effective theory are in general different from the ones of the full theory. To relate the two theories we introduce decoupling constants in the following way

$$g^{0,f} = \zeta_g^0\, g^0, \qquad X^{0,f} = \sqrt{\zeta_X^0}\, X^0\,, \tag{9.46}$$

where $g$ and $X$ stand for parameters and fields of the theory, respectively. In this way we are able to relate the full and the effective bare QCD Lagrangian in terms of

the re-scaled parameters and fields

$$\mathcal{L}^f\left(g_s^{0,f},\, g_e^{0,f},\, \hat{A}^{0,f},\, \tilde{A}^{0,f}, \psi^{0,f}, \dots\right) = \mathcal{L}\left(g_s^0,\, g_e^0,\, \hat{A}^0,\, \tilde{A}^0,\, \psi^0, \dots, \{\zeta_X^0\}\right). \tag{9.47}$$

The decoupling constants can be obtained from a matching calculation. For $\zeta_{\hat{A}}^0$, which is related to the gluon field decoupling, for example, we get

$$\frac{-\hat{g}_{\mu\nu}}{p^2\left(1+\hat{\Pi}^{0,f}\right)} = i\int \mathrm{d}^4x\, e^{i\,px}\,\langle\, T\,\hat{A}_\mu^{0,f}(x)\,\hat{A}_\nu^{0,f}(0)\rangle \tag{9.48a}$$

$$= i\,\zeta_{\hat{A}}^0\int \mathrm{d}^4x\, e^{i\,px}\,\langle\, T\,\hat{A}_\mu^{0}(x)\,\hat{A}_\nu^{0}(0)\rangle = \zeta_{\hat{A}}^0\,\frac{-\hat{g}_{\mu\nu}}{p^2\left(1+\hat{\Pi}^{0}\right)}\,, \tag{9.48b}$$

where $\hat{\Pi}^0$ only contains light degrees of freedom and $\hat{\Pi}^{0,f}$ receives virtual contributions from the heavy quarks. From Eq. (9.48b) we then get

$$\zeta_{\hat{A}}^0 = \frac{1+\hat{\Pi}^0}{1+\hat{\Pi}^{0,f}}\,. \tag{9.49}$$

Since the l. h. s. does not depend on the kinematics of the process it is possible to consider the special case $p = 0$. The renormalization of the decoupling constant is done in the usual way by means of the renormalization constants in the effective and the full theory: $\zeta_{\hat{A}} = \bar{Z}_{\hat{A}}/\bar{Z}_{\hat{A}}^f\,\zeta_A^0$.

The same method also applies to the decoupling of the $\epsilon$-scalar field where, however, according to the discussion in Sec. 9.1.1 a mass counterterm has to be added

$$\tilde{\zeta}_{\tilde{A}}^0 = \left.\frac{1+\tilde{\Pi}^0}{1+\tilde{\Pi}^{0,f}+\delta m_\epsilon^2}\right|_{p\to 0}\,. \tag{9.50}$$

For the calculations in this work we need the decoupling transformations for $\alpha_s$ and $\alpha_e$ at the one loop level which can be obtained from a matching of the $\hat{g}q\bar{q}$ and $\tilde{g}q\bar{q}$ vertices, in analogy to Eqs. (9.48)

$$\zeta_{g_s}^0 = \frac{1}{\zeta_\psi^0\sqrt{\zeta_{\hat{A}}^0}}\,\frac{1+\Gamma_{\hat{g}q\bar{q}}^{0,f}}{1+\Gamma_{\hat{g}q\bar{q}}^0}\,, \qquad \zeta_{g_e}^0 = \frac{1}{\zeta_\psi^0\sqrt{\zeta_{\tilde{A}}^0}}\,\frac{1+\Gamma_{\tilde{g}q\bar{q}}^{0,f}}{1+\Gamma_{\tilde{g}q\bar{q}}^0}\,. \tag{9.51}$$

Since $\zeta_\psi^0$, $(\Gamma_{\hat{g}q\bar{q}}^{0,f}-\Gamma_{\hat{g}q\bar{q}}^0)$, and $(\Gamma_{\tilde{g}q\bar{q}}^{0,f}-\Gamma_{\tilde{g}q\bar{q}}^0)$ are of $\mathcal{O}(\alpha^2)$, the (bare) one-loop decoupling constants for $g_s$ and $g_e$ are entirely given by $\xi_{\hat{A}}^0$ and $\tilde{\xi}_{\tilde{A}}^0$, respectively. Using $(\zeta_{g_s}^0)^2 = \zeta_{\alpha_s}^0$ and $\zeta_{\alpha_s} = \bar{Z}_{\alpha_s}/\bar{Z}_{\alpha_s}^f$ and similar for the evanescent coupling we finally obtain

$$\zeta_{\alpha_s} = 1 + \left(\frac{\alpha_s}{4\pi}\right) N_H\,\frac{2}{3}\ln(\frac{\mu^2}{m^2}) + \mathcal{O}(\alpha^2)\,, \tag{9.52a}$$

$$\zeta_{\alpha_e} = 1 + \left(\frac{\alpha_e}{4\pi}\right) N_H\,\ln(\frac{\mu^2}{m^2}) + \mathcal{O}(\alpha^2) \tag{9.52b}$$

for the renormalized decoupling constants of $\alpha_s$ and $\alpha_e$.

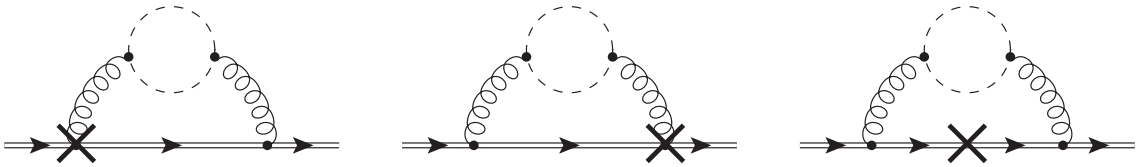

**Figure 19**. Two-loop graphs containing $\epsilon$-scalar contribution, which induce the scheme dependence in FDH. Double line denote heavy-quark propagators, while the crosses denote the insertion of the operator $(\omega + in \cdot D + i0)^{-1}$.

## 9.4 Alternative computation of the anomalous dimensions through SCET

As in the massless case we can determine the anomalous dimensions through a SCET computation. In that way we can determine $\gamma_Q$ by computing the heavy-to-light soft function and $\bar{\gamma}_{\text{cusp}}(\beta, \alpha_s)$ by computing the heavy-to-heavy anomalous dimension.

### 9.4.1 Scheme dependence of the heavy-to-light soft function and $\gamma_Q$

In Ref. [35] it has been shown that the top quark decay factorizes into regions where only soft radiations and (or) radiations collinear to the massless partons are present. The factorization consists of a hard function whose the renormalization group equation (RGE) depends on the heavy quark anomalous dimension, a quark jet function, and a soft function. In CDR, the jet and soft functions have been calculated up to the two-loop level in Refs. [31] and [90], respectively. In FDH, so far only the jet function is known [11] and it has been computed in Section 7.3.

The general relation between the corresponding IR anomalous dimensions is given by

$$\gamma_Q^{\text{RS}} = \gamma_S^{\text{RS}} + \gamma_J^{\text{RS}} - \gamma_q^{\text{RS}} \,, \tag{9.53}$$

where $\gamma_S^{\text{RS}}$ and $\gamma_J^{\text{RS}}$ are the (regularization-scheme dependent) anomalous dimensions of the soft and jet function. Eq. (9.53) is a direct consequence of the fact that the RGE of the factorization formula does not depend on the factorization scale. The values of $\gamma_J^{\text{RS}}$ and $\gamma_q^{\text{RS}}$ have been calculated in Section 7.3 (see also Ref. [11]) up to the two-loop level. In order to obtain the scheme-dependent quantity $\gamma_Q^{\text{RS}}$ we therefore have to compute $\gamma_S^{\text{RS}}$.

Extending the approach of Ref. [90], we define the scheme-dependent (bare) soft function as

$$S_{\text{bare}}^{\text{RS}}\left(\ln\frac{\Omega}{\mu}, \mu\right) := \int_0^{\Omega} d\omega \, \langle b_v | \, \bar{h}_v \, \delta(\omega + in \cdot D) \, h_v \, | b_v \rangle \,, \tag{9.54}$$

where $h_v$ are effective quark fields in HQET [91], $b_v$ are on-shell $b$-quark states with velocity $v$, and $n$ is a light-like 4-vector with $n \cdot v = 1$ and $n^2 = 0$. The normalization is fixed by $\langle b_v | \, \bar{h}_v \, h_v \, | b_v \rangle = 1$.

For the explicit calculations it is useful to express the soft function as a contour integral

$$S^{\rm RS}_{\rm bare}\Big(\ln\frac{\Omega}{\mu},\mu\Big)=\frac{1}{2\pi i}\oint\limits_{|\omega|=\Omega}d\omega\,\langle b_v|\,\bar h_v\,\frac{1}{\omega+in\cdot D+i0}\,h_v\,|b_v\rangle=\frac{1}{2\pi i}\oint\limits_{|\omega|=\Omega}d\omega\,\mathcal{S}^{\rm RS}_{\rm bare}\Big(\omega,\mu\Big) \tag{9.55}$$

and to work in Laplace space

$$s^{\rm RS}_{\rm bare}(\Omega):=\int_0^\infty d\omega\,\exp\Big(-\frac{\omega}{\Omega\,e^{\gamma_E}}\Big)\,\frac{1}{\pi}{\rm Im}\Big[\mathcal{S}^{\rm RS}_{\rm bare}(\omega)\Big]\,. \tag{9.56}$$

Since $h_v$ and $b_v$ are Heisenberg fields, the usual perturbative expansion results in loop diagrams contributing to the heavy quark propagator. As in the massless case, the scheme dependence is related to the UV singularities of such diagrams.

At the one-loop level there are no evanescent contributions since the $\epsilon$-scalar does not couple to heavy quark lines[13]. It is exactly three diagrams that induce a scheme-dependence of the soft function at the two-loop level. These are shown in Figure 19. For the explicit computation we generated the diagrams with QGRAF and applied a tensor reduction of the integrals with Reduze 2, where the master integrals needed in FDH are identical to the ones of CDR [90].

In FDH we then get up to the two-loop level

$$\begin{aligned}\bar s_{\rm bare}(\Omega)=1+a_s(\Omega)\,C_F\bigg[&-\frac{2}{\epsilon^2}+\frac{2}{\epsilon}-\frac{5}{6}\pi^2+\epsilon\Big(\frac{5}{6}\pi^2-\frac{14}{3}\,\zeta_3\Big)-\epsilon^2\Big(\frac{193}{720}\pi^4-\frac{14}{3}\,\zeta_3\Big)\bigg]\\&+a_s^2(\Omega)\,C_F\Big[C_F\bar K_F(\epsilon)+C_A\bar K_A(\epsilon)+T_RN_F\bar K_f(\epsilon)\Big]+\mathcal{O}(a^3)\,,\end{aligned} \tag{9.57}$$

where explicit NNLO expressions are given in Appendix A. Taking the limit $N_\epsilon\to 0$ in Eq. (9.57) we obtain the CDR result which is in agreement with the one given in Ref. [90].

As for the quark and gluon jet functions, the divergences of the soft function can be removed multiplicatively by means of a $Z$ factor

$$s^{\rm RS}_{\rm sub}(\Omega,\mu)=Z^{\rm RS}_S(\Omega,\mu)\,s^{\rm RS}_{\rm bare}(\Omega)\,. \tag{9.58}$$

To relate $Z^{\rm RS}_S(\Omega,\mu)$ with $\gamma^{\rm RS}_S$ we compare the RGE of the soft function,

$$\frac{d}{d\ln\mu}\,s^{\rm RS}_{\rm sub}(\Omega,\mu)=\bigg[\Big(\frac{d}{d\ln\mu}\,Z^{\rm RS}_S(\Omega,\mu)\Big)\Big(Z^{\rm RS}_S(\Omega,\mu)\Big)^{-1}\bigg]\,s^{\rm RS}_{\rm sub}(\Omega,\mu)\;, \tag{9.59}$$

[13]The explanation for the vanishing of the $\epsilon$-scalar coupling in the eikonal approximation will be shown explicitly in Section 9.4.2.

with the RGE written in terms of $\gamma_S^{\rm RS}$,

$$\frac{d}{d\ln\mu} s_{\rm sub}^{\rm RS}(\Omega,\mu) = \left[ C_F\,\gamma_{\rm cusp}^{\rm RS}\,L_\Omega - 2\gamma_S^{\rm RS} \right] s_{\rm sub}^{\rm RS}(\Omega,\mu)\,, \tag{9.60}$$

where $L_\Omega \equiv \ln(\Omega/\mu^2)$ and the cusp anomalous dimension is known from the massless case [11, 30, 34]. In FDH, the factor $\bar{Z}_S$ is given by

$$\begin{aligned}
\ln \bar{Z}_S = {} & \left(\frac{\alpha_s}{4\pi}\right)\left[\frac{C_F\,\bar{\gamma}_{10}^{\rm cusp}}{2\epsilon^2} - \frac{1}{\epsilon}\left(\frac{C_F\,\bar{\gamma}_{10}^{\rm cusp}}{2}\,L_\Omega - \bar{\gamma}_{10}^{S}\right)\right] \\
& + \left(\frac{\alpha_s}{4\pi}\right)^2\left[ - \frac{3\,C_F\,\bar{\gamma}_{10}^{\rm cusp}\,\bar{\beta}_{20}^{s}}{8\epsilon^3} + \frac{\bar{\beta}_{20}^{s}}{2\,\epsilon^2}\left(\frac{C_F\,\bar{\gamma}_{10}^{\rm cusp}}{2}\,L_\Omega - \bar{\gamma}_{10}^{S}\right) + \frac{C_F\,\bar{\gamma}_{20}^{\rm cusp}}{8\,\epsilon^2}\right. \\
& \left. - \frac{1}{2\,\epsilon}\left(\frac{C_F\,\bar{\gamma}_{20}^{\rm cusp}}{2}\,L_\Omega - \bar{\gamma}_{20}^{S}\right)\right] + \mathcal{O}(\alpha^3)\,.
\end{aligned} \tag{9.61}$$

Imposing minimal subtraction with $N_\epsilon$ as an independent quantity we can read off the soft anomalous dimension

$$\begin{aligned}
\bar{\gamma}_S = {} & \left(\frac{\alpha_s}{4\pi}\right)(-2C_F) \\
& + \left(\frac{\alpha_s}{4\pi}\right)^2\left\{ C_A C_F\left[\frac{110}{27} + \frac{\pi^2}{18} - 18\zeta(3) - \left(\frac{2}{27} - \frac{\pi^2}{36}\right)N_\epsilon\right] + C_F N_F\left[\frac{4}{27} + \frac{\pi^2}{9}\right]\right\} \\
& + \mathcal{O}(\alpha^3).
\end{aligned} \tag{9.62}$$

As a result, the soft anomalous dimension is scheme-independent at the one-loop level. Apart from $\bar{\gamma}_S$ it is also possible to extract the already known values of the cusp anomalous dimension as well as the $\beta$ functions in the FDH scheme. This provides a strong consistency check on the applied procedure. Using the obtained results together with Eq. (9.53) we finally find

$$\begin{aligned}
\bar{\gamma}_Q = {} & \left(\frac{\alpha_s}{4\pi}\right)(-2C_F) \\
& + \left(\frac{\alpha_s}{4\pi}\right)^2\left\{ C_A C_F\left[ - \frac{98}{9} + \frac{2}{3}\pi^2 - 4\zeta(3) + \frac{8}{9}N_\epsilon\right] + C_F N_F\,\frac{20}{9}\right\} + \mathcal{O}(\alpha^3)\,,
\end{aligned} \tag{9.63}$$

in perfect agreement with Eq. (9.45). For the IR anomalous dimension of the heavy quarks in the FDH scheme like $\bar{\gamma}_S$, it does not depend on $N_\epsilon$ at the one-loop level and receives RS-dependent contributions $\propto N_\epsilon$ at NNLO. Eq. (9.63) is the main result of this chapter. Finally we can obtain a finite and scheme independent soft function as

$$s_{\rm fin}(\Omega,\mu) = \lim_{(N)_\epsilon \to 0} s_{\rm sub}^{\rm RS}(\Omega,\mu)\,. \tag{9.64}$$

For completeness the explicit result is listed in Appendix A.

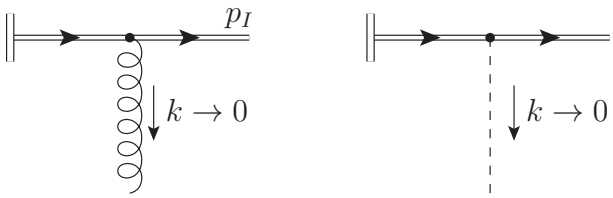


**Figure 20**. Coupling of gluons and $\epsilon$-scalars to heavy quark propagators in the eikonal approximation.

### 9.4.2 Determination of $\bar{\gamma}_{\text{cusp}}(\beta, \alpha_s)$

The velocity-dependent cusp anomalous dimensions can be extracted from the heavy-to-heavy anomalous dimension $\Gamma_{hh}$ for the pair production of massive quarks. Using CDR, $\Gamma_{hh}$ has been calculated in Ref. [92] in the framework of the eikonal approximation. This method can also be used to derive the respective quantity in FDH.

In general, the eikonal approximation is suited for describing the emission of soft gluons from partons in a hard scattering process, see the l. h. s. of Figure 20. For a vanishing gluon momentum, the Feynman rule for the coupling of gluons to massive quark propagators can be reduced to

$$\bar{u}(p_I)(-ig_s T^a)\,\hat{\gamma}^\mu \left[ i\frac{\not{p}_I + \not{k} + m_I}{(p_I+k)^2 - m_I^2} \right] \to \bar{u}(p_I)\, g_s T^a\, \hat{\gamma}^\mu \left[ \frac{\not{p}_I + m_I}{2\, p_I \cdot k} \right] \tag{9.65a}$$

$$= \bar{u}(p_I)\, g_s T^a \left[ (p_I)_\nu \frac{\{\hat{\gamma}^\mu, \hat{\gamma}^\nu\}}{2\, p_I \cdot k} \right] \tag{9.65b}$$

$$= \bar{u}(p_I)\, g_s T^a \left[ \frac{v_I^\mu}{v_I \cdot k} \right], \tag{9.65c}$$

where in the second line the Dirac equation $\bar{u}(p_I)(\not{p}_I - m_I) = 0$ has been used. Since the Feynman rule (9.65c) does not contain a Dirac matrix anymore, the evaluation of loop contributions is much simpler compared to ordinary QCD.

Extending this to the case of an $\epsilon$-scalar we get

$$\bar{u}(p_I)(-ig_e T^a)\,\tilde{\gamma}^\mu \left[ i\frac{\not{p}_I + \not{k} + m_I}{(p_I+k)^2 - m_I^2} \right] \to \bar{u}(p_I)\, g_e T^a \left[ (p_I)_\nu \frac{\{\tilde{\gamma}^\mu, \hat{\gamma}^\nu\}}{2\, p_I \cdot k} \right] = 0\,. \tag{9.66}$$

Due to the vanishing anticommutator, a direct coupling of $\epsilon$-scalars to massive quark propagators does not exist in the eikonal approximation.

Following the approach of Ref. [92], the heavy-to-heavy anomalous dimension for heavy quark pair production can be obtained from the UV-poles of corresponding eikonal diagrams with one- and two-loop examples shown in Figure 21. The scalar product of the two outgoing velocity vectors is in the following fixed by $v_I \cdot v_J = -\cosh \beta_{IJ}$ with $\beta_{IJ}$ given in Eq. (3.37). Since there is no direct coupling of $\epsilon$-scalars to massive quarks, the heavy-to-heavy anomalous dimension is scheme-independent

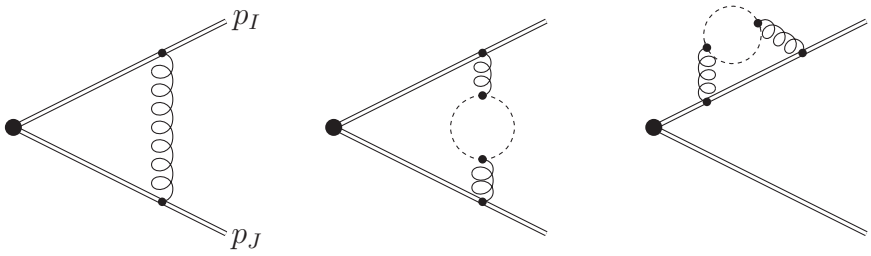


**Figure 21**. One- and two-loop contributions to the heavy-to-heavy anomalous dimension in the eikonal approximation. Since there is no direct coupling of $\epsilon$-scalars to massive quark propagators there is no evanescent contribution at the one-loop level.

at the one-loop level. At the two-loop level, however, closed $\epsilon$-scalar loops yield evanescent contributions $\propto \alpha_s N_\epsilon$.

Generalizing Eq. (14) of Ref. [47] to the case of FDH, the obtained result for the anomalous dimension can be represented as

$$\bar{\Gamma}_{hh}(v_I, v_J, \alpha_s) = C_F\, \bar{\gamma}_{\rm cusp}(\beta, \alpha_s) + 2\, \bar{\gamma}_Q(\alpha_s)\,. \tag{9.67}$$

Using Eq. (9.63), it is then possible to extract the velocity-dependent cusp anomalous dimension in FDH, which is

$$\begin{aligned}\bar{\gamma}_{\rm cusp}(\beta, \alpha_s) = \bar{\gamma}_{\rm cusp}(\alpha_s)\, \beta \coth\beta + 8\, C_A \left(\frac{\alpha_s}{4\pi}\right)^2 \Bigg\{ & \beta^2 + \frac{\pi^2}{6} + \zeta_3 \\ & + \coth\beta \left[ {\rm Li}_2(e^{-2\beta}) - 2\beta\, \ln(1 - e^{-2\beta}) - \frac{\pi^2}{6}\,(1+\beta) - \beta^2 - \frac{\beta^3}{3} \right] \\ & + \coth^2\beta \left[ {\rm Li}_3(e^{-2\beta}) + \beta\, {\rm Li}_2(e^{-2\beta}) - \zeta_3 + \frac{\pi^2}{6}\,\beta + \frac{\beta^3}{3} \right] \Bigg\} + \mathcal{O}(\alpha^3)\end{aligned} \tag{9.68}$$

in terms of the renormalized couplings. Eq. (9.68) is in perfect agreement with the previous extraction given in Eq. (9.45).

# 10 Concluding remarks

With the results presented in this thesis we complete the understanding of the scheme dependence of IR divergent NNLO virtual amplitudes. In particular, we have presented the generalization of this dependence to DRED, where we have to consider amplitudes with external $\epsilon$-scalars and, hence, need the corresponding anomalous dimension $\bar{\gamma}_\epsilon$. Furthermore, we have presented a SCET approach to the scheme dependence and derived all anomalous dimensions again in this approach. In this way FDH and DRED are shown to be perfectly consistent IR regularization schemes (at least) up to NNLO, as long as the UV renormalization is done consistently. Concretely, this means that the various couplings $\alpha_s$, $\alpha_e$ and $\alpha_{4\epsilon,i}$ have to be distinguished. This is also the case in FDH, where at NNLO the only concrete modification appears due to the UV renormalization of the NLO virtual amplitudes. Our results and definitions of FDH are perfectly consistent with the results and definitions proposed in [23, 29].

Obviously, the virtual amplitudes are not the only ingredients needed for a calculation of a physical quantity. At NNLO, also double-real and real-virtual corrections must be considered. Furthermore, if there are initial-state hadrons, a counterterm for the initial-state collinear singularities is required. All these additional contributions are also regularization-scheme dependent and only once all parts are combined to a physical cross section, the regularization-scheme dependence cancels.

In virtually all NNLO calculations of cross sections completed so far, CDR has been used. The results presented in this thesis allow for using any of the other regularization schemes for the calculation of the virtual corrections. Using a scheme different from CDR often facilitates the use of efficient calculational techniques for loop amplitudes. The results can then be translated to obtain the virtual corrections in CDR and can be combined with the additional parts mentioned above, obtained again in CDR.

Of course, it is not imperative to treat the additional contributions (i.e. the contributions other than the NNLO virtual corrections) in CDR. Also for these terms other schemes might offer advantages. In fact, a modification of a subtraction scheme at NNLO to the HV scheme has been presented recently [93], resulting in a reduction of the algebraic complexity.

The question of the scheme (in)dependence of a full cross section at NNLO becomes particularly transparent if the calculation is performed in a SCET inspired way. Following ideas of the slicing method [94] and the $q_T$-subtraction method [95], the cross section is split into two regions, a 'hard' region and a 'soft' region. In the hard region not all radiation in addition to the final state under consideration is soft (or collinear). At least one of the emitted gluons is hard. Here we are effectively dealing with a NLO calculation of a process for a final state with an additional parton and the scheme independence of cross sections at NLO is well established [16]. In the soft region all additional radiation is soft (or collinear) and a true NNLO calculation

is required. For this part a SCET approach is used. This idea has first been applied to the decay of a top quark [35] $t \to W\,b\,X$ where the invariant mass of the jet $b + X$ has been used for the split. Recently, the N-jettiness event-shape variable has been used to obtain a similar setup for differential NNLO calculations of Higgs plus jet [36], $W$ plus jet [37] and Drell-Yan production [38].

In the soft region, the cross section factorizes into a product of hard-, soft- and jet functions (and beam functions if there are initial-state hadrons). The corresponding bare functions are all IR divergent and scheme dependent. However, we have shown that the properly IR subtracted soft functions $s_{\text{fin}}$, Eqs. (7.31) and (A.25), and jet functions $\jmath_{q\,\text{fin}}$ and $\jmath_{g\,\text{fin}}$, Eqs. (7.44) and (7.50), are not only finite but also scheme independent, at least up to NNLO. The same holds true for the hard function [96, 97] that is closely related to $\mathcal{M}_{\text{fin}}$, Eq. (6.3). Hence the cross section in the soft limit can be expressed in terms of these IR subtracted quantities in a manifestly scheme-independent way.

The soft function that is required for the processes mentioned above is not the soft function for Drell-Yan or Higgs production as we have computed. However, the procedure to perform the IR subtraction (or UV renormalization in SCET language) consistent with the regularization scheme used in the computation of the bare soft function is exactly the same.

Since the soft, hard and jet functions are separately scheme independent, it is possible to use different schemes in the computation of the various parts contributing to the cross section. For example, the calculation of the virtual corrections (i.e. the hard function) in FDH, where the helicity and unitarity methods are applicable, can easily be combined with the soft or jet function computed in CDR. We are convinced that this flexibility will be very beneficial for further developments of fully differential NNLO calculations.

## Acknowledgments

First of all I wish to express all my gratitude to my supervisor Adrian Signer for the trust he decided to put in me. I must thank him for having been a firm guide and for supporting and helping me in my daily work. His suggestions and advice on technical aspects have been fundamentally helpful. I must thank him for all the time he has spent in listening to my doubts, problems and sometimes even crazy ideas I had in mind. And not least I appreciate his human side, which created such a great atmosphere at work during these four years of PhD. So thanks a lot Adrian, I am indebted to you!

My gratitude goes then to my collaborators Dominik Stöckinger, Alessandro Broggio and Christoph Gnendiger for the fruitful discussions and successful work we had: without them the results in this thesis would not have been possible.

Special thanks also to Thomas Gehrmann, who helped me in looking for the PhD position. I am also very grateful to him for having always been available and willing to help.

I would like to thank Gionata Luisoni and Pier Francesco Monni from whom I learned a lot about physics and mostly for being great friends with whom I shared unforgettable time! To Lorenzo Tancredi for his patience in listening to my doubts and helping me in computer programming: his expertise has been fundamentally helpful. To Paolo Torrielli and Marco Pruna for their help and suggestions in debugging my codes and for always being available for fruitful discussions.

I am grateful to all the members of the physics institute at the university of Zurich and at the Paul Scherrer Institute for having made such a great environment in which to work.

I am very thankful to Steven Knight, Daniel Hulme, Christoph Gnendiger and Cristina Morisoli for reading my thesis and for pointing out some typographical mistakes. I also thanks Daniel for having played top level tennis with me.

Big thanks to all my friends in Zurich (in particular to Danilo and Adriano) for all the great time spent together and for having always made me feel right at home. A special thanks goes to my flatmates Steven, Elisa and Diogo.

I am also very grateful to my old friends, especially to all the members of my band: going back to Ticino on Friday night to play with you has always been indispensable. A big hug to Moyra and Trevor Elliot, whom are always in my heart and whom I consider part of my family. My deepest gratitude goes then to my mother, brothers and relatives without whom I could never become the person I am today.

Not least all my deepest gratitude and love to Cristina for always filling my heart with joy and being my biggest support I have in life. I must thank her for always being there for me and for sharing her life with me!

Last but not least I have to conclude by saying that these years of my PhD have been unfortunately the most difficult in my life, and not because of physics.

The loss of my grandfather at the beginning of my PhD and especially losing my father and my sister in law later, pushed me seriously through the mill. These big losses made an enormous change in my life and hence, I can not consider myself the same person I was at the beginning of the PhD. I would like to express my deepest gratitude to those people for having been a big part of my life. For that reason I would like to thank *nonno* Remo for his wisdom and love and for having founded H.C. Ambrí-Piotta, thus far the best ice hockey team in the world! Thanks to Leda, for having not only been my sister in law, but also my colleague clarinet in our band and mostly a friend with whom I have shared unforgettable time, together with my brother and the rest of my family. I will never forget your shiny smile until the very end, for the rest of my life. Last but not least you *papà*, for the infinite love you gave me! Apart from being my father, you have been the most important teacher in my life: almost everything I am today I owe to you. From you I inherited the passion of skiing, hiking, studying, playing music, among many other activities. I inherited the love of our region and their traditions. You were for many years the conductor of our band and my teacher at secondary school. I shared with you so many things that it is impossible for me to even try to classify them. And mostly you have always put incredible trust in me, especially in my studies. I will never forget the pride you felt because I was doing a PhD. Unfortunately you can not see the end of this journey, but this thesis is for you *papà*!

# A Explicit expressions for the soft and jet functions and for the form factors

In this appendix we give the explicit results for several quantities as a perturbative expansion. We use the conventions specified in Section 7.1. For most results it will be sufficient to expand a quantity $X$ in $\alpha_s$ and $\alpha_e$ and write, instead of Eq. (5.1),

$$X^{\rm RS} = \sum_{m,n}^{\infty} \left(\frac{\alpha_s}{4\pi}\right)^m \left(\frac{\alpha_e}{4\pi}\right)^n X^{\rm RS}_{mn} \,. \tag{A.1}$$

As in Eq. (7.5) we will use the short-hand notation $X_{mn} \equiv X^{\rm HV}_{mn} = X^{\rm CDR}_{mn}$ and $\bar{X}_{mn} \equiv X^{\rm FDH}_{mn} = X^{\rm DRED}_{mn}$. The explicit results for scheme-dependent quantities will be given in the FDH/DRED scheme but we can obtain the corresponding coefficients in the HV/CDR scheme as $X_{mn} = \lim_{N_\epsilon \to 0} \bar{X}_{mn}$.

## A.1 Soft function

It is convenient to solve the RGEs for the soft functions in Eq. (7.28) order by order in $\alpha_s$. By using the expansion coefficients of the anomalous dimensions in Eq. (7.8) one obtains the following scheme independent result

$$\begin{aligned} s_{\rm fin}(\kappa,\mu) = 1 &+ \left(\frac{\alpha_s}{4\pi}\right)\left[2\Gamma_{10}L_\kappa^2 + 2\gamma^W_{10}L_\kappa + c^W_1\right] \\ &+ \left(\frac{\alpha_s}{4\pi}\right)^2\left[2\left(\Gamma_{10}\right)^2 L_\kappa^4 - \frac{4\Gamma_{10}}{3}\left(\beta^s_{20} - 3\gamma^W_{10}\right)L_\kappa^3\right. \\ &+ 2\left(\Gamma_{20} + \left(\gamma^W_{10}\right)^2 - \beta^s_{20}\gamma^W_{10} + \Gamma_{10}c^W_1\right)L_\kappa^2 \\ &\left.+ 2\left(\gamma^W_{20} + \gamma^W_{10}c^W_1 - \beta^s_{20}c^W_1\right)L_\kappa + c^W_2\right], \end{aligned} \tag{A.2}$$

where $\Gamma_{\rm cusp} = C_R\,\gamma_{\rm cusp}$ and

$$\gamma^W_{10} = 0\,, \tag{A.3a}$$

$$\gamma^W_{20} = C_R\left[C_A\left(-\frac{808}{27} + \frac{11}{9}\pi^2 + 28\zeta_3\right) + N_F\left(\frac{112}{27} - \frac{2}{9}\pi^2\right)\right], \tag{A.3b}$$

and the one and two-loop non-logarithmic coefficients have the expressions

$$c^W_1 = C_R\frac{\pi^2}{3}\,, \tag{A.4a}$$

$$c^W_2 = C_R\left[C_A\left(-\frac{22\zeta_3}{9} + \frac{2428}{81} + \frac{67\pi^2}{54} - \frac{\pi^4}{3}\right) + C_R\frac{\pi^4}{18} + N_F\left(\frac{4\zeta_3}{9} - \frac{5\pi^2}{27} - \frac{328}{81}\right)\right]. \tag{A.4b}$$

The result in Eq. (A.2) is in agreement with previous calculations in [58, 62].

### A.2 Quark jet function

Here we list the explicit two-loop coefficients entering Eq. (7.37):

$$\bar{\jmath}_{20}^{q;F} = \frac{8}{\epsilon^4} + \frac{12}{\epsilon^3} + \Big(\frac{65}{2} - \frac{8\pi^2}{3}\Big)\frac{1}{\epsilon^2} + \Big(\frac{311}{4} - 5\pi^2 - 20\,\zeta_3\Big)\frac{1}{\epsilon} + \frac{1437}{8} - \frac{57\pi^2}{4} + \frac{5\pi^4}{18} - 54\zeta_3\,, \tag{A.5a}$$

$$\bar{\jmath}_{20}^{q;A} = \frac{11}{3\epsilon^3} + \Big(\frac{233}{18} - \frac{\pi^2}{3}\Big)\frac{1}{\epsilon^2} + \Big(\frac{4541}{108} - \frac{11\pi^2}{6} - 20\zeta_3\Big)\frac{1}{\epsilon} + \frac{86393}{648} - \frac{221\pi^2}{36} - \frac{37\pi^4}{180} - \frac{142}{3}\zeta_3 + \frac{N_\epsilon}{2}\Big(-\frac{1}{3\epsilon^3} - \frac{25}{18\epsilon^2} + \big(\frac{\pi^2}{6} - \frac{523}{108}\big)\frac{1}{\epsilon} - \frac{10219}{648} + \frac{25\pi^2}{36} + \frac{8\zeta_3}{3}\Big)\,, \tag{A.5b}$$

$$\bar{\jmath}_{20}^{q;f} = -\frac{4}{3\epsilon^3} - \frac{38}{9\epsilon^2} + \Big(-\frac{373}{27} + \frac{2\pi^2}{3}\Big)\frac{1}{\epsilon} - \frac{7081}{162} + \frac{19\pi^2}{9} + \frac{32}{3}\zeta_3\,, \tag{A.5c}$$

$$\bar{\jmath}_{02}^{q;F} = \frac{N_\epsilon^2}{4}\Big(-\frac{1}{2\epsilon^2} - \frac{7}{4\epsilon} - \frac{33}{8} + \frac{\pi^2}{4}\Big) + \frac{N_\epsilon}{2}\Big(\frac{2}{\epsilon^2} + \frac{8}{\epsilon} + 24 - \pi^2\Big)\,, \tag{A.5d}$$

$$\bar{\jmath}_{02}^{q;A} = \frac{N_\epsilon^2}{4}\Big(\frac{1}{\epsilon^2} + \frac{4}{\epsilon} + 12 - \frac{\pi^2}{2}\Big) + \frac{N_\epsilon}{2}\Big(-\frac{1}{\epsilon^2} - \frac{4}{\epsilon} - 12 + \frac{\pi^2}{2}\Big)\,, \tag{A.5e}$$

$$\bar{\jmath}_{02}^{q;f} = \frac{N_\epsilon}{2}\Big(\frac{1}{\epsilon^2} + \frac{11}{2\epsilon} + \frac{89}{4} - \frac{\pi^2}{2}\Big)\,, \tag{A.5f}$$

$$\bar{\jmath}_{11}^{q;F} = \frac{N_\epsilon}{2}\Big(-\frac{4}{\epsilon^3} - \frac{14}{\epsilon^2} + \big(\frac{5\pi^2}{3} - 39\big)\frac{1}{\epsilon} - \frac{201}{2} + 6\pi^2 + 18\zeta_3\Big)\,, \tag{A.5g}$$

$$\bar{\jmath}_{11}^{q;A} = \frac{N_\epsilon}{2}\Big(-\frac{11}{2\epsilon} - \frac{129}{4} + \frac{\pi^2}{3} + 6\zeta_3\Big)\,. \tag{A.5h}$$

After renormalization and setting $\epsilon \to 0$ we obtain a finite and scheme independent quark-jet function. The terms containing $\alpha_e$ cancel and we are left with only $\alpha_s$ dependent terms. In Laplace space the quark-jet function reads

$$\begin{aligned} \jmath_{q\,\mathrm{fin}}(Q^2,\mu) = 1 &+ \frac{\alpha_s}{4\pi}\Big[\Gamma_{10}\frac{L_Q^2}{2} + \gamma_{10}^{J_q} L_Q + c_1^{J_q}\Big] \\ &+ \Big(\frac{\alpha_s}{4\pi}\Big)^2\Big[(\Gamma_{10})^2\,\frac{L_Q^4}{8} + \Big(-\beta_{20}^s + 3\gamma_{10}^{J_q}\Big)\Gamma_{10}\frac{L_Q^3}{6} \\ &\qquad + \Big(\Gamma_{20} + \big(\gamma_{10}^{J_q}\big)^2 - \beta_{20}^s\gamma_{10}^{J_q} + c_1^{J_q}\Gamma_{10}\Big)\frac{L_Q^2}{2} \\ &\qquad + \Big(\gamma_{20}^{J_q} + \gamma_{10}^{J_q}c_1^{J_q} - \beta_{20}^s c_1^{J_q}\Big)L_Q + c_2^{J_q}\Big]\,, \end{aligned} \tag{A.6}$$

where here $\Gamma_{\mathrm{cusp}} = C_F\,\gamma_{\mathrm{cusp}}$ and

$$c_1^{J_q} = C_F\Big(7 - \frac{2\pi^2}{3}\Big)\,, \tag{A.7a}$$

$$c_2^{J_q} = C_F^2\Big(\frac{205}{8} - \frac{97\pi^2}{12} + \frac{61\pi^4}{90} - 6\zeta_3\Big) + C_F C_A\Big(\frac{53129}{648} - \frac{155\pi^2}{36} - \frac{37\pi^4}{180} - 18\zeta_3\Big)$$

$$+ C_F T_R N_F \Big(\frac{13\pi^2}{9} - \frac{4057}{162}\Big) \tag{A.7b}$$

and is in agreement with previous results [31].

### A.3 Gluon jet function

Here we list the explicit two-loop coefficients entering Eq. (7.48):

$$\begin{aligned}
\bar{\jmath}_{20}^{g;\,AA} &= \frac{8}{\epsilon^4} + \frac{55}{3\epsilon^3} + \frac{1}{\epsilon^2}\Big(-3\pi^2 + \frac{152}{3}\Big) + \frac{1}{\epsilon}\Big(-40\zeta_3 - \frac{143\pi^2}{18} + \frac{3638}{27}\Big) \\
&\quad + \frac{13\pi^4}{180} - \frac{352\zeta_3}{3} - \frac{617\pi^2}{27} + \frac{57415}{162} \\
&\quad + \frac{N_\epsilon}{2}\Big[-\frac{5}{3\epsilon^3} - \frac{62}{9\epsilon^2} + \frac{1}{\epsilon}\Big(\frac{13\pi^2}{18} - \frac{214}{9}\Big) + \frac{85\pi^2}{27} - \frac{12371}{162} + \frac{32}{3}\zeta_3\Big] \\
&\quad + \frac{N_\epsilon^2}{4}\Big[\frac{1}{9\epsilon^2} + \frac{16}{27\epsilon} + \frac{56}{27} - \frac{\pi^2}{18}\Big], \qquad \text{(A.8a)} \\
\bar{\jmath}_{20}^{g;\,Af} &= -\frac{20}{3\epsilon^3} - \frac{188}{9\epsilon^2} + \frac{1}{\epsilon}\Big(\frac{26\pi^2}{9} - \frac{536}{9}\Big) + \frac{80\zeta_3}{3} + \frac{262\pi^2}{27} - \frac{12880}{81} \\
&\quad + \frac{N_\epsilon}{2}\Big(\frac{8}{9\epsilon^2} + \frac{104}{27\epsilon} + \frac{320}{27} - \frac{4\pi^2}{9}\Big), \qquad \text{(A.8b)} \\
\bar{\jmath}_{20}^{g;\,Ff} &= -\frac{2}{\epsilon} - \frac{55}{3} + 16\zeta_3\,, \qquad \text{(A.8c)} \\
\bar{\jmath}_{20}^{g;\,ff} &= \frac{16}{9\epsilon^2} + \frac{160}{27\epsilon} + 16 - \frac{8\pi^2}{9}\,, \qquad \text{(A.8d)} \\
\bar{\jmath}_{11}^{g;\,Af} &= 3\frac{N_\epsilon}{2}\,, \qquad \text{(A.8e)} \\
\bar{\jmath}_{11}^{g;\,Ff} &= \frac{N_\epsilon}{2}\Big(\frac{2}{\epsilon} + 11\Big). \qquad \text{(A.8f)}
\end{aligned}$$

After renormalization and setting $\epsilon \to 0$ we obtain a finite and scheme independent gluon jet function. The structure in Laplace space is the same as for the quark jet function, Eq. (A.6),

$$\begin{aligned}
\jmath_{g\,\mathrm{fin}}(Q^2,\mu) &= 1 + \frac{\alpha_s}{4\pi}\Big[\Gamma_{10}\frac{L_Q^2}{2} + \gamma_{10}^{J_g} L_Q + c_1^{J_g}\Big] \\
&\quad + \Big(\frac{\alpha_s}{4\pi}\Big)^2\Big[(\Gamma_{10})^2\frac{L_Q^4}{8} + \Big(-\beta_{20}^s + 3\gamma_{10}^{J_g}\Big)\Gamma_{10}\frac{L_Q^3}{6} \\
&\qquad + \Big(\Gamma_{20} + \big(\gamma_{10}^{J_g}\big)^2 - \beta_{20}^s\gamma_{10}^{J_g} + c_1^{J_g}\Gamma_{10}\Big)\frac{L_Q^2}{2} \\
&\qquad + \Big(\gamma_{20}^{J_g} + \gamma_{10}^{J_g} c_1^{J_g} - \beta_{20}^s c_1^{J_g}\Big)L_Q + c_2^{J_g}\Big]\,, \qquad \text{(A.9)}
\end{aligned}$$

where here $\Gamma_{\mathrm{cusp}} = C_A\,\gamma_{\mathrm{cusp}}$. The coefficients are given by

$$c_1^{J_g} = C_A\Big(\frac{67}{9} - \frac{2\pi^2}{3}\Big) - \frac{20}{9}N_F T_R\,, \qquad \text{(A.10a)}$$

$$
\begin{aligned}
c_2^{J_g} &= C_A^2\Big(\frac{20215}{162} - \frac{362\pi^2}{27} - \frac{88\zeta_3}{3} + \frac{17\pi^4}{36}\Big) \\
&+ C_A N_F T_R\Big( - \frac{1520}{27} + \frac{134\pi^2}{27} - \frac{16\zeta_3}{3}\Big) \\
&+ C_F N_F T_R\Big( - \frac{55}{3} + 16\zeta_3\Big) + N_F^2 T_R^2\Big(\frac{400}{81} - \frac{8\pi^2}{27}\Big)
\end{aligned} \tag{A.10b}
$$

and agree with Ref. [32].

### A.4 $\epsilon$-scalar jet function

The results in this subsection depend on $\alpha_{4\epsilon}$ as well as $\alpha_s$ and $\alpha_e$. We start by listing the explicit two-loop coefficients entering Eq. (7.53):

$$
\begin{aligned}
\bar{\jmath}_{200}^{\epsilon;\,AA} &= \frac{8}{\epsilon^4} + \frac{1}{\epsilon^3}\Big(\frac{59}{3} - \frac{N_\epsilon}{6}\Big) + \frac{1}{\epsilon^2}\Big(\frac{493}{9} - 3\pi^2 - \frac{7\,N_\epsilon}{9}\Big) \\
&+ \frac{1}{\epsilon}\Big(\frac{31675}{216} - \frac{17\pi^2}{2} - 40\zeta_3 + N_\epsilon(\frac{\pi^2}{12} - \frac{625}{216})\Big) \\
&+ \frac{502189}{1296} - \frac{445\pi^2}{18} + \frac{13\pi^4}{180} - \frac{376}{3}\zeta_3 + N_\epsilon\Big( - \frac{12787}{1296} + \frac{7\pi^2}{18} + \frac{4}{3}\zeta_3\Big)\,,
\end{aligned} \tag{A.11a}
$$

$$
\bar{\jmath}_{200}^{\epsilon;\,Af} = -\frac{4}{3\epsilon^3} - \frac{44}{9\epsilon^2} + \frac{1}{\epsilon}\Big(\frac{2\pi^2}{3} - \frac{457}{27}\Big) - \frac{9037}{162} + \frac{22\pi^2}{9} + \frac{32}{3}\zeta_3\,, \tag{A.11b}
$$

$$
\bar{\jmath}_{020}^{\epsilon;\,Af} = \frac{1}{\epsilon^2}\Big( - 2 + N_\epsilon\Big) + \frac{1}{\epsilon}\Big( - 9 + N_\epsilon\frac{9}{2}\Big) - \frac{61}{2} + N_\epsilon\frac{61}{4} + \pi^2 - N_\epsilon\frac{\pi^2}{2}\,, \tag{A.11c}
$$

$$
\bar{\jmath}_{020}^{\epsilon;\,Ff} = \frac{1}{\epsilon^2}\big(4 - N_\epsilon\big) + \frac{1}{\epsilon}\big(18 - 7\frac{N_\epsilon}{2}\big) + 61 - N_\epsilon\frac{33}{4} - 2\pi^2 + N_\epsilon\frac{\pi^2}{2}\,, \tag{A.11d}
$$

$$
\bar{\jmath}_{020}^{\epsilon;\,ff} = \frac{4}{\epsilon^2} + \frac{16}{\epsilon} + 48 - 2\pi^2\,, \tag{A.11e}
$$

$$
\bar{\jmath}_{002}^{\epsilon;\,AA} = \frac{3}{8\epsilon}\big(1 - N_\epsilon\big) + \frac{39}{16} - N_\epsilon\frac{39}{16}\,, \tag{A.11f}
$$

$$
\bar{\jmath}_{110}^{\epsilon;\,Af} = -\frac{8}{\epsilon^3} - \frac{24}{\epsilon^2} + \frac{1}{\epsilon}\big(\frac{10\pi^2}{3} - 64\big) - 156 + \frac{32\pi^2}{3} + 24\zeta_3\,, \tag{A.11g}
$$

$$
\bar{\jmath}_{110}^{\epsilon;\,Ff} = -\frac{6}{\epsilon^2} - \frac{29}{\epsilon} - \frac{227}{2} + 3\pi^2 + 24\zeta_3\,. \tag{A.11h}
$$

The expression for the renormalized $\epsilon$-scalar jet function in Laplace space is considerably more complicated than the corresponding expression for the quark- or gluon-jet function. Contrary to the quark- and gluon-jet function, there is still a dependence on $\alpha_e$ and $\alpha_{4\epsilon}$. The finite $\epsilon$-scalar jet function is given by

$$
\begin{aligned}
&\jmath_{\epsilon\,\mathrm{fin}}(Q^2,\mu) = 1 + \frac{\alpha_s}{4\pi}\Big[\Gamma_{100}\frac{L_Q^2}{2} + \gamma_{100}^{J_\epsilon}L_Q + c_{100}^{J_\epsilon}\Big] + \frac{\alpha_e}{4\pi}\Big[\Gamma_{010}\frac{L_Q^2}{2} + \gamma_{010}^{J_\epsilon}L_Q + c_{010}^{J_\epsilon}\Big] \\
&+ \Big(\frac{\alpha_s}{4\pi}\Big)^2\Big[\Gamma_{100}^2\frac{L_Q^4}{8} + (-\beta_{200}^s + 3\gamma_{100}^{J_\epsilon})\Gamma_{100}\frac{L_Q^3}{6} \\
&\quad + (\Gamma_{200} + (\gamma_{100}^{J_\epsilon})^2 - \beta_{200}^s\gamma_{100}^{J_\epsilon} + c_{100}^{J_\epsilon}\Gamma_{100})\frac{L_Q^2}{2} + (\gamma_{200}^{J_\epsilon} + \gamma_{100}^{J_\epsilon}c_{100} - \beta_{200}^s c_{100}^{J_\epsilon})L_Q + c_{200}^{J_\epsilon}\Big]
\end{aligned}
$$

$$
\begin{aligned}
&+\left(\frac{\alpha_e}{4\pi}\right)^2\Big[\Gamma_{010}^2\frac{L_Q^4}{8}+(-\beta_{020}^e+3\gamma_{010}^{J_\epsilon})\Gamma_{010}\frac{L_Q^3}{6}\\
&\quad+(\Gamma_{020}+(\gamma_{010}^{J_\epsilon})^2-\beta_{020}^e\gamma_{010}^{J_\epsilon}+c_{010}^{J_\epsilon}\Gamma_{010})\frac{L_Q^2}{2}+(\gamma_{020}^{J_\epsilon}+\gamma_{010}^{J_\epsilon}c_{010}-\beta_{020}^e c_{010}^{J_\epsilon})L_Q+c_{020}^{J_\epsilon}\Big]\\
&+\left(\frac{\alpha_{4\epsilon}}{4\pi}\right)^2\Big[\Gamma_{001}^2\frac{L_Q^4}{8}+(-\beta_{002}^{4\epsilon}+3\gamma_{001}^{J_\epsilon})\Gamma_{001}\frac{L_Q^3}{6}\\
&\quad+(\Gamma_{002}+(\gamma_{001}^{J_\epsilon})^2-\beta_{002}^{4\epsilon}\gamma_{001}^{J_\epsilon}+c_{001}^{J_\epsilon}\Gamma_{001})\frac{L_Q^2}{2}+(\gamma_{002}^{J_\epsilon}+\gamma_{001}^{J_\epsilon}c_{001}^{J_\epsilon}-\beta_{002}^{4\epsilon}c_{001}^{J_\epsilon})L_Q+c_{002}^{J_\epsilon}\Big]\\
&+\left(\frac{\alpha_s}{4\pi}\right)\left(\frac{\alpha_e}{4\pi}\right)\Big[\Gamma_{010}\Gamma_{100}\frac{L_Q^4}{4}+(-(\beta_{110}^e\Gamma_{010}+\beta_{110}^s\Gamma_{100})+3(\Gamma_{010}\gamma_{100}^{J_\epsilon}+\Gamma_{100}\gamma_{010}^{J_\epsilon}))\frac{L_Q^3}{6}\\
&\quad+(\Gamma_{110}+2\gamma_{010}^{J_\epsilon}\gamma_{100}^{J_\epsilon}-(\beta_{110}^e\gamma_{010}^{J_\epsilon}+\beta_{110}^s\gamma_{100}^{J_\epsilon})+c_{100}^{J_\epsilon}\Gamma_{010}+c_{010}^{J_\epsilon}\Gamma_{100})\frac{L_Q^2}{2}\\
&\quad+(\gamma_{110}^{J_\epsilon}+\gamma_{100}^{J_\epsilon}c_{010}^{J_\epsilon}+\gamma_{010}^{J_\epsilon}c_{100}^{J_\epsilon}-(\beta_{110}^e c_{010}^{J_\epsilon}+\beta_{110}^s c_{100}^{J_\epsilon}))L_Q+c_{110}^{J_\epsilon}\Big]\,,
\end{aligned}
\tag{A.12}
$$

where we have kept all terms of $\mathcal{O}(\alpha_s^2)$, $\mathcal{O}(\alpha_e^2)$, $\mathcal{O}(\alpha_{4\epsilon}^2)$ and $\mathcal{O}(\alpha_s\,\alpha_e)$, that appear in the structure of the equation, even if they are zero. The limit $N_\epsilon \to 0$ has been taken and as usual we indicate this in the notation by dropping the bar, e.g. $\beta^e = \lim_{N_\epsilon\to 0}\bar{\beta}^e$. The coefficients of the anomalous dimension of the $\epsilon$-scalar jet can be read off Eq. (7.56). In particular $\gamma_{001}^{J_\epsilon}=0$. The coefficients of the cusp anomalous dimensions can be read off Eq. (B.1f) and only $\Gamma_{100}$ and $\Gamma_{200}$ are non-vanishing.

The non-logarithmic terms of Eq. (A.12) read

$$c_{100}^{J_\epsilon} = 8\,C_A - \frac{2\pi^2}{3}C_A\,, \tag{A.13a}$$

$$c_{010}^{J_\epsilon} = -4N_F T_R\,, \tag{A.13b}$$

$$c_{001}^{J_\epsilon} = 0\,, \tag{A.13c}$$

$$c_{200}^{J_\epsilon} = \Big[\frac{177325}{1296}-\frac{257\pi^2}{18}+\frac{17\pi^4}{36}-32\zeta_3\Big]C_A^2+\Big[\frac{14}{9}\pi^2-\frac{5581}{162}\Big]C_A N_F T_R\,, \tag{A.13d}$$

$$c_{020}^{J_\epsilon} = \Big[\frac{\pi^2}{3}-\frac{29}{2}\Big]C_A N_F T_R+\Big[29-\frac{2\pi^2}{3}\Big]C_F N_F T_R+\Big[16-\frac{2\pi^2}{3}\Big]N_F^2 T_R^2\,, \tag{A.13e}$$

$$c_{002}^{J_\epsilon} = \frac{39}{16}C_A^2\,, \tag{A.13f}$$

$$c_{110}^{J_\epsilon} = \Big[\frac{16\pi^2}{3}-28-8\zeta_3\Big]C_A N_F T_R+\Big[\pi^2-\frac{131}{2}+24\zeta_3\Big]C_F N_F T_R\,. \tag{A.13g}$$

### A.5 Heavy form factor

We give here only the expressions for the renormalized result that contributes in FDH and not in CDR. In addition to that, the full FDH result includes the already known expression in CDR given in [78]. We follow the notation given in 9.11.

$$\mathcal{F}_{01}(x) = -\frac{2C_F N_\epsilon (x-1)H(0,x)}{4(x+1)}. \tag{A.14}$$

The two-loop contribution is given by

$$
\begin{aligned}
\mathcal{F}_{20}(x) = 4\frac{C_A C_F N_\epsilon}{1-x^2}\Big[&\frac{1}{\epsilon^2}\Big(-\frac{1}{24}x^2H(0,x)-\frac{1}{24}H(0,x)+\frac{x^2}{24}-\frac{1}{24}\Big)\\
&+\frac{1}{\epsilon}\Big(\frac{1}{9}x^2H(0,x)+\frac{1}{9}H(0,x)-\frac{x^2}{9}+\frac{1}{9}+L(\frac{1}{12}x^2H(0,x)+\frac{1}{12}H(0,x)\\
&-\frac{x^2}{12}+\frac{1}{12})\Big)+\frac{1}{36}\pi^2x^2H(-1,x)+\frac{1}{72}\pi^2x^2H(0,x)+\frac{311}{432}x^2H(0,x)\\
&-\frac{25}{36}x^2H(-1,0,x)+\frac{25}{72}x^2H(0,0,x)+\frac{1}{3}x^2H(-1,-1,0,x)-\frac{1}{6}x^2H(-1,0,0,x)\\
&-\frac{1}{6}x^2H(0,-1,0,x)+\frac{1}{12}x^2H(0,0,0,x)+\frac{7}{72}xH(0,x)-\frac{1}{6}xH(-1,0,x)\\
&+\frac{1}{12}xH(0,0,x)+\frac{1}{36}\pi^2H(-1,x)+\frac{1}{72}\pi^2H(0,x)+\frac{311}{432}H(0,x)\\
&-\frac{25}{36}H(-1,0,x)+\frac{25}{72}H(0,0,x)+\frac{1}{3}H(-1,-1,0,x)-\frac{1}{6}H(-1,0,0,x)\\
&-\frac{1}{6}H(0,-1,0,x)+\frac{1}{12}H(0,0,0,x)-\frac{x^2\zeta(3)}{6}-\frac{37\pi^2x^2}{432}-\frac{83x^2}{108}\\
&-\frac{\pi^2x}{72}-\frac{\zeta(3)}{6}-\frac{13\pi^2}{432}+\frac{83}{108}+L(\frac{1}{8}x^2H(0,x)-\frac{1}{6}x^2H(-1,0,x)\\
&+\frac{1}{12}x^2H(0,0,x)+\frac{1}{12}xH(0,x)+\frac{1}{8}H(0,x)-\frac{1}{6}H(-1,0,x)+\frac{1}{12}H(0,0,x)\\
&-\frac{\pi^2x^2}{72}-\frac{x^2}{6}-\frac{\pi^2}{72}+\frac{1}{6})+L^2(-\frac{1}{24}x^2H(0,x)-\frac{1}{24}H(0,x)+\frac{x^2}{24}-\frac{1}{24})\\
&-\frac{1}{144}\pi^2x^2H(0,x)-\frac{1}{144}\pi^2H(0,x)+\frac{\pi^2x^2}{144}-\frac{\pi^2}{144}\Big], \qquad \text{(A.15)}
\end{aligned}
$$

$$
\begin{aligned}
\mathcal{F}_{02}(x) = 4C_AC_F\Bigg\{&\frac{N_\epsilon}{(-1+x)(1+x)^5}\Big[-\frac{1}{4}H(0,x)x^6+\frac{1}{4}H(-1,0,x)x^6+\frac{\pi^2x^6}{24}+\frac{x^6}{8}\\
&+\frac{5}{4}\pi^2H(-1,x)x^5+\frac{5}{4}\pi^2H(0,x)x^5-\frac{7}{4}H(0,x)x^5-13H(-1,0,x)x^5\\
&-\frac{1}{2}\pi^2H(0,-1,x)x^5+\frac{1}{6}\pi^2H(0,0,x)x^5+15H(0,0,x)x^5+\frac{1}{3}\pi^2H(1,0,x)x^5\\
&-\frac{25}{2}H(-1,0,0,x)x^5+10H(0,-1,0,x)x^5+\frac{25}{2}H(0,0,0,x)x^5\\
&+10H(1,0,0,x)x^5+3H(0,-1,0,0,x)x^5-3H(0,0,-1,0,x)x^5\\
&-\frac{1}{2}H(0,0,0,0,x)x^5-3H(0,1,0,0,x)x^5+2H(1,0,0,0,x)x^5\\
&-3H(0,x)\zeta(3)x^5+\frac{25\zeta(3)x^5}{2}+\frac{2\pi^4x^5}{45}\\
&-\frac{17\pi^2x^5}{4}+x^5-2\pi^2H(-1,x)x^4-\frac{25}{4}\pi^2H(0,x)x^4\\
&-\frac{7}{4}H(0,x)x^4-\frac{1}{4}H(-1,0,x)x^4+2\pi^2H(0,-1,x)x^4
\end{aligned}
$$

$$
\begin{aligned}
&- \frac{11}{6}\pi^2 H(0,0,x)x^4 - \frac{53}{4}H(0,0,x)x^4 - 6\pi^2 H(1,0,x)x^4 \\
&+ 56H(-1,0,0,x)x^4 - 34H(0,-1,0,x)x^4 - \frac{109}{2}H(0,0,0,x)x^4 \\
&- 34H(1,0,0,x)x^4 - 40H(0,-1,0,0,x)x^4 + 26H(0,0,-1,0,x)x^4 \\
&+ 2H(0,0,0,0,x)x^4 + 26H(0,1,0,0,x)x^4 - 36H(1,0,0,0,x)x^4 \\
&+ 40H(0,x)\zeta(3)x^4 - 56\zeta(3)x^4 - \frac{61\pi^4 x^4}{120} + \frac{79\pi^2 x^4}{12} + \frac{13x^4}{8} \\
&+ \frac{73}{12}\pi^2 H(0,x)x^3 - \frac{1}{2}H(0,x)x^3 + 26H(-1,0,x)x^3 - 4\pi^2 H(0,-1,x)x^3 \\
&+ \frac{7}{2}\pi^2 H(0,0,x)x^3 - 13H(0,0,x)x^3 + \frac{34}{3}\pi^2 H(1,0,x)x^3 \\
&+ \frac{73}{2}H(0,0,0,x)x^3 + 76H(0,-1,0,0,x)x^3 - 50H(0,0,-1,0,x)x^3 \\
&- 4H(0,0,0,0,x)x^3 - 50H(0,1,0,0,x)x^3 + 68H(1,0,0,0,x)x^3 \\
&- 76H(0,x)\zeta(3)x^3 + \frac{349\pi^4 x^3}{360} + \frac{13\pi^2 x^3}{6} + 2\pi^2 H(-1,x)x^2 \\
&- \frac{31}{12}\pi^2 H(0,x)x^2 - \frac{7}{4}H(0,x)x^2 - \frac{1}{4}H(-1,0,x)x^2 \\
&+ 2\pi^2 H(0,-1,x)x^2 - \frac{11}{6}\pi^2 H(0,0,x)x^2 + \frac{27}{2}H(0,0,x)x^2 \\
&- 6\pi^2 H(1,0,x)x^2 - 56H(-1,0,0,x)x^2 + 34H(0,-1,0,x)x^2 \\
&+ \frac{3}{2}H(0,0,0,x)x^2 + 34H(1,0,0,x)x^2 - 40H(0,-1,0,0,x)x^2 \\
&+ 26H(0,0,-1,0,x)x^2 + 2H(0,0,0,0,x)x^2 + 26H(0,1,0,0,x)x^2 \\
&- 36H(1,0,0,0,x)x^2 + 40H(0,x)\zeta(3)x^2 + 56\zeta(3)x^2 \\
&- \frac{61\pi^4 x^2}{120} - \frac{53\pi^2 x^2}{8} - \frac{13x^2}{8} - \frac{5}{4}\pi^2 H(-1,x)x \\
&+ \frac{5}{6}\pi^2 H(0,x)x - \frac{7}{4}H(0,x)x - 13H(-1,0,x)x \\
&- \frac{1}{2}\pi^2 H(0,-1,x)x + \frac{1}{6}\pi^2 H(0,0,x)x - 2H(0,0,x)x \\
&+ \frac{1}{3}\pi^2 H(1,0,x)x + \frac{25}{2}H(-1,0,0,x)x - 10H(0,-1,0,x)x - 10H(1,0,0,x)x \\
&+ 3H(0,-1,0,0,x)x - 3H(0,0,-1,0,x)x - \frac{1}{2}H(0,0,0,0,x)x \\
&- 3H(0,1,0,0,x)x + 2H(1,0,0,0,x)x - 3H(0,x)\zeta(3)x \\
&- \frac{25\zeta(3)x}{2} + \frac{2\pi^4 x}{45} + \frac{25\pi^2 x}{12} - x - \frac{1}{4}H(0,x) \\
&+ \frac{1}{4}H(-1,0,x) - \frac{1}{4}H(0,0,x) - \frac{1}{8} \\
&+ L(-\frac{1}{4}x^6 H(0,x) - \frac{1}{2}x^5 H(0,x) + \frac{1}{4}x^4 H(0,x)
\end{aligned}
$$

$$
\begin{aligned}
&+ x^3 H(0,x) + \frac{1}{4}x^2 H(0,x) - \frac{1}{2}xH(0,x) - \frac{1}{4}H(0,x))\Big] \\
&+ \frac{N_\epsilon^2}{(-1+x)(1+x)^5}\Big[\frac{1}{8}H(0,x)x^6 - \frac{1}{8}H(-1,0,x)x^6 \\
&- \frac{\pi^2 x^6}{48} - \frac{x^6}{16} - \frac{5}{8}\pi^2 H(-1,x)x^5 \\
&- \frac{5}{8}\pi^2 H(0,x)x^5 + \frac{7}{8}H(0,x)x^5 + \frac{13}{2}H(-1,0,x)x^5 \\
&+ \frac{1}{4}\pi^2 H(0,-1,x)x^5 - \frac{1}{12}\pi^2 H(0,0,x)x^5 - \frac{15}{2}H(0,0,x)x^5 \\
&- \frac{1}{6}\pi^2 H(1,0,x)x^5 + \frac{25}{4}H(-1,0,0,x)x^5 - 5H(0,-1,0,x)x^5 \\
&- \frac{25}{4}H(0,0,0,x)x^5 - 5H(1,0,0,x)x^5 - \frac{3}{2}H(0,-1,0,0,x)x^5 \\
&+ \frac{3}{2}H(0,0,-1,0,x)x^5 + \frac{1}{4}H(0,0,0,0,x)x^5 + \frac{3}{2}H(0,1,0,0,x)x^5 \\
&- H(1,0,0,0,x)x^5 + \frac{3}{2}H(0,x)\zeta(3)x^5 - \frac{25\zeta(3)x^5}{4} \\
&- \frac{\pi^4 x^5}{45} + \frac{17\pi^2 x^5}{8} - \frac{x^5}{2} \\
&+ \pi^2 H(-1,x)x^4 + \frac{25}{8}\pi^2 H(0,x)x^4 + \frac{7}{8}H(0,x)x^4 + \frac{1}{8}H(-1,0,x)x^4 \\
&- \pi^2 H(0,-1,x)x^4 + \frac{11}{12}\pi^2 H(0,0,x)x^4 + \frac{53}{8}H(0,0,x)x^4 \\
&+ 3\pi^2 H(1,0,x)x^4 - 28H(-1,0,0,x)x^4 + 17H(0,-1,0,x)x^4 \\
&+ \frac{109}{4}H(0,0,0,x)x^4 + 17H(1,0,0,x)x^4 + 20H(0,-1,0,0,x)x^4 \\
&- 13H(0,0,-1,0,x)x^4 - H(0,0,0,0,x)x^4 - 13H(0,1,0,0,x)x^4 \\
&+ 18H(1,0,0,0,x)x^4 - 20H(0,x)\zeta(3)x^4 + 28\zeta(3)x^4 \\
&+ \frac{61\pi^4 x^4}{240} - \frac{79\pi^2 x^4}{24} - \frac{13x^4}{16} - \frac{73}{24}\pi^2 H(0,x)x^3 + \\
&\frac{1}{4}H(0,x)x^3 - 13H(-1,0,x)x^3 + 2\pi^2 H(0,-1,x)x^3 \\
&- \frac{7}{4}\pi^2 H(0,0,x)x^3 + \frac{13}{2}H(0,0,x)x^3 - \frac{17}{3}\pi^2 H(1,0,x)x^3 \\
&- \frac{73}{4}H(0,0,0,x)x^3 - 38H(0,-1,0,0,x)x^3 + 25H(0,0,-1,0,x)x^3 \\
&+ 2H(0,0,0,0,x)x^3 + 25H(0,1,0,0,x)x^3 - 34H(1,0,0,0,x)x^3 \\
&+ 38H(0,x)\zeta(3)x^3 - \frac{349\pi^4 x^3}{720} - \frac{13\pi^2 x^3}{12} \\
&- \pi^2 H(-1,x)x^2 + \frac{31}{24}\pi^2 H(0,x)x^2 + \frac{7}{8}H(0,x)x^2 + \frac{1}{8}H(-1,0,x)x^2 \\
&- \pi^2 H(0,-1,x)x^2 + \frac{11}{12}\pi^2 H(0,0,x)x^2 - \frac{27}{4}H(0,0,x)x^2
\end{aligned}
$$

$$
\begin{aligned}
&+ 3\pi^2 H(1,0,x)x^2 + 28H(-1,0,0,x)x^2 - 17H(0,-1,0,x)x^2 \\
&- \frac{3}{4}H(0,0,0,x)x^2 - 17H(1,0,0,x)x^2 + 20H(0,-1,0,0,x)x^2 \\
&- 13H(0,0,-1,0,x)x^2 - H(0,0,0,0,x)x^2 - 13H(0,1,0,0,x)x^2 \\
&+ 18H(1,0,0,0,x)x^2 - 20H(0,x)\zeta(3)x^2 - 28\zeta(3)x^2 + \frac{61\pi^4 x^2}{240} \\
&+ \frac{53\pi^2 x^2}{16} + \frac{13x^2}{16} + \frac{5}{8}\pi^2 H(-1,x)x - \frac{5}{12}\pi^2 H(0,x)x \\
&+ \frac{7}{8}H(0,x)x + \frac{13}{2}H(-1,0,x)x + \frac{1}{4}\pi^2 H(0,-1,x)x \\
&- \frac{1}{12}\pi^2 H(0,0,x)x + H(0,0,x)x - \frac{1}{6}\pi^2 H(1,0,x)x \\
&- \frac{25}{4}H(-1,0,0,x)x + 5H(0,-1,0,x)x + 5H(1,0,0,x)x \\
&- \frac{3}{2}H(0,-1,0,0,x)x + \frac{3}{2}H(0,0,-1,0,x)x + \frac{1}{4}H(0,0,0,0,x)x \\
&+ \frac{3}{2}H(0,1,0,0,x)x - H(1,0,0,0,x)x + \frac{3}{2}H(0,x)\zeta(3)x \\
&+ \frac{25\zeta(3)x}{4} - \frac{\pi^4 x}{45} - \frac{25\pi^2 x}{24} \\
&+ \frac{x}{2} + \frac{1}{8}H(0,x) - \frac{1}{8}H(-1,0,x) + \frac{1}{8}H(0,0,x) + \frac{1}{16} \\
&+ L(\frac{1}{8}x^6 H(0,x) + \frac{1}{4}x^5 H(0,x) - \frac{1}{8}x^4 H(0,x) \\
&- \frac{1}{2}x^3 H(0,x) - \frac{1}{8}x^2 H(0,x) + \frac{1}{4}xH(0,x) + \frac{1}{8}H(0,x))\Big]\Bigg\} \\
&+ 4C_F^2\Bigg\{\frac{N_\epsilon}{(-1+x)(1+x)^5}\Big[\frac{1}{2}H(0,x)x^6 - \frac{1}{2}H(-1,0,x)x^6 - \frac{\pi^2 x^6}{12} \\
&- \frac{x^6}{4} - \frac{5}{2}\pi^2 H(-1,x)x^5 - \frac{5}{2}\pi^2 H(0,x)x^5 + \frac{7}{2}H(0,x)x^5 + 26H(-1,0,x)x^5 \\
&+ \pi^2 H(0,-1,x)x^5 - \frac{1}{3}\pi^2 H(0,0,x)x^5 - 30H(0,0,x)x^5 - \frac{2}{3}\pi^2 H(1,0,x)x^5 \\
&+ 25H(-1,0,0,x)x^5 - 20H(0,-1,0,x)x^5 - 25H(0,0,0,x)x^5 \\
&- 20H(1,0,0,x)x^5 - 6H(0,-1,0,0,x)x^5 + 6H(0,0,-1,0,x)x^5 \\
&+ H(0,0,0,0,x)x^5 + 6H(0,1,0,0,x)x^5 - 4H(1,0,0,0,x)x^5 \\
&+ 6H(0,x)\zeta(3)x^5 - 25\zeta(3)x^5 - \frac{4\pi^4 x^5}{45} \\
&+ \frac{17\pi^2 x^5}{2} - 2x^5 + 4\pi^2 H(-1,x)x^4 + \frac{25}{2}\pi^2 H(0,x)x^4 \\
&+ \frac{7}{2}H(0,x)x^4 + \frac{1}{2}H(-1,0,x)x^4 - 4\pi^2 H(0,-1,x)x^4
\end{aligned}
$$

$$+\frac{11}{3}\pi^2 H(0,0,x)x^4+\frac{53}{2}H(0,0,x)x^4+12\pi^2 H(1,0,x)x^4$$
$$-112H(-1,0,0,x)x^4+68H(0,-1,0,x)x^4+109H(0,0,0,x)x^4$$
$$+68H(1,0,0,x)x^4+80H(0,-1,0,0,x)x^4-52H(0,0,-1,0,x)x^4$$
$$-4H(0,0,0,0,x)x^4-52H(0,1,0,0,x)x^4+72H(1,0,0,0,x)x^4$$
$$-80H(0,x)\zeta(3)x^4+112\zeta(3)x^4+\frac{61\pi^4x^4}{60}$$
$$-\frac{79\pi^2x^4}{6}-\frac{13x^4}{4}-\frac{73}{6}\pi^2H(0,x)x^3+H(0,x)x^3$$
$$-52H(-1,0,x)x^3+8\pi^2H(0,-1,x)x^3-7\pi^2H(0,0,x)x^3$$
$$+26H(0,0,x)x^3-\frac{68}{3}\pi^2H(1,0,x)x^3-73H(0,0,0,x)x^3$$
$$-152H(0,-1,0,0,x)x^3+100H(0,0,-1,0,x)x^3+8H(0,0,0,0,x)x^3$$
$$+100H(0,1,0,0,x)x^3-136H(1,0,0,0,x)x^3+152H(0,x)\zeta(3)x^3$$
$$-\frac{349\pi^4x^3}{180}-\frac{13\pi^2x^3}{3}-4\pi^2H(-1,x)x^2$$
$$+\frac{31}{6}\pi^2H(0,x)x^2+\frac{7}{2}H(0,x)x^2+\frac{1}{2}H(-1,0,x)x^2$$
$$-4\pi^2H(0,-1,x)x^2+\frac{11}{3}\pi^2H(0,0,x)x^2-27H(0,0,x)x^2$$
$$+12\pi^2H(1,0,x)x^2+112H(-1,0,0,x)x^2-68H(0,-1,0,x)x^2$$
$$-3H(0,0,0,x)x^2-68H(1,0,0,x)x^2+80H(0,-1,0,0,x)x^2$$
$$-52H(0,0,-1,0,x)x^2-4H(0,0,0,0,x)x^2-52H(0,1,0,0,x)x^2$$
$$+72H(1,0,0,0,x)x^2-80H(0,x)\zeta(3)x^2-112\zeta(3)x^2$$
$$+\frac{61\pi^4x^2}{60}+\frac{53\pi^2x^2}{4}+\frac{13x^2}{4}$$
$$+\frac{5}{2}\pi^2H(-1,x)x-\frac{5}{3}\pi^2H(0,x)x+\frac{7}{2}H(0,x)x$$
$$+26H(-1,0,x)x+\pi^2H(0,-1,x)x-\frac{1}{3}\pi^2H(0,0,x)x$$
$$+4H(0,0,x)x-\frac{2}{3}\pi^2H(1,0,x)x-25H(-1,0,0,x)x$$
$$+20H(0,-1,0,x)x+20H(1,0,0,x)x-6H(0,-1,0,0,x)x$$
$$+6H(0,0,-1,0,x)x+H(0,0,0,0,x)x+6H(0,1,0,0,x)x$$
$$-4H(1,0,0,0,x)x+6H(0,x)\zeta(3)x+25\zeta(3)x-\frac{4\pi^4x}{45}$$
$$-\frac{25\pi^2x}{6}+2x+\frac{1}{2}H(0,x)-\frac{1}{2}H(-1,0,x)$$
$$+\frac{1}{2}H(0,0,x)+\frac{1}{4}+L(\frac{1}{2}x^6H(0,x)$$

$$
\begin{aligned}
&+ x^5 H(0,x) - \frac{1}{2} x^4 H(0,x) - 2x^3 H(0,x) \\
&- \frac{1}{2} x^2 H(0,x) + x H(0,x) + \frac{1}{2} H(0,x)) \Big] \\
&+ \frac{N_\epsilon^2}{(-1+x)(1+x)^5} \Big[ - \frac{3}{32} H(0,x) x^6 + \frac{1}{8} H(-1,0,x) x^6 \\
&+ \frac{1}{16} H(0,0,x) x^6 - \frac{\pi^2 x^6}{96} + \frac{3x^6}{8} \\
&+ \frac{5}{4} \pi^2 H(-1,x) x^5 - \frac{5}{8} \pi^2 H(0,x) x^5 + \frac{17}{16} H(0,x) x^5 \\
&- \frac{7}{4} H(-1,0,x) x^5 - \frac{1}{2} \pi^2 H(0,-1,x) x^5 + \frac{11}{8} H(0,0,x) x^5 \\
&- \frac{1}{3} \pi^2 H(1,0,x) x^5 + \frac{5}{2} H(-1,0,0,x) x^5 + \frac{5}{2} H(0,-1,0,x) x^5 \\
&- \frac{5}{2} H(0,0,0,x) x^5 + \frac{5}{2} H(1,0,0,x) x^5 - H(0,-1,0,0,x) x^5 \\
&- H(0,0,-1,0,x) x^5 - \frac{1}{2} H(0,0,0,0,x) x^5 - H(0,1,0,0,x) x^5 \\
&- 2H(1,0,0,0,x) x^5 + H(0,x) \zeta(3) x^5 - \frac{5\zeta(3) x^5}{2} \\
&- \frac{\pi^4 x^5}{360} - \frac{17\pi^2 x^5}{16} + \frac{x^5}{2} - 2\pi^2 H(-1,x) x^4 \\
&+ \frac{23}{6} \pi^2 H(0,x) x^4 - \frac{29}{32} H(0,x) x^4 - \frac{65}{8} H(-1,0,x) x^4 \\
&+ 2\pi^2 H(0,-1,x) x^4 + \frac{1}{4} \pi^2 H(0,0,x) x^4 + \frac{171}{16} H(0,0,x) x^4 \\
&+ \frac{7}{3} \pi^2 H(1,0,x) x^4 - 22 H(-1,0,0,x) x^4 + 5 H(0,-1,0,x) x^4 \\
&+ \frac{51}{2} H(0,0,0,x) x^4 + 5 H(1,0,0,x) x^4 + 10 H(0,-1,0,0,x) x^4 \\
&+ H(0,0,-1,0,x) x^4 + 2H(0,0,0,0,x) x^4 + H(0,1,0,0,x) x^4 \\
&+ 14 H(1,0,0,0,x) x^4 - 10 H(0,x) \zeta(3) x^4 + 22 \zeta(3) x^4 + \frac{59\pi^4 x^4}{720} \\
&- \frac{139\pi^2 x^4}{96} - \frac{x^4}{8} - \frac{7}{4} \pi^2 H(0,x) x^3 \\
&- \frac{33}{8} H(0,x) x^3 - \frac{25}{2} H(-1,0,x) x^3 - 4\pi^2 H(0,-1,x) x^3 \\
&- \pi^2 H(0,0,x) x^3 + \frac{25}{4} H(0,0,x) x^3 - \frac{20}{3} \pi^2 H(1,0,x) x^3 \\
&- \frac{21}{2} H(0,0,0,x) x^3 - 32 H(0,-1,0,0,x) x^3 + 4 H(0,0,-1,0,x) x^3 \\
&- 4H(0,0,0,0,x) x^3 + 4 H(0,1,0,0,x) x^3 - 40 H(1,0,0,0,x) x^3 \\
&+ 32 H(0,x) \zeta(3) x^3 - \frac{11\pi^4 x^3}{36} - \frac{25\pi^2 x^3}{24}
\end{aligned}
$$

$$
\begin{aligned}
&+ 2\pi^2 H(-1,x)x^2 + \pi^2 H(0,x)x^2 - \frac{29}{32}H(0,x)x^2 \\
&- \frac{65}{8}H(-1,0,x)x^2 + 2\pi^2 H(0,-1,x)x^2 + \frac{1}{4}\pi^2 H(0,0,x)x^2 \\
&- \frac{41}{16}H(0,0,x)x^2 + \frac{7}{3}\pi^2 H(1,0,x)x^2 + 22H(-1,0,0,x)x^2 \\
&- 5H(0,-1,0,x)x^2 + \frac{7}{2}H(0,0,0,x)x^2 - 5H(1,0,0,x)x^2 \\
&+ 10H(0,-1,0,0,x)x^2 + H(0,0,-1,0,x)x^2 + 2H(0,0,0,0,x)x^2 \\
&+ H(0,1,0,0,x)x^2 + 14H(1,0,0,0,x)x^2 - 10H(0,x)\zeta(3)x^2 \\
&- 22\zeta(3)x^2 + \frac{59\pi^4 x^2}{720} + \frac{3\pi^2 x^2}{32} + \frac{x^2}{8} \\
&- \frac{5}{4}\pi^2 H(-1,x)x + \frac{5}{24}\pi^2 H(0,x)x + \frac{17}{16}H(0,x)x \\
&- \frac{7}{4}H(-1,0,x)x - \frac{1}{2}\pi^2 H(0,-1,x)x + \frac{3}{8}H(0,0,x)x \\
&- \frac{1}{3}\pi^2 H(1,0,x)x - \frac{5}{2}H(-1,0,0,x)x - \frac{5}{2}H(0,-1,0,x)x \\
&- \frac{5}{2}H(1,0,0,x)x - H(0,-1,0,0,x)x - H(0,0,-1,0,x)x \\
&- \frac{1}{2}H(0,0,0,0,x)x - H(0,1,0,0,x)x - 2H(1,0,0,0,x)x \\
&+ H(0,x)\zeta(3)x + \frac{5\zeta(3)x}{2} - \frac{\pi^4 x}{360} \\
&+ \frac{37\pi^2 x}{48} - \frac{x}{2} - \frac{3}{32}H(0,x) + \frac{1}{8}H(-1,0,x) \\
&- \frac{3}{16}H(0,0,x) + \frac{\pi^2}{32} - \frac{3}{8} \\
&+ L(-\frac{1}{8}x^6 H(0,x) - \frac{1}{4}x^5 H(0,x) + \frac{1}{8}x^4 H(0,x) \\
&+ \frac{1}{2}x^3 H(0,x) + \frac{1}{8}x^2 H(0,x) - \frac{1}{4}xH(0,x) - \frac{1}{8}H(0,x))\Big]\Bigg\} \\
&+ 4C_F N_F N_\epsilon \Bigg\{ \frac{1}{(-1+x)(1+x)^5}\Big[\frac{5}{16}x^6 H(0,x) - \frac{1}{4}x^6 H(-1,0,x) \\
&+ \frac{1}{8}x^6 H(0,0,x) + \frac{9}{8}x^5 H(0,x) - \frac{1}{2}x^5 H(-1,0,x) + \frac{1}{4}x^5 H(0,0,x) \\
&+ \frac{27}{16}x^4 H(0,x) + \frac{1}{4}x^4 H(-1,0,x) - \frac{1}{8}x^4 H(0,0,x) + \frac{7}{4}x^3 H(0,x) \\
&+ x^3 H(-1,0,x) - \frac{1}{2}x^3 H(0,0,x) + \frac{27}{16}x^2 H(0,x) + \frac{1}{4}x^2 H(-1,0,x) \\
&- \frac{1}{8}x^2 H(0,0,x) + \frac{9}{8}xH(0,x) - \frac{1}{2}xH(-1,0,x) + \frac{1}{4}xH(0,0,x)
\end{aligned}
$$

$$
\begin{aligned}
&+\frac{5}{16}H(0,x)-\frac{1}{4}H(-1,0,x)+\frac{1}{8}H(0,0,x)-\frac{\pi^2x^6}{48}-\frac{x^6}{4}\\
&-\frac{\pi^2x^5}{24}-x^5+\frac{\pi^2x^4}{48}-\frac{5x^4}{4}+\frac{\pi^2x^3}{12}+\frac{\pi^2x^2}{48}+\frac{5x^2}{4}-\frac{\pi^2x}{24}\\
&+x-\frac{\pi^2}{48}+\frac{1}{4}+L(\frac{1}{8}x^6H(0,x)+\frac{1}{4}x^5H(0,x)\\
&-\frac{1}{8}x^4H(0,x)-\frac{1}{2}x^3H(0,x)-\frac{1}{8}x^2H(0,x)+\frac{1}{4}xH(0,x)+\frac{1}{8}H(0,x))\Big]\Bigg\}\\
&+4C_FN_HN_\epsilon\Bigg\{\frac{1}{(-1+x)(1+x)^5}\Big[\frac{5}{16}x^6H(0,x)-\frac{1}{8}x^6H(0,0,x)\\
&+\frac{7}{8}x^5H(0,x)+\frac{1}{4}x^5H(0,0,x)+\frac{5}{12}\pi^2x^4H(0,x)\\
&+\frac{59}{16}x^4H(0,x)-\frac{17}{8}x^4H(0,0,x)+\frac{5}{2}x^4H(0,0,0,x)\\
&-\frac{1}{6}\pi^2x^3H(0,x)+\frac{25}{4}x^3H(0,x)-x^3H(0,0,0,x)\\
&+\frac{5}{12}\pi^2x^2H(0,x)+\frac{59}{16}x^2H(0,x)+\frac{17}{8}x^2H(0,0,x)\\
&+\frac{5}{2}x^2H(0,0,0,x)+\frac{7}{8}xH(0,x)-\frac{1}{4}xH(0,0,x)\\
&+\frac{5}{16}H(0,x)+\frac{1}{8}H(0,0,x)-\frac{\pi^2x^6}{48}\\
&-\frac{5x^6}{8}+\frac{\pi^2x^5}{24}-2x^5-\frac{17\pi^2x^4}{48}\\
&-\frac{17x^4}{8}+\frac{17\pi^2x^2}{48}+\frac{17x^2}{8}-\frac{\pi^2x}{24}+2x\\
&+\frac{\pi^2}{48}+\frac{5}{8}+L(\frac{1}{8}x^6H(0,x)+\frac{1}{4}x^5H(0,x)\\
&-\frac{1}{8}x^4H(0,x)-\frac{1}{2}x^3H(0,x)-\frac{1}{8}x^2H(0,x)\\
&+\frac{1}{4}xH(0,x)+\frac{1}{8}H(0,x))+L^2(x^4H(0,x)\\
&+2x^3H(0,x)+x^2H(0,x)+\frac{x^5}{2}+x^4-x^2-\frac{x}{2})\Big]\Bigg\},
\end{aligned}
\tag{A.16}
$$

$$
\begin{aligned}
\mathcal{F}_{11}(x)=&\frac{4C_F^2N_\epsilon}{(-1+x)(1+x)^5}\Big[\frac{1}{\epsilon}\Big(\frac{1}{4}x^6H(0,x)-\frac{1}{2}x^6H(0,0,x)\\
&+\frac{1}{2}x^5H(0,x)-x^5H(0,0,x)-\frac{1}{4}x^4H(0,x)-\frac{1}{2}x^4H(0,0,x)\\
&-x^3H(0,x)-\frac{1}{4}x^2H(0,x)+\frac{1}{2}x^2H(0,0,x)+\frac{1}{2}xH(0,x)+xH(0,0,x)
\end{aligned}
$$

$$+\frac{1}{4}H(0,x)+\frac{1}{2}H(0,0,x)\Big)-\frac{3}{4}LH(0,x)x^6+\frac{1}{6}\pi^2H(0,x)x^6$$
$$+\frac{1}{2}H(0,x)x^6+H(-1,0,x)x^6-\frac{7}{4}H(0,0,x)x^6$$
$$+2H(-1,0,0,x)x^6-H(0,-1,0,x)x^6-\frac{1}{2}H(0,0,0,x)x^6$$
$$+H(0,1,0,x)x^6-2H(1,0,0,x)x^6+\zeta(3)x^6-\frac{\pi^2x^6}{24}$$
$$-\frac{x^6}{4}-\frac{3}{2}LH(0,x)x^5+\frac{5}{2}\pi^2H(0,x)x^5$$
$$+\frac{7}{2}H(0,x)x^5+18H(-1,0,x)x^5-\frac{69}{2}H(0,0,x)x^5$$
$$-12H(1,0,x)x^5-2H(0,-1,0,x)x^5+15H(0,0,0,x)x^5$$
$$+6H(0,1,0,x)x^5+2H(1,0,0,x)x^5+7\zeta(3)x^5-\frac{37\pi^2x^5}{12}$$
$$-2x^5+\frac{3}{4}LH(0,x)x^4+\frac{3}{2}\pi^2H(0,x)x^4+\frac{7}{2}H(0,x)x^4$$
$$-33H(-1,0,x)x^4+\frac{1}{3}\pi^2H(0,0,x)x^4+\frac{141}{4}H(0,0,x)x^4$$
$$-30H(-1,0,0,x)x^4+95H(0,-1,0,x)x^4-\frac{9}{2}H(0,0,0,x)x^4$$
$$-39H(0,1,0,x)x^4+94H(1,0,0,x)x^4-12H(0,0,-1,0,x)x^4$$
$$+6H(0,0,0,0,x)x^4+8H(0,0,1,0,x)x^4-8H(0,1,0,0,x)x^4$$
$$+6H(0,x)\zeta(3)x^4-7\zeta(3)x^4+\frac{11\pi^4x^4}{60}-\frac{61\pi^2x^4}{24}$$
$$-\frac{13x^4}{4}+3LH(0,x)x^3+7\pi^2H(0,x)x^3+H(0,x)x^3$$
$$-100H(-1,0,x)x^3+\frac{2}{3}\pi^2H(0,0,x)x^3+62H(0,0,x)x^3$$
$$+24H(1,0,x)x^3+42H(0,0,0,x)x^3-48H(0,-1,0,0,x)x^3$$
$$+168H(0,0,-1,0,x)x^3-24H(0,0,0,0,x)x^3-80H(0,0,1,0,x)x^3$$
$$+152H(0,1,0,0,x)x^3-24H(0,x)\zeta(3)x^3-\frac{43\pi^4x^3}{30}$$
$$-\frac{13\pi^2x^3}{3}+\frac{3}{4}LH(0,x)x^2-\frac{4}{3}\pi^2H(0,x)x^2$$
$$+\frac{7}{2}H(0,x)x^2-33H(-1,0,x)x^2+\frac{1}{3}\pi^2H(0,0,x)x^2$$
$$-\frac{9}{4}H(0,0,x)x^2+30H(-1,0,0,x)x^2-95H(0,-1,0,x)x^2$$
$$+\frac{11}{2}H(0,0,0,x)x^2+39H(0,1,0,x)x^2-94H(1,0,0,x)x^2$$
$$-12H(0,0,-1,0,x)x^2+6H(0,0,0,0,x)x^2+8H(0,0,1,0,x)x^2$$

$$
\begin{aligned}
&- 8H(0,1,0,0,x)x^2 + 6H(0,x)\zeta(3)x^2 + 7\zeta(3)x^2 + \frac{11\pi^4 x^2}{60} \\
&- \frac{71\pi^2 x^2}{24} + \frac{13x^2}{4} - \frac{3}{2}LH(0,x)x \\
&+ \frac{5}{6}\pi^2 H(0,x)x + \frac{7}{2}H(0,x)x + 18H(-1,0,x)x \\
&+ \frac{9}{2}H(0,0,x)x - 12H(1,0,x)x + 2H(0,-1,0,x)x \\
&+ 5H(0,0,0,x)x - 6H(0,1,0,x)x - 2H(1,0,0,x)x \\
&- 7\zeta(3)x + \frac{25\pi^2 x}{12} + 2x - \frac{3}{4}LH(0,x) \\
&+ \frac{1}{2}H(0,x) + H(-1,0,x) + \frac{3}{4}H(0,0,x) \\
&- 2H(-1,0,0,x) + H(0,-1,0,x) + \frac{3}{2}H(0,0,0,x) \\
&- H(0,1,0,x) + 2H(1,0,0,x) - \zeta(3) + \frac{5\pi^2}{24} + \frac{1}{4}\Big] \\
&+ \frac{4C_A C_F N_\epsilon}{(-1+x)(1+x)^5}\Big[\frac{1}{12}\pi^2 H(0,x)x^6 - \frac{11}{8}H(0,x)x^6 - \frac{3}{4}H(-1,0,x)x^6 \\
&+ \frac{1}{4}H(0,0,x)x^6 - \frac{1}{2}H(1,0,x)x^6 + \frac{1}{2}H(0,-1,0,x)x^6 \\
&+ \frac{1}{2}H(0,0,0,x)x^6 + H(1,0,0,x)x^6 - \frac{\zeta(3)x^6}{4} \\
&- \frac{\pi^2 x^6}{3} + \frac{7x^6}{8} - \frac{95}{12}\pi^2 H(0,x)x^5 \\
&+ \frac{1}{2}H(0,x)x^5 + \frac{57}{2}H(-1,0,x)x^5 - \frac{2}{3}\pi^2 H(0,0,x)x^5 \\
&- \frac{57}{2}H(0,0,x)x^5 - \frac{8}{3}\pi^2 H(1,0,x)x^5 + 5H(1,0,x)x^5 \\
&+ 58H(-1,0,0,x)x^5 - 27H(0,-1,0,x)x^5 - 63H(0,0,0,x)x^5 \\
&- 2H(0,1,0,x)x^5 - 29H(1,0,0,x)x^5 - 16H(0,-1,0,0,x)x^5 \\
&+ 8H(0,0,-1,0,x)x^5 + 8H(0,1,0,0,x)x^5 - 16H(1,0,0,0,x)x^5 \\
&+ 16H(0,x)\zeta(3)x^5 - 59\zeta(3)x^5 - \frac{17\pi^4 x^5}{90} + \frac{25\pi^2 x^5}{2} \\
&+ x^5 + \frac{121}{4}\pi^2 H(0,x)x^4 - \frac{5}{8}H(0,x)x^4 + \frac{3}{4}H(-1,0,x)x^4 \\
&+ \frac{13}{2}\pi^2 H(0,0,x)x^4 + 41H(0,0,x)x^4 + \frac{80}{3}\pi^2 H(1,0,x)x^4 \\
&+ \frac{1}{2}H(1,0,x)x^4 - 208H(-1,0,0,x)x^4 + \frac{129}{2}H(0,-1,0,x)x^4 \\
&+ \frac{487}{2}H(0,0,0,x)x^4 + 20H(0,1,0,x)x^4 + 65H(1,0,0,x)x^4 \\
&+ 160H(0,-1,0,0,x)x^4 - 74H(0,0,-1,0,x)x^4 - 3H(0,0,0,0,x)x^4
\end{aligned}
$$

$$
\begin{aligned}
&- 4H(0,0,1,0,x)x^4 - 76H(0,1,0,0,x)x^4 + 160H(1,0,0,0,x)x^4 \\
&- 163H(0,x)\zeta(3)x^4 + \frac{911\zeta(3)x^4}{4} + \frac{647\pi^4x^4}{360} \\
&- \frac{533\pi^2x^4}{24} - \frac{5x^4}{8} - \frac{175}{6}\pi^2H(0,x)x^3 \\
&- 5H(0,x)x^3 - 57H(-1,0,x)x^3 - \frac{41}{3}\pi^2H(0,0,x)x^3 \\
&+ \frac{47}{2}H(0,0,x)x^3 - \frac{160}{3}\pi^2H(1,0,x)x^3 - 10H(1,0,x)x^3 \\
&- 175H(0,0,0,x)x^3 - 296H(0,-1,0,0,x)x^3 + 76H(0,0,-1,0,x)x^3 \\
&+ 12H(0,0,0,0,x)x^3 + 40H(0,0,1,0,x)x^3 + 84H(0,1,0,0,x)x^3 \\
&- 320H(1,0,0,0,x)x^3 + 332H(0,x)\zeta(3)x^3 - \frac{551\pi^4x^3}{180} \\
&- \frac{77\pi^2x^3}{12} + \frac{77}{6}\pi^2H(0,x)x^2 - \frac{5}{8}H(0,x)x^2 \\
&+ \frac{3}{4}H(-1,0,x)x^2 + \frac{13}{2}\pi^2H(0,0,x)x^2 - \frac{165}{4}H(0,0,x)x^2 \\
&+ \frac{80}{3}\pi^2H(1,0,x)x^2 + \frac{1}{2}H(1,0,x)x^2 + 208H(-1,0,0,x)x^2 \\
&- \frac{129}{2}H(0,-1,0,x)x^2 + 15H(0,0,0,x)x^2 - 20H(0,1,0,x)x^2 \\
&- 65H(1,0,0,x)x^2 + 160H(0,-1,0,0,x)x^2 - 74H(0,0,-1,0,x)x^2 \\
&- 3H(0,0,0,0,x)x^2 - 4H(0,0,1,0,x)x^2 - 76H(0,1,0,0,x)x^2 \\
&+ 160H(1,0,0,0,x)x^2 - 163H(0,x)\zeta(3)x^2 - \frac{911\zeta(3)x^2}{4} \\
&+ \frac{647\pi^4x^2}{360} + \frac{45\pi^2x^2}{2} + \frac{5x^2}{8} - \frac{11}{4}\pi^2H(0,x)x \\
&+ \frac{1}{2}H(0,x)x + \frac{57}{2}H(-1,0,x)x - \frac{2}{3}\pi^2H(0,0,x)x \\
&+ 5H(0,0,x)x - \frac{8}{3}\pi^2H(1,0,x)x + 5H(1,0,x)x \\
&- 58H(-1,0,0,x)x + 27H(0,-1,0,x)x - H(0,0,0,x)x \\
&+ 2H(0,1,0,x)x + 29H(1,0,0,x)x - 16H(0,-1,0,0,x)x \\
&+ 8H(0,0,-1,0,x)x + 8H(0,1,0,0,x)x - 16H(1,0,0,0,x)x \\
&+ 16H(0,x)\zeta(3)x + 59\zeta(3)x - \frac{17\pi^4x}{90} - \frac{73\pi^2x}{12} \\
&- x - \frac{11}{8}H(0,x) - \frac{3}{4}H(-1,0,x) - \frac{1}{2}H(1,0,x) \\
&- \frac{1}{2}H(0,-1,0,x) - H(1,0,0,x) + \frac{\zeta(3)}{4} + \frac{\pi^2}{24} - \frac{7}{8}\Big], \qquad \text{(A.17)}
\end{aligned}
$$

where $L = \ln\left(\frac{\mu^2}{m^2}\right)$.

### A.6 Heavy-to-light form factor

We give here only the expressions for the renormalized result that contributes in FDH and not in CDR. In addition to that, the full FDH result includes the already known expression in CDR given in [84]. We follow the notation given in 9.11.

$$\mathcal{F}_{01}(y) = N_\epsilon C_F \left[ + \frac{1}{4\epsilon} + \frac{1}{4} - \frac{1}{2} H(-1,-x) \right]. \tag{A.18}$$

$$\begin{aligned}
\mathcal{F}_{20}(y) = C_F C_A N_\epsilon \Bigg\{ & - \frac{1}{8\epsilon^3} + \frac{\frac{1}{6}H(-1,-y) + \frac{L}{6} - \frac{7}{72}}{\epsilon^2} \\
& + \frac{-\frac{1}{3}LH(-1,-y) - \frac{4}{9}H(-1,-y) - \frac{L^2}{12} + \frac{5L}{12} + \frac{\pi^2}{48} + \frac{263}{432}}{\epsilon} \\
& + \frac{1}{6}L^2 H(-1,-y) - \frac{1}{2}LH(-1,-y) + \frac{2}{3}LH(-1,-1,-y) \\
& - \frac{1}{3}LH(0,-1,-y) - \frac{H(-1,-y)}{6y} - \frac{5}{36}\pi^2 H(-1,-y) - \frac{311}{108}H(-1,-y) \\
& + \frac{25}{9}H(-1,-1,-y) - \frac{25}{18}H(0,-1,-y) - \frac{4}{3}H(-1,-1,-1,-y) \\
& + \frac{2}{3}H(-1,0,-1,-y) + \frac{2}{3}H(0,-1,-1,-y) - \frac{1}{3}H(0,0,-1,-y) \\
& + \frac{L^3}{36} - \frac{5L^2}{24} - \frac{\pi^2 L}{72} + L + \frac{5\zeta(3)}{18} + \frac{107\pi^2}{432} + \frac{10799}{2592} \\
& + \frac{1}{36}\pi^2 H(-1,-y) + \frac{\pi^2 L}{36} + \frac{\zeta(3)}{12} - \frac{7\pi^2}{432} \Bigg\},
\end{aligned} \tag{A.19}$$

$$\begin{aligned}
\mathcal{F}_{02}(y) = C_F^2 \Bigg\{ & N_\epsilon \left[ \frac{1}{2\epsilon^2} - \frac{L}{\epsilon} + (y-1)^4 \Big( \frac{L^2 y^4}{2} - L y^4 + 2LH(-1,-y)y^4 \right. \\
& + 2H(-1,-y)y^4 - 3H(-1,-1,-y)y^4 + H(0,-1,-y)y^4 \\
& - \frac{5\pi^2 y^4}{12} + \frac{3y^4}{2} - 2L^2 y^3 + 4Ly^3 \\
& + \frac{1}{2}\pi^2 H(-2,-y)y^3 - 8LH(-1,-y)y^3 + \frac{15}{2}\pi^2 H(-1,-y)y^3 \\
& - 13H(-1,-y)y^3 - 31H(-1,-1,-y)y^3 - 2\pi^2 H(0,-1,-y)y^3 \\
& + 45H(0,-1,-y)y^3 + H(-2,-1,-1,-y)y^3 - 15H(-1,0,-1,-y)y^3 \\
& + 31H(0,-1,-1,-y)y^3 - 17H(0,0,-1,-y)y^3 + 4H(0,-1,0,-1,-y)y^3 \\
& - 8H(0,0,-1,-1,-y)y^3 + 4H(0,0,0,-1,-y)y^3 - \frac{9\zeta(3)y^3}{4} \\
& \left. + \frac{1}{4}\pi^2 \ln(4) y^3 - \frac{3\pi^4 y^3}{10} - \frac{77\pi^2 y^3}{6} \right.
\end{aligned}$$

$$
\begin{aligned}
&- 5y^3 + 3L^2y^2 - 6Ly^2 - \frac{7}{2}\pi^2 H(-2,-y)y^2 \\
&+ 12LH(-1,-y)y^2 + \frac{33}{2}\pi^2 H(-1,-y)y^2 + 29H(-1,-y)y^2 \\
&+ 45H(-1,-1,-y)y^2 - 18\pi^2 H(0,-1,-y)y^2 - 19H(0,-1,-y)y^2 \\
&- 7H(-2,-1,-1,-y)y^2 - 33H(-1,0,-1,-y)y^2 + 59H(0,-1,-1,-y)y^2 \\
&- 19H(0,0,-1,-y)y^2 + 36H(0,-1,0,-1,-y)y^2 - 72H(0,0,-1,-1,-y)y^2 \\
&+ 36H(0,0,0,-1,-y)y^2 + \frac{63\zeta(3)y^2}{4} - \frac{7}{2}\pi^2\ln(2)y^2 \\
&- \frac{27\pi^4 y^2}{10} - \frac{17\pi^2 y^2}{3} + 6y^2 - 2L^2 y + 4Ly \\
&+ 5\pi^2 H(-2,-y)y - 8LH(-1,-y)y - \frac{39}{2}\pi^2 H(-1,-y)y \\
&- 29H(-1,-y)y + 15H(-1,-1,-y)y - 15\pi^2 H(0,-1,-y)y \\
&- 35H(0,-1,-y)y + 10H(-2,-1,-1,-y)y + 39H(-1,0,-1,-y)y \\
&- 68H(0,-1,-1,-y)y + 32H(0,0,-1,-y)y + 30H(0,-1,0,-1,-y)y \\
&- 60H(0,0,-1,-1,-y)y + 30H(0,0,0,-1,-y)y - \frac{19\zeta(3)y}{2} \\
&+ 5\pi^2\ln(2)y - \frac{9\pi^4 y}{4} + \frac{37\pi^2 y}{2} - 3y \\
&+ \frac{L^2}{2} - L + \pi^2 H(-2,-y) + 2LH(-1,-y) \\
&- \frac{9}{2}\pi^2 H(-1,-y) + 13H(-1,-y) - 26H(-1,-1,-y) \\
&- \pi^2 H(0,-1,-y) + 8H(0,-1,-y) + 2H(-2,-1,-1,-y) \\
&+ 9H(-1,0,-1,-y) - 16H(0,-1,-1,-y) + 10H(0,0,-1,-y) \\
&+ 2H(0,-1,0,-1,-y) - 4H(0,0,-1,-1,-y) + 2H(0,0,0,-1,-y) \\
&+ \frac{\zeta(3)}{2} + \frac{1}{4}\pi^2\ln(16) - \frac{3\pi^4}{20} \\
&+ \frac{5\pi^2}{12} + \frac{1}{2} - \frac{2H(-1,-y)}{y}\Big) + \frac{\pi^2}{12}\Bigg] \\
&+ N_\epsilon^2\Bigg[ - \frac{3}{32\epsilon^2} + \frac{-4H(-1,-y) + 8L + 1}{32\epsilon} + (y-1)^4\Big( - \frac{1}{8}L^2 y^4 \\
&+ \frac{Ly^4}{4} - \frac{1}{2}LH(-1,-y)y^4 - \frac{5}{8}H(-1,-y)y^4 \\
&+ \frac{5}{4}H(-1,-1,-y)y^4 - \frac{3}{8}H(0,-1,-y)y^4 + \frac{\pi^2 y^4}{16} \\
&+ \frac{7y^4}{64} + \frac{L^2 y^3}{2} - Ly^3 - \frac{1}{4}\pi^2 H(-2,-y)y^3
\end{aligned}
$$

$$
\begin{aligned}
&+ 2LH(-1,-y)y^3 + \frac{7}{4}H(-1,-y)y^3 - 6H(-1,-1,-y)y^3 \\
&+ \frac{5}{2}H(0,-1,-y)y^3 - \frac{1}{2}H(-2,-1,-1,-y)y^3 - \frac{1}{2}H(0,-1,-1,-y)y^3 \\
&+ H(0,0,-1,-y)y^3 + \frac{9\zeta(3)y^3}{8} - \frac{1}{8}\pi^2\ln(4)y^3 \\
&- \frac{\pi^2y^3}{12} + \frac{9y^3}{16} - \frac{3L^2y^2}{4} + \frac{3Ly^2}{2} \\
&+ \frac{7}{4}\pi^2H(-2,-y)y^2 - 3LH(-1,-y)y^2 + \frac{9}{2}\pi^2H(-1,-y)y^2 \\
&- \frac{15}{4}H(-1,-y)y^2 - 9H(-1,-1,-y)y^2 - \frac{3}{2}\pi^2H(0,-1,-y)y^2 \\
&+ \frac{87}{4}H(0,-1,-y)y^2 + \frac{7}{2}H(-2,-1,-1,-y)y^2 - 9H(-1,0,-1,-y)y^2 \\
&+ \frac{43}{2}H(0,-1,-1,-y)y^2 - 16H(0,0,-1,-y)y^2 + 3H(0,-1,0,-1,-y)y^2 \\
&- 6H(0,0,-1,-1,-y)y^2 + 3H(0,0,0,-1,-y)y^2 - \frac{63\zeta(3)y^2}{8} \\
&+ \frac{7}{4}\pi^2\ln(2)y^2 - \frac{9\pi^4y^2}{40} - \frac{181\pi^2y^2}{24} \\
&- \frac{75y^2}{32} + \frac{L^2y}{2} - Ly - \frac{5}{2}\pi^2H(-2,-y)y \\
&+ 2LH(-1,-y)y + 7H(-1,-y)y + \frac{59}{2}H(-1,-1,-y)y \\
&- 6\pi^2H(0,-1,-y)y - 28H(0,-1,-y)y - 5H(-2,-1,-1,-y)y \\
&- 5H(0,-1,-1,-y)y + \frac{7}{2}H(0,0,-1,-y)y + 12H(0,-1,0,-1,-y)y \\
&- 24H(0,0,-1,-1,-y)y + 12H(0,0,0,-1,-y)y + \frac{19\zeta(3)y}{4} \\
&- \frac{5}{2}\pi^2\ln(2)y - \frac{9\pi^4y}{10} + \frac{55\pi^2y}{12} + \frac{41y}{16} \\
&- \frac{L^2}{8} + \frac{L}{4} - \frac{1}{2}\pi^2H(-2,-y) - \frac{1}{2}LH(-1,-y) \\
&- \frac{9}{2}\pi^2H(-1,-y) - \frac{53}{8}H(-1,-y) - \frac{57}{4}H(-1,-1,-y) \\
&- \frac{3}{2}\pi^2H(0,-1,-y) + \frac{29}{8}H(0,-1,-y) - H(-2,-1,-1,-y) \\
&+ 9H(-1,0,-1,-y) - 19H(0,-1,-1,-y) + \frac{17}{2}H(0,0,-1,-y) \\
&+ 3H(0,-1,0,-1,-y) - 6H(0,0,-1,-1,-y) + 3H(0,0,0,-1,-y) \\
&- \frac{\zeta(3)}{4} - \frac{1}{8}\pi^2\ln(16) - \frac{9\pi^4}{40} + \frac{143\pi^2}{48} \\
&- \frac{57}{64} + \frac{9H(-1,-y)}{4y} - \frac{3H(-1,-1,-y)}{2y} + \frac{H(0,-1,-y)}{2y}\Big) - \frac{\pi^2}{64}\Bigg]\Bigg\}
\end{aligned}
$$

$$
\begin{aligned}
&+ C_F C_A \Bigg\{ N_\epsilon \Bigg[ - \frac{1}{4\epsilon^2} + \frac{L}{2\epsilon} + (y-1)^4 \Big( - \frac{1}{4} L^2 y^4 + \frac{L y^4}{2} \\
&- L H(-1,-y) y^4 - H(-1,-y) y^4 + \frac{3}{2} H(-1,-1,-y) y^4 \\
&- \frac{1}{2} H(0,-1,-y) y^4 + \frac{5\pi^2 y^4}{24} - \frac{3y^4}{4} + L^2 y^3 \\
&- 2Ly^3 - \frac{1}{4}\pi^2 H(-2,-y) y^3 + 4LH(-1,-y) y^3 - \frac{15}{4}\pi^2 H(-1,-y) y^3 \\
&+ \frac{13}{2} H(-1,-y) y^3 + \frac{31}{2} H(-1,-1,-y) y^3 + \pi^2 H(0,-1,-y) y^3 \\
&- \frac{45}{2} H(0,-1,-y) y^3 - \frac{1}{2} H(-2,-1,-1,-y) y^3 + \frac{15}{2} H(-1,0,-1,-y) y^3 \\
&- \frac{31}{2} H(0,-1,-1,-y) y^3 + \frac{17}{2} H(0,0,-1,-y) y^3 - 2H(0,-1,0,-1,-y) y^3 \\
&+ 4H(0,0,-1,-1,-y) y^3 - 2H(0,0,0,-1,-y) y^3 + \frac{9\zeta(3) y^3}{8} \\
&- \frac{1}{8}\pi^2 \ln(4) y^3 + \frac{3\pi^4 y^3}{20} + \frac{77\pi^2 y^3}{12} \\
&+ \frac{5y^3}{2} - \frac{3L^2 y^2}{2} + 3Ly^2 + \frac{7}{4}\pi^2 H(-2,-y) y^2 \\
&- 6LH(-1,-y) y^2 - \frac{33}{4}\pi^2 H(-1,-y) y^2 - \frac{29}{2} H(-1,-y) y^2 \\
&- \frac{45}{2} H(-1,-1,-y) y^2 + 9\pi^2 H(0,-1,-y) y^2 + \frac{19}{2} H(0,-1,-y) y^2 \\
&+ \frac{7}{2} H(-2,-1,-1,-y) y^2 + \frac{33}{2} H(-1,0,-1,-y) y^2 - \frac{59}{2} H(0,-1,-1,-y) y^2 \\
&+ \frac{19}{2} H(0,0,-1,-y) y^2 - 18H(0,-1,0,-1,-y) y^2 + 36H(0,0,-1,-1,-y) y^2 \\
&- 18H(0,0,0,-1,-y) y^2 - \frac{63\zeta(3) y^2}{8} + \frac{7}{4}\pi^2 \ln(2) y^2 \\
&+ \frac{27\pi^4 y^2}{20} + \frac{17\pi^2 y^2}{6} - 3y^2 + L^2 y - 2Ly - \frac{5}{2}\pi^2 H(-2,-y) y \\
&+ 4LH(-1,-y) y + \frac{39}{4}\pi^2 H(-1,-y) y + \frac{29}{2} H(-1,-y) y \\
&- \frac{15}{2} H(-1,-1,-y) y + \frac{15}{2}\pi^2 H(0,-1,-y) y + \frac{35}{2} H(0,-1,-y) y \\
&- 5H(-2,-1,-1,-y) y - \frac{39}{2} H(-1,0,-1,-y) y + 34H(0,-1,-1,-y) y \\
&- 16H(0,0,-1,-y) y - 15H(0,-1,0,-1,-y) y + 30H(0,0,-1,-1,-y) y \\
&- 15H(0,0,0,-1,-y) y + \frac{19\zeta(3) y}{4} - \frac{5}{2}\pi^2 \ln(2) y \\
&+ \frac{9\pi^4 y}{8} - \frac{37\pi^2 y}{4} + \frac{3y}{2} - \frac{L^2}{4} + \frac{L}{2}
\end{aligned}
$$

$$
\begin{aligned}
&- \frac{1}{2}\pi^2 H(-2,-y) - LH(-1,-y) + \frac{9}{4}\pi^2 H(-1,-y) \\
&- \frac{13}{2}H(-1,-y) + 13H(-1,-1,-y) + \frac{1}{2}\pi^2 H(0,-1,-y) \\
&- 4H(0,-1,-y) - H(-2,-1,-1,-y) - \frac{9}{2}H(-1,0,-1,-y) \\
&+ 8H(0,-1,-1,-y) - 5H(0,0,-1,-y) - H(0,-1,0,-1,-y) \\
&+ 2H(0,0,-1,-1,-y) - H(0,0,0,-1,-y) - \frac{\zeta(3)}{4} - \frac{1}{8}\pi^2 \ln(16) \\
&+ \frac{3\pi^4}{40} - \frac{5\pi^2}{24} - \frac{1}{4} + \frac{H(-1,-y)}{y}\Big) - \frac{\pi^2}{24}\Bigg] \\
&+ N_\epsilon^2 \Bigg[ \frac{1}{8\epsilon^2} - \frac{L}{4\epsilon} + (y-1)^4 \Big( \frac{L^2 y^4}{8} - \frac{L y^4}{4} \\
&+ \frac{1}{2}LH(-1,-y)y^4 + \frac{1}{2}H(-1,-y)y^4 - \frac{3}{4}H(-1,-1,-y)y^4 \\
&+ \frac{1}{4}H(0,-1,-y)y^4 - \frac{5\pi^2 y^4}{48} + \frac{3y^4}{8} - \frac{L^2 y^3}{2} \\
&+ Ly^3 + \frac{1}{8}\pi^2 H(-2,-y)y^3 - 2LH(-1,-y)y^3 + \frac{15}{8}\pi^2 H(-1,-y)y^3 \\
&- \frac{13}{4}H(-1,-y)y^3 - \frac{31}{4}H(-1,-1,-y)y^3 - \frac{1}{2}\pi^2 H(0,-1,-y)y^3 \\
&+ \frac{45}{4}H(0,-1,-y)y^3 + \frac{1}{4}H(-2,-1,-1,-y)y^3 - \frac{15}{4}H(-1,0,-1,-y)y^3 \\
&+ \frac{31}{4}H(0,-1,-1,-y)y^3 - \frac{17}{4}H(0,0,-1,-y)y^3 + H(0,-1,0,-1,-y)y^3 \\
&- 2H(0,0,-1,-1,-y)y^3 + H(0,0,0,-1,-y)y^3 - \frac{9\zeta(3)y^3}{16} \\
&+ \frac{1}{16}\pi^2 \ln(4)y^3 - \frac{3\pi^4 y^3}{40} - \frac{77\pi^2 y^3}{24} \\
&- \frac{5y^3}{4} + \frac{3L^2 y^2}{4} - \frac{3Ly^2}{2} - \frac{7}{8}\pi^2 H(-2,-y)y^2 \\
&+ 3LH(-1,-y)y^2 + \frac{33}{8}\pi^2 H(-1,-y)y^2 + \frac{29}{4}H(-1,-y)y^2 \\
&+ \frac{45}{4}H(-1,-1,-y)y^2 - \frac{9}{2}\pi^2 H(0,-1,-y)y^2 - \frac{19}{4}H(0,-1,-y)y^2 \\
&- \frac{7}{4}H(-2,-1,-1,-y)y^2 - \frac{33}{4}H(-1,0,-1,-y)y^2 + \frac{59}{4}H(0,-1,-1,-y)y^2 \\
&- \frac{19}{4}H(0,0,-1,-y)y^2 + 9H(0,-1,0,-1,-y)y^2 - 18H(0,0,-1,-1,-y)y^2 \\
&+ 9H(0,0,0,-1,-y)y^2 + \frac{63\zeta(3)y^2}{16} - \frac{7}{8}\pi^2 \ln(2)y^2 - \frac{27\pi^4 y^2}{40} \\
&- \frac{17\pi^2 y^2}{12} + \frac{3y^2}{2} - \frac{L^2 y}{2} + Ly + \frac{5}{4}\pi^2 H(-2,-y)y
\end{aligned}
$$

$$
\begin{aligned}
&- 2LH(-1,-y)y - \frac{39}{8}\pi^2 H(-1,-y)y - \frac{29}{4}H(-1,-y)y \\
&+ \frac{15}{4}H(-1,-1,-y)y - \frac{15}{4}\pi^2 H(0,-1,-y)y - \frac{35}{4}H(0,-1,-y)y \\
&+ \frac{5}{2}H(-2,-1,-1,-y)y + \frac{39}{4}H(-1,0,-1,-y)y - 17H(0,-1,-1,-y)y \\
&+ 8H(0,0,-1,-y)y + \frac{15}{2}H(0,-1,0,-1,-y)y - 15H(0,0,-1,-1,-y)y \\
&+ \frac{15}{2}H(0,0,0,-1,-y)y - \frac{19\zeta(3)y}{8} + \frac{5}{4}\pi^2\ln(2)y \\
&- \frac{9\pi^4 y}{16} + \frac{37\pi^2 y}{8} - \frac{3y}{4} + \frac{L^2}{8} - \frac{L}{4} + \frac{1}{4}\pi^2 H(-2,-y) \\
&+ \frac{1}{2}LH(-1,-y) - \frac{9}{8}\pi^2 H(-1,-y) + \frac{13}{4}H(-1,-y) \\
&- \frac{13}{2}H(-1,-1,-y) - \frac{1}{4}\pi^2 H(0,-1,-y) + 2H(0,-1,-y) \\
&+ \frac{1}{2}H(-2,-1,-1,-y) + \frac{9}{4}H(-1,0,-1,-y) - 4H(0,-1,-1,-y) \\
&+ \frac{5}{2}H(0,0,-1,-y) + \frac{1}{2}H(0,-1,0,-1,-y) - H(0,0,-1,-1,-y) \\
&+ \frac{1}{2}H(0,0,0,-1,-y) + \frac{\zeta(3)}{8} + \frac{1}{16}\pi^2\ln(16) \\
&- \frac{3\pi^4}{80} + \frac{5\pi^2}{48} + \frac{1}{8} - \frac{H(-1,-y)}{2y}\Big) + \frac{\pi^2}{48}\Big]\Big\} \\
&+ C_F N_F N_\epsilon \Big\{ \frac{1}{8\epsilon^2} + \frac{1}{\epsilon}\Big( - \frac{3}{16} - \frac{L}{4}\Big) + \frac{1}{2}LH(-1,-y) - \frac{H(-1,-y)}{2y} \\
&+ \frac{5}{4}H(-1,-y) - H(-1,-1,-y) + \frac{1}{2}H(0,-1,-y) \\
&+ \frac{L^2}{8} - \frac{L}{4} - \frac{5\pi^2}{48} - \frac{45}{32} + \frac{\pi^2}{48}\Big\} \\
&+ C_F N_H N_\epsilon \Big\{ - \frac{L}{4\epsilon} + (y-1)^4\Big(\frac{1}{2}Ly^4 H(-1,-y) \\
&- 2Ly^3 H(-1,-y) + 3Ly^2 H(-1,-y) - 2LyH(-1,-y) \\
&+ \frac{1}{2}LH(-1,-y) + \frac{5}{4}y^4 H(-1,-y) - \frac{1}{2}y^4 H(0,-1,-y) \\
&- \frac{9}{2}y^3 H(-1,-y) + \frac{19}{2}y^2 H(-1,-y) - 2y^2 H(0,-1,-y) \\
&+ 4y^2 H(0,0,-1,-y) - 11yH(-1,-y) + \frac{21}{4}H(-1,-y) \\
&+ \frac{5}{2}H(0,-1,-y) + 2H(0,0,-1,-y) - \frac{H(-1,-y)}{2y}
\end{aligned}
$$

$$
\begin{aligned}
&+\frac{L^2y^4}{8}-\frac{L^2y^3}{2}+\frac{3L^2y^2}{4}-\frac{L^2y}{2}\\
&+\frac{L^2}{8}-\frac{Ly^4}{4}+Ly^3-\frac{3Ly^2}{2}+Ly\\
&-\frac{L}{4}-\frac{\pi^2y^4}{48}-\frac{41y^4}{16}+\frac{\pi^2y^3}{12}+\frac{37y^3}{4}\\
&+4y^2\zeta(3)-\frac{\pi^2y^2}{8}-\frac{111y^2}{8}+\frac{\pi^2y}{12}+\frac{41y}{4}+2\zeta(3)-\frac{\pi^2}{48}-\frac{49}{16}\Big)+\Bigg\}, \qquad \text{(A.20)}
\end{aligned}
$$

$$
\begin{aligned}
\mathcal{F}_{11}(y) = C_F^2N_\epsilon\Bigg\{&-\frac{1}{4\epsilon^3}+\frac{H(-1,-y)-\frac{13}{8}}{\epsilon^2}\\
&+\frac{3H(-1,-y)-4H(-1,-1,-y)+H(0,-1,-y)+\frac{3L}{2}-\frac{\pi^2}{8}-\frac{23}{8}}{\epsilon}\\
&+\frac{1}{6}\pi^2H(-1,-y)+\frac{\zeta(3)}{6}-\frac{13\pi^2}{48}+(y-1)^4\Big(-\frac{3}{4}L^2y^4+\frac{3Ly^4}{2}\\
&-3LH(-1,-y)y^4+\frac{1}{3}\pi^2H(-1,-y)y^4+7H(-1,-y)y^4\\
&+\frac{1}{3}\pi^2H(1,-y)y^4-5H(-1,-1,-y)y^4+16H(-1,-1,-1,-y)y^4\\
&-4H(-1,0,-1,-y)y^4-8H(0,-1,-1,-y)y^4-H(0,0,-1,-y)y^4\\
&-4H(1,0,-1,-y)y^4+\frac{\zeta(3)y^4}{2}+\frac{5\pi^2y^4}{24}\\
&-10y^4+3L^2y^3-6Ly^3-\frac{5}{2}\pi^2H(-2,-y)y^3\\
&+12LH(-1,-y)y^3-2\pi^2H(-1,-y)y^3-26H(-1,-y)y^3\\
&-\frac{4}{3}\pi^2H(1,-y)y^3+24H(-1,-1,-y)y^3-10H(0,-1,-y)y^3\\
&-5H(-2,-1,-1,-y)y^3-64H(-1,-1,-1,-y)y^3+20H(-1,0,-1,-y)y^3\\
&+23H(0,-1,-1,-y)y^3+14H(0,0,-1,-y)y^3+16H(1,0,-1,-y)y^3\\
&+\frac{45\zeta(3)y^3}{4}-\frac{5}{2}\pi^2\ln(2)y^3+\frac{13\pi^2y^3}{6}+41y^3-\frac{9L^2y^2}{2}+9Ly^2\\
&+8\pi^2H(-2,-y)y^2-18LH(-1,-y)y^2+\frac{22}{3}\pi^2H(-1,-y)y^2\\
&+30H(-1,-y)y^2-\frac{4}{3}\pi^2H(1,-y)y^2-82H(-1,-1,-y)y^2\\
&+\frac{2}{3}\pi^2H(0,-1,-y)y^2+75H(0,-1,-y)y^2+\frac{4}{3}\pi^2H(0,1,-y)y^2\\
&+16H(-2,-1,-1,-y)y^2+96H(-1,-1,-1,-y)y^2-56H(-1,0,-1,-y)y^2\\
&+20H(0,-1,-1,-y)y^2-12H(0,0,-1,-y)y^2+16H(1,0,-1,-y)y^2\\
&+4H(0,-1,0,-1,-y)y^2-8H(0,0,-1,-1,-y)y^2-12H(0,0,0,-1,-y)y^2
\end{aligned}
$$

$$
- 16H(0,1,0,-1,-y)y^2 - 33\zeta(3)y^2 + 8\pi^2\ln(2)y^2 + \frac{\pi^4 y^2}{9}
$$
$$
- \frac{157\pi^2 y^2}{12} - 63y^2 + 3L^2 y - 6Ly - 6\pi^2 H(-2,-y)y
$$
$$
+ 12LH(-1,-y)y + 6\pi^2 H(-1,-y)y - 4H(-1,-y)y
$$
$$
+ \frac{4}{3}\pi^2 H(1,-y)y + 107H(-1,-1,-y)y - \frac{38}{3}\pi^2 H(0,-1,-y)y
$$
$$
- 73H(0,-1,-y)y + \frac{8}{3}\pi^2 H(0,1,-y)y - 12H(-2,-1,-1,-y)y
$$
$$
- 64H(-1,-1,-1,-y)y + 20H(-1,0,-1,-y)y + 24H(0,-1,-1,-y)y
$$
$$
- 17H(0,0,-1,-y)y - 16H(1,0,-1,-y)y + 36H(0,-1,0,-1,-y)y
$$
$$
- 72H(0,0,-1,-1,-y)y + 4H(0,0,0,-1,-y)y - 32H(0,1,0,-1,-y)y
$$
$$
+ 26\zeta(3)y - 6\pi^2\ln(2)y - \frac{169\pi^4 y}{90} + \frac{13\pi^2 y}{3}
$$
$$
+ 43y - \frac{3L^2}{4} + \frac{3L}{2} + 2\pi^2 H(-2,-y)
$$
$$
- 3LH(-1,-y) - \frac{35}{3}\pi^2 H(-1,-y) - 13H(-1,-y)
$$
$$
+ \pi^2 H(1,-y) - 39H(-1,-1,-y) - 4\pi^2 H(0,-1,-y)
$$
$$
+ 6H(0,-1,-y) + 4H(-2,-1,-1,-y) + 16H(-1,-1,-1,-y)
$$
$$
+ 20H(-1,0,-1,-y) - 56H(0,-1,-1,-y) + 19H(0,0,-1,-y)
$$
$$
- 12H(1,0,-1,-y) + 8H(0,-1,0,-1,-y) - 16H(0,0,-1,-1,-y)
$$
$$
+ 8H(0,0,0,-1,-y) - \frac{5\zeta(3)}{2} + \pi^2\ln(4) - \frac{3\pi^4}{5} + \frac{51\pi^2}{8} - 11
$$
$$
+ \frac{6H(-1,-y)}{y} - \frac{5H(-1,-1,-y)}{y} + \frac{2H(0,-1,-y)}{y}\Big)\Bigg\}
$$
$$
+ C_F C_A N_\epsilon \Bigg\{ \frac{11}{8\epsilon} + (y-1)^4\Big( - \frac{11}{2}H(-1,-y)y^4 - \frac{1}{6}\pi^2 H(1,-y)y^4
$$
$$
- \frac{5}{2}H(-1,-1,-y)y^4 + \frac{5}{2}H(0,-1,-y)y^4 + H(0,-1,-1,-y)y^4
$$
$$
+ H(0,0,-1,-y)y^4 + 2H(1,0,-1,-y)y^4 - \frac{3\zeta(3)y^4}{2}
$$
$$
- \frac{2\pi^2 y^4}{3} + \frac{161y^4}{16} + \frac{5}{4}\pi^2 H(-2,-y)y^3
$$
$$
+ \frac{145}{12}\pi^2 H(-1,-y)y^3 + \frac{29}{2}H(-1,-y)y^3 + \frac{2}{3}\pi^2 H(1,-y)y^3
$$
$$
- \frac{105}{2}H(-1,-1,-y)y^3 - \frac{7}{2}\pi^2 H(0,-1,-y)y^3 + \frac{131}{2}H(0,-1,-y)y^3
$$
$$
+ \frac{5}{2}H(-2,-1,-1,-y)y^3 - \frac{51}{2}H(-1,0,-1,-y)y^3 + \frac{95}{2}H(0,-1,-1,-y)y^3
$$

$$
\begin{aligned}
&- \frac{65}{2}H(0,0,-1,-y)y^3 - 8H(1,0,-1,-y)y^3 + 7H(0,-1,0,-1,-y)y^3 \\
&- 14H(0,0,-1,-1,-y)y^3 + 7H(0,0,0,-1,-y)y^3 - \frac{5\zeta(3)y^3}{8} \\
&+ \frac{5}{4}\pi^2\ln(2)y^3 - \frac{21\pi^4y^3}{40} - \frac{235\pi^2y^3}{12} \\
&- \frac{151y^3}{4} - 4\pi^2H(-2,-y)y^2 + \frac{61}{3}\pi^2H(-1,-y)y^2 \\
&- \frac{21}{2}H(-1,-y)y^2 + \frac{2}{3}\pi^2H(1,-y)y^2 + 78H(-1,-1,-y)y^2 \\
&- \frac{155}{6}\pi^2H(0,-1,-y)y^2 - 31H(0,-1,-y)y^2 - \frac{2}{3}\pi^2H(0,1,-y)y^2 \\
&- 8H(-2,-1,-1,-y)y^2 - 30H(-1,0,-1,-y)y^2 + 64H(0,-1,-1,-y)y^2 \\
&- 37H(0,0,-1,-y)y^2 - 8H(1,0,-1,-y)y^2 + 49H(0,-1,0,-1,-y)y^2 \\
&- 98H(0,0,-1,-1,-y)y^2 + 57H(0,0,0,-1,-y)y^2 + 8H(0,1,0,-1,-y)y^2 \\
&+ 9\zeta(3)y^2 - 4\pi^2\ln(2)y^2 - \frac{1397\pi^4y^2}{360} - \frac{15\pi^2y^2}{2} \\
&+ \frac{423y^2}{8} + 3\pi^2H(-2,-y)y - \frac{317}{12}\pi^2H(-1,-y)y \\
&- \frac{1}{2}H(-1,-y)y - \frac{2}{3}\pi^2H(1,-y)y + \frac{23}{2}H(-1,-1,-y)y \\
&- \frac{59}{3}\pi^2H(0,-1,-y)y - 50H(0,-1,-y)y - \frac{4}{3}\pi^2H(0,1,-y)y \\
&+ 6H(-2,-1,-1,-y)y + \frac{87}{2}H(-1,0,-1,-y)y - 91H(0,-1,-1,-y)y \\
&+ 52H(0,0,-1,-y)y + 8H(1,0,-1,-y)y + 34H(0,-1,0,-1,-y)y \\
&- 68H(0,0,-1,-1,-y)y + 50H(0,0,0,-1,-y)y + 16H(0,1,0,-1,-y)y \\
&- 8\zeta(3)y + \pi^2\ln(8)y - \frac{533\pi^4y}{180} + \frac{151\pi^2y}{6} \\
&- \frac{131y}{4} - \pi^2H(-2,-y) - 6\pi^2H(-1,-y) + 2H(-1,-y) \\
&- \frac{1}{2}\pi^2H(1,-y) - \frac{69}{2}H(-1,-1,-y) \\
&- \frac{3}{2}\pi^2H(0,-1,-y) + 13H(0,-1,-y) - 2H(-2,-1,-1,-y) \\
&+ 12H(-1,0,-1,-y) - 23H(0,-1,-1,-y) + 15H(0,0,-1,-y) \\
&+ 6H(1,0,-1,-y) + 3H(0,-1,0,-1,-y) - 6H(0,0,-1,-1,-y) \\
&+ 3H(0,0,0,-1,-y) - \pi^2\ln(2) - \frac{9\pi^4}{40} + \frac{31\pi^2}{12} + \frac{121}{16}\Big)\Bigg\}. \qquad \text{(A.21)}
\end{aligned}
$$

### A.7 Heavy-to-light soft function

Here we list the explicit two-loop coefficients entering Eq. (9.57):

$$\bar{K}_F = \frac{2}{\epsilon^4} - \frac{4}{\epsilon^3} + \frac{2+\frac{5\pi^2}{3}}{\epsilon^2} + \frac{2\left(14\zeta(3)-5\pi^2\right)}{3\epsilon} - \frac{56\zeta(3)}{3} + \frac{5\pi^2}{3} + \frac{53\pi^4}{60}\,, \tag{A.22}$$

$$\begin{aligned}\bar{K}_A = &-\frac{11}{6\epsilon^3} + \frac{3\pi^2-1}{18\epsilon^2} + \frac{9\zeta(3)-\frac{55}{27}-\frac{37\pi^2}{12}}{\epsilon} + \frac{-78660\zeta(3)-6520-5535\pi^2+963\pi^4}{1620} \\ &+ N_\epsilon\Big(\frac{1}{12\epsilon^3} + \frac{1}{18\epsilon^2} + \frac{\frac{1}{27}+\frac{\pi^2}{8}}{\epsilon} + \frac{1}{324}\left(450\zeta(3)+8+27\pi^2\right)\Big)\,,\end{aligned} \tag{A.23}$$

$$\bar{K}_f = \frac{2}{3\epsilon^3} - \frac{2}{9\epsilon^2} + \frac{27\pi^2-4}{27\epsilon} + \frac{1}{81}\left(900\zeta(3)-8-27\pi^2\right). \tag{A.24}$$

After renormalization and setting $\epsilon \to 0$ we obtain a finite and scheme independent soft function. The structure in Laplace space is given by

$$\begin{aligned}s_{\text{fin}}(\Omega,\mu) = 1 &+ \frac{\alpha_s}{4\pi}\left[-\Gamma_{10}\frac{L^2}{4} + \gamma^S_{10}L + c^S_1\right] \\ &+ \left(\frac{\alpha_s}{4\pi}\right)^2\left[\left(\Gamma_{10}\right)^2\frac{L^4}{32} + \left(\beta^s_{20} - 3\gamma^S_{10}\right)\Gamma_{10}\frac{L^3}{12}\right. \\ &\qquad + \left(24\gamma^S_{10}(-\beta^s_{20}+\gamma^S_{10}) - 12\Gamma_{10}c^S_1 - 12\Gamma_{20}\right)\frac{L^2}{48} \\ &\qquad \left. + \left(c^S_1(-\beta^s_{20}+\gamma^S_{10}) + \gamma^S_{20}\right)L + c^S_2\right],\end{aligned} \tag{A.25}$$

where here $\Gamma_{\text{cusp}} = C_F\,\gamma_{\text{cusp}}$ and

$$c^S_1 = C_F\Big(-\frac{5\pi^2}{6}\Big), \tag{A.26}$$

$$\begin{aligned}c^S_2 = &\,C_F^2\Big(\frac{25\pi^4}{72}\Big) + C_F C_A\Big(-\frac{283\zeta(3)}{9} - \frac{326}{81} - \frac{233\pi^2}{36} + \frac{107\pi^4}{180}\Big) \\ &+ C_F T_R N_F\Big(\frac{1}{81}\left(396\zeta(3)-8+63\pi^2\right)\Big)\end{aligned} \tag{A.27}$$

and is in agreement with previous results [90].

# B Anomalous dimensions

In this appendix we collect all results for the anomalous dimensions relevant for this work without distinguishing the various $\alpha_{4\epsilon,i}$.

We give the explicit results with $T_R = 1/2$ in the FDH/DRED scheme, see Eqs. (6.18) and (6.19) for definitions and relations. The CDR/HV results are obtained by setting $N_\epsilon = 0$. Of course, $\bar{\gamma}_\epsilon$ is only meaningful for DRED.

$$\begin{aligned}
\bar{\gamma}_Q &= \Big(\frac{\alpha_s}{4\pi}\Big)\big(-2C_F\big) \\
&\quad + \Big(\frac{\alpha_s}{4\pi}\Big)^2\bigg\{C_AC_F\bigg[-\frac{98}{9}+\frac{2}{3}\pi^2-4\zeta(3)+\frac{8}{9}N_\epsilon\bigg]+C_FN_F\,\frac{20}{9}\bigg\}+\mathcal{O}(\alpha^3)\,,
\end{aligned} \tag{B.1a}$$

$$\begin{aligned}
\bar{\gamma}_q &= \Big(\frac{\alpha_s}{4\pi}\Big)(-3\,C_F)+\Big(\frac{\alpha_e}{4\pi}\Big)N_\epsilon\frac{C_F}{2} \\
&\quad + \Big(\frac{\alpha_s}{4\pi}\Big)^2\Big[C_AC_F\Big(-\frac{961}{54}-\frac{11}{6}\pi^2+26\zeta_3\Big)+C_F^2\Big(-\frac{3}{2}+2\pi^2-24\zeta_3\Big) \\
&\qquad\qquad + C_FN_F\Big(\frac{65}{27}+\frac{\pi^2}{3}\Big)+N_\epsilon\Big(\frac{167}{108}+\frac{\pi^2}{12}\Big)C_AC_F\Big] \\
&\quad + \Big(\frac{\alpha_s}{4\pi}\Big)\Big(\frac{\alpha_e}{4\pi}\Big)N_\epsilon\Big[\frac{11}{2}C_AC_F-\Big(2+\frac{\pi^2}{3}\Big)C_F^2\Big] \\
&\quad + \Big(\frac{\alpha_e}{4\pi}\Big)^2\Big[-N_\epsilon\frac{3}{4}C_FN_F-N_\epsilon^2\frac{C_F^2}{8}\Big]+\mathcal{O}(\alpha^3)\,,
\end{aligned} \tag{B.1b}$$

$$\begin{aligned}
\bar{\gamma}_g &= \Big(\frac{\alpha_s}{4\pi}\Big)\Big[-\frac{11}{3}C_A+\frac{2}{3}N_F+N_\epsilon\frac{C_A}{6}\Big] \\
&\quad + \Big(\frac{\alpha_s}{4\pi}\Big)^2\Big[C_A^2\Big(-\frac{692}{27}+\frac{11}{18}\pi^2+2\zeta_3\Big)+C_AN_F\Big(\frac{128}{27}-\frac{\pi^2}{9}\Big) \\
&\qquad\qquad + 2C_FN_F+N_\epsilon\Big(\frac{98}{27}-\frac{\pi^2}{36}\Big)C_A^2\Big] \\
&\quad + \Big(\frac{\alpha_s}{4\pi}\Big)\Big(\frac{\alpha_e}{4\pi}\Big)(-N_\epsilon C_FN_F)+\mathcal{O}(\alpha^3)\,,
\end{aligned} \tag{B.1c}$$

$$\begin{aligned}
\bar{\gamma}_\epsilon &= \Big(\frac{\alpha_s}{4\pi}\Big)\,(-4\,C_A)+\Big(\frac{\alpha_e}{4\pi}\Big)\,(N_F) \\
&\quad + \Big(\frac{\alpha_s}{4\pi}\Big)^2\,\Big[C_A^2\Big(-\frac{2987}{108}+\frac{5\pi^2}{6}+2\zeta_3+N_\epsilon\frac{233}{108}+N_\epsilon\frac{\pi^2}{12}\Big)+C_AN_F\Big(\frac{113}{27}+\frac{\pi^2}{3}\Big)\Big] \\
&\quad + \Big(\frac{\alpha_s}{4\pi}\Big)\,\Big(\frac{\alpha_e}{4\pi}\Big)\,\Big[5\,C_FN_F-\frac{2\pi^2}{3}C_AN_F\Big] \\
&\quad + \Big(\frac{\alpha_e}{4\pi}\Big)^2\,\Big[N_F\Big(\,C_A-2\,C_F-\frac{N_\epsilon}{2}(C_A+C_F)\Big)\Big] \\
&\quad + \Big(\frac{\alpha_{4\epsilon}}{4\pi}\Big)^2\,\Big[C_A^2\frac{3}{4}(-1+N_\epsilon)\Big]+\mathcal{O}(\alpha^3)\,,
\end{aligned} \tag{B.1d}$$

$$\bar{\gamma}_{\text{cusp}} = \Big(\frac{\alpha_s}{4\pi}\Big)\,(\,4\,)$$

$$+\left(\frac{\alpha_s}{4\pi}\right)^2\left[C_A\left(\frac{268}{9}-\frac{4}{3}\pi^2\right)-\frac{40}{9}N_F-N_\epsilon\frac{16}{9}C_A\right]+\mathcal{O}(\alpha^3)\,, \tag{B.1e}$$

$$\begin{aligned}\bar{\gamma}_{\rm cusp}(\beta) = \bar{\gamma}_{\rm cusp}(\alpha_s)\,\beta\coth\beta + 8\,C_A\left(\frac{\alpha_s}{4\pi}\right)^2\Bigg\{&\beta^2+\frac{\pi^2}{6}+\zeta_3\\ &+\coth\beta\left[\mathrm{Li}_2(e^{-2\beta})-2\beta\,\ln(1-e^{-2\beta})-\frac{\pi^2}{6}(1+\beta)-\beta^2-\frac{\beta^3}{3}\right]\\ &+\coth^2\beta\left[\mathrm{Li}_3(e^{-2\beta})+\beta\,\mathrm{Li}_2(e^{-2\beta})-\zeta_3+\frac{\pi^2}{6}\beta+\frac{\beta^3}{3}\right]\Bigg\}+\mathcal{O}(\alpha^3)\,.\end{aligned} \tag{B.1f}$$

where $\mathcal{O}(\alpha^3)$ stands for a generic coupling $\alpha \in \{\alpha_s, \alpha_e, \alpha_{4\epsilon,i}\}$.

For the $\beta$ functions we have

$$\bar{\beta}^s = -\left(\frac{\alpha_s}{4\pi}\right)^2\left[\frac{11}{3}C_A-\frac{2}{3}N_F+N_\epsilon\left(-\frac{C_A}{6}\right)\right]+\mathcal{O}(\alpha^3)\,, \tag{B.2a}$$

$$\begin{aligned}\bar{\beta}^e = &-\left(\frac{\alpha_s}{4\pi}\right)\left(\frac{\alpha_e}{4\pi}\right)(6\,C_F)\\ &-\left(\frac{\alpha_e}{4\pi}\right)^2\left[-4\,C_F+2\,C_A-N_F+N_\epsilon\Big(C_F-C_A\Big)\right]+\mathcal{O}(\alpha^3)\,.\end{aligned} \tag{B.2b}$$

A more complete list of coefficients for the $\beta$ functions can be found in Ref. [29].

## References


[1] J. C. Collins, D. E. Soper, and G. F. Sterman, *Factorization of Hard Processes in QCD*, *Adv. Ser. Direct. High Energy Phys.* **5** (1989) 1–91, [hep-ph/0409313].

[2] C. W. Bauer, S. Fleming, and M. E. Luke, *Summing Sudakov logarithms in $B \to X_s\gamma$ in effective field theory*, *Phys. Rev.* **D63** (2000) 014006, [hep-ph/0005275].

[3] C. W. Bauer, S. Fleming, D. Pirjol, and I. W. Stewart, *An Effective field theory for collinear and soft gluons: Heavy to light decays*, *Phys. Rev.* **D63** (2001) 114020, [hep-ph/0011336].

[4] C. W. Bauer and I. W. Stewart, *Invariant operators in collinear effective theory*, *Phys. Lett.* **B516** (2001) 134–142, [hep-ph/0107001].

[5] C. W. Bauer, D. Pirjol, and I. W. Stewart, *Soft collinear factorization in effective field theory*, *Phys. Rev.* **D65** (2002) 054022, [hep-ph/0109045].

[6] M. Beneke, A. P. Chapovsky, M. Diehl, and T. Feldmann, *Soft collinear effective theory and heavy to light currents beyond leading power*, *Nucl. Phys.* **B643** (2002) 431–476, [hep-ph/0206152].

[7] M. Beneke and T. Feldmann, *Multipole expanded soft collinear effective theory with nonAbelian gauge symmetry*, *Phys. Lett.* **B553** (2003) 267–276, [hep-ph/0211358].

[8] R. J. Hill and M. Neubert, *Spectator interactions in soft collinear effective theory*, *Nucl. Phys.* **B657** (2003) 229–256, [hep-ph/0211018].

[9] T. Becher, A. Broggio, and A. Ferroglia, *Introduction to Soft-Collinear Effective Theory*, arXiv:1410.1892.

[10] C. Lee, *The Evolution of Soft Collinear Effective Theory*, *Int. J. Mod. Phys. Conf. Ser.* **37** (2015) 1560045, [arXiv:1410.4216].

[11] A. Broggio, C. Gnendiger, A. Signer, D. Stöckinger, and A. Visconti, *SCET approach to regularization-scheme dependence of QCD amplitudes*, *JHEP* **01** (2016) 078, [arXiv:1506.0530].

[12] C. Gnendiger, A. Signer, and A. Visconti, *Regularization-scheme dependence of QCD amplitudes in the massive case*, arXiv:1607.0824.

[13] G. 't Hooft and M. Veltman, *Regularization and Renormalization of Gauge Fields*, *Nucl.Phys.* **B44** (1972) 189–213.

[14] W. Siegel, *Supersymmetric Dimensional Regularization via Dimensional Reduction*, *Phys.Lett.* **B84** (1979) 193.

[15] Z. Bern and D. A. Kosower, *The Computation of loop amplitudes in gauge theories*, *Nucl.Phys.* **B379** (1992) 451–561.

[16] A. Signer and D. Stöckinger, *Using Dimensional Reduction for Hadronic Collisions*, *Nucl.Phys.* **B808** (2009) 88–120, [arXiv:0807.4424].

[17] D. Capper, D. Jones, and P. van Nieuwenhuizen, *Regularization by Dimensional Reduction of Supersymmetric and Nonsupersymmetric Gauge Theories*, *Nucl.Phys.* **B167** (1980) 479.

[18] I. Jack, D. Jones, and K. Roberts, *Equivalence of dimensional reduction and dimensional regularization*, *Z.Phys.* **C63** (1994) 151–160, [hep-ph/9401349].

[19] I. Jack, D. Jones, and K. Roberts, *Dimensional reduction in nonsupersymmetric theories*, *Z.Phys.* **C62** (1994) 161–166, [hep-ph/9310301].

[20] R. Harlander, P. Kant, L. Mihaila, and M. Steinhauser, *Dimensional Reduction applied to QCD at three loops*, *JHEP* **0609** (2006) 053, [hep-ph/0607240].

[21] R. Harlander, D. Jones, P. Kant, L. Mihaila, and M. Steinhauser, *Four-loop beta function and mass anomalous dimension in dimensional reduction*, *JHEP* **0612** (2006) 024, [hep-ph/0610206].

[22] R. Harlander, P. Kant, L. Mihaila, and M. Steinhauser, *Dimensional reduction applied to QCD at higher orders*, arXiv:0706.2982.

[23] W. B. Kilgore, *Regularization Schemes and Higher Order Corrections*, *Phys.Rev.* **D83** (2011) 114005, [arXiv:1102.5353].

[24] E. Gardi and L. Magnea, *Factorization constraints for soft anomalous dimensions in QCD scattering amplitudes*, *JHEP* **03** (2009) 079, [arXiv:0901.1091].

[25] E. Gardi and L. Magnea, *Infrared singularities in QCD amplitudes*, *Nuovo Cim.* **C32N5-6** (2009) 137–157, [arXiv:0908.3273].

[26] T. Becher and M. Neubert, *Infrared singularities of scattering amplitudes in perturbative QCD*, *Phys.Rev.Lett.* **102** (2009) 162001, [arXiv:0901.0722].

[27] T. Becher and M. Neubert, *On the Structure of Infrared Singularities of Gauge-Theory Amplitudes*, *JHEP* **0906** (2009) 081, [arXiv:0903.1126].

[28] Z. Kunszt, A. Signer, and Z. Trocsanyi, *One loop helicity amplitudes for all $2 \to 2$ processes in QCD and N=1 supersymmetric Yang-Mills theory*, *Nucl.Phys.* **B411** (1994) 397–442, [hep-ph/9305239].

[29] W. B. Kilgore, *The Four Dimensional Helicity Scheme Beyond One Loop*, *Phys.Rev.* **D86** (2012) 014019, [arXiv:1205.4015].

[30] C. Gnendiger, A. Signer, and D. Stöckinger, *The infrared structure of QCD amplitudes and $H \to gg$ in FDH and DRED*, *Phys.Lett.* **B733** (2014) 296–304, [arXiv:1404.2171].

[31] T. Becher and M. Neubert, *Toward a NNLO calculation of the $\bar{B} \to X_s\gamma$ decay rate with a cut on photon energy. II. Two-loop result for the jet function*, *Phys. Lett.* **B637** (2006) 251–259, [hep-ph/0603140].

[32] T. Becher and G. Bell, *The gluon jet function at two-loop order*, *Phys. Lett.* **B695** (2011) 252–258, [arXiv:1008.1936].

[33] Z. Bern, A. De Freitas, L. J. Dixon, and H. L. Wong, *Supersymmetric regularization, two loop QCD amplitudes and coupling shifts*, *Phys. Rev.* **D66** (2002) 085002, [hep-ph/0202271].

[34] A. Broggio, C. Gnendiger, A. Signer, D. Stöckinger, and A. Visconti, *Computation of $H \to gg$ in DRED and FDH: renormalization, operator mixing, and explicit two-loop results*, *Eur. Phys. J.* **C75** (2015), no. 9 418, [arXiv:1503.0910].

[35] J. Gao, C. S. Li, and H. X. Zhu, *Top Quark Decay at Next-to-Next-to Leading Order in QCD*, *Phys. Rev. Lett.* **110** (2013), no. 4 042001, [arXiv:1210.2808].

[36] R. Boughezal, C. Focke, X. Liu, and F. Petriello, *$W$-boson production in association with a jet at next-to-next-to-leading order in perturbative QCD*, *Phys. Rev. Lett.* **115** (2015), no. 6 062002, [arXiv:1504.0213].

[37] R. Boughezal, C. Focke, W. Giele, X. Liu, and F. Petriello, *Higgs boson production in association with a jet at NNLO using jettiness subtraction*, *Phys. Lett.* **B748** (2015) 5–8, [arXiv:1505.0389].

[38] J. Gaunt, M. Stahlhofen, F. J. Tackmann, and J. R. Walsh, *N-jettiness Subtractions for NNLO QCD Calculations*, *JHEP* **09** (2015) 058, [arXiv:1505.0479].

[39] D. Farhi, I. Feige, M. Freytsis, and M. D. Schwartz, *Streamlining resummed QCD calculations using Monte Carlo integration*, arXiv:1507.0631.

[40] I. W. Stewart, F. J. Tackmann, J. Thaler, C. K. Vermilion, and T. F. Wilkason, *XCone: N-jettiness as an Exclusive Cone Jet Algorithm*, *JHEP* **11** (2015) 072, [arXiv:1508.0151].

[41] T. Kasemets, W. J. Waalewijn, and L. Zeune, *Calculating Soft Radiation at One Loop*, *JHEP* **03** (2016) 153, [arXiv:1512.0085].

[42] R. Boughezal, J. M. Campbell, R. K. Ellis, C. Focke, W. T. Giele, X. Liu, and F. Petriello, *Z-boson production in association with a jet at next-to-next-to-leading order in perturbative QCD*, *Phys. Rev. Lett.* **116** (2016), no. 15 152001, [arXiv:1512.0129].

[43] J. M. Campbell, R. K. Ellis, and C. Williams, *Associated Production of a Higgs Boson at NNLO*, arXiv:1601.0065.

[44] R. Boughezal, *NNLO phenomenology using N-jettiness subtraction*, in *Proceedings, 12th International Symposium on Radiative Corrections (Radcor 2015) and LoopFest XIV (Radiative Corrections for the LHC and Future Colliders)*, 2016. arXiv:1601.0492.

[45] R. Boughezal, J. M. Campbell, R. K. Ellis, C. Focke, W. Giele, X. Liu, F. Petriello, and C. Williams, *Color singlet production at NNLO in MCFM*, arXiv:1605.0801.

[46] S. Catani, *The Singular behavior of QCD amplitudes at two loop order*, *Phys.Lett.* **B427** (1998) 161–171, [hep-ph/9802439].

[47] T. Becher and M. Neubert, *Infrared singularities of QCD amplitudes with massive*

*partons*, *Phys. Rev.* **D79** (2009) 125004, [arXiv:0904.1021]. [Erratum: Phys. Rev.D80,109901(2009)].

[48] . Almelid, C. Duhr, and E. Gardi, *Three-loop corrections to the soft anomalous dimension in multi-leg scattering*, arXiv:1507.0004.

[49] M. Steinhauser, *Results and techniques of multiloop calculations*, *Phys. Rept.* **364** (2002) 247–357, [hep-ph/0201075].

[50] W. Siegel, *Inconsistency of Supersymmetric Dimensional Regularization*, *Phys. Lett.* **B94** (1980) 37–40.

[51] D. Stöckinger, *Regularization by dimensional reduction: consistency, quantum action principle, and supersymmetry*, *JHEP* **0503** (2005) 076, [hep-ph/0503129].

[52] K. G. Wilson, *Quantum field theory models in less than four-dimensions*, *Phys. Rev.* **D7** (1973) 2911–2926.

[53] J. C. Collins, *Renormalization*, vol. 26 of *Cambridge Monographs on Mathematical Physics*. Cambridge University Press, Cambridge, 1986.

[54] A. Signer and D. Stockinger, *Factorization and regularization by dimensional reduction*, *Phys.Lett.* **B626** (2005) 127–138, [hep-ph/0508203].

[55] L. Magnea, V. Del Duca, C. Duhr, E. Gardi, and C. D. White, *Infrared singularities in the high-energy limit*, *PoS* **LL2012** (2012) 008, [arXiv:1210.6786].

[56] V. Del Duca, C. Duhr, E. Gardi, L. Magnea, and C. D. White, *The Infrared structure of gauge theory amplitudes in the high-energy limit*, *JHEP* **12** (2011) 021, [arXiv:1109.3581].

[57] V. Del Duca, C. Duhr, E. Gardi, L. Magnea, and C. D. White, *An infrared approach to Reggeization*, *Phys. Rev.* **D85** (2012) 071104, [arXiv:1108.5947].

[58] T. Becher, M. Neubert, and G. Xu, *Dynamical Threshold Enhancement and Resummation in Drell-Yan Production*, *JHEP* **07** (2008) 030, [arXiv:0710.0680].

[59] T. Becher, M. Neubert, and B. D. Pecjak, *Factorization and Momentum-Space Resummation in Deep-Inelastic Scattering*, *JHEP* **0701** (2007) 076, [hep-ph/0607228].

[60] Y. Li, A. von Manteuffel, R. M. Schabinger, and H. X. Zhu, *Soft-virtual corrections to Higgs production at $N^3LO$*, *Phys. Rev.* **D91** (2015) 036008, [arXiv:1412.2771].

[61] V. Ahrens, T. Becher, M. Neubert, and L. L. Yang, *Renormalization-Group Improved Prediction for Higgs Production at Hadron Colliders*, *Eur. Phys. J.* **C62** (2009) 333–353, [arXiv:0809.4283].

[62] A. V. Belitsky, *Two loop renormalization of Wilson loop for Drell-Yan production*, *Phys. Lett.* **B442** (1998) 307–314, [hep-ph/9808389].

[63] Y. Li, S. Mantry, and F. Petriello, *An Exclusive Soft Function for Drell-Yan at Next-to-Next-to-Leading Order*, *Phys. Rev.* **D84** (2011) 094014, [arXiv:1105.5171].

[64] Y. Li and H. X. Zhu, *Single soft gluon emission at two loops*, *JHEP* **11** (2013) 080, [arXiv:1309.4391].

[65] Y. Li, A. von Manteuffel, R. M. Schabinger, and H. X. Zhu, *$N^3LO$ Higgs boson and Drell-Yan production at threshold: The one-loop two-emission contribution*, *Phys. Rev.* **D90** (2014), no. 5 053006, [arXiv:1404.5839].

[66] P. F. Monni, T. Gehrmann, and G. Luisoni, *Two-Loop Soft Corrections and Resummation of the Thrust Distribution in the Dijet Region*, *JHEP* **08** (2011) 010, [arXiv:1105.4560].

[67] R. Kelley, M. D. Schwartz, R. M. Schabinger, and H. X. Zhu, *The two-loop hemisphere soft function*, *Phys. Rev.* **D84** (2011) 045022, [arXiv:1105.3676].

[68] R. Boughezal, X. Liu, and F. Petriello, *N-jettiness soft function at next-to-next-to-leading order*, *Phys. Rev.* **D91** (2015), no. 9 094035, [arXiv:1504.0254].

[69] T. Becher, G. Bell, and S. Marti, *NNLO soft function for electroweak boson production at large transverse momentum*, *JHEP* **04** (2012) 034, [arXiv:1201.5572].

[70] A. Ferroglia, B. D. Pecjak, L. L. Yang, B. D. Pecjak, and L. L. Yang, *The NNLO soft function for the pair invariant mass distribution of boosted top quarks*, *JHEP* **10** (2012) 180, [arXiv:1207.4798].

[71] P. Nogueira, *Automatic Feynman graph generation*, *J. Comput. Phys.* **105** (1993) 279–289.

[72] M. Sjödahl, *ColorMath - A package for color summed calculations in SU(Nc)*, *Eur. Phys. J.* **C73** (2013), no. 2 2310, [arXiv:1211.2099].

[73] A. von Manteuffel and C. Studerus, *Reduze 2 - Distributed Feynman Integral Reduction*, arXiv:1201.4330.

[74] E. N. Glover, C. Oleari, and M. Tejeda-Yeomans, *Two loop QCD corrections to gluon-gluon scattering*, *Nucl.Phys.* **B605** (2001) 467–485, [hep-ph/0102201].

[75] C. Anastasiou, E. N. Glover, C. Oleari, and M. Tejeda-Yeomans, *Two loop QCD corrections to massless quark gluon scattering*, *Nucl.Phys.* **B605** (2001) 486–516, [hep-ph/0101304].

[76] Z. Bern, A. De Freitas, and L. J. Dixon, *Two loop helicity amplitudes for gluon-gluon scattering in QCD and supersymmetric Yang-Mills theory*, *JHEP* **0203** (2002) 018, [hep-ph/0201161].

[77] Z. Bern, A. De Freitas, and L. J. Dixon, *Two loop helicity amplitudes for quark gluon scattering in QCD and gluino gluon scattering in supersymmetric Yang-Mills theory*, *JHEP* **0306** (2003) 028, [hep-ph/0304168].

[78] W. Bernreuther, R. Bonciani, T. Gehrmann, R. Heinesch, T. Leineweber, P. Mastrolia, and E. Remiddi, *Two-loop QCD corrections to the heavy quark form-factors: The Vector contributions*, *Nucl. Phys.* **B706** (2005) 245–324, [hep-ph/0406046].

[79] E. Remiddi and J. A. M. Vermaseren, *Harmonic polylogarithms*, *Int. J. Mod. Phys.* **A15** (2000) 725–754, [hep-ph/9905237].

[80] T. Gehrmann and E. Remiddi, *Numerical evaluation of harmonic polylogarithms*, *Comput. Phys. Commun.* **141** (2001) 296–312, [hep-ph/0107173].

[81] R. Bonciani, P. Mastrolia, and E. Remiddi, *Vertex diagrams for the QED form-factors at the two loop level*, *Nucl. Phys.* **B661** (2003) 289–343, [hep-ph/0301170]. [Erratum: Nucl. Phys.B702,359(2004)].

[82] R. Bonciani, P. Mastrolia, and E. Remiddi, *Master integrals for the two loop QCD virtual corrections to the forward backward asymmetry*, *Nucl. Phys.* **B690** (2004) 138–176, [hep-ph/0311145].

[83] I. Jack, D. R. T. Jones, S. P. Martin, M. T. Vaughn, and Y. Yamada, *Decoupling of the epsilon scalar mass in softly broken supersymmetry*, *Phys. Rev.* **D50** (1994) 5481–5483, [hep-ph/9407291].

[84] R. Bonciani and A. Ferroglia, *Two-Loop QCD Corrections to the Heavy-to-Light Quark Decay*, *JHEP* **11** (2008) 065, [arXiv:0809.4687].

[85] H. M. Asatrian, C. Greub, and B. D. Pecjak, *NNLO corrections to $\bar{B} \to X_u l \bar{\nu}$ in the shape-function region*, *Phys. Rev.* **D78** (2008) 114028, [arXiv:0810.0987].

[86] M. Beneke, T. Huber, and X. Q. Li, *Two-loop QCD correction to differential semi-leptonic $b \to u$ decays in the shape-function region*, *Nucl. Phys.* **B811** (2009) 77–97, [arXiv:0810.1230].

[87] G. Bell, *NNLO corrections to inclusive semileptonic B decays in the shape-function region*, *Nucl. Phys.* **B812** (2009) 264–289, [arXiv:0810.5695].

[88] S. Catani, S. Dittmaier, and Z. Trocsanyi, *One loop singular behavior of QCD and SUSY QCD amplitudes with massive partons*, *Phys. Lett.* **B500** (2001) 149–160, [hep-ph/0011222].

[89] K. Chetyrkin, B. A. Kniehl, and M. Steinhauser, *Decoupling relations to O (alpha-s**3) and their connection to low-energy theorems*, *Nucl.Phys.* **B510** (1998) 61–87, [hep-ph/9708255].

[90] T. Becher and M. Neubert, *Toward a NNLO calculation of the $\bar{B} \to X_s \gamma$ decay rate with a cut on photon energy: I. Two-loop result for the soft function*, *Phys. Lett.* **B633** (2006) 739–747, [hep-ph/0512208].

[91] M. Neubert, *Heavy quark symmetry*, *Phys. Rept.* **245** (1994) 259–396, [hep-ph/9306320].

[92] N. Kidonakis, *Two-loop soft anomalous dimensions and NNLL resummation for heavy quark production*, *Phys. Rev. Lett.* **102** (2009) 232003, [arXiv:0903.2561].

[93] M. Czakon and D. Heymes, *Four-dimensional formulation of the sector-improved residue subtraction scheme*, *Nucl. Phys.* **B890** (2014) 152–227, [arXiv:1408.2500].

[94] W. T. Giele and E. W. N. Glover, *Higher order corrections to jet cross-sections in e+ e- annihilation*, *Phys. Rev.* **D46** (1992) 1980–2010.

[95] S. Catani and M. Grazzini, *An NNLO subtraction formalism in hadron collisions and its application to Higgs boson production at the LHC*, *Phys. Rev. Lett.* **98** (2007) 222002, [hep-ph/0703012].

[96] R. Kelley and M. D. Schwartz, *1-loop matching and NNLL resummation for all partonic 2 to 2 processes in QCD*, *Phys. Rev.* **D83** (2011) 045022, [arXiv:1008.2759].

[97] A. Broggio, A. Ferroglia, B. D. Pecjak, and Z. Zhang, *NNLO hard functions in massless QCD*, *JHEP* **12** (2014) 005, [arXiv:1409.5294].